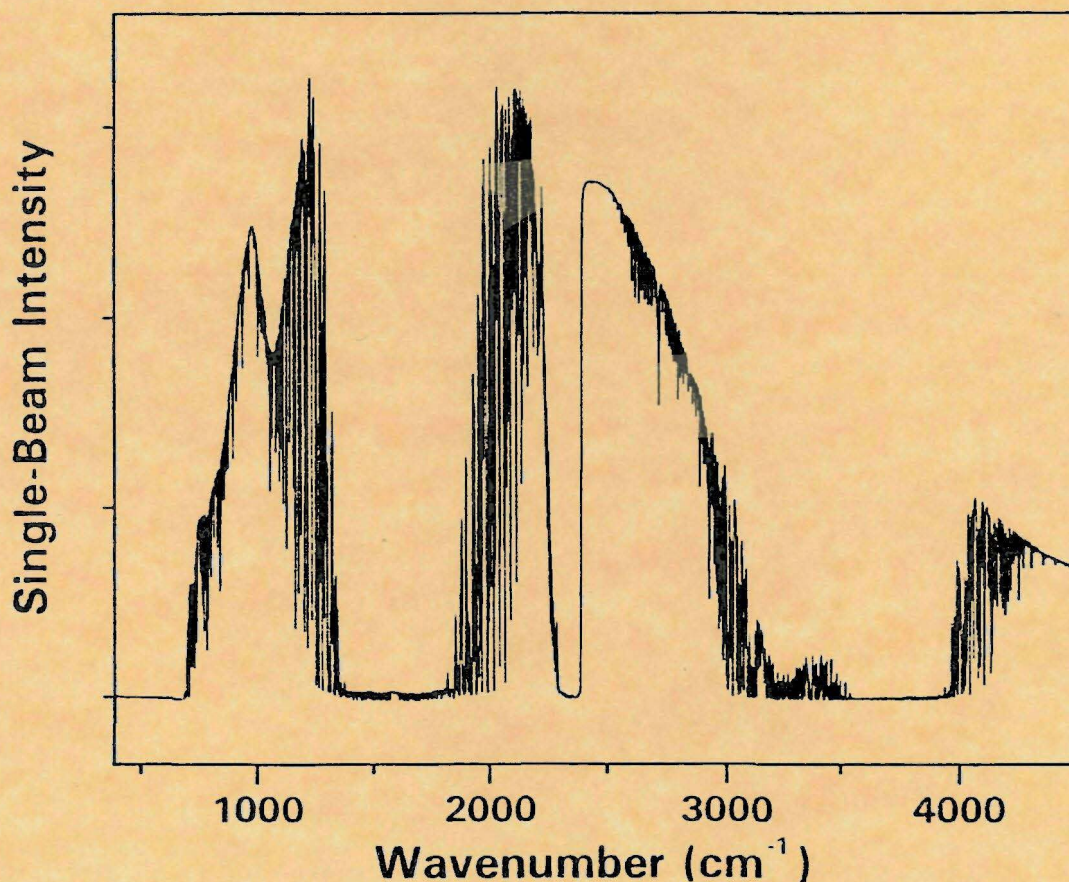


# FT-IR Open-Path Monitoring Guidance Document

Third Edition



ManTech Environmental Technology, Inc.  
P.O. Box 12313  
Research Triangle Park, NC 27709

*A ManTech International Company*

# FT-IR Open-Path Monitoring Guidance Document

Third Edition

by

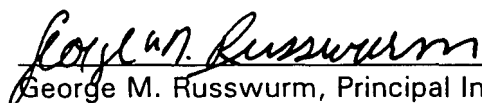
**George M. Russwurm and Jeffrey W. Childers**  
ManTech Environmental Technology, Inc.  
Research Triangle Park, North Carolina 27709

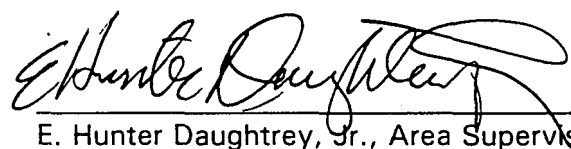
*Submitted to:*

William A. McClenny  
Work Assignment Manager  
Human Exposure and Atmospheric Sciences Division  
National Exposure Research Laboratory  
Research Triangle Park, North Carolina 27711

Contract 68-D5-0049

*Reviewed and Approved by:*

  
George M. Russwurm, Principal Investigator

  
E. Hunter Daughtrey, Jr., Area Supervisor

ManTech Environmental Technology, Inc.  
P.O. Box 12313  
Research Triangle Park, NC 27709

*A ManTech International Company*

## Foreword

This report presents the results of work performed by ManTech Environmental Technology, Inc., under Contract 68-D5-0049 for the Atmospheric Methods and Monitoring Branch, National Exposure Research Laboratory, U.S. Environmental Protection Agency, Research Triangle Park, NC. This report has been reviewed by ManTech Environmental Technology, Inc., and approved for publication. Mention of trade names or commercial products does not constitute endorsement or recommendation for use.

## Preface to the Third Edition

The Fourier transform infrared remote sensing technique for measuring gas concentrations in the atmosphere has undergone a vigorous growth and development period over the last 10 years. There seems to be an expanding awareness of the capabilities of this technique and therefore a continuing demand for a guidance document that is useful to the people entering the field for the first time. It is our hope that this document will fulfill that need. The intent of this document is to provide information about the FT-IR technique that will assist the user in understanding how the system functions.

While there is some difficulty in producing a document that addresses all the questions operators may have about the FT-IR remote sensing technique, we have tried to include as much pertinent information as is available at this time. Some of the topics included here are more rigorous than would at first be deemed necessary. But both authors have come to understand that the operator should have an in-depth understanding of the instrumentation in order to make appropriate choices about the data acquisition and processing.

The data that has been used to compile the information in this document was acquired over a several year period and with several different instruments. We have tried to present guidance that would be common to all instruments, but in some instances that is not possible. The judgements included in this document are based on our study of spectra acquired with high ( $0.125\text{ cm}^{-1}$ ) resolution and with low ( $1.0\text{ cm}^{-1}$ ) resolution instruments and with both the monostatic and the bistatic systems. During the data acquisition phase of this project we also acquired the ancillary data of relative humidity, temperature, and atmospheric pressure. This provided us with much of the information necessary to understand the effects of water vapor on the data and the manufacture of a background spectrum and a water vapor reference.

The document contains 12 chapters that we believe address the most important aspects of atmospheric monitoring with the FT-IR remote sensing technique. As we have defined this technique, we mean the use of an open-air path up to 1 km long. Chapter 12 is a bibliography that contains more than 330 citations of papers and presentations that describe the technique. While this is not an exhaustive compilation, it shows that there is a wealth of information about the use and efficacy of the technique.

The authors wish to emphasize that this document is meant to be a primer for the new users of the FT-IR remote sensing technique and to give them some guidance in the overall operation of the instrument. It is not meant to be a standard operating procedure. For that,

there is an EPA-approved method (compendium method TO-16) and also two ASTM methods that are available. These are cited in the text and in the bibliography.

GMR

JWC

June 1999

## Contents

Foreword .....	iii
Preface to the Third Edition .....	v
Figures .....	xi
Tables .....	xv
Acknowledgement .....	xvii
1 Introduction .....	1-1
1.1 Overview of Document .....	1-1
1.2 References .....	1-2
2 The Fourier Transform Spectrometer .....	2-1
2.1 Introduction and Overview .....	2-1
2.2 The Michelson Interferometer .....	2-3
2.2.1 Interference .....	2-3
2.2.2 Resolution .....	2-7
2.2.3 Throughput .....	2-8
2.2.4 The Detector .....	2-8
2.2.5 The IR Source .....	2-10
2.3 Transfer Optics, Telescopes, and Beam-Return Optics .....	2-10
2.3.1 Bistatic System .....	2-13
2.3.2 Monostatic System .....	2-14
2.4 The Electronics .....	2-15
2.5 The Computer .....	2-16
2.6 The Data Output .....	2-17
2.6.1 Beer's Law .....	2-17
2.6.2 The Interferogram .....	2-19
2.6.2.1 Truncation .....	2-19
2.6.2.2 Phase Shift .....	2-19
2.6.3 The Transform .....	2-20
2.6.4 The Single-Beam Spectrum .....	2-20
2.6.5 Data Analysis .....	2-21
2.6.5.1 Generation of the Absorption Spectrum .....	2-21
2.6.5.2 Generation of the Reference Spectrum .....	2-21
2.6.5.3 Analytical Methods .....	2-22
2.6.5.3.1 Comparison Technique .....	2-23
2.6.5.3.2 Scaled Subtraction Technique .....	2-23
2.6.5.3.3 Multicomponent Analysis Techniques .....	2-24
2.7 References .....	2-24
3 Initial Instrument Operation .....	3-1
3.1 Introduction and Overview .....	3-1
3.2 The Single-Beam Spectrum .....	3-2
3.2.1 Wave Number Shift .....	3-4
3.2.2 Change in Resolution .....	3-4
3.3 Distance to Saturation .....	3-5

3.4	Return Intensity as a Function of Distance	3-5
3.5	Determination of the Stray Light Signal	3-6
3.6	Determination of the Random Noise of the System	3-7
3.7	Return Intensity as a Function of Water Vapor	3-10
3.8	References	3-10
4	Background Spectra	4-1
4.1	Introduction and Overview	4-1
4.2	Synthetic Background Spectra	4-3
4.3	Upwind Background Spectra	4-3
4.4	Short-Path Background Spectra	4-4
4.5	Averaged Background Spectra	4-6
4.6	Why Use a Background	4-7
4.7	General Advice About Background Spectra	4-8
5	Water Vapor Spectra	5-1
5.1	Introduction and Overview	5-1
5.2	Water Vapor Spectra Considerations	5-2
5.3	General Process for the Production of a Water Vapor Spectrum	5-2
5.3.1	Selection of Spectra	5-3
5.3.2	Creation of Synthetic Background	5-3
5.3.3	Creation of the Absorption Spectrum	5-3
5.3.4	Subtraction of the Target Gas	5-4
5.4	Calculated Water Spectra	5-4
5.5	Methane and Ozone Examples	5-5
6	Siting	6-1
6.1	Introduction and Overview	6-1
6.2	Selecting the Path	6-3
6.2.1	The Longest Path	6-5
6.2.2	Shortest Path Requirements	6-5
6.2.3	Short Path Versus Long Path	6-6
6.2.4	Prevailing Winds	6-8
6.2.5	Slant Path Versus Horizontal Path	6-8
6.3	Changing the Path	6-8
6.4	Ancillary Measurements	6-9
6.5	A Specific Case	6-9
6.6	References	6-12
7	Resolution Considerations in Long-Path, Open-Path FT-IR Spectrometry	7-1
7.1	Introduction and Overview	7-1
7.2	Definition of Resolution	7-3
7.3	Trading Rules in FT-IR Spectrometry	7-4
7.4	Example Spectra of CO <sub>2</sub> and Water Vapor	7-6
7.4.1	Resolution Effects	7-8
7.4.1.1	Laboratory Measurements	7-8
7.4.1.2	Long-Path Measurements	7-10
7.4.2	Zero-Filling Effects	7-11

7.4.3	Apodization Effects	7-12
7.5	Effect of Resolution on Quantitative Analyses	7-14
7.5.1	Studies from the Literature	7-15
7.5.2	Case Study: The Effect of Resolution and Related Parameters on the CLS Analysis of Multicomponent Mixtures	7-17
7.5.2.1	Mixtures of CO and <sup>13</sup> CO	7-18
7.5.2.2	Mixtures of Acetone, Methylene Chloride, and Ethanol	7-19
7.5.2.2.1	Effect of the Number of Data Points on the CLS Analysis	7-20
7.5.2.2.2	Effect of S/N Ratio on the CLS Analysis	7-22
7.5.2.3	Mixtures of Methylene Chloride and Nitrous Oxide	7-22
7.5.2.4	Conclusions and Recommendations Based on Case Study	7-23
7.6	General Conclusions and Recommendations	7-24
7.7	Guidance for Selecting Resolution and Related Parameters	7-25
7.8	References	7-28
8	Nonlinear Response Caused by Apodization Functions and Its Effect on FTIR Data	8-1
8.1	Introduction and Overview	8-1
8.2	Procedure and Theoretical Basis	8-4
8.3	Results of Calculations	8-7
8.4	Analysis	8-13
8.5	Discussion	8-17
8.6	Conclusions and Recommendations	8-19
8.7	References	8-20
9	The Technique of Classical Least Squares	9-1
9.1	Introduction and Overview	9-1
9.2	Least Squares Analysis for One Gas	9-1
9.3	Matrices	9-5
9.3.1	Matrix Types	9-5
9.3.2	Some Matrix Properties	9-6
9.3.3	Multiplication of Matrices	9-7
9.3.4	The Identity Matrix	9-8
9.3.5	The Transpose of a Matrix	9-9
9.3.6	The Determinant of a Matrix	9-9
9.3.7	Cofactors of Matrices	9-11
9.3.8	The Inverse of a Matrix	9-11
9.4	Matrices and Algebraic Equations	9-13
9.5	Least Squares and Matrices	9-14
9.6	Expansion to Many Gases	9-18
9.7	Least Squares Errors	9-20
9.8	References	9-21



10	Quality Assurance and Quality Control	10-1
10.1	Introduction and Overview	10-1
10.2	Project Plan Categories	10-2
10.2.1	Category Definitions	10-3
10.2.2	Category I Points to be Addressed	10-3
10.2.2.1	Project Description	10-4
10.2.2.2	Project Organization and Responsibilities	10-4
10.2.2.3	QA Objectives	10-5
10.2.2.4	Site Selection and Sampling Procedures	10-5
10.2.2.5	Sample Custody	10-6
10.2.2.6	Calibration Procedures and Frequency	10-6
10.2.2.7	Analytical Procedures	10-7
10.2.2.8	Data Reduction, Validation, and Reporting	10-7
10.2.2.9	Internal Quality Control Checks	10-8
10.2.2.10	Performance and System Audits	10-8
10.2.2.11	Preventive Maintenance	10-8
10.2.2.12	Calculation of Data Quality Indicators	10-9
10.2.2.13	Corrective Action	10-9
10.2.2.14	Quality Control Reports to Management	10-9
10.2.2.15	References	10-9
10.2.2.16	Other Items	10-9
10.3	Case Study: QA Data Collected Over Two and One-Half Months at a Semipermanent Field Site	10-10
10.4	Recommendations of Tests to Be Included in a QA Program for FT-IR Long-Path Monitors	10-14
10.4.1	Noise Measurements	10-15
10.4.2	Stability of Instrument	10-15
10.4.3	Accuracy and Precision	10-16
10.4.4	Completeness and Representativeness of Data	10-18
10.4.5	Comparability of the Data	10-18
10.4.6	Ancillary Measurements	10-19
10.4.7	Documentation	10-19
10.5	References	10-19
11	Glossary of Terms for FT-IR Open-Path Remote Sensing	11-1
11.1	Introduction and Overview	11-1
11.2	Terms	11-1
11.3	References	11-7
12	Bibliography	12-1
12.1	Introduction and Overview	12-1
12.2	Publications	12-1

## Figures

Number		Page
2-1	A Schematic of the Simplest Form of a Michelson Interferometer . . . . .	2-4
2-2	Schematic of Interference Created by Division of Amplitude . . . . .	2-5
2-3	Center Burst Increasing as the Wave Number Range Expands . . . . .	2-6
2-4	Interferograms for a Range of 3500 cm <sup>-1</sup> . . . . .	2-6
2-5	Interferogram of Two Cosine Waves as a Function of $\Delta T$ . . . . .	2-7
2-6	The Bistatic Configuration . . . . .	2-11
2-7	The Monostatic Configuration . . . . .	2-12
2-8	Data Reduction Flow Chart . . . . .	2-22
3-1	Single-Beam Spectrum Along a 414-m Path . . . . .	3-2
3-2	Single-Beam Spectrum Recorded at a 20-m Total Path Length Indicating Nonlinear Operation . . . . .	3-3
3-3	Region Between 1000 and 1025 cm <sup>-1</sup> . . . . .	3-4
3-4	Subtraction of Spectra for the Determination of Line Shifts and Resolution Changes . . . . .	3-5
3-5	Effect of Stray Light . . . . .	3-7
3-6	The RMS Baseline Noise Measured Between 980 and 1020 cm <sup>-1</sup> , 2480 and 2520 cm <sup>-1</sup> , and 4380 and 4420 cm <sup>-1</sup> . . . . .	3-9
4-1	Synthetic $I_0$ Spectrum . . . . .	4-3
4-2	A Possible Configuration for $I_0$ Spectrum Acquisition . . . . .	4-4
4-3	Procedure for Acquiring a Short-Path Background Spectrum . . . . .	4-5
5-1	The Portion of a Single-Beam Spectrum over Which Methane Absorbs . . . . .	5-5
5-2	Methane Region with Synthetic Background Spectrum Superimposed . . . . .	5-5
5-3	Methane Reference Spectrum and the Calculated Absorption Spectrum . . . . .	5-6
5-4	Water Vapor Spectrum Made for the Methane Absorption Region . . . . .	5-6
5-5	Atmospheric Ozone Absorption Spectrum and Ozone Reference Spectrum . . . . .	5-6
5-6	Ozone Measured at Research Triangle Park During June . . . . .	5-7
6-1	Sulfur Hexafluoride Reference Spectrum . . . . .	6-7
6-2	Aerial Photograph of a Superfund Site . . . . .	6-11
7-1	Single-Beam IR Spectra of CO <sub>2</sub> Measured at 0.25-, 0.50-, 1.0-, and 2.0-cm <sup>-1</sup> Resolution with No Apodization and No Additional Zero Filling . . . . .	7-7
7-2	Single-Beam IR Spectra of Water Vapor Measured at 0.25-, 0.50-, 1.0-, and 2.0-cm <sup>-1</sup> Resolution with No Apodization and No Additional Zero Filling . . . . .	7-7
7-3	Single-Beam IR Spectra of Water Vapor Measured at 2-, 1-, and 0.5-cm <sup>-1</sup> Resolution over a 150-m Path . . . . .	7-7

7-4	IR Spectra of Water	7-11
7-5	Absorption Spectra of CO <sub>2</sub> Measured at 0.25-cm <sup>-1</sup> Resolution with a Zero-Filling Factor of 1, 0.5-cm <sup>-1</sup> Resolution with No Zero-Filling, and 0.5-cm <sup>-1</sup> with a Zero-Filling Factor of 2	7-11
7-6	Absorption Spectra of Water Vapor Measured at 0.25-cm <sup>-1</sup> Resolution with a Zero-Filling Factor of 1, 0.5-cm <sup>-1</sup> Resolution with a Zero-Filling Factor of 2, and 1-cm <sup>-1</sup> Resolution with a Zero-Filling Factor of 4	7-12
7-7	Absorption Spectra of CO Measured at a Nominal 0.125-cm <sup>-1</sup> Resolution with No, Triangular, Happ-Genzel, and Norton-Beer-Medium Apodization Functions	7-13
7-8	Absorption Spectra of Water Vapor Measured at 0.5-cm <sup>-1</sup> Resolution with a Zero-Filling Factor of 2 and with No, Triangular, Happ-Genzel, and Norton-Beer-Medium Apodization Functions	7-13
7-9	Reference 0.25-cm <sup>-1</sup> Spectra of <sup>13</sup> CO and CO and Spectra of Synthetic Mixtures of 150 ppm CO and 100 ppm <sup>13</sup> CO Measured at 0.25-, 0.5-, 1.0-, and 2.0-cm <sup>-1</sup> Resolution	7-19
7-10	Concentration Calculated from CLS Analysis vs. Known Concentration for <sup>13</sup> CO/CO Mixtures Measured at 2-cm <sup>-1</sup> Resolution	7-19
7-11	Reference 0.25-cm <sup>-1</sup> Spectra of Acetone, Methylene Chloride, and Ethanol and Spectra of Synthetic Mixtures of 100 ppm Acetone, 100 ppm Methylene Chloride, and 500 ppm Ethanol Measured at 1.0-, 2.0-, and 4.0-cm <sup>-1</sup> Resolution	7-20
7-12	Spectra of Synthetic Mixtures of 100 ppm Acetone, 100 ppm Methylene Chloride, and 500 ppm Ethanol Measured at 1-cm <sup>-1</sup> Resolution with 0, 1, 5, 10, and 25% Noise Added	7-22
7-13	Reference 0.25-cm <sup>-1</sup> Spectra of N <sub>2</sub> O and Methylene Chloride and Spectra of Synthetic Mixtures of 50 ppm N <sub>2</sub> O and 100 ppm Methylene Chloride Measured at 0.25-, 0.5-, and 1.0-cm <sup>-1</sup> Resolution	7-23
7-14	Concentration Calculated from CLS Analysis vs. Known Concentration for N <sub>2</sub> O/Methylene Chloride Mixtures Measured at 0.25-cm <sup>-1</sup> Resolution	7-23
8-1	A Portion of a Water Spectrum Using Boxcar Apodization and Triangular Apodization	8-2
8-2	Schematic of Actual and Assumed FT-IR Responses	8-3
8-3	Measured Concentration of Methane vs. the Experimental Response of the FT-IR	8-7
8-4	Methane Absorbance at 2927 cm <sup>-1</sup>	8-9
8-5	Ammonia Absorbance at 967 cm <sup>-1</sup>	8-9
8-6	Water Absorbance at 1014.5 cm <sup>-1</sup>	8-10
8-7	Methane Absorbance vs. <i>CL</i> at 2927 cm <sup>-1</sup>	8-10
8-8	Ammonia Absorbance at 2927 cm <sup>-1</sup>	8-11
8-9	Water Absorbance vs. <i>P</i> at 1014.5 cm <sup>-1</sup>	8-11
8-10	Water Absorbance for 0.5 torr at 1014.5 cm <sup>-1</sup>	8-12
8-11	Water Absorbance for 35 torr at 1014.5 cm <sup>-1</sup>	8-12
8-12	Match of Water Absorbance at 1014.5 cm <sup>-1</sup>	8-14
8-13	Analysis Results for Methane from 2915 to 2929 cm <sup>-1</sup>	8-16

8-14	Analysis Results for Methane from 2900 to 3000 $\text{cm}^{-1}$ . . . . .	8-16
8-15	Methane Analysis Allowing the Water Reference Concentration to Vary . . . . .	8-17
8-16	Plot of Regression Slopes vs. Temperature . . . . .	8-18
8-17	Difference After Regression Coefficients Have Been Applied . . . . .	8-19
9-1	Least Squares Fit of a Data Set . . . . .	9-3
10-1	Return Signal Magnitude of the FT-IR Monitor Measured Daily at 0700 and 1200 . . . . .	10-11
10-2	The RMS Baseline Noise Measured Between 980 and 1020 $\text{cm}^{-1}$ , 2480 and 2520 $\text{cm}^{-1}$ , and 4380 and 4420 $\text{cm}^{-1}$ . . . . .	10-11
10-3	Repeatability of the Position of the Water Vapor Singlet at 1014.2 $\text{cm}^{-1}$ Measured on November 10, 1993, December 22, 1993, and January 4, 1994 . . . . .	10-12
10-4	Measurement of Ambient Methane Concentration and Single Beam Intensity at 987 $\text{cm}^{-1}$ on November 17 and 18, 1993 . . . . .	10-13
10-5	Peak Area of 2998.8- $\text{cm}^{-1}$ Absorption Band of $\text{CH}_4$ and the 1014.2- $\text{cm}^{-1}$ Absorption Band of Water Vapor Measured on November 17-18, 1993 . . .	10-14

## Tables

Number		Page
6-1	Estimated Method Detection Limits for Selected Gases . . . . .	6-4
6-2	Minimum Usable Path Lengths . . . . .	6-7
7-1	Resolution Test Data . . . . .	7-6
7-2	Optimal Wave Number Region and Minimum Resolution . . . . .	7-16
7-3	Effect of the Number of Data Points on the CLS Analysis . . . . .	7-21
7-4	The Effect of Zero Filling on the CLS Analysis . . . . .	7-21
7-5	Effect of Noise on the CLS Analysis . . . . .	7-22
8-1	Maximum Values Over Which Response Can be Considered Linear and Associate Errors . . . . .	8-13
9-1	Partial Listing of Spectral Absorbance Data . . . . .	9-2

## Acknowledgement

There have been many helpful comments and reviews of this document that the authors have received from many people since the first edition was published. In particular, we would like to thank the following people. Dr. William Herget (now deceased) reviewed the original document and the contents of Chapter 8 in this version. Dr. Steven Levine of the University of Michigan provided much support and an excellent review of an earlier version. Dr. Peter Griffiths of the University of Idaho provided an excellent and comprehensive review of the second edition of this document.

Professor Konradin Weber of the Fachhochschule in Dusseldorf, Germany, and a doctoral candidate, Mr. Alexander Ropertz, provided us with the experimental verification of the nonlinear response discussed in Chapter 8. Professor Weber was also the first person to provide us with the information that the detection limits when measured from the actual data do not seem to change with path length.

Dr. William Phillips of SpectraSoft Technology in Tullahoma, Tennessee, provided us with much of the mathematical development and some of the software that allowed us to perform the calculations in Chapter 8.

The authors wish to thank two companies for their support in this endeavor. The MIDAC Corporation in Irvine, California, provided us with a bistatic system capable of acquiring data at  $0.5\text{-cm}^{-1}$  resolution. Kayser-Threde GmbH in Munich, Germany, provided us with a high-resolution instrument which gave us a great deal of insight about the need for higher resolution spectra.

We must also express our gratitude to Ms. Janet Parsons for editing this entire document again. We are convinced that Ms. Parsons has made this document a more readable document.

Finally, we wish to thank Dr. William McClenny for his support in the preparation of this work.

## Chapter 1

### Introduction

The Michelson interferometer has had a remarkable history in that new uses for the device have been found for more than 100 years. One use of the interferometer that has experienced rapid growth since the mid-1960s is as the main optical component of Fourier transform infrared (FT-IR) spectrometers. Although there have been several applications of FT-IR spectrometers to unique and difficult problems, the majority of FT-IR systems have been used to make qualitative measurements under controlled conditions in the laboratory. More than 20 years ago, some efforts were made to use the instrument for making quantitative measurements of atmospheric gaseous pollutants over extended open paths (Hanst 1970; Herget and Brasher 1979). Although these efforts were largely successful, they were overlooked by the great majority of people engaged in environmental monitoring. During the 1980s there was steady but slow progress in development of the technique. In the late 1980s, a revival of the technique occurred, initiated in part during a meeting of the Chemical Manufacturer's Association in Houston (Russwurm and McClenny 1990; Levine et al. 1991; McClenny et al. 1991), and today there is a large amount of developmental activity taking place. (See the bibliography in Chapter 10.)

This document describes the components of FT-IR monitors and is

intended to provide guidance for the FT-IR operator in field monitoring applications. It is a point of reference for further development and evaluation of FT-IR open-path monitors as field instruments.

#### 1.1 Overview of Document

A brief discussion of the FT-IR open-path monitor and its function is given in Chapter 2, along with a more in-depth description of the various components of the sensor. Chapter 3 includes the preliminary procedures for setting up the FT-IR instrumentation for monitoring. Chapter 4 is a discussion of background spectra, and Chapter 5 is a discussion of water vapor spectra. Chapter 6 presents guidance on how to set up the monitoring instruments within the physical constraints of a site. Chapter 7 presents experimental data that illustrate the effect of resolution and related parameters on the spectral data. Chapter 8 contains a discussion of the effects of the apodization function on the FTIR data using classical least squares analysis. It also discusses some of the effects due to ambient temperature. Chapter 9 describes the classical least squares analysis technique itself. It starts with a description of a linear regression for a dependent and one independent variable and proceeds to the multiple regression case using matrix notation. Chapter 10 contains quality control

and quality assurance guidelines, incorporating portions of an approved quality assurance plan, and includes selected QA data we collected over a recent one-year period. Chapter 11 is a glossary of terms, and Chapter 12 is a general bibliography of work that addresses FT-IR monitoring and the principles of FT-IR spectrometry.

Each chapter begins with a summary highlighting the primary contents of the chapter. This is followed by an introduction and overview of the chapter.

## 1.2 References

- Hanst, P.L. 1970. Infrared Spectroscopy and Infrared Lasers in Air Pollution Research and Monitoring. *Appl. Spectrosc.* 24:161-174.
- Herget, W.F., and J.D. Brasher. 1979. Remote Measurement of Gaseous Pollutant Concentrations Using a Mobile Fourier Transform Interferometer System. *Appl. Opt.* 18(20):3404-3420.
- Levine, S., H. Xiao, W. Herget, R. Spear, and T. Pritchett. 1991. Remote Sensing (ROSE) FTIR. In *Proceedings of the 1991 U.S. EPA/A&WMA International Symposium on the Measurement of Toxic and Related Air Pollutants*, Air & Waste Management Association, Pittsburgh, PA, pp. 707-711.
- McClenny, W.A., G.M. Russwurm, M.W. Holdren, A.J. Pollack, J.D. Pleil, J.L. Varns, J.D. Mulik, K.D. Oliver, R.E. Berkley, D.D. Williams, K.J. Krost, and W.T. McLeod. 1991. *Superfund Innovative Technology Evaluation. The Delaware SITE Study, 1989*. U.S. Environmental Protection Agency, Research Triangle Park, NC.
- Russwurm, G.M., and W.A. McClenny. 1990. A Comparison of FTIR Open Path Ambient Data with Method TO-14 Canister Data. In *Proceedings of the 1990 U.S. EPA/A&WMA International Symposium on the Measurement of Toxic and Related Air Pollutants*, Air & Waste Management Association, Pittsburgh, PA, pp. 248-253.



## Chapter 2

### The Fourier Transform Spectrometer

#### SUMMARY

The major topics discussed in this chapter are the following.

- The basic principles of FT-IR spectrometers
  - Resolution and throughput
  - Detectors and sources
  - Electronics and computer requirements
- The fundamental aspects of the interferogram, the Fourier transform, and single-beam spectra
- The optics used in long-path, open-path FT-IR monitors
  - Transfer optics, telescopes, and beam return optics
  - Monostatic and bistatic configurations
- Beer's law and data analysis procedures

#### 2.1 Introduction and Overview

This chapter describes the components of a complete FT-IR monitoring system, which include the following: the FT-IR spectrometer, the transmitting and receiving optics, the electronics, the computer, and the data output. The discussions in this chapter are based on the general configurations of instruments that are commercially available at the time of this writing. There are currently other manufacturers with instruments in the design or developmental stages.

It is not necessary to have a thorough understanding of the underlying physics describing how an FT-IR spectrometer

functions to obtain reliable data with a long-path, open-path FT-IR monitoring system. However, familiarity with the basic principles of FT-IR spectrometry is required if proper operational choices are to be made under varying field conditions. And, the better the operator understands the functions of the instrument, the more likely it is that reliable data will be produced. This chapter includes a description of long-path, open-path FT-IR monitors and an in-depth discussion of the various components of FT-IR spectrometers. The integral components of an FT-IR monitoring system, which include the interferometer, detector, IR source, transfer and beam-return optics, electronics, and computers, are described. The fundamental processes of FT-IR spectrometry, including

the interference phenomenon, generation of the interferogram, optical throughput, resolution, and the Fourier transform, are explained. A brief discussion of Beer's law and its application to the data analysis is provided. In addition to providing quantitative results, the relationships that are explained by Beer's law are important when estimating detection limits and determining optimum path lengths.

The heart of an FT-IR system is the interferometer. Most, but not all, commercial instruments use the Michelson interferometer. A detailed description of the Michelson interferometer is provided in Section 2.2. The trace of the output of the interferometer is referred to as an interferogram. The interferogram is the actual data produced by an FT-IR spectrometer and contains all of the information about the spectrum. However, the information contained in the interferogram is not in a form that is readily recognizable to most spectroscopists. To change the data into a form that is more easily interpretable, the raw data are converted into a spectrum (a plot of intensity versus wave number) by performing a Fourier transform on the interferogram. A computer system with the appropriate software packages is used to apply this and all other necessary mathematical functions to the data. Although the execution of these calculations is virtually invisible to the operator, a basic understanding of the principles involved is necessary to ensure that the optimum

parameters are used to collect and process the FT-IR data.

All quantitative data analysis in long-path, open-path FT-IR spectrometry is based on Beer's law. Beer's law states that for a constant path length, the IR energy traversing an absorbing medium diminishes exponentially with concentration. Mathematically, this is written as

$$I(\nu) = I_0(\nu)e^{-\alpha(\nu)CL}$$

where  $I_0(\nu)$  is the intensity of the incident beam,  $\alpha(\nu)$  is the optical absorption coefficient of the absorbing material (e.g., target gas) as a function of wave number ( $\nu$ ),  $C$  is the concentration of the target gas, and  $L$  is the path length.

Two primary configurations, monostatic and bistatic, are used to transmit the IR beam along the path, as described in Section 2.3. The monostatic system has both the IR source and the detector at one end of the path and a retroreflector at the other. The retroreflector returns the beam either along or collinear to the original path, which doubles the effective path length and thus the measured absorbance of the target gas. The bistatic system has the detector at one end of the path and the source at the other. This configuration minimizes the optical components that are required for open-path monitoring. However, in the bistatic system, the IR beam is limited to a single pass along the path. Both types of configurations are currently in use for environmental monitoring.

## 2.2 The Michelson Interferometer

The primary optical component in an FT-IR instrument is a Michelson interferometer. It is not generally necessary to have a fundamental understanding of how the interferometer functions to obtain reliable data with an FT-IR instrument. However, familiarity with some of the aspects of the interferometer is required if proper operational choices are to be made under varying field conditions. To that purpose, a brief discussion of the optics of the FT-IR instrument is included in this subsection. The following major topics are discussed: interference (Section 2.2.1), resolution (Section 2.2.2), throughput (Section 2.2.3), the detector (Section 2.2.4), and the IR source (Section 2.2.5).

A variety of devices have been used over the last 200 years to study interference phenomena. These devices are conveniently classified by the amount of four primary attributes that they exhibit: monochromatism, fringe localization, fringe production by division of wave front or by division of amplitude, and double or multiple beams. The interferometric device that today bears his name was first introduced by A. A. Michelson in 1881 (Michelson 1881). It is the most famous of a group of interferometers that produce interference fringes by the division of amplitude. Four years after Michelson introduced the interferometer, it was shown that the Fourier transform of the interferogram was the original spectrum or intensity as a function of wavelength. The Michelson interferometer

has been used to define and measure the standard meter, to measure the angular separation of binary stars, and to provide the experimental data for one of the four cornerstones of relativity theory. During recent times, the Michelson interferometer has been used successfully to measure the concentrations of various chemicals that absorb energy in the IR portion of the electromagnetic spectrum. (See Chapter 10, Bibliography.) It is currently being developed as an instrument to make similar measurements over extended open paths, and it is in this context that the interferometer is discussed here.

A schematic of the simplest form of a Michelson interferometer is shown in Figure 2-1. It consists of a beam splitter and two mirrors, one of them movable. The figure also shows an arrangement for the light source and the detector. For the most accurate use, the two mirrors must be kept perpendicular to one another. One of the two mirrors moves along the optic axis. During this motion the perpendicularity cannot change. This requirement can represent a stringent limitation for the mechanisms involved with the motion. The light incident on the beam splitter should be collimated, because uncollimated light gives rise to poor resolution.

### 2.2.1 Interference

This section is presented for completeness and because there seems to be some confusion as to how the interferogram arises. It is somewhat

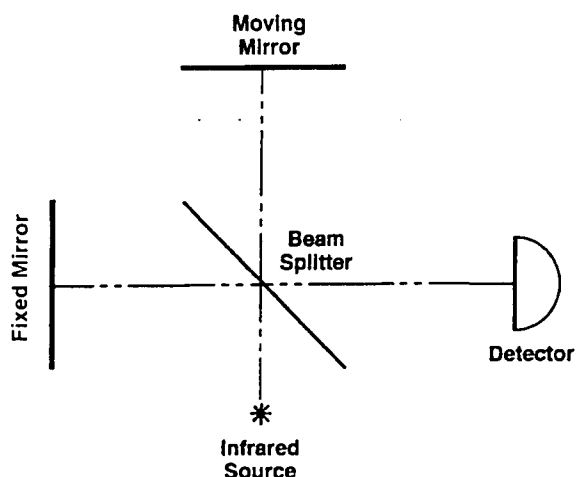


Figure 2-1. A Schematic of the Simplest Form of a Michelson Interferometer.

mathematically rigorous and can be omitted without jeopardizing the ability of the operator to obtain reliable FT-IR data.

Interference is the underlying physical phenomenon that allows a Fourier transform instrument to obtain spectrometric data. The interference phenomenon cannot be physically explained by the simple addition of the intensities of two or more optical beams. The amplitudes of the individual interfering beams must be added according to the principle of superposition, and the total intensity must be calculated from that result. Interference phenomena are linear in amplitude. The principle of linear superposition, which is operating here, follows directly from Maxwell's equations and the fact that these equations are linear differential equations. To arrive at the basic equation that describes how the Michelson works, consider the arrangement of Figure 2-2. A monochromatic electromagnetic plane wave is incident on a device at *A* that divides its amplitude into two

components. After the division, the individual beams traverse a medium along different paths and are somehow recombined at a point *P* in space. On arrival at point *P*, the two beams, which need not be collinear, have the following amplitudes.

$$A_1 = A_0 e^{i(\omega t - 2\pi n T_1 / \lambda)}$$

$$A_2 = A'_0 e^{i(\omega t - 2\pi n T_2 / \lambda)}$$

The two  $A_0$  terms are the amplitudes of the individual beams, the  $\omega$  is the angular frequency of the radiation,  $n$  is the index of refraction of the medium, and the two  $T$  terms are the physical path lengths that each beam has traversed. The product  $nT$  is called the optical path length that the beam has traveled. At point *P*, where the two beams are recombined, the total amplitude is the sum of these terms. The intensity is then given by the product of this sum and its complex conjugate. Thus the intensity at point *P* is given by Equation 2-1.

$$I(P) = A_0 A_0^* + A'_0 A_0'^* + A_0 A_0'^* e^{i[2\pi n(T_2 - T_1) / \lambda]} + A_0'^* A_0 e^{-i[2\pi n(T_2 - T_1) / \lambda]} \quad (2-1)$$

The first two terms are the intensities of the original two beams, and the last two terms are called the interference terms. When the amplitudes  $A_0$  and  $A_0'$  are equal, they can be combined.

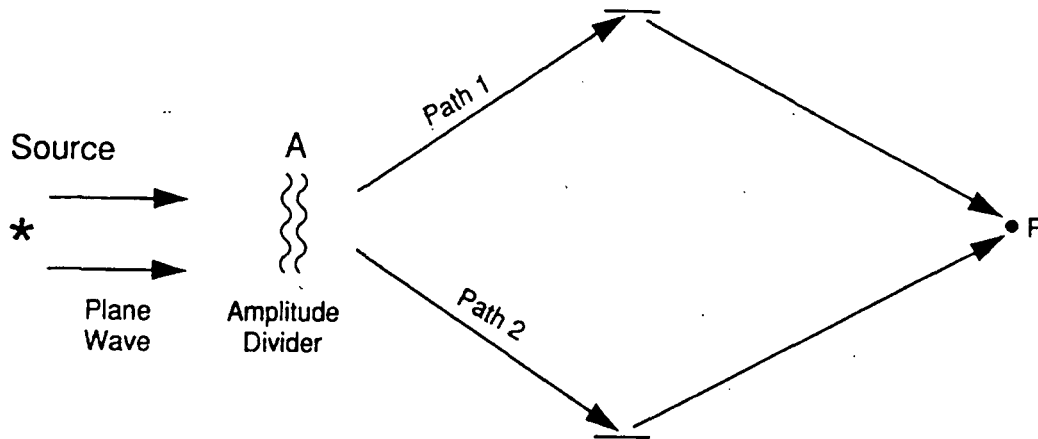


**Figure 2-2. Schematic of Interference Created by Division of Amplitude.**  
 Path 1 has physical length  $T_1$ , and Path 2 has physical length  $T_2$ .

By using the relation  $2\cos x = e^{ix} + e^{-ix}$ , the intensity at point  $P$  is given by Equation 2-2.

$$I(P) = 2I_0 \left\{ 1 + \cos \left[ 2\pi n (T_2 - T_1) / \lambda \right] \right\} \quad (2-2)$$

Here  $I_0$  is the intensity of either beam. Thus as the difference of the path length,  $T_2 - T_1$ , changes, the intensity at point  $P$  can vary from 0 to  $4I_0$ . The fact that  $I$  can be  $4I_0$  does not violate the conservation of energy law. There is no physical requirement that the intensity at every point in space be  $2I_0$ . The requirement is that the interference term averaged over space must be zero (Rossi 1957).

When a plane monochromatic wave is incident on the beam splitter of the Michelson interferometer, the amplitude ideally is evenly divided along each leg. At any position of the moving mirror, the detector output is proportional to the integral of the intensities over wavelength, and this

recording is called the interferogram. From Equation 2-2, it is seen that at zero path ( $T_2 - T_1 = 0$ ) difference, the cosine term is 1 for all wavelengths. Thus for all wavelengths, the intensity is  $4I_0$ , and the output of the detector is large compared to any other mirror position. This is quite noticeable in the interferogram and is commonly called the center burst.

This center burst does not appear when the radiation is monochromatic. Figure 2-3 shows how the center burst builds as the wave number range is expanded to include more wavelengths. The interferograms in this figure were calculated from Equation 2-1 in the following way. All the wave numbers have the same intensity and add incoherently. The wave number value was stepped in increments of  $0.1 \text{ cm}^{-1}$ . The retardation (actually, the term  $T_2 - T_1$ ) was taken in increments of the wavelength of a He-Ne laser. At each position of the mirror the proper phase for each wave

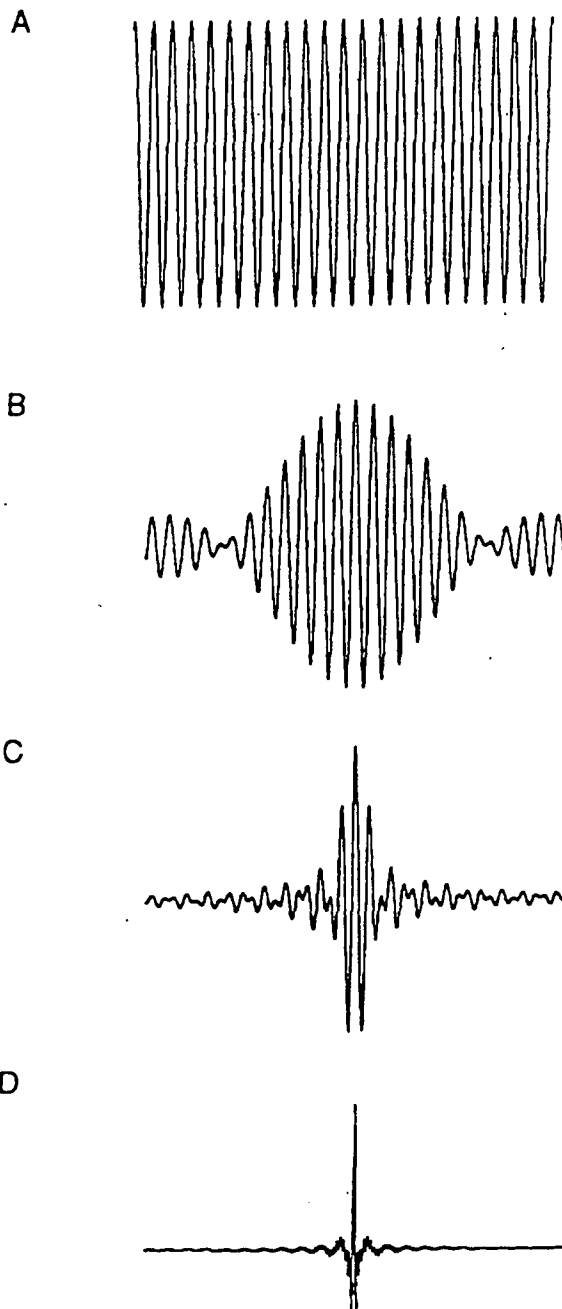


**Figure 2-3. Center Burst Increasing as the Wave Number Range Expands.**

number was used to calculate the intensity, and then the intensities were added. The interferograms were actually calculated for 6000 incremental movements of the mirror; however, only a portion of the data is shown for clarity. The interferograms in Figure 2-3

are for (A) a 2-cm<sup>-1</sup> range, (B) a 50-cm<sup>-1</sup> range, (C) a 500-cm<sup>-1</sup> range, and (D) a 3500-cm<sup>-1</sup> range. The two interferograms shown in Figure 2-4 are for a range of 3500 cm<sup>-1</sup>, but curve B has a 1500 K blackbody radiation curve superimposed on it, and it appears quite similar to the interferogram actually recorded by the FT-IR spectrometers.

Equation 2-2 shows that as the mirror moves, the path difference causes a modulation of the intensity at each wavelength. The modulation can be used to advantage in open-path FT-IR monitors. For example, if the IR beam traverses the interferometer before it is sent along the open path, any background radiation entering

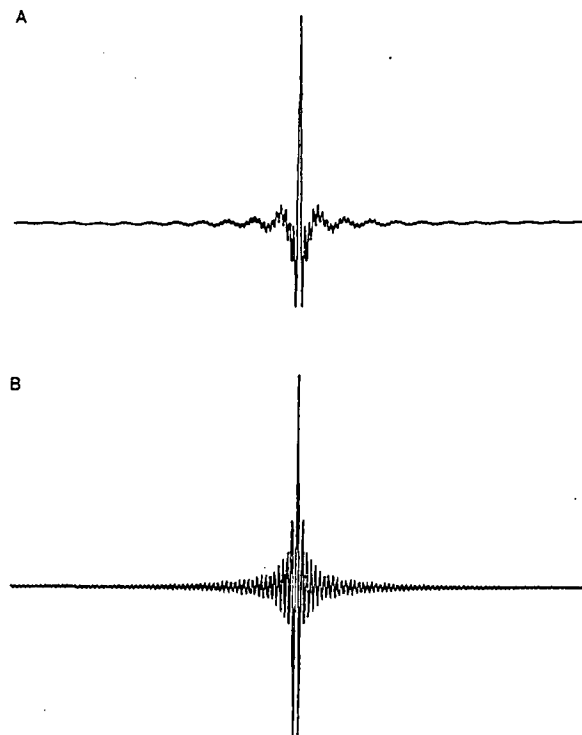


**Figure 2-4. Interferograms for a Range of 3500 cm<sup>-1</sup>. Interferogram B has a 1500 K blackbody radiation spectrum superimposed on it.**

the system from the surroundings is not modulated and will not be processed by the electronics. However, a portion of this unmodulated light will still be incident on the detector and in extreme situations could cause the detector to become saturated. Therefore, it is prudent to avoid setting the instrument up along a path that includes bright (hot) IR sources.

### 2.2.2 Resolution

The resolution of an instrument determines how close two absorption features can be and still be separated enough for analysis. There are several criteria for this instrument parameter, but the one most often used for the FT-IR instrument is described below. Equation 2-2 shows that all wavelengths have a maximum and are in phase with one another at zero path difference. The most common definition of resolution for the FT-IR spectrometer states that two absorbing features centered at wavelengths  $\lambda_1$  and  $\lambda_2$  will be resolved if the mirror moves at least to the point where these two wavelengths are again in phase. To determine when this occurs, the following example may be considered. If only two spectral features situated at  $\lambda_1$  and  $\lambda_2$  make up the spectrum, then the interferogram is made up of two spectra, each described by Equation 2-2. The result of adding these two spectra is shown in Figure 2-5 and is given by Equation 2-3.

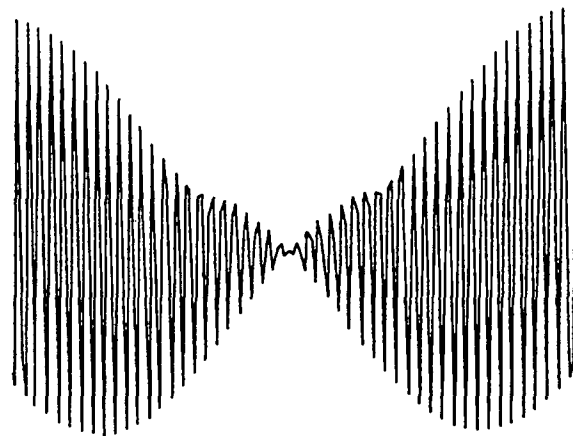


**Figure 2-5. Interferogram of Two Cosine Waves vs.  $\Delta T$ .** The wavelengths differ by  $10 \text{ cm}^{-1}$ . The minimum occurs when the two waves are  $180^\circ$  out of phase.

$$I(P) = 4I_0 \left\{ 1 + \cos \left[ \pi n \Delta T \left( \frac{1}{\lambda_1} - \frac{1}{\lambda_2} \right) \right] \cos \left[ \pi n \Delta T \left( \frac{1}{\lambda_1} + \frac{1}{\lambda_2} \right) \right] \right\} \quad (2-3)$$

The second cosine term produces a high-frequency signal that is modulated by a low-frequency signal described by the first cosine term. It is the first term that is of interest when determining the resolution of the system. The signal is a maximum when the argument of this cosine term is  $2N\pi$ , where  $N = 0, 1, 2, \dots$ . Thus, setting  $n$  the index of refraction equal to 1, the first time that the two wavelengths are in phase after the center burst is when  $N = 1$ , so that

$$\pi \Delta T (1/\lambda_2 - 1/\lambda_1) = 2\pi$$

This implies that

$$\Delta T = 2 / (1/\lambda_2 - 1/\lambda_1)$$

However, the term in the denominator is the difference in the wave numbers of the absorption peaks, so that  $\Delta T = 2/\Delta v$ . Thus, if the operator desires a resolution of  $0.5 \text{ cm}^{-1}$ , the optical path difference must be 4 cm. Because the beam traverses the path in the interferometer twice, the actual motion of the mirror must be only 2 cm. It should be noted here that this is an idealized result. The fact that the interferogram is first truncated and then apodized changes this result somewhat (Marshall and Verdun 1990; Beer 1992).

The question of what resolution should be used for a specific data collection task is not addressed in this section. It is discussed in more depth in Chapter 7 and Chapter 8. The answers to the resolution questions are specific to the gases to be monitored and the effects of water vapor in their regions of absorbance. At the present time, each monitoring situation must be considered separately.

### 2.2.3 Throughput

The throughput of an optical system is defined as the product of the area of an aperture  $A$  and the solid angle  $\Omega$  of the light beam at that aperture. This quantity is theoretically a constant throughout the system, so that once it is defined for an aperture it is known for all apertures. For small angles, the solid angle of the beam can be shown to be equivalent to the product  $\pi\theta^2$ , where  $\theta$  is the half angle of the field of view of the instrument. It can be shown that the throughput is related to the  $f\#$  of the system by recognizing that  $\theta = 1/(2f\#)$ , so

that the throughput is equal to  $A\pi[1/(4f\#)]^2$ . With FT-IR instruments, the selection of the system  $f\#$  is generally a compromise. An important consideration is the solid angle of the beam as it traverses the interferometer. A portion of the beam traversing the interferometer at a large angle will travel over a longer path through the interferometer, and a beam traversing at a smaller angle will travel over a shorter path. This angular dispersion tends to degrade the resolution of the instrument, because energy at the same wavelength appears to the interferometer as though it covers a range of wavelengths. Smaller  $f\#$ s are at first attractive because they indicate that a smaller aperture can be used. However, small  $f\#$ s imply large solid angles and therefore a loss in resolution. The manufacturers of these instruments have taken this into account in the instrument design, but nevertheless the aperture size is fixed, and once a specific instrument is purchased, there is little, if anything, the operator can do to change the throughput.

### 2.2.4 The Detector

The detector in most FT-IR instruments used for monitoring atmospheric pollutant gases is a semiconductor device made of mercury, cadmium, and telluride, commonly called an MCT detector. There are three modes of operation for this device, as a photovoltaic device, as a photoelectromagnetic device, and as a photoconductive device. The MCT photoconductive detector is the one most often used in the FT-IR instrument. This device converts a beam of



photons to an electrical current that can be measured. In addition to the spectral region that the detector responds to, the two most important parameters of the detector are the noise equivalent power (NEP) and the sensitivity of the detector in terms of a quantity called  $D^*$  (pronounced "Dee Star"). For an MCT photoconductive device, the spectral response ranges from 2 to 20  $\mu\text{m}$ , or from 500 to 5000  $\text{cm}^{-1}$ . The NEP is given in terms of  $\text{W}/(\text{Hz})^{1/2}$ . For the detectors used in FT-IR instruments, this parameter has a value of about  $5 \times 10^{-12}$ . The user should be aware that this parameter represents a measure of the inherent noise in the detector and that small numbers are better than large numbers. The  $D^*$  is a measure of the sensitivity of the detector and has units of  $\text{cm}(\text{Hz})^{1/2}/\text{W}$ . This number is actually defined as the ratio of the square root of the detector area to the NEP, or  $D^* = \sqrt{A}/\text{NEP}$ . For the MCT photoconductive detectors, this number is about  $5 \times 10^{10}$  at 10  $\mu\text{m}$ . Here, larger numbers are better. However, there is little that the operator can do about the magnitude of these parameters once the instrument is purchased. But if the detector has to be replaced, some acceptance criteria for the NEP and the  $D^*$  should be specified.

There are, in general, two types of MCT detectors available, wide band and narrow band. Each has somewhat different characteristics. Wide band MCT detectors cut off at around 500  $\text{cm}^{-1}$ , whereas the narrow band MCT detectors cut off near 600  $\text{cm}^{-1}$ . For long-path measurements the region below 722  $\text{cm}^{-1}$  is nearly opaque because of absorption by  $\text{CO}_2$  in the

atmosphere, so a wide band detector does not offer any real advantages. Also, the  $D^*$  for the narrow band detector is 5 to 10 times higher than that for the wide band detector. There is also an indium antimonide (In-Sb) detector that can be used in the higher wave number region with advantage. One particular application for using this type of detector is the measurement of HF.

An important requirement for the detectors in FT-IR monitoring systems is that they must be cooled to operate properly. Liquid nitrogen temperatures (77 K) allow optimum operation of these detectors. Currently, two techniques are used to cool the detector. The first is to place the detector in a Dewar that uses liquid nitrogen as a refrigerant. For this mode, a supply of liquid nitrogen must be available for use in the field, and the operator must fill the Dewar periodically. This has not been a major problem in the past, as the liquid nitrogen requirement is only a few pints per day of operation. The second technique to achieve cold temperatures is with a cryogenic cooler, such as a Stirling engine, a Joule-Thompson cooler, or a closed-cycle helium refrigeration system. In the Stirling engine, the heat is exchanged through a wall from the enclosure to cool the gas. Currently, the major problems with this cooling device is the mean time between failures is too short, and these coolers seem to add noise to the spectra. One-half year of continuous operation is about the maximum that can be expected. If unattended operation is a necessity, the Stirling engine is one choice. The Joule-Thompson cooler forces dry

nitrogen through an orifice, after which it expands and cools. This device uses nitrogen, which has to be of high purity, at the rate of about one 300 size cylinder in 40 h of operation. Other options for unattended operation are the use of larger detector Dewars with longer hold times or devices that automatically refill the detector Dewar.

### 2.2.5 The IR Source

All IR sources that are available today for use with the FT-IR monitor are heated elements that are open to the atmosphere. They are resistive devices that radiate approximately as black body radiators. These devices operate at a color temperature from 1200 to 1500 K. The Wien displacement law states that the product of the wavelength of maximum power output and the temperature of the source,  $\lambda_{\max}T$ , is a constant equal to  $0.2987 \text{ cm K}^{-1}$ . This indicates that there is an inverse relation between peak wavelength and source temperature. Planck's radiation law shows that there is more energy at all wavelengths for hotter sources. The ideal would be a source that is at about 3000 K, so it would have a peak at about  $1.1 \mu\text{m}$ . The materials that are necessary to make such a source have not been available until now.

Perhaps the most detrimental characteristic of the available sources is that they are large compared to the focal length of the collimating optics. From geometrical optics, it is clearly seen that the beam can never be better collimated than the angle

that the source subtends at the collimating optics (lens or mirror). Thus, all available FT-IR spectrometers have beam divergences that are too large for the rest of the optics. This means that retroreflectors or receiving optics are overfilled, and much of the initially available energy is lost. Ultimately, this divergence restricts the path length that can be used to advantage. Perhaps as further developments occur, a small hot source will be developed that will minimize this difficulty.

## 2.3 Transfer Optics, Telescopes, and Beam-Return Optics

There are two primary geometrical configurations available for transmitting the IR beam along the path. One is a bistatic system (Figure 2-6); the other a monostatic system (Figure 2-7). The monostatic system has both the IR source and the detector at the same end of the path, whereas the bistatic system has the detector at one end of the path and the source at the other. In the bistatic system, the optical path length is equal to the physical path length, whereas in the monostatic configuration, the optical path length is twice the physical path length. In this document, we always refer to the optical path length. The reflecting optics for a bistatic FT-IR monitoring system are relatively straightforward (see Section 2.3.1), whereas the optics in a monostatic system may include one or more telescopes, an additional beam splitter, and return-beam optics. The possible configurations for a monostatic system are described in Section 2.3.2.

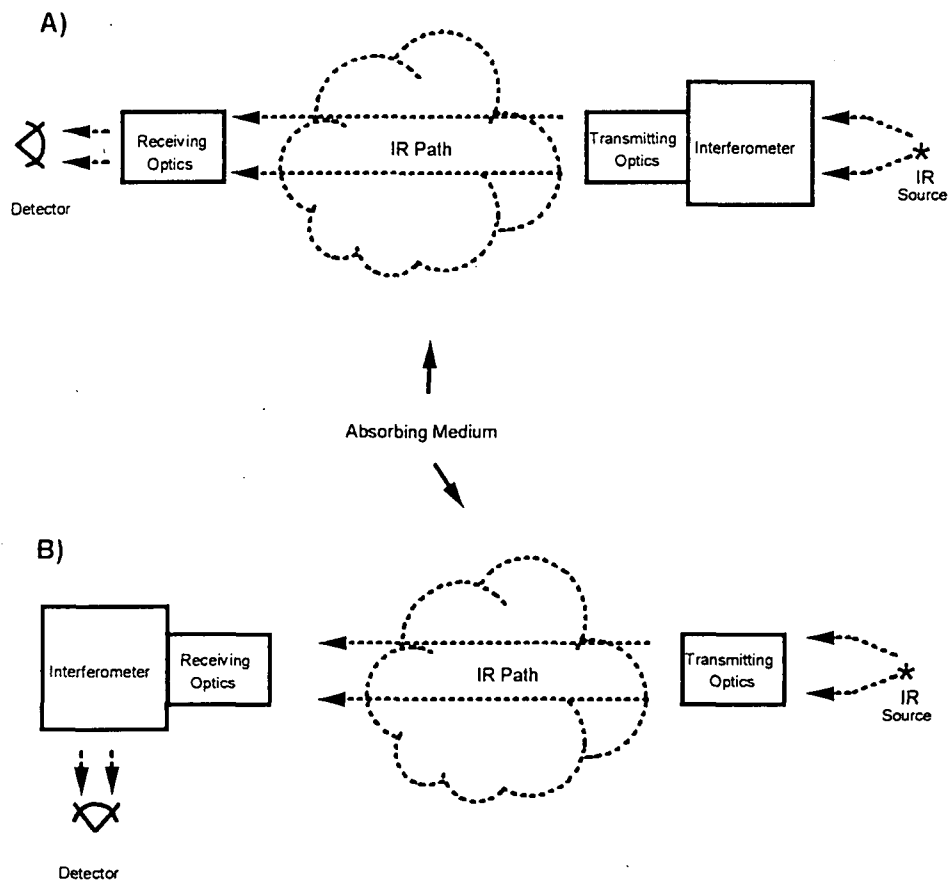


Figure 2-6. The Bistatic Configuration.

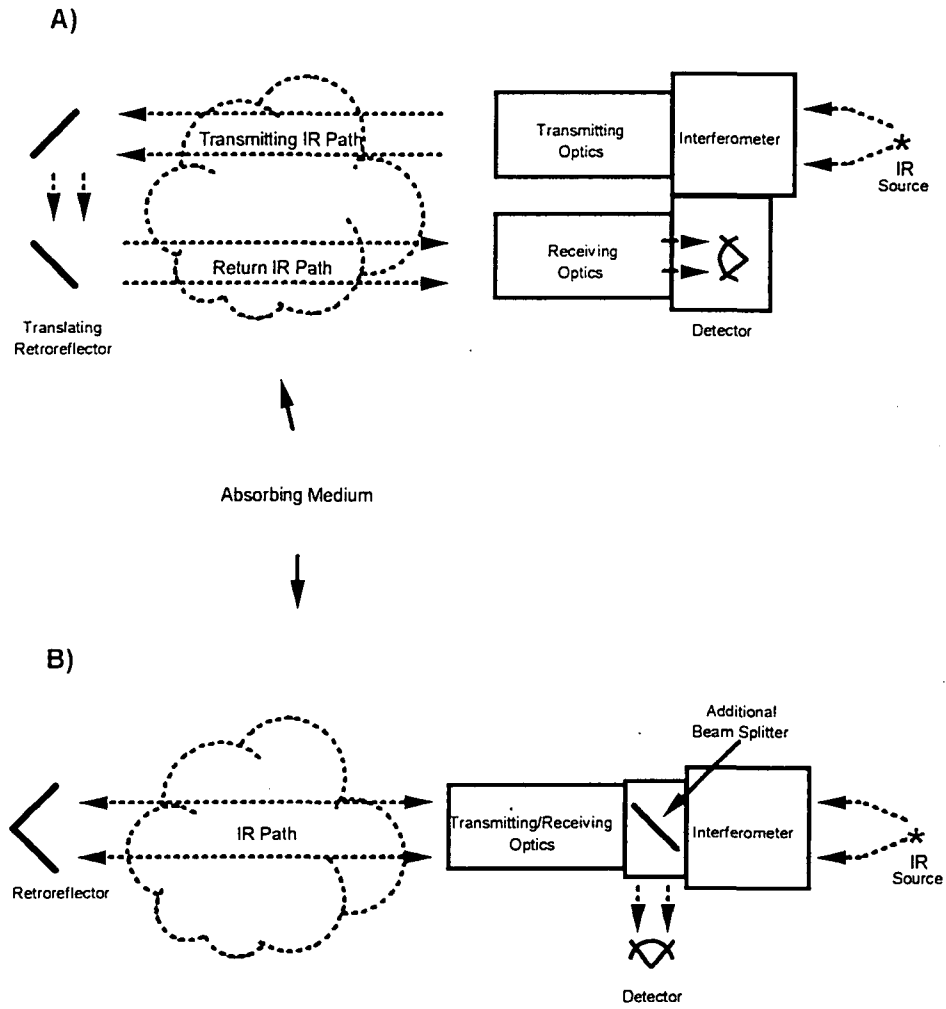


Figure 2-7. The Monostatic Configuration.

There are several types of telescopes that could be used to transmit and collect the IR beam. Those in current use are the Cassegrain and the Newtonian telescopes. They are optically equivalent, and the only difference is the placement of the diagonal mirror that removes the beam from the telescope. In the Cassegrain, the beam exits from the end of the telescope, and for the Newtonian it exits from the side. Optically, the number of reflections is the same, and other things being equal, the reflection losses are also essentially the same. The geometrical configuration for the whole instrument is slightly different for these two designs. In one, the overall package enlarges vertically, whereas in the other it grows longitudinally. These are minor points as far as instrument operation is concerned.

In most cases, the beam is expanded before it is sent along the path, and in principle there are essentially no size limits. The physical quantity that is of interest to the operator is how much of the IR beam is absorbed by the gases of interest. This is, in general, very small (about 1 part in a 1000). This fact is not changed by expanding the beam. In general, beam expansion allows more energy to be transmitted along the path, thereby increasing the overall signal-to-noise ratio (S/N). There are, of course, practical limitations to the size of the optics that can be accommodated.

As a rule, the optics in either system are reflecting optics rather than refracting optics to avoid transmission losses. Once the IR energy has been collected, the optics

must reduce the size of the beam so that it can pass through the system to the detector without vignetting and also to set the solid angle of the beam so that the resolution remains acceptable.

### 2.3.1 Bistatic System

The bistatic configuration minimizes the optical components that are required for open-path monitoring. At the source end of the path there must be some method for collimating the beam. This can easily be done with a mirror shaped as a parabola or one of the other conic sections. At the receiving end of the path, a collector, similar in design to the collimator, may be used to transfer the beam to the interferometer and the detector. In commercially available instruments, the diameter of the collector generally is the same as that of the transmitter, although there is no optical necessity for this choice.

There are two configurations that can be used for bistatic systems. One configuration places the IR source, interferometer, and transmitting optics at one end of the path and the receiving optics and detector at the other end (Figure 2-6A). The advantage of this configuration is that the IR beam is modulated along the path, which enables the unmodulated background radiation to be rejected by the system's electronics.

The other configuration places the IR source and transmitting optics at one end of the path and the receiving optics, interferometer, and detector at the other end

of the path (Figure 2-6B). This is the more common configuration of bistatic systems in current use. The main drawback to this configuration is that the IR source is not modulated before it is transmitted along the path. Therefore, the system has no way to distinguish between the active IR source and the background IR radiation.

Still another version is being tested at the present time. In this bistatic system the light source is modulated by some mechanical means. This configuration requires a feedback loop to the interferometer (via radio link or optical cable) so that proper phasing can be obtained.

Because the IR radiation makes only a single pass through the optics, less of the radiation is lost in bistatic systems. Also, this makes the systems more amenable to passive measurements, such as emission measurements or absorption measurements with a natural background hot source. For various reasons, this single pass through the absorbing medium is not seen as a severe drawback.

Ambient monitoring in confined areas or rough terrain may pose certain logistics problems with a bistatic system. One is that this mode of operation requires two power sources, one at each end of the path. Another is that there is only one pass through the absorbers. The absorbance for most gases of interest is very small, and for short paths, as those encountered with plumes, a single pass through the gas may be insufficient.

### 2.3.2 Monostatic System

There are currently two techniques in use for returning the beam along the optical path when the monostatic mode is used. One is to set up an arrangement of mirrors that translates the beam slightly for its return path, and another is to place a retroreflector array at the end of the path. These two configurations are optically equivalent.

In the first configuration, an optical system is placed at the end of the path that translates the IR beam slightly so that it does not fold back on itself (Figure 2-7A). The receiving end then has a second telescope slightly removed from the transmitter with the detector at the primary focus. This technique circumvents a possible objection to the second monostatic configuration.

The second configuration for the monostatic monitoring mode uses the same telescope for the transmitting and the receiving optics and uses a retroreflector array at the end of the beam (Figure 2-7B). A retroreflector is an arrangement of mirrors that reflects the beam so that the incident and reflected directions of propagation are collinear but opposite to one another. It is made of three reflecting surfaces that are mutually orthogonal, such as the floor and two adjacent walls of a room. It is often assumed that after reflection the beam returns along the same path over which it was transmitted. That is true only in a gross sense because if the beam is small compared to the reflecting surfaces, a measurable translation takes place, and there is always

an inversion and a reversion of the beam. In order to transmit and receive with the same optics, a beam splitter must be placed in the optical path. An objection to this configuration is that the IR energy must traverse this beam splitter twice, once on the transmitting end and once on the receiving end. The most effective beam splitter transmits 50% of the light and rejects the other 50%. Thus, in two passes, the transmission is only 25% of the original beam. Because this loss affects the S/N, it may be a significant drawback of this configuration of the monostatic mode.

Because of the design of the orthogonal mirror retroreflector, it is quite insensitive to small motions such as those caused by a wind. Retroreflector arrays are also very easy to align with the transmitting-receiving telescope, and a few degrees of misalignment will pose no problem to the operator. This does not seem to be the case with the spherical mirror configuration. Although this arrangement is also easy to align, it seems somewhat more sensitive to a small error.

## 2.4 The Electronics

An in-depth discussion of the electronics of the FT-IR system is beyond the scope of this document. However, some points that are of interest to the operator are covered. The interferogram is in the form of intensity versus position of the moving mirror. As the mirror moves, the detector measures a varying intensity, and this signal is first amplified and then sent to an analog-

to-digital (A/D) converter for digitization. There are two important features that pertain to this digitization process.

The first concerns the dynamic range of the signal, which can actually be too large. There must be enough resolution in the A/D converter so that the least significant bit can always be reserved for recording the noise in the system. If this not the case, the spectrum derived by performing the Fourier transform on the interferogram will be distorted. For this reason, most commercially available instruments today use a 16-bit A/D converter. Higher range converters exist but the trade-off comes in the noise and the speed of the device. So a 20-bit converter may not offer much of an advantage over a 16-bit converter. This means that if the noise is recorded on the least significant bit, the highest signal that can be recorded is a factor of  $2^{15}$  above the noise. This is not really as high as it seems. For example, if the noise is about  $1 \mu\text{V}$ , the largest signal that can be recorded is about 0.5 V.

The second feature concerns the amount of data that has to be recorded in digital form so that the original waveform can be reproduced. There is some relation between the rate at which a signal varies and the number of sampling pulses that are needed to reproduce it exactly. The sampling theorem from modern communication theory, sometimes called the Nyquist theorem, states that at least  $2f_m$  equally spaced samples are needed each second to reproduce the waveform without distortion. Here  $f_m$  is the maximum frequency

component that is contained in the original waveform.

As the mirror of the Michelson interferometer moves, each wavelength is modulated at a frequency that is related to the velocity of the mirror and the particular wavelength. Since the light must traverse the distance from the beam splitter to the mirror twice (down and back) in any one cycle, 2 times the actual velocity can be used for the determination of the frequency range to which the electronics must respond. If the mirror moves at a speed of 1 cm/s and the wavelength range is from 2.5  $\mu\text{m}$  to 20  $\mu\text{m}$ , then the frequency range is from 8000 Hz to 1000 Hz. Thus, according to the Nyquist theorem, the digital sampling rate must be at least 16000 equally spaced samples per second.

There is also a need for measuring the position of the mirror and for signaling to the electronics when to record data. This is done by using an He-Ne laser. The laser beam is sent through the interferometer and modulated in the same way as all other wavelengths are. The amplifier output is capacitively coupled to the rest of the electronics so that the He-Ne interferogram is an ac signal with negative and positive parts. The zero crossings of this ac signal are sensed, and the instrument records a data point at the zero crossings. Electronically, zero crossings are easier to detect than maxima or minima because of the sign change.

## 2.5 The Computer

The final requirement for an FT-IR system is a computer. This discussion is meant to be a discussion of the minimum requirements only.

The data storage requirements depend on the resolution used, and the capacity must be fairly large if the interferogram is stored. This requires about 100 kilobytes for each interferogram recorded at 1-cm<sup>-1</sup> resolution, and some means for archiving the data must be available. Most software packages that are currently available are written for Windows'95, so a computer with a Pentium processor is required. For ordinary field work at monitoring sites such as Superfund sites or waste sites, the ideal system seems to be either a single computer with the ability to operate in both foreground and background modes or two computers—one to control the instrument and to record the data and the other, a much more powerful machine, to be used for data analysis.

In addition to the computer hardware, a software package is required that will control the FT-IR system and record either the interferogram (preferably) or the single-beam spectrum (Section 2.7.4) produced by the Fourier transform performed on the interferogram. There is currently one generic software package that can be configured for any of the commercially available FT-IR systems. Other FT-IR systems use proprietary software for data collection. In addition to data collection, the software



should also provide some means for data analysis. This is discussed further in Section 2.6.5.

## 2.6 The Data Output

This section contains a discussion of the interferogram generated by the FT-IR system, the Fourier transform that is applied to the interferogram, and the single-beam spectrum into which the interferogram is transformed. The data reduction process, starting with the interferogram and ending with the unknown gas concentration, is described. A discussion of Beer's law of how energy diminishes as it traverses an absorbing medium is presented first.

### 2.6.1 Beer's Law

The fundamental physical law that is quoted as the basis for all FT-IR data analysis is Beer's law (Beer 1852). It states that, for a constant path length, the intensity of the incident light energy traversing an absorbing medium diminishes exponentially with concentration. Mathematically, this is written as

$$I(\nu) = I_0(\nu)e^{-\alpha(\nu)CL} \quad (2-4)$$

where  $I_0(\nu)$  is the intensity of the incident spectrum,  $\alpha$  is the optical absorption coefficient of the gas and is a function of the wave number  $\nu$ ,  $C$  is the concentration of the gas, and  $L$  is the path length. There are many possible sets of units for these quantities that are variously used by the workers in

FT-IR open-path monitoring. Whatever the set chosen, it must be noted that the product  $\alpha CL$  must be a unitless quantity. Thus, if the absorption coefficient has units of  $(\text{cm} \cdot \text{atm})^{-1}$ , the concentration must be in atmospheres and the path length must be in centimeters. One primary difficulty that confronts the user of FT-IR open-path monitors is determining the quantity  $I_0$ . This is discussed in detail in Chapter 4, Background Spectra.

The mathematical functional form of Beer's law explains many physical phenomena. These include atmospheric pressure as a function of altitude, thermal expansion of metal rods, radioactive decay, and the electrical discharge of capacitors, to name but a few. Although there is no physical basis for doing so, in the field of optical spectroscopy, this functional form is often stated by using logarithm to the base 10. The available analysis software also uses logarithms to the base 10. To understand how the change is to be made, consider the following.

The fundamental formula is  $Y = a^X$ . The problem is to solve this equation for the quantity  $X$ , which is the power that  $a$  must be raised to obtain  $Y$ . To solve this, the concept of logarithms is introduced so that  $\log_a(Y) = X \log_a(a)$ . This is read as "the logarithm of  $Y$  to the base  $a$  equals  $X$  times the logarithm of  $a$  to the base  $a$ ." By definition,  $\log_a(a) = 1$  so that

$$X = \log_a(Y)$$

Logarithms can be determined by using any number for the base, but only two are commonly used in the physical sciences. They are the base 10 and the base  $e$ . The number  $e$  is defined as the limit of  $(1 + 1/N)^N$  as  $N$  goes to infinity. The number  $e$  occurs naturally in mathematics, and particularly it occurs naturally in equations like Beer's law. The question is then how must Beer's law be written to account for the change to base 10.

The logarithmic form of the equation  $Y = a^X$  can be written in any other base  $b$  such that

$$\log_b(Y) = X \log_b(a)$$

Solving this for  $X$  gives

$$X = \log_b(Y) / \log_b(a)$$

Substituting this  $X$  into the original equation gives

$$\log_b(Y) = \log_b(Y) \log_b(a)$$

In terms of the bases  $e$  and 10, this is written as

$$\log_{10}(Y) = \log_{10}(e) \log_e(Y)$$

Historically, natural logarithms are written by using the prefix  $\ln$ , while logarithms to the base 10 are written with the conventional  $\log$  as a designator. Logarithms to all other bases also use the convention  $\log$  as nomenclature, but then the actual base is specified as a subscript.

If the power of 10 is used, Beer's law is written as follows.

$$I(\lambda) = I_0(\lambda) 10^{-\ln(10)\alpha(v)CL}$$

For convenience, the exponential term in this expression is defined as the absorbance. The mathematics given here is transparent to the operator and of little significance throughout the remainder of this document. However, it should be noted that when absorbances are given as numerical values, the logarithm to the base 10 has been used.

Although most FT-IR workers cite and discuss Beer's law, it is not directly used. The absorption coefficient is generally not known. One implication of Beer's law that is used is the concept of reciprocity. That is, if the concentration diminishes by a factor of 2 but the path length increases by a factor of 2, the measurement will yield the same results. This is not always true, and it is generally accepted that if the quantity  $\alpha CL$  becomes larger than about 0.1, the concept of reciprocity is no longer valid.

Beer's law has been restated so that it includes many applications, and, as restated, the law has assumed several other names, as the Lambert-Beer law or the Bouguer-Lambert-Beer law, but these other names are not correctly used. Beer wrote the law for a purpose other than the way it is used today. When Beer published his original work in 1852, he was conducting experiments designed to measure the absorption of various materials that were then being used in the field of photometry.

His entire endeavor was directed toward investigating the effects of the thickness of a material. He therefore did not write the law in terms of concentration, nor is there any evidence that he considered the effects of a changing concentration. The law as used today, with concentration as an explicit term in the exponent, seems to have first been published by B. Walter almost 40 years after Beer's original work (Walter 1889).

## 2.6.2 The Interferogram

The primary data produced by an FT-IR instrument is the interferogram, and it is the piece of data that should be recorded. However, the mechanics of the FT-IR instrument itself can alter the appearance of the interferogram, and this influence must be accounted for during data analysis. Two of these effects, truncation and phase shift, are discussed below.

### 2.6.2.1 Truncation

As discussed earlier, the interferogram is the intensity measured by the detector as a function of the position of the moving mirror. It contains all the information about the spectrum that is familiar to most operators. In actual operation, the mirror in the interferometer moves, at most, a few centimeters and stops and then returns to its original position. This finite movement truncates the interferogram at each end. It can be shown that this truncation actually limits the sharpness of the absorbing features that are of interest to the experimentalist. This is analogous to creating a square wave

from a series of sine and cosine functions. There it is seen that the higher frequency components sharpen the edges of the square wave. The situation with the FT-IR data is identical. The information at the ends of the interferogram is really information about the high-frequency components. A simple truncation (stopping the mirror motion after a certain distance) behaves mathematically as though the interferogram were multiplied by what is called a boxcar function. That is, the interferogram is multiplied by a function that is 1 in a region from mirror position 1 to mirror position 2 and is zero elsewhere. The effect of this multiplication is to broaden the spectral line features. Truncation also causes a phenomenon called ringing in the wings of the spectral features. That is, the truncation of the interferogram adds oscillations into the wings of the spectral features. These unwanted features can be removed by applying an apodization function to the interferogram prior to the Fourier transform. There are several apodization functions (see Filler or Norton and Beer) that can be applied to the data, but an in-depth description is beyond the scope of this chapter. They are addressed briefly in Chapters 7 and 8. The point is that the operator should be aware of this effect and that some choices can be made during data analysis that will affect the shape and intensity of the spectral features.

### 2.6.2.2 Phase Shift

A second instrumental effect on the data that occurs is a shifting in the relative phase of the wavelength, which is caused by the optics and the electronics. There are two

components for each of the wavelengths whose intensities are added to make up the interferogram. They are the magnitude of the intensity and the relative phase. The optics and the electronics cause slight phase shifts as the signals are processed, and these are frequency dependent. The shifts are normally accounted for when the Fourier transform is done, but no record of them is saved. Therefore, if the interferogram is not recorded, it cannot be retrieved by simply performing an inverse transform on the spectrum itself. It is primarily for this reason that the interferogram should be saved, even though it is somewhat more costly in disk space.

### 2.6.3 The Transform

The transform is performed on the interferogram by machine and therefore is done numerically. There are many algorithms to accomplish this, and which of these is used in the software provided with the commercially available instruments is not known. The mathematical basis for the transform is described below.

The complex motion of items such as vibrating strings or drumheads or other periodically varying quantities can always be described by a sum of sine and cosine terms known as a Fourier series. The frequencies in these terms are called the fundamental frequencies at which the item or quantity can vibrate. The actual motion is then a linear combination of these fundamental frequencies. When this summing of terms is done, it is said that a harmonic analysis has

been performed on the original vibratory motion. A study of such analyses shows that there are related pairs of variables such as time and frequency or position and momentum. In an analogous manner, functions can be analyzed, but here the more general Fourier transform must be used. The Fourier series is used to describe a periodic function as an infinite sum of sine and cosine terms whose frequencies are multiples of some fundamental. The transform allows the analysis of nonperiodic functions as an integral (also a summation) over a continuous range of frequencies. In one of its forms that relates time and frequency, the Fourier transform  $F(\omega)$ , a function of frequency, is related to  $G(t)$ , a function of time, as is shown in Equation 2-5. In the present situation, the function  $G(t)$  is the interferogram produced by the system, and  $F(\omega)$  is called the single-beam spectrum. The  $t$  in the term  $G(t)$  is a dummy variable, but in this case it is really the position of the moving mirror from the center burst position.

$$F(\omega) = \frac{1}{\sqrt{2\pi}} \int_{-\infty}^{+\infty} G(t) e^{-i\omega t} dt \quad (2-5)$$

### 2.6.4 The Single-Beam Spectrum

Some of the literature in this field refers to the single-beam spectrum as the inverse transform of the interferogram because the instrument takes the transform of the incoming signal to start with. Mathematically, this merely changes the sign in the exponent of Equation 2-5, which implies a phase shift in the sine and cosine terms. The term single-beam spectrum is a

historical holdover from the time when spectroscopists used a double-beam instrument and determined the transmission directly from a ratiometer in the electronics of the instrument. The present-day FT-IR systems do not use a double-beam system, but some of the terminology remains.

The single-beam spectrum contains all the information about the absorbing species of interest. But most workers do not use this spectrum for any direct data analysis. In some systems, it is this spectrum that has been stored on disk. At  $1\text{-cm}^{-1}$  resolution this spectrum takes about 35 kilobytes of memory, which is much less than the interferogram (100 kilobytes). However, storage capacity of the computers available today makes this a non-issue.

### 2.6.5 Data Analysis

The data analysis includes generating an absorption spectrum from the raw interferogram data, developing or obtaining the appropriate reference spectra, and then applying the chosen analytical method to determine the concentration of the target gases. The analytical methods and the procedures for generating an absorption spectrum from the interferogram and reference spectra of the target compounds are discussed below.

#### 2.6.5.1 *Generation of the Absorption Spectrum*

As shown in Figure 2-8, the data analysis generally starts with the recording of

the interferogram. Although in some cases the interferogram is analyzed directly to determine the concentration of the target gas, more commonly, the interferogram is automatically converted into a single-beam spectrum through the numeric process that is called a fast Fourier transform. A single-beam spectrum is generated and recorded for each sampling period. We call this spectrum the analytical, or field, spectrum. A background spectrum is generated by one of the methods described in Chapter 4. Then a transmission spectrum is obtained by dividing the field spectrum by the background. The absorption spectrum is obtained by taking the negative logarithm of the transmission spectrum. The absorption spectrum is used for all further data analysis.

#### 2.6.5.2 *Generation of the Reference Spectrum*

A reference spectrum is usually generated by using a high concentration of gas in a relatively short cell. The cell is usually at least 1 m long, although multipass cells with longer path lengths are also used. A pure sample of gas mixed with an inert gas, such as nitrogen, is used. The concentration of gas used to generate the reference spectrum should yield a range of absorbance values that match as closely as possible those expected to be found in atmospheric measurements. The system can use a flowing stream of gas, but the total pressure should be around 1 atm. The process of producing a reference spectrum is then the same as outlined above.

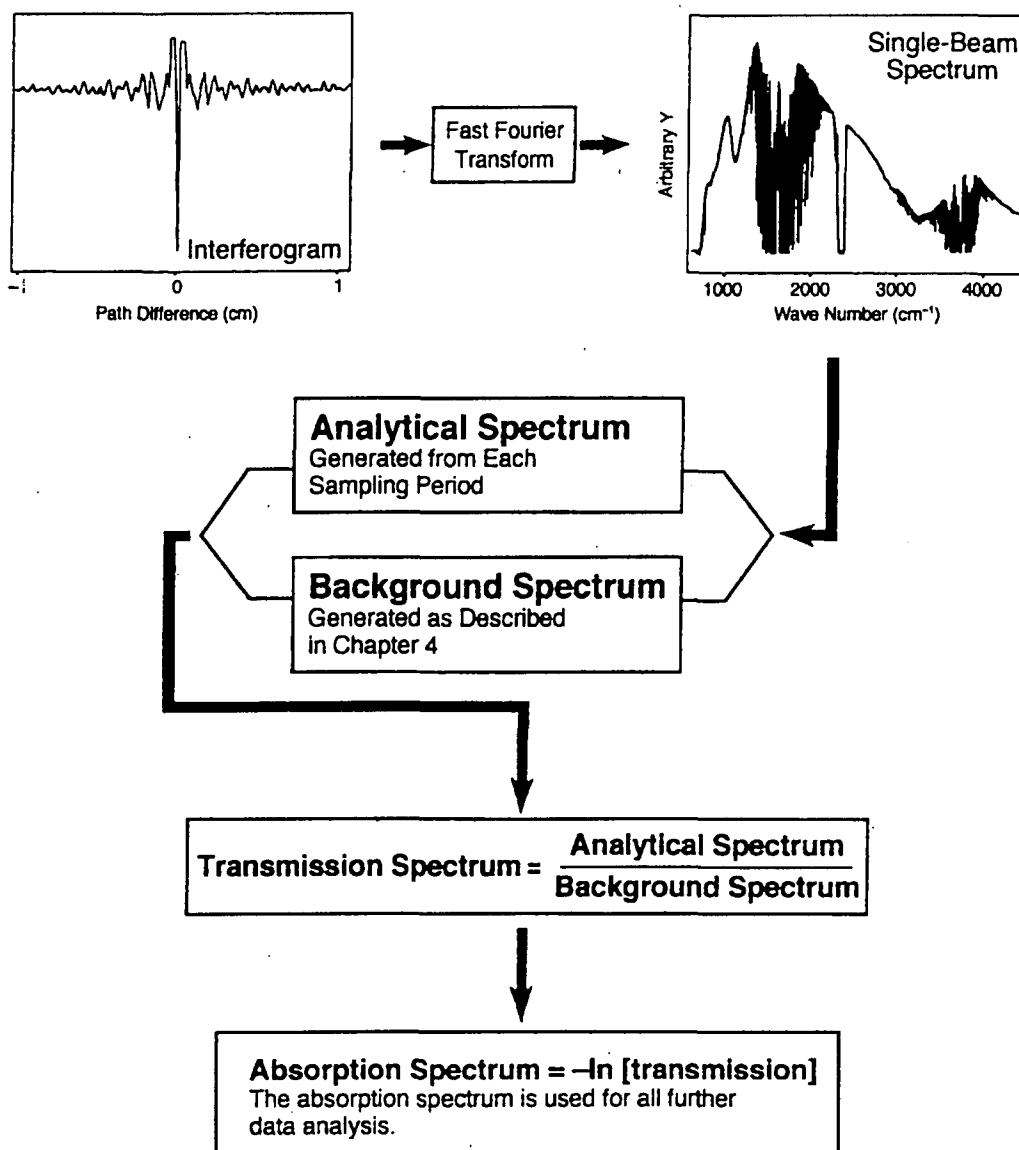


Figure 2-8. Data Reduction Flow Chart.

The production of reference spectra is an exacting undertaking and requires great attention to the experimental details. It is not likely that most users of the FT-IR technique will prepare their own reference spectra. Reference spectra are currently available commercially. The National Institute for Standards and Technology (NIST) has undertaken the task of producing reference spectra that are available at a minimal cost.

The investigators can at present (1999) be contacted at 301-975-3108 or on the Internet at <http://gases.nist.gov>.

### 2.6.5.3 Analytical Methods

After the reference spectra of the target gases are obtained, the appropriate wave number region for analysis must be selected. The selection should be based on

an examination of reference spectra and the type of analytical method chosen. Two issues must be addressed to make this selection. Ideally, the gas should have a high absorption coefficient in the selected region, and the region should be free of absorption bands from interfering species. If interfering species are present they must be identified and accounted for in the analysis methods.

Once an appropriate wave number region is selected, data analysis can proceed. The concentration of the unknown gas can be determined in three general ways, as described below: the comparison method, scaled subtraction, and multicomponent analysis techniques. Each method uses a reference spectrum of the gas being investigated.

#### 2.6.5.3.1 Comparison Technique

One method of determining the concentration is to measure the absorbance at a particular wave number and compare it with the absorbance of the reference spectrum at the same wave number. Then, if reciprocity holds (as implied by Beer's law), the concentration is obtained as follows. The absorbance ( $A$ ) is the product of  $\alpha$ , the optical absorption coefficient,  $C$ , the concentration of the gas and  $L$ , the path length. Thus  $A = \alpha CL$  and the unknown concentration can be found from the following expression.

$$A_{ref} / A_{unk} = C_{ref} L_{ref} / C_{unk} L_{unk} \quad (2-6)$$

Solving for the unknown concentration gives the following.

$$C_{unk} = C_{ref} L_{ref} A_{unk} / L_{unk} A_{ref} \quad (2-7)$$

This concentration has the same units as the units of the reference concentration, which is prepared as described in Section 2.6.5.2.

#### 2.6.5.3.2 Scaled Subtraction Technique

The scaled subtraction technique is similar in principle to the comparison technique. This technique is particularly useful if there are spectral features due to interfering species that overlap with those of the target compound. However, for scaled subtraction to be successful, either the target compound or the interfering species should have at least one unique absorption band. High-resolution data can be used to an advantage with this technique.

The scaled subtraction can be done as follows. Most software packages allow two spectra to be subtracted interactively. In this case the reference spectrum should be subtracted from the analytical spectrum until the absorption maximum of the band of interest is zero. Once the subtraction is completed the software reports a scaling factor. This factor can be multiplied by the concentration used to generate the reference spectrum to obtain the concentration of the target gas in the analytical spectrum. There is some operator skill involved in subtracting spectra interactively; therefore, some practice in using this technique is

recommended before the actual field spectra are measured.

### 2.6.5.3.3 *Multicomponent Analysis Techniques*

Multicomponent analysis techniques can be used to advantage when there are several target compounds to be analyzed for and there are several interfering species present. This is the case often encountered in open-path FT-IR monitoring, so some type of multicomponent analysis technique is generally the preferred method of analysis. There are several techniques that are used to perform multicomponent analyses of IR spectra. Multicomponent analysis techniques encompass a discipline unto themselves, and a complete discussion of the various techniques is beyond the scope of this document. Chapter 9 includes a discussion of classical least squares analysis. But this is intended to be only an introduction. The reader is referred to an excellent review by Haaland (1990). The most common multicomponent analysis method used in open-path FT-IR monitoring is based on a classical least squares (CLS) fitting algorithm. This is discussed below.

The CLS technique performs a linear regression by using the unknown and the reference spectra over a wave number region. The slope calculated in the regression is then used as a multiplier of the reference concentration to obtain the unknown. The ratio of the path lengths must also be accounted for. Thus if the slope is found to be 1 and the ratio of the reference path

length to the path length used for the measurement is 1/10, then the unknown concentration is 1/10 of the reference concentration.

The process of using the linear regression is more suitable than either the comparison technique or the scaled subtraction technique because the shape of one spectrum is compared with the shape of the reference spectrum. If the correlation coefficient is also calculated, it gives a measure of this comparison. There is one significant problem with this technique that has generally been overlooked. The procedures are generally written by assuming a linear response of the instrument to changes in concentration. The response is actually slightly nonlinear, and this contributes to the overall error in the data. This topic is discussed in depth in Chapter 8.

## 2.7 References

- Beer, A. 1852. *Ann. Physik.* 86:78
- Beer, R. 1992. *Remote Sensing by Fourier Transform Spectrometry*, John Wiley & Sons, New York.
- Filler, A.S. 1964. Apodization and Interpolation in Fourier Transform Spectroscopy, *J. Opt. Soc. Am.* 54: 762
- Haaland, D.M. 1990. Multivariate Calibration Methods Applied to Quantitative FT-IR Analyses. *Practical Fourier Transform Infrared Spectroscopy-Industrial and Laboratory Chemical Analysis*, J.R. Ferrar and K. Krishnan, Eds., Academic Press, San Diego, CA, pp. 396-468.



Marshall, A.G., and F.R. Verdun. 1990. *Fourier Transforms in NMR, Optical, and Mass Spectrometry*, Elsevier, Amsterdam.

Norton, R.H. and Beer, R. 1976, New Apodizing Functions for Fourier Spectrometry. *J. Opt. Soc. Am.* 66: 259.

Michelson, A.A. 1881. The Relative Motion of the Earth and the Luminiferous Ether. *Am. J. Sci.* 22: 120-129.

Rossi, B. 1957. *Optics*. Addison-Wesley Publishing Company, Inc., Reading, MA.

Walter, B. 1889. *Ann. Physik* (Wiedemann) 36: 502, 518.

## Chapter 3

### Initial Instrument Operation

#### SUMMARY

This chapter offers guidance and recommendations with respect to the initial tests that should be performed on the FT-IR system to verify that the instrument is set up to operate properly. Specific areas that are addressed include the following.

- The characteristic features of the single-beam spectrum
- The distance at which the detector is saturated and operating in a nonlinear fashion
- The return signal intensity as a function of distance
- The uniformity of the IR beam intensity
- The contribution of stray light to the total return signal
- The determination of the system noise
- The effect of water vapor concentration on the return signal intensity

#### 3.1 Introduction and Overview

The assumption made for the discussion in this chapter is that the manufacturer has set up the FT-IR and it is running according to his specifications. Initially, the setup procedure for each field study should be the same, although certain procedural differences are dictated by specific data requirements.

Before putting the instrument into continuous monitoring service, the operator should conduct some initial tests and determine the following.

- The distance at which the detector is saturated and operating in a nonlinear fashion (Section 3.4)
- The return signal as a function of distance (Section 3.5)
- The stray light inside the instrument (Section 3.6)
- The uniformity of the beam intensity (Section 3.7)

The operator should become quite familiar with the single-beam intensity profile and with the gross features of the single-beam spectrum. Beyond that, the operator must start several control charts that will provide long-term information about the return

intensity and the noise levels. Some ancillary items such as water vapor concentration, ambient temperature, and ambient pressure should also be recorded.

This chapter includes a discussion of each of these items and also addresses the items that must be recorded so that adequate information concerning the long-term stability of the FT-IR can be obtained. In addition, some data are presented that have been recorded by FT-IR instruments in the past.

The tests outlined in this chapter should be performed before data are recorded with the FT-IR monitor. A failure to do so could result in the acquisition of erroneous data that could lead to inaccurate concentration measurements. Many of the tests involving the initial instrument setup are similar to those proposed for use in the routine quality assurance procedures presented in Chapter 10 of this document.

### 3.2 The Single-Beam Spectrum

Figure 3-1 shows a single-beam spectrum taken with  $1\text{-cm}^{-1}$  resolution. The total scan time was 5 min and the total path length was 414 m. The vapor pressure of water during this measurement was 12 torr. There are several features in the spectrum that should be noted. First, the regions 1415 to  $1815\text{ cm}^{-1}$  and 3547 to  $3900\text{ cm}^{-1}$  are where the infrared energy in the beam is totally absorbed by water vapor. The operator will notice that, for a given path length, the width of the region for complete

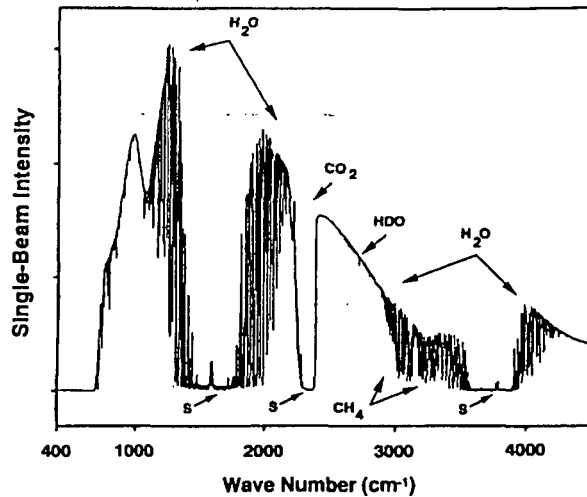


Figure 3-1. Single-Beam Spectrum Along a 414-m Path. S indicates stray light.

absorption varies as the amount water vapor in the atmosphere changes from one day to the next. Also the center of the region should become somewhat transparent as the path is made shorter.

The strong absorption in the 2234- to  $2389\text{-cm}^{-1}$  region is due to carbon dioxide, and the atmosphere in this wave number region should remain opaque at all times, even when the instrument is used to monitor over short paths. The opaque regions should be flat, and they represent the baseline of the spectrum. Any deviation from zero in these regions indicates that something is wrong with the instrument operation. However, Figure 3-1 shows these regions to be elevated. This is due to stray light in the instrument, and these regions are marked "S" in the figure.

The operator should pay particular attention to the spectrum in the region around  $600\text{--}700\text{ cm}^{-1}$ . The spectrum below this wave number region should be flat and

at the baseline. If the spectrum has an elevated baseline below the detector cutoff, in this example the  $650\text{-cm}^{-1}$  region, the instrument may be operating in a nonlinear manner. If this is the case, the operator will see what seems like a dip appear as the retroreflector or source is brought closer to the FT-IR. An example of this is given in Figure 3-2 for a single-beam spectrum recorded at a 20-m path length.

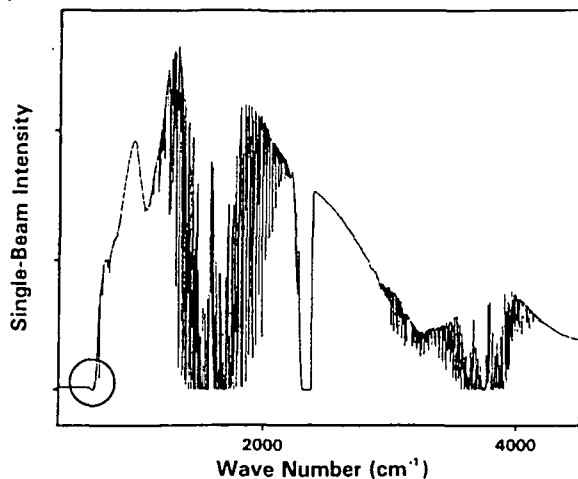


**Figure 3-2. Single-Beam Spectrum Recorded at a 20-m Total Path Length Indicating Nonlinear Operation.**

When the path is sufficiently long (200 m and 10 torr  $\text{H}_2\text{O}$ ) or the water vapor concentration is large, an absorption band should be noticeable at  $2720\text{ cm}^{-1}$ . This peak is the Q-branch of deuterated water ( $\text{HDO}$ ), and it is also possible to observe the P and the R branches.

The spectral region around  $3000\text{ cm}^{-1}$  is also strongly absorbed by water vapor, although it is not opaque. The absorption features of methane are in this region. This

is also the region of the C-H stretching frequencies. The atmosphere from  $3500$  to  $3900\text{ cm}^{-1}$  is opaque, again because of water vapor. There is still some sensitivity and therefore an elevated signal return above  $4200\text{ cm}^{-1}$ , and this is the region where hydrogen fluoride is absorbing.

The return beam intensity at approximately  $987$ ,  $2500$ , and  $4400\text{ cm}^{-1}$  should be recorded so as to form a basic set of data about the instrument's operation. Along with this, the operator should record the path length. The total return signal is dependent on the path length and the amount of water vapor in the atmosphere. When using the single-beam spectrum to gauge how well the instrument is functioning, the operator should try to select regions that are not greatly impacted by water vapor.

Figure 3-3 shows the region between  $1000$  and  $1025\text{ cm}^{-1}$  enlarged and plotted in absorbance. The operator should notice that there are water vapor lines at  $1010$ ,  $1014$ , and  $1017\text{ cm}^{-1}$ . These lines will be in every spectrum as long as the product of the water vapor concentration and the path length is large enough. The lines at  $1010$  and  $1017$  are actually doublets and cannot be resolved at  $1\text{-cm}^{-1}$  resolution. The line at  $1014.2\text{ cm}^{-1}$  is a singlet and can be used as a check for wave number shifts and resolution. A procedure for doing each of these is given in the subsections below.

Both wave number shifts and resolution changes indicate that something has

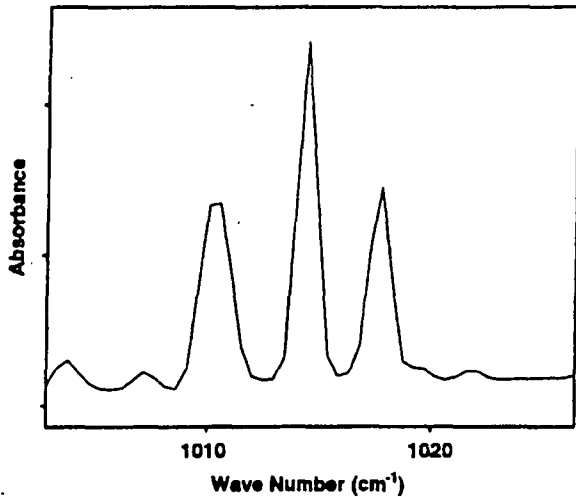


**Figure 3-3. Region Between 1000 and 1025  $\text{cm}^{-1}$ .** The line at  $1014.2 \text{ cm}^{-1}$  can be used as a check for wave number shifts and resolution.

changed in the instrument geometry, and if these occur they should be discussed with the instrument manufacturer. A subtle, apparent wave number shift can be observed if the atmospheric absorption line used for a shift determination is an unresolved doublet. In this case, if one line becomes more intense with respect to the other, the envelope peak will appear to be shifted.

### 3.2.1 Wave Number Shift

To determine whether wave number shifts have occurred, the operator should have an absorption spectrum that contains the water vapor line at  $1014.2 \text{ cm}^{-1}$  and one for which there is no shift present. The HITRAN database for water vapor is used in this document as a guide (University of South Florida 1993), and it positions this water vapor line at  $1014.2 \text{ cm}^{-1}$ .

For any particular instrument, the line assignment may be slightly different ( $\pm 0.2 \text{ cm}^{-1}$ ) because of the instrument's geometry, but it should not shift in time. However that may be, it is the responsibility of the operator to determine precisely where the water line is and whether shifts occur with time. The operator may also choose to determine wave number shifts by using the HDO lines in the  $2720\text{-cm}^{-1}$  region. This measurement is somewhat more sensitive to shifts in the higher wave number (shorter wavelength) region.

In principle, any absorption or single beam spectrum can be used as a guide to determine wave number shifts. There are two methods available for determining shifts. The first is simply to compare the positions of the peaks of the two spectra on the computer monitor. The second is to subtract the second spectrum from the first and study the result. The second spectrum should be normalized to the first by a simple multiplication before the subtraction is done, or the subtraction can be done interactively. After subtraction, wave number shifts will result in a curve that appears to be the first derivative of the line shape. The wave number where zero amplitude occurs will be shifted from the original peak wave number by an amount that is proportional to the wave number shift. This is shown schematically in Figure 3-4A.

### 3.2.2 Change in Resolution

The other possible change that can occur in the spectra as time passes is a

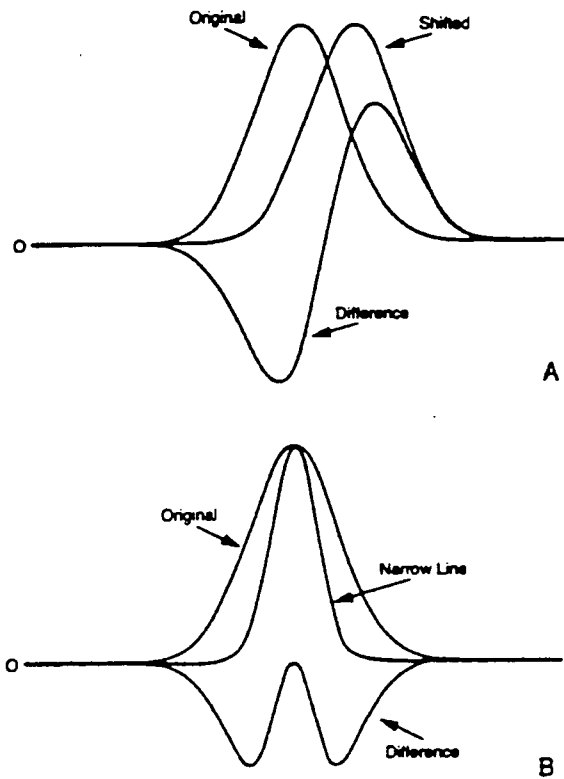


**Figure 3-4. Subtraction of Spectra for the Determination of (A) Line Shifts and (B) Resolution Changes.**

resolution change in the instrument. If a change in the resolution has occurred but there is no peak shift, the result will appear to have the shape of an 'M' or a 'W', depending on which spectrum has been recorded with the largest amount of water vapor. This is shown schematically in Figure 3-4B. If there are no changes in the line, then the result of subtraction will be random noise.

### 3.3 Distance to Saturation

One of the early pieces of information to obtain with an FT-IR monitor is the path length at which the detector is saturated. As

discussed in Section 3.2, this is easily noticed by a negative dip in the single-beam return in the  $650\text{-}750\text{-cm}^{-1}$  region below the detector cutoff. As the retroreflector or the light source is brought closer to the detector, this dip will appear. This response is opposite to the response that is due to an absorption feature in the spectrum. This distance is important because it represents the minimum path length over which it is possible to operate without making changes to the instrument. In the monostatic case, it is possible to rotate the retroreflector to lower the return intensity. If necessary, it is possible to lower the intensity of the FT-IR instruments by simply using a fine wire mesh screen to cover the aperture. A plastic screen should not be used because plastics have absorption features in the infrared.

To measure this distance, simply move the light source or the retroreflector away from the transmitting telescope until the negative dip just disappears from the single-beam spectrum. This distance should be recorded as the minimum working distance available without making instrument changes.

### 3.4 Return Intensity as a Function of Distance

Some attempt is made to collimate the infrared beam before it is transmitted along the path. It is, however, impossible to completely collimate the beam because of the size of the light source. Therefore, most beams either are always diverging as they traverse the path or become diverging at

some point along the path. Once the beam is bigger than the retroreflector or the receiving telescope, the return signal should diminish as the square of the distance. That is, beyond some distance the signal is reduced by a factor of 4 when the path length is doubled. The reason that this return signal versus distance determination is necessary is twofold. The first is that the commercially available instruments that use the monostatic configuration both have a stray light signal when the telescope is blocked. The return beam should never be allowed to approach this signal. The second is that at some distance the system noise will become an appreciable part of the signal, and this represents the maximum usable distance.

To determine the return signal as a function of distance, the operator must start with the retroreflector or the light source at the minimum working distance as determined above. Then, the operator should move the light source or the retroreflector back by some distance and record the signal. This process should be continued until the signal level reaches the noise level or just levels off. It should be noted that the leveling-off effect can also be caused by the return signal's reaching the stray light level. These data should then be plotted and used for quality assurance/quality control purposes.

### **3.5 Determination of the Stray Light Signal**

The stray light in the instrument can be measured without regard to the distance to the light source or the retroreflector. It is not

expected that instruments using the bistatic configuration will have any measurable stray light, but a one-time check is appropriate. To measure the stray light, the operator must block the receiving telescope while the signal is being recorded. It is important to use an appropriate blocking material to do this. No surface that can reflect any of the infrared energy back to the instrument can be used, nor any material that is transparent. The best blocking material is a piece of black cloth such as is used in the construction of a photographic film changing bag. For systems that transmit the beam through the interferometer before transmitting it along the path, the beam can simply be slewed away from the retroreflector. This return signal should be recorded and then plotted on the graph as return signal versus distance, discussed above. A record of the stray light spectrum should be made and compared to the single-beam spectrum recorded at the selected working distance.

Stray light inside the instrument can also be caused by strong sources of IR energy that are in the field of view of the instrument. For example, it is possible to have the sun in the instrument's field of view during sunrise and sunset. This will probably give rise to an unwanted signal that actually comes from reflections inside the instrument.

The stray light actually causes an error in the determination of the gas concentrations and must be subtracted from the data spectra before processing. Thus it has to be recorded at every monitoring session and periodically in the case of a

permanent installation. The effect of stray light on photometric accuracy is illustrated by the absorption feature shown in Figure 3-5.

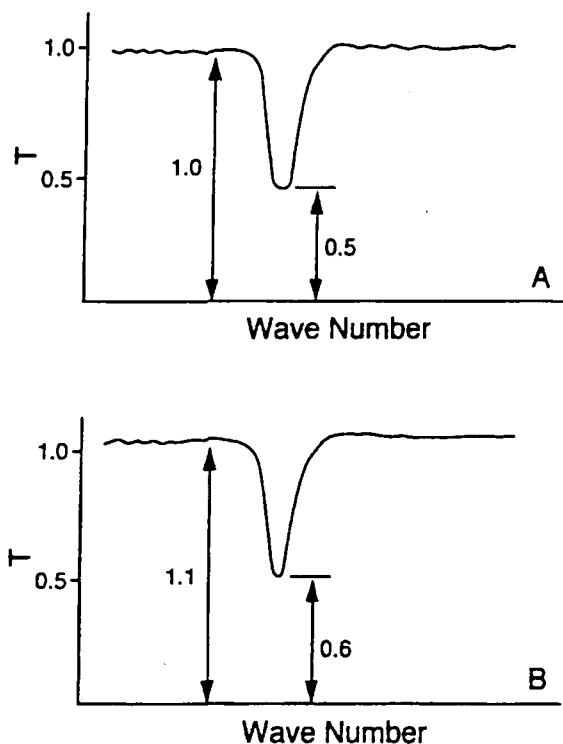


**Figure 3-5. Effect of Stray Light.** A. Spectral feature without stray light. B. Spectral feature with stray light.

The absorption line in Figure 3-5A has a transmission of 0.5 at the peak. The baseline (100% transmission) has unity amplitude. Now suppose that stray light exists in the instrument in the amount of 10% of the original return signal. This means that the baseline goes to an amplitude of 1.1, but the absorption feature goes to an amplitude of 0.6, as shown in Figure 3-5B. Thus the new transmission of the absorption is 0.6/1.1, and this is not equal to 0.5 but to 0.5454, or is in error by about 9.2%.

Mathematically, this is just verifying the fact that  $A/B \neq (A + C)/(B + C)$ . It might be questioned whether the effect of this stray light is offset by the effect of the air in the interferometer enclosure, which most likely contains the pollutant gas also.

However, the transmission due to the gas in the cell is increased from that along the path in the ratio of the path lengths. Thus, for our data taken at Research Triangle Park, NC, along a 414-m path, the ratio of the path lengths is at most 1/414, and therefore the additional absorption is negligible. A more in-depth analysis of the problems introduced by stray light indicates that actual line shape distortions may take place. It is also quite likely that the simple subtraction of stray light as suggested above will not remove all the error incurred. Therefore, all efforts should be made to at least minimize the amount of stray light reaching the detector.

### 3.6 Determination of the Random Noise of the System

The random noise of the system is determined from an absorption spectrum made from two single-beam spectra taken sequentially. These spectra are to be taken under the same operating conditions as will be used for the acquisition of data spectra. That is, the same acquisition time and path length should be used for the noise determination as will be used for data acquisition. There should be no time allowed to elapse between the acquisition of the two



spectra. This determination will be somewhat dependent on the water vapor concentration in the atmosphere, so the water vapor concentration should also be determined.

The use of the word "noise" suggests a random signal that is primarily produced by the system electronics. When measurements are taken in the open air, this may not exactly be the case. If the period of data acquisition for the two spectra is long (because of a large number of scans, for example), then atmospheric effects may contribute to the measurement. For that reason, the wave number regions that are used for the determination should be carefully chosen. Three regions are suggested below, but the low wave number region may not be suitable in all situations because of the presence of gases other than water vapor.

The actual wave number range over which the noise should be calculated will vary with the resolution used. Statistically, it can be shown that about 98 data points is an optimum number (Mark and Workman, 1991). For 1-cm<sup>-1</sup> resolution, this means that data should be taken over a 50-cm<sup>-1</sup> region.

Once the two spectra have been acquired, an absorption spectrum should be made by using one of the two spectra as a reference or background spectrum. Which one is used for the background is not important. The noise is then determined in

the three regions 958-1008 cm<sup>-1</sup>, 2480-2530 cm<sup>-1</sup>, and 4380-4430 cm<sup>-1</sup>.

There are several ways that are described in statistics texts to determine the noise. We will specify the use of the root mean square (RMS) deviation as the appropriate measure of the noise. The first step is to perform a linear regression over the wave number region and determine the slope and the intercept of the line. At each wave number, the next step is then to calculate the difference between the calculated line and the actual ordinate value. The squares of these differences are then used to calculate the RMS deviation as is described below.

To calculate the slope and the intercept from a linear regression, use the following expressions.

$$NUMERATOR = N \sum X_i Y_i - \sum X_i \sum Y_i$$

$$DENOMINATOR = N \sum (X_i)^2 - \sum X_i \sum X_i$$

$$SLOPE = NUMERATOR / DENOMINATOR$$

$$INTERCEPT = \frac{1}{N} (\sum Y_i - SLOPE * \sum X_i)$$

In this case the X<sub>i</sub> values are the wave numbers and the Y<sub>i</sub> values are the

absorbance values at the particular wave numbers.

The differences are then found as  $D_i = Y_i - y_i$ , where now the  $Y_i$  values are calculated from the line by using the expression  $Y_i = \text{slope} * X_i - \text{intercept}$ .

Once this is accomplished the RMS deviation is determined with the following expression.

$$RMSDEVATION = \left( \sum \frac{D_i^2}{N-2} \right)^{1/2}$$

Mathematical representations of the RMS deviation vary in what the denominator is. Quite often the denominator is written simply as  $N$ . The term  $N-2$  is used here because the slope and the intercept are calculated from the data. This reduces the degrees of freedom by 2 and hence the  $N-2$  (see, e.g., Mark and Workman 1991).

Some results of these measurements are shown in Figure 3-6. The data shown in the figure were taken over the region 980-1020  $\text{cm}^{-1}$  in order to include the water vapor peaks at 1014  $\text{cm}^{-1}$ . To reduce the effect of water vapor to a minimum it is possible to create two spectra by using an artificial background, subtract the water vapor of one from the other, and then make the noise determination.

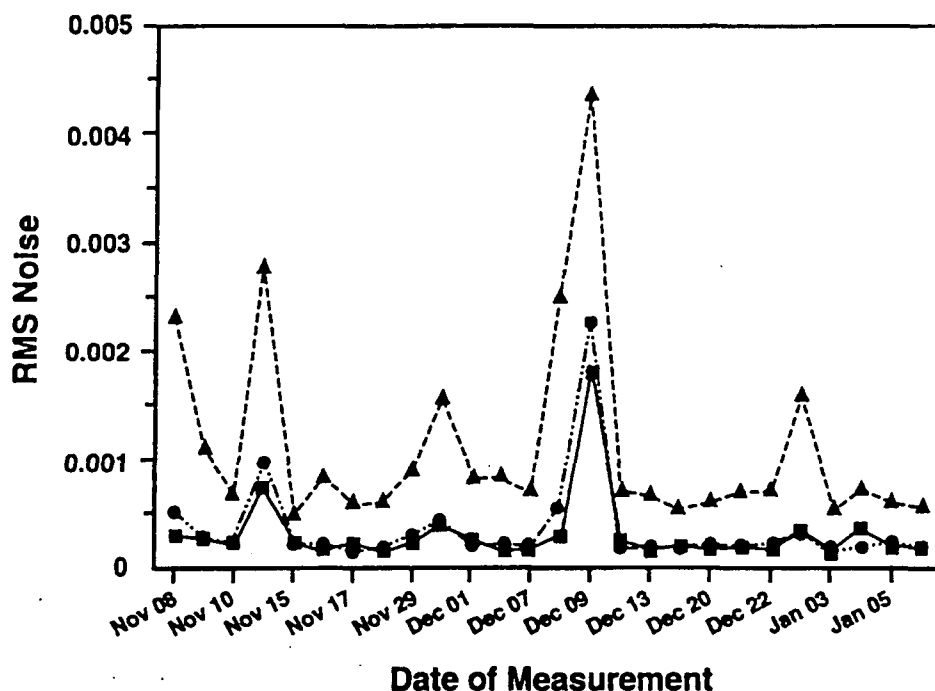


Figure 3-6. The RMS Baseline Noise Measured Between 980 and 1020  $\text{cm}^{-1}$  (■), 2480 and 2520  $\text{cm}^{-1}$  (●), and 4380 and 4420  $\text{cm}^{-1}$  (▲).

### 3.7 Return Intensity as a Function of Water Vapor

The return-beam intensity is a function of the absorption due to water vapor in the atmosphere. It is therefore a function not only of the path length but also the water vapor concentration in the atmosphere. It must be clear to the operator that relative humidity is not important in this case and has no relevance to the FT-IR data, and it is actually the water vapor partial pressure in torr that must be used. However, over a period of one day, the water vapor concentration may not change very much, so acquiring a set of data over a range of water vapor concentrations will take some time. Some thought must also be given to the problem of measuring the water vapor concentration when the temperature is below freezing. The Smithsonian psychrometric tables give data to an ambient temperature of 5 °F, but it is not clear that a simple sling psychrometer should be used to make the wet and dry bulb measurements.

The measurements for water vapor can be made at any place along the path. The

operator should note, however, that some investigators feel that the concentration of water vapor along the path actually changes. We have made some measurements with a sling psychrometer and have not seen any appreciable changes along the path. We have seen rather subtle changes in the absorption due to water vapor from the spectra themselves. This is most easily noticed if the subtraction technique is used. For example, we acquired a set of data taken at 1-min intervals. After the spectra were converted to absorption spectra, the first spectrum was subtracted from the others in order. The residual water in the spectra indicated that minor but noticeable changes take place minute by minute.

### 3.8 References

University of South Florida. 1993. USF HITRAN-PC. University of South Florida, Tampa, FL

Mark, H., and J. Workman. 1991. *Statistics in Spectroscopy*. Academic Press, New York.

## Chapter 4

### Background Spectra

#### SUMMARY

The topics and specific points of emphasis discussed in this chapter include the following.

- The generation of the transmission spectrum and the absorption spectrum
- The need for a background spectrum and the difficulties in obtaining one that is adequate
- The methods for generating a suitable background spectrum
  - Synthetic backgrounds
  - Upwind backgrounds
  - Short-path backgrounds
  - Averaged backgrounds
- Specific field guidance for measuring the background spectrum

#### 4.1 Introduction and Overview

In current use, long-path, open-path FT-IR data are obtained from single-beam measurements. That is, there is no reference, or background, spectrum taken simultaneously with the sample spectrum to null the spectral features due to the characteristics of the source, beam splitter, detector, and interfering species in the atmosphere. To remove these background spectral features, the single-beam field spectrum is divided by a single-beam background spectrum, or  $I_0$  spectrum. This operation (illustrated in Figure 2-8) generates a transmission spectrum. According to Beer's law, the absorption spectrum is then calculated by taking the negative logarithm of the transmission spectrum. It is the

absorption spectrum that is used for data analysis.

Ideally, the background spectrum is collected under the same experimental conditions as those for the sample spectrum, but without the target gas or gases present. However, in the field it is not possible to obtain the  $I_0$  spectrum directly because the target gas cannot be easily removed from the atmosphere. This chapter presents a discussion of the problems associated with obtaining the  $I_0$  spectrum and the methods that are used to generate a background spectrum.

There are currently four methods for obtaining  $I_0$ : synthetic, upwind, short-path, and averaged background spectra. Synthetic

background spectra can be generated by selecting data points along a single-beam spectrum and then calculating the high-order polynomial function that best fits the selected points or by repeatedly subtracting the spectral features due to interfering species from a single-beam spectrum. Both of these methods can introduce distortions or spurious features in the actual intensity profile. Therefore, much care must be taken when generating synthetic background spectra.

For short-term monitoring efforts, the FT-IR path is generally chosen to be perpendicular to the wind field. If the area of the emission source is relatively small, a background spectrum can be acquired along a path that is upwind from the source. However, it is difficult to make this type of measurement frequently if the FT-IR system has to be moved from one side of the source area to another. Also, errors may be introduced in the measurements if the water vapor in the atmosphere changes significantly between the times that the background spectrum and the sample spectra are acquired.

Another option for obtaining the  $I_0$  spectrum is to bring the retroreflector or external IR source close to the receiving telescope. This effectively eliminates the absorption caused by the target gases and records a true instrument background. One problem with this method is that the detector can be saturated at short paths because too much IR radiation is incident on the detector element.

When the experimental conditions are fairly constant over a measurement period, it is possible to average several backgrounds that have been taken over this time. This average  $I_0$  can then be used for the entire data set for that period. However, most of the time, the experimental conditions are not constant enough to perform this type of long-term averaging. For example, the concentrations of water vapor,  $\text{CO}_2$ , and gases emanating from other sources are constantly changing.

The change in water vapor concentration must be considered the biggest potential source of error in the background measurement. This is because changes in water vapor concentration can change the curvature of the baseline in the field spectra. When that happens, the background spectrum and the field spectra do not properly match, and errors occur. An accurate record of the partial pressure of water vapor should be maintained. These data should be taken continuously.

Acquisition of the  $I_0$  spectrum represents one of the more difficult tasks in FT-IR long-path, open-path monitoring. Currently, there is not a universal method for obtaining a satisfactory background spectrum. The method chosen to obtain  $I_0$  must be determined on a site-by-site basis. This chapter includes a rationale for the use of an  $I_0$  spectrum, as well as advice on the appropriate techniques for generating it. These techniques are each discussed below.

## 4.2 Synthetic Background Spectra

The software that is supplied with the commercially available instruments has a routine that allows a synthetic spectrum to be generated. This is best accomplished by selecting data points along some original single-beam spectra and then calculating a high-order polynomial function that best fits the selected points. Generally, however, the individual data points are connected with straight line segments, and in most instances this is satisfactory. Thus, once a single-beam spectrum is produced, it can be used to generate a synthetic  $I_0$ . Synthetic  $I_0$  spectra can be made that cover only selected wave number regions, or they can be made to cover the entire wave number region that the FT-IR uses. An example synthetic spectrum is shown in Figure 4-1.

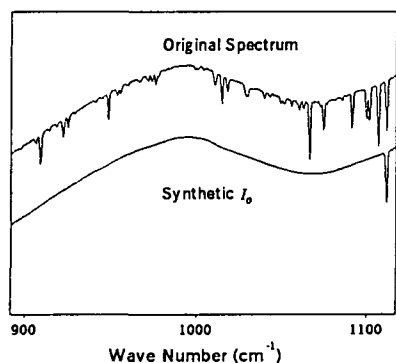


**Figure 4-1. Synthetic  $I_0$  Spectrum.** The peak at  $1110\text{ cm}^{-1}$  has intentionally been left in as a fiducial point.

Some care must be used when synthetic  $I_0$  spectra are generated so that distortions are not introduced into the intensity function. For this reason, when

data points are selected, they should never be selected at the peaks or even within an absorbing feature. The final curve that is produced must be a smooth function without artificial dips and peaks and must follow the baseline of the single-beam spectrum from which it is made.

It is essentially impossible to construct a synthetic spectrum in the wave number regions where water vapor and carbon dioxide absorb strongly. The individual lines are overlapping so that it is very difficult to judge where the background curve should be set, and in much of the region there is almost no energy being returned to the detector. Even at the shortest path length possible, there are still portions of the spectrum that are completely absorbed by the water vapor and the carbon dioxide. Because of this strong absorption, these regions of the spectrum are not used in the data analysis.

## 4.3 Upwind Background Spectra

For short-term monitoring efforts, the path is generally set out so as to be perpendicular to the wind field. If need be, the operator can change the orientation of the path so that this geometry is maintained. If the area of the source is relatively small and its upwind side is accessible, an upwind  $I_0$  spectrum can be acquired. A usable background spectrum can also be acquired by taking data along the side of source. (See Figure 4-2.) As long as the wind is not blowing across the source area and transporting the emissions across the path

used for  $I_0$ , these spectra should be satisfactory.

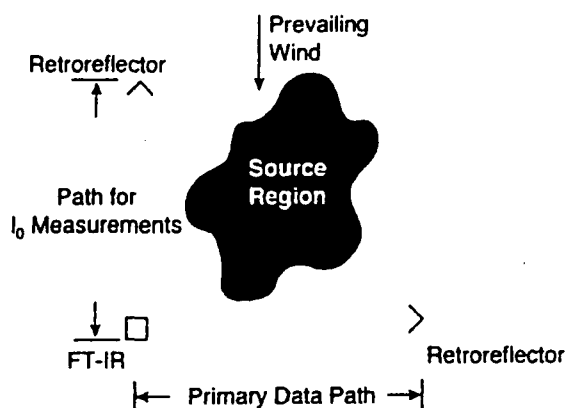


Figure 4-2. A Possible Configuration for  $I_0$  Spectrum Acquisition.

Another technique for acquiring an upwind background spectrum is to wait until the wind shifts so that the path is along an upwind side of the source. This works well for isolated sources, but if there are other places emitting chemicals, then this method can lead to errors in identifying compounds and in quantifying just what is coming from the source under study.

There are some advantages to taking true upwind background spectra this way. First, it is likely that sources are not isolated and the chemical species of interest are emanating from several places in the area. The compounds entering the area being investigated are thus included in the upwind background spectrum. If the configuration can be set up so the side of the source area can be used, a second retroreflector or IR source can be used, and the  $I_0$  spectrum can be taken frequently and without having to

transport the entire system from one place to another.

There are also some disadvantages to this procedure. It is difficult to take upwind and downwind spectra frequently if the system has to be moved from one side of the source area to another. Generally, this type of spectrum is taken once at the beginning of the monitoring period and once at the end (each day).

#### 4.4 Short-Path Background Spectra

Another possible technique for obtaining the  $I_0$  spectrum is to bring the retroreflector or external IR source close to the receiving telescope. This effectively eliminates the absorption caused by the compounds of interest and records a true background. This background is called the short-path  $I_0$ . If two retroreflectors are available, this task is fairly easy to perform. The FT-IR monitor can be pointed first to one retroreflector and then the other quite easily with some regularity.

Figure 4-3 presents a procedure for acquiring a short-path background spectrum. The recommendation for the frequency of repeating this procedure is that a background should be considered valid for no longer than one day or until there is a major change in the operational parameters. Although a short-path background spectrum may be valid for an extended period, it should be revalidated on a daily basis. Necessary checks for a short-path background spectrum include the following.

### ACQUIRING A SHORT-PATH BACKGROUND SPECTRUM

1. Calculate the required path length for each gas that is being measured.
  - a. Calculate the absorption coefficient of the gas in the wave number region that is being used for analysis. From the reference spectrum, obtain the product of the concentration and the path length used to generate the reference data. Then measure the absorbance of the peak that is being used for analysis. The absorption coefficient is given by the following.

$$\alpha = A/CL$$

- b. Estimate the maximum anticipated concentration of the target gas. Express this in the same units as the concentration of the reference has been expressed (generally, ppm).
  - c. Set the absorbance to the number that has been experimentally determined from the RMS noise as an estimate of the lowest possible detection limit for the FT-IR system, for example,  $10^{-4}$ , and use the expression

$$L = A/\alpha C$$

to find the path length to be used for the background spectrum.

- d. A sample calculation with the toluene peak at  $1031.6 \text{ cm}^{-1}$  is given below.

$$\alpha = A/CL$$

Read  $A$  at  $1031.6$  as  $0.0203$ .

The  $CL$  product =  $496 \text{ ppm-m}$

$$\alpha = 0.0203/496 = 4.1 \times 10^{-5}$$

Estimate the maximum concentration to be  $0.050 \text{ ppm}$ .

Calculate  $L$ :

$$L = A/\alpha C = 10^{-4}/(0.000041 \times 0.050)$$

or

$$L = 48.8 \text{ m}$$

2. Repeat Step 1 for each target gas and set up the retroreflector or light source at the minimum calculated distance.
3. Take a spectrum at the same resolution as will be used to take data. So that the noise in the data spectrum will be the predominant source of noise, take the background spectrum for at least 4 times the number of scans used for the data spectrum. (This judgement should be based on the time involved with taking a spectrum.)
4. Use this spectrum for the background spectrum.

Figure 4-3. Procedure for Acquiring a Short-Path Background Spectrum.



- Comparison of the curvature of the baseline in the short-path spectrum with the curvature of the baseline in the field spectra
- Inspection of the spectrum for wavelength shifts and resolution changes, as discussed in Section 3.2

One difficulty with this procedure is deciding on an appropriate distance for placing the retroreflector or external IR source. One difficulty is that the detector can easily be saturated when the path length is too short. However, if the reflector is placed far enough away to overcome this problem, then the absorption may become large enough to be detrimental. Thus, this distance must be determined for each instrument at least once. When the detector is saturated, the signal seems to drop below zero at the low-wave-number end of the single-beam spectrum, and the response of the detector is nonlinear. The retroreflector or external IR source must be far enough away so that this dip in the signal strength disappears. One way to accomplish this is to reduce the light intensity by rotating the retroreflector or using wire mesh screens to attenuate the signal. (See Section 3.3.)

A second difficulty in monostatic systems is that the retroreflector will subtend different angles when it is at different distances. The retroreflector may be the actual optical field stop of the instrument, and changing the distance can cause distortions in the spectrum. When the distance is increased, the retroreflector subtends smaller angles, and the instrument

uses different cones of light. This problem can be overcome by placing a field stop in the instrument that uses a smaller field of view than the smallest anticipated from the retroreflector. However, that is a job for the manufacturer because stops cannot be placed just anywhere in the optical train without causing other problems

#### 4.5 Averaged Background Spectra

When the experimental conditions are fairly constant over a measurement period, it is possible to average several background spectra that have been taken over this time. This average  $I_0$  can then be used for the entire data set for that period. Because all the individual spectra making up the average should have the same noise and there should be no other errors, the final error in this average background should be smaller by a factor of  $\sqrt{N}$ . Here,  $N$  is the number of spectra in the average.

However, most of the time the experimental conditions are not constant enough to perform the averaging. The water vapor concentration is changing most of the time, and so is the concentration of carbon dioxide. If other sources are in the area, the concentrations of the gases emanating from them are not likely to be constant. If any of these gases are also being monitored, the use of an average  $I_0$  will not give true absorption spectra for the entire monitoring period.

Currently, no published data seem to be available that have been taken over

periods of more than a few weeks. Therefore it is not known whether  $I_0$  spectra can be taken over extended periods, sorted according to the similarity of conditions, and then averaged. If this could be done, it might be possible to acquire a set of  $I_0$  spectra that are universal. The experimenter could use these as he uses the library of pure compound spectra. Thus, with 10 torr of water vapor and a path length of 200 m, background VII might be used, etc.

Acquisition of the  $I_0$  spectrum represents one of the more difficult tasks associated with using an FT-IR spectrometer. Most of the data that have been published until now has come from short-term monitoring programs. The  $I_0$  spectra that have been used have been taken at various times during the days of operation. These spectra have then been used for the next series of atmospheric spectra to be analyzed until the next background is taken. Although shifts in the wind direction have been used to determine the need for a new background, changes in water vapor concentration have not. Little information has been published on the stability of the instrument itself or on the effect of taking a new background after some instability develops. There is some evidence that has been derived from bench-top laboratory work that indicates the  $I_0$  should be taken as often as every other atmospheric spectrum. There is also some evidence that a single  $I_0$  can be used over a long period of time with no detrimental effects. Neither of these observations has been corroborated by any in-depth study of the background spectra.

The work performed at Research Triangle Park, NC, indicates that a synthetic background ( $I_0$ )-spectrum can be used for extended periods with some care. After one year of operation, the  $I_0$  spectrum had to be changed four times. Three times were caused by instrument component changes, and only one time did the atmospheric conditions require a change in  $I_0$ . That time the water vapor concentration changed from 23 torr to 9 torr in a 15-min period.

Thus, much work is yet to be done in establishing the appropriate manner and frequency for acquiring the  $I_0$  data.

#### 4.6 Why Use a Background

The primary data that is produced by an FT-IR is the interferogram. It contains all the information that is required to obtain the concentrations of the gases that the experimenter wants. However, the information in the interferogram is in a form that is somewhat cumbersome to most people that are familiar with spectroscopy. In addition, the primary physical law that governs the analysis of the data is Beer's law, and this is defined in terms of the more conventional spectra that are familiar to most people. Thus, with few exceptions, the interferogram is converted to a single-beam spectrum via a Fourier transform and divided by a background, or  $I_0$ , spectrum to get a transmission spectrum. This is then converted to an absorption spectrum by finding the negative logarithm of the transmission spectrum. At this point, the absorption spectrum is compared with the

absorption spectrum (after it has undergone the same mathematical processing) of a pure gas to obtain the concentration.

All this mathematical processing is performed by computer and therefore is done numerically with whatever algorithms were available at the time the analysis software was written. A relevant question is whether all the processing is necessary, or if it is being done merely because it has always been done that way.

It is likely that most workers would essentially refuse to work with the interferogram directly because spectra have historically been used. However, this does not seem to be true of the single-beam spectrum. The single-beam spectrum also contains all the information about the concentrations, and it looks like a normal spectrum. The water vapor and the carbon dioxide absorption peaks are readily discernable, and any absorption due to other gases should also be discernable. Thus, for identification purposes, using the single-beam spectrum should not be a problem.

The problem seems to arise when quantitation is required. If the reference spectrum were also available in terms of a single-beam spectrum, a direct comparison could be made between the data spectrum and the reference spectrum, but only if the intensity levels of each were known on some absolute basis. Beer's law gives no hint of how the data are to be analyzed in the absence of an  $I_0$  spectrum. It is true that the single-beam spectrum is recorded with some

intensity level for the ordinate. But unless it is put on an absolute basis, the single-beam spectrum alone is not a sufficient piece of information to determine the transmission through the atmosphere.

Currently, there does not seem to be a satisfactory way to use the single-beam spectrum alone for the final analysis.

#### **4.7 General Advice About Background Spectra**

All of the currently used methods for generating a background spectrum are fraught with difficulties. No one method is generally accepted as the best method for acquiring a background. It is crucial for the operator to be aware of the importance of this spectrum and of two criteria for a valid background.

1. The background cannot contain any absorption features due to the target gas or gases.
2. The background spectrum must be valid for the time period over which it is used.

Although there seems to be agreement that the first point above is a requirement, no such consensus has been reached for the second. The time periods over which single backgrounds are used by various workers vary from a day to several months. However, one point has become clear. Whenever any optical component (light source, mirror, window, etc.) is changed in

the instrument, a new background must be acquired.

There are few guidelines as to what represents a valid background spectrum for the production of accurate data. One point is that the curvature of the baseline (maximum intensity) must be quite close to the curvature of the baseline of the field spectra.

There are two primary choices for the background that is to be used with a specific data set. If the absorbing peaks are narrow, as they are for methane or hydrogen fluoride, it is possible to construct a synthetic

background for the analysis. But for broad absorbing features like those exhibited by acetone, this is difficult. With broad features, even small changes in the curvature of the baseline can produce large errors. In general, the operator is advised to use a synthetic background whenever possible. Taking a short-path background should be considered only when the absorption feature of the target gas is very broad. A final reason to consider the use of a synthetic background is that it is essentially the only background that allows actual atmospheric concentrations to be determined.

## Chapter 5

### Water Vapor Spectra

#### SUMMARY

Specific topics that are addressed in this chapter are the following.

- Selection of spectra that can be used for generating a water vapor reference spectrum
- Creation of the water vapor reference spectrum itself
- Subtraction from the water vapor spectrum all absorption features of  $\text{CO}_2$ ,  $\text{N}_2\text{O}$ ,  $\text{CH}_4$ ,  $\text{CO}$ , and the so-called pollutant gases
- Example water vapor spectra for methane and ozone, selected because they present different problems to the operator

#### 5.1 Introduction and Overview

Water vapor absorption lines are present in all regions of the mid-IR wavelength region, as was shown in Figure 3-1. The water vapor spectrum interferes with the spectrum of almost every volatile organic compound in the atmosphere. Because of this, the absorption features of water vapor have to be accounted for during the analysis of field spectra.

Some amount of the water vapor absorption is accounted for if there is water vapor absorption in the background spectrum, as described in the previous chapter. However, when a synthetic background is used, all the water will still be in the field spectrum, and some residual amount will be there when other backgrounds are used. It is possible to

account for the water vapor by considering it as an interfering species in the analysis package. The software commercially available for performing a classical least squares analysis allows the operator to choose interfering gas species that are present in the wave number region of interest. To do this, however, a water vapor spectrum must be available. Although there are water vapor spectra available commercially, they are not suitable for use in this application because of line shape differences and other small instrumental effects, as well as insufficient path length.

This chapter explains how to use field spectra on site to produce a spectrum of pure water that can subsequently be used in the analysis of field spectra. Examples of water vapor spectra that can be used for the analysis of methane and ozone are

discussed, as these gases represent, perhaps, the extreme challenges that the operator will encounter.

## 5.2 Water Vapor Spectra Considerations

Any single-beam spectrum that exhibits a sufficient amount of water vapor absorption in the wave number region of interest can be used for the production of a water vapor reference spectrum. Spectra taken at short path lengths or during very dry periods may not be satisfactory. At Research Triangle Park, NC, we have seen the water vapor partial pressure change from a low of less than 1 torr in the winter to a high of 28 torr during the summer. Changes in the water vapor concentration of this magnitude, along with any instrument changes, may require that a new water vapor spectrum be produced. It is the responsibility of the operator to determine when the water vapor spectrum has to be remade, and no hard and fast rules on the frequency for creating a new spectrum are presently available. If the error bars of the analysis increase from one data set to another, a first step in determining the cause is to compare the water vapor reference spectrum with the water vapor in the field spectra.

The primary concern for the production of a water vapor spectrum is that the final result must not contain any of the target gas. If the water vapor spectrum does contain even a small amount of a target gas, the analysis will be in error by that amount. The ease with which the absorption features of the target gas can be removed from the

water vapor reference spectrum is dependent on many instrumental factors, and the process can be quite time-consuming. The removal of the target gas absorption is done by subtraction and in some instances requires great attention to detail.

## 5.3 General Process for the Production of a Water Vapor Spectrum

The general procedure that is to be followed to produce a water vapor reference spectrum is given below.

1. Select two single-beam spectra that will be combined into a water vapor absorption spectrum.
2. Use one of the spectra to create a synthetic spectrum that is to be used as the background.
3. Create the absorption spectrum that is to be used as the water vapor reference spectrum.
4. Subtract any absorption features that are known to be present from the target gas.
5. Analyze a number of the field spectra for the target gas, using the water vapor reference spectrum as an interfering species.
6. Determine if any of the target gas absorption remains in the water vapor spectrum.
7. Repeat Steps 4-6 until you are sure that there is no absorbance due to the target gases remaining.

A word of caution is necessary here. If analysis is to be done for more than one gas, the synthetic background in Step 2 should be created for all the gases of interest at the same time. Otherwise, when the absorption spectrum is created, some or all of the water vapor absorbance will disappear. If this occurs the process has to be started over.

### 5.3.1 Selection of Spectra

The spectra selected in Step 1 that are to be used to produce a water vapor reference spectrum should be taken at the same resolution as the field spectra. The water vapor spectrum should have a signal-to-noise ratio that is the same as or better than the field spectra. If possible, the water vapor concentration for these two spectra should be representative of the water vapor concentration in the field spectra to be analyzed. Curvatures and any other special features of the baselines of these spectra should be the same as those of the field spectra baselines over the wave number regions of interest. If both of these spectra are closely spaced in time, they should contain approximately the same amount of the target gas. The operator should select spectra at times when a minimum of the target gas is expected to be present. However, the operator should be aware that the target gas will be present in both spectra and should consider the ramifications of that fact.

### 5.3.2 Generation of Synthetic Background

Either of the two spectra selected above (Step 1) can be used to create a synthetic background that is then used to create an absorption spectrum. The synthetic background must be created over the same wave number region as will be used for the final analysis. The wave number region can be larger than that used for analysis, but it cannot be smaller. If the two spectra selected above are closely spaced in time they will probably both contain approximately the same amount of the target gas. This will certainly be the case with methane and nitrous oxide regardless of the time selected, but any set of spectra for ozone may have widely varying absorption due to ozone. Again, which one of the spectra is used for the synthetic background generation is arbitrary. Once the synthetic background has been prepared, it should be stored with an appropriate name.

### 5.3.3 Generation of the Absorption Spectrum

Use the remaining spectrum (after Step 2) as the data spectrum and the newly created synthetic background to create an absorption spectrum (Step 3). This is done exactly as all the other absorption spectra are created. (See Figure 2-8.) At this point it is not likely that the baseline of the absorption spectrum is at zero absorbance. To make the baseline zero, measure the height of the baseline above zero and simply subtract that amount from the spectrum. This completes the process of creating an

absorption spectrum, and it should be saved with an appropriate name.

#### 5.3.4 Subtraction of the Target Gas

This step (Step 4) is really an iterative process. The newly created water vapor spectrum must be used in the analysis of other spectra. The results of these analyses must be examined in an attempt to determine whether any of the target gas remains. If some remains, it must be subtracted from the water vapor spectrum. The process must then be repeated until the operator is sure that no target gas absorbance remains.

To analyze the water vapor spectrum, the operator must process several data spectra and use the newly created water vapor spectrum as an interfering species spectrum. The field spectra to be used should be chosen so that the target gas is a minimum. If the analysis shows the target gas to go through zero and actually become negative, then the water vapor spectrum still contains an absorbance due to the target gas. The negative concentration should be subtracted from the water vapor reference spectrum. Some gas concentrations will not go to zero at any time but will reach a minimum. This minimum can be set to zero in some instances, but it should at least be set to the minimum that the gas is known to achieve from other sources.

The actual subtraction can be done in two ways. The first way is to use the reference spectrum of the target gas and create a spectrum that represents the

amount of the target gas to be subtracted. This is done by multiplying the reference spectrum by an appropriate factor. This factor can be calculated by using the concentration path length product used in the reference gas and the path length that was used for data acquisition.

The second way is to do the subtraction interactively with the software. In this way, the operator can see the results of the subtraction directly and has a little more control of the process. Both procedures require some practice, and the operator must be aware that his first attempt may not be satisfactory.

#### 5.4 Calculated Water Spectra

Some time ago investigators at the Air Force Geophysics Laboratory in Cambridge, Massachusetts, compiled a high-resolution transmission molecular absorption database for the primary atmospheric gaseous constituents. This database is known as HITRAN and contains the data for calculating a water spectrum. Software has been developed that allows for the actual generation of the spectrum, and that software is called FASCODE. FASCODE generates a high-resolution spectrum using Lorentzian line shapes. These calculated spectra can then be mathematically shaped to fit the spectra produced by a particular FT-IR instrument by using the mathematics described in Chapter 8.

While the software is not readily available, this procedure has been tested for



several different resolutions and for several different FTIR instruments. It has been determined that this procedure works well, and all of the observable absorption features are quite accurately reproduced.

The above-referenced mathematical procedure will probably be used by NIST to generate lower resolution reference spectra from the high-resolution spectra that they are acquiring.

If this procedure can be used, it is recommended as the method of choice for the production of a water vapor reference. It eliminates all of the difficulties described in the previous sections about having to remove the absorptions of the other gases in the atmosphere. It has a flat baseline, and once the procedure is determined, a new reference can be generated in a few minutes' time.

### 5.5 Methane and Ozone Examples

Figure 5-1 shows the portion of a single-beam spectrum over which methane absorbs. The methane concentrations at Research Triangle Park are generally measured at about 2.5 ppm. We have seen methane concentrations as high as about 6 ppm in this area. The spectrum in Figure 5-1 actually contains water vapor and methane, although the methane is not very noticeable. Figure 5-2 has superimposed on it the synthetic background that will be used to manufacture an absorption spectrum. The synthetic background has been raised slightly above the single beam spectrum for clarity.

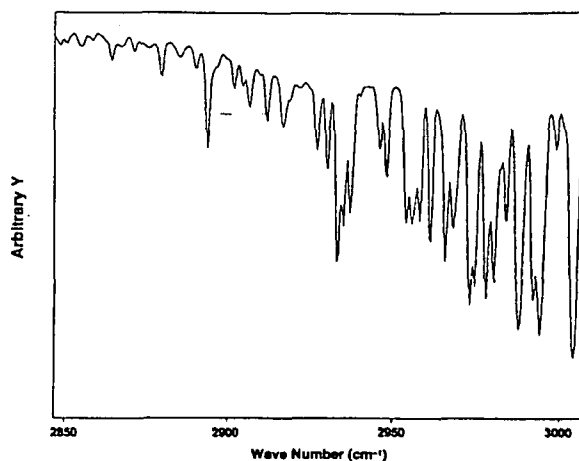


Figure 5-1. The Portion of a Single-Beam Spectrum Over Which Methane Absorbs.

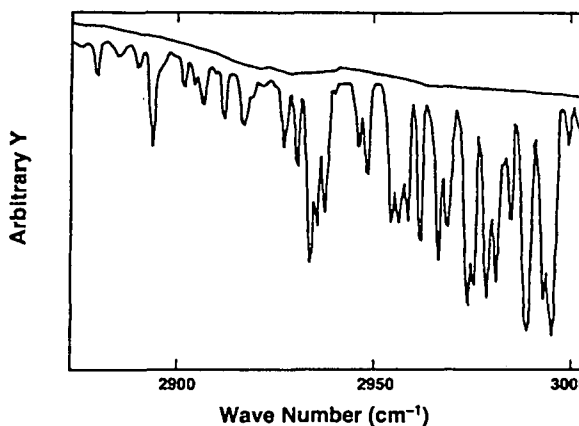
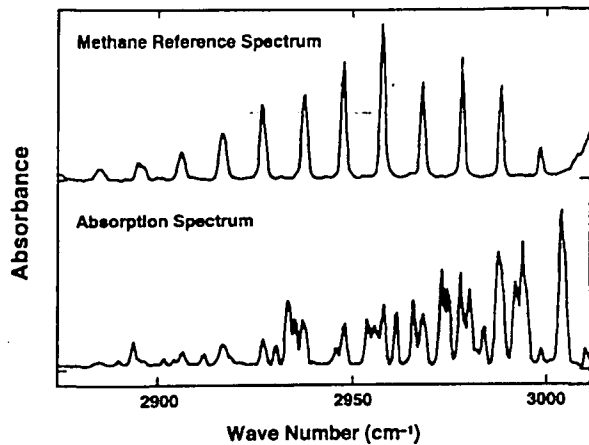


Figure 5-2. Methane Region with Synthetic Background Spectrum Superimposed.

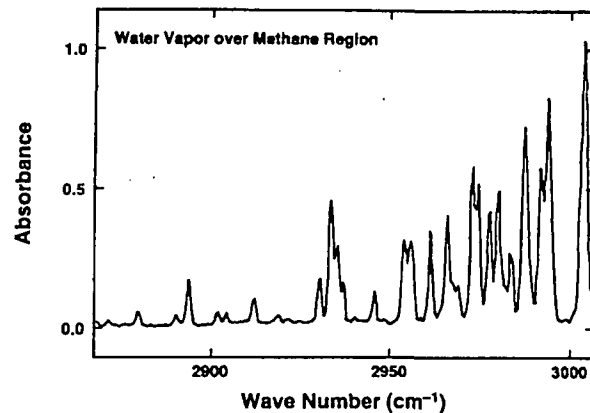
Figure 5-3 shows the absorption spectrum that has been made from the two spectra shown in Figure 5-2. Also shown in this figure is the methane reference spectrum. The task is now to subtract out the methane that is present in this absorption spectrum. There are two absorption peaks in



**Figure 5-3. Methane Reference Spectrum and the Calculated Absorption Spectrum.**

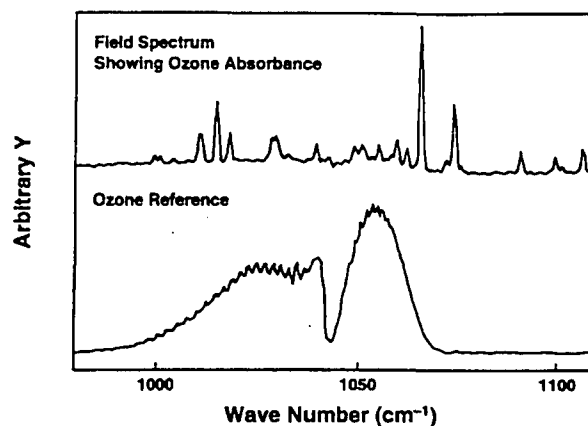
the methane spectrum that are virtually not impacted by water vapor. They are at 2916.7 and 2926.8  $\text{cm}^{-1}$ . The methane concentration can be calculated from the peak height of these two peaks. The concentration path length product of the reference spectrum is 81 ppm-m. The field spectrum was taken at a path length of 414 m, so the reference spectrum represents a concentration of  $81/414 = 196$  ppb. The measured peak height of the 2926.8- $\text{cm}^{-1}$  line is 0.00771 absorbance units for the reference spectrum and 0.1069 absorbance units for the field spectrum. Thus if the reference spectrum is multiplied by the factor  $0.1069/0.00771 = 13.9$  it will represent the same amount of methane as is in the field spectrum. That is to say that the absorbance in the data spectrum is indicative of  $196 \text{ ppb} \times 13.9 = 2.7$  ppm of methane. After multiplication, the reference can be subtracted from the field spectrum, and the methane should be removed from the water vapor spectrum.

Figure 5-4 shows the spectrum that has the methane removed and is now usable as a water vapor spectrum in the region of the methane absorbance. The operator must note, however, that many gases other than methane absorb in this region and, if they are still in the spectrum, they will cause errors in the analysis.



**Figure 5-4. Water Vapor Spectrum Made for the Methane Absorption Region.**

Removal of ozone from the water vapor spectrum is much more difficult, primarily because the absorption feature is broad. Figure 5-5 shows an atmospheric



**Figure 5-5. Atmospheric Ozone Absorption Spectrum and Ozone Reference Spectrum.**

ozone absorption spectrum and the ozone reference spectrum. The slight elevation of the absorption spectrum in the vicinity of  $1050\text{ cm}^{-1}$  is indicative of an absorbance due to ozone with a concentration of about 100 ppb. A significant problem with ozone occurs when the synthetic background is made. Here the absorption spectrum is so broad that at least one point in the ozone spectrum region must be chosen for the baseline. It is easiest to think that the point in the center of the spectrum where the absorbance dips almost to the baseline should be used. However, the ozone absorbance does not go to zero at that wave number. So, a very careful estimate for where that point should be placed needs to be made. A difficulty arises that is associated with the MCT detector, for which there is a curvature of the baseline in this wave number region. This means that the baseline cannot be made by connecting a line between two points along the curve.

Once the synthetic background has been made and the operator has an absorption spectrum, the ozone still has to be subtracted from it. There is almost no possibility that the ozone concentration will actually go to zero at any location but it should go through a minimum. For areas such as Research Triangle Park, where the atmospheric ozone is produced locally and not transported into the area from elsewhere, that minimum occurs at about 6:00 in the morning.

A plot of several days of ozone concentration taken at Research Triangle

Park during the month of June is shown in Figure 5-6. The negative values indicate that there is a significant amount of ozone in the water vapor spectrum. The question is just

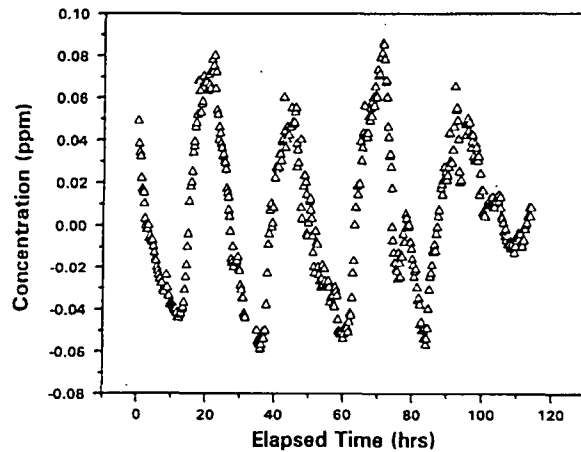


Figure 5-6. Ozone Measured at Research Triangle Park During June.

how much to subtract from the spectrum, because the ozone concentration does not go to zero. In this area, we are fortunate because there are other instruments that make measurements of ozone, and they can be used to determine the ozone minimum. Ozone is a criteria pollutant and is also monitored by the individual states. These data are generally available as hourly averages and may be useful to the operator who is trying to subtract the correct amount of ozone from the water vapor reference spectrum.

The operator must be aware that gases other than methane and ozone must be subtracted from the water vapor reference spectrum, even though they are all not covered here. Certainly the gases  $\text{CO}_2$ ,  $\text{N}_2\text{O}$ ,

and CO must be subtracted from the water vapor reference. When data are taken at industrial sites, any gas that is to be monitored or used as an interfering species must be subtracted from the water vapor reference spectrum.

## Chapter 6

### Siting

#### SUMMARY

The topics and specific points of emphasis discussed in this chapter include the following

- Siting considerations for long-term and short-term monitoring efforts
- Factors to consider when selecting the path
  - Short path versus long path
  - Prevailing winds
  - Slant path versus horizontal path
- What conditions warrant changing the path
- What ancillary measurements are required
- Calculation of the minimum path length required to detect specific concentrations of selected target gases
- An example of a specific monitoring site

#### 6.1 Introduction and Overview

There are two kinds of monitoring programs for which siting needs to be discussed. One is a long-term effort with the instrument placed in a more or less permanent position. The second is a short-term program designed to take data at a site for a period from a few days to a few weeks. Each of these situations, while similar, requires somewhat different thinking to actually site the instrument. The short-term program is more flexible in that the path configuration can be based on the meteorological conditions at the time of the monitoring program. Long-term monitoring programs must be designed

to allow for changes in the direction of the path as dictated by changing meteorological conditions, or useful data might be lost. Siting considerations for both situations are described in this chapter. Criteria for selecting the path, changing the path, and choosing the ancillary measurements to make at a monitoring site are also discussed.

There is little information in the literature pertaining to the long-term monitoring program. Even for the short-term program, the parameters that were considered in selecting the actual direction and length of the path have been discussed in only a cursory manner. A typical

statement is "The path was set up based on a knowledge of the prevailing winds." But what the wind field actually was during the observation period or where the prevailing wind data were taken is almost never presented. There is a similar lack of information concerning the selection of the path length and the partial pressure of water vapor in the atmosphere. For that matter, there is almost no discussion in the literature about how the length of the path is selected.

There are some sophisticated methods being studied by various groups that use real-time meteorological data for making decisions about the path. It seems that these techniques are more suited for permanent monitoring installations and not for short-term programs such as monitoring at small waste sites. Under any circumstances these methods have not been adequately tested, and an evaluation of these methods is considered to be beyond the scope of this document at the present time.

Other ongoing relevant work is being documented by the U.S. Environmental Protection Agency, which has prepared a set of changes to Part 58 of Chapter 1 of Title 40 of the *Code of Federal Regulations* (40CFR58) that define the appropriate ambient air monitoring criteria for open-path (long-path) monitors (U.S. Environmental Protection Agency, 1994). These amendments have been finalized and approved, and they specifically address the monitoring of the gases called the criteria pollutants. The amendments are significant in that they describe just how the path is to be chosen in terms of obstructions, height above the

ground, and changes in path height. They also describe the appropriate positioning of the path in relation to buildings, stacks, and roadways.

Several factors must be considered when selecting the path. These factors include (1) instrumental parameters, such as the signal-to-noise ratio (S/N) of the system and the divergence of the IR beam; (2) the characteristics of the target gases, such as concentrations and absorption coefficients; (3) the presence and concentrations of interfering species, such as water vapor and CO<sub>2</sub>; (4) meteorological data, such as wind direction and speed; and (5) physical constraints, such as the area of the emission source, the extent of the plume, and the availability of suitable sites to accommodate the instrument and peripherals.

Example calculations using Beer's law are given in this chapter to illustrate the minimum path length required to measure a specific concentration of a target gas. For example, the minimum path length required to measure ammonia at a concentration of 10 ppb would be approximately 21 m, assuming a minimum detection limit of  $3 \times 10^{-4}$  absorbance units, no interfering species, and a uniform concentration throughout the path. In contrast, the minimum path length required to measure 10 ppb of chlorobenzene would be 230 m. In general, the length of the path must be chosen to be the minimum length that will allow the measurement to be made with a meaningful statistical accuracy.

As an aid to the operator, Table 6-1, listing minimum detection limits for various

gases, is included. The limits in Table 6-1 were calculated by using a minimum detectable absorbance of  $10^{-3}$ . The units used in this table are ppm·m.

An example using a specific Superfund site is given in this chapter. Procedures are described for selecting a usable path for a short-term intensive study.

## 6.2 Selecting the Path

To select the length and the position of the path, the investigator must have some understanding of the ramifications of these choices. The immediate questions concern (1) the effect that the path has on the data that is produced and (2) the procedure that the operator follows for selecting a path.

Preliminary answers to those questions are found by referring to Beer's law. But the complete answers are more complicated. They include scattering and absorption by aerosols, the effects of water vapor and carbon dioxide on the S/N, and spectral interferences. When measuring plumes of finite extent, a path longer than the width of the plume is actually detrimental.

The amendments to 40CFR58 describe the following considerations for selecting the path.

- At least 80% of the path must be between 3 and 15 m above the ground.

- At least 90% of the path must be at least 1 m vertically or horizontally away from walls, etc.
- If the path has to be near a building, then it must be on the windward side of the building.
- Buildings or other obstructions may possibly scavenge the gases of interest. At least 90% of the path must have unrestricted airflow and be located away from obstructions so that it is removed by at least twice the height that the obstacle protrudes above the path.
- At least 90% of the path must be at least 20 m from the drip lines of trees.
- When monitoring is done for ozone, 90% of the path must be at least 10 m from a road that carries fewer than 10,000 cars a day. This criterion changes to 250 m for heavily traveled roads (> 110,000 cars per day).

There are other changes to 40 CFR Part 58 that are applicable to the use of FT-IR open-path monitors, but they are for concerns other than siting. The interested reader should obtain a copy of 40 CFR Part 58 from the Office of *Federal Register*, National Archives and Records Administration, Washington, DC. It is also available in most public libraries.

**TABLE 6-1. Estimated Method Detection Limits (MDLs) for Selected Gases<sup>†</sup>**

Compound	Class <sup>a</sup>	$v_{\max}^b$ ( $\text{cm}^{-1}$ )	MDL <sup>b</sup> (ppb-m)	$v_{\max}^c$ ( $\text{cm}^{-1}$ )	MDL <sup>c</sup> (ppb-m)
acetaldehyde	caa	1761	2063	2729	6674
acetonitrile	caa	1463	8403	1042	46095
acrolein	pp,caa	1730	1297	958	4509
acrylic acid	caa	1726	639	1439	1326
acrylonitrile	pp,caa	954	3398	971	4548
ammonia	pp	967	620	931	718
benzene	pp,caa	673	266	3047	4449
bis-(2-chloroethyl)ether	pp,caa	1138	2157	767	4372
bromomethane	pp,caa	1306	11547	2983	12455
1,3-butadiene	caa	908	1445	1014	5719
2-butanone	pp,caa	1745	1483	1175	3224
carbon dioxide	ag	2361	637	668	608
carbon disulfide	pp,caa	1541	191	1527	266
carbon monoxide	cp	2173	4583	2112	5417
carbon tetrachloride	pp,caa	795	178	773	1027
carbonyl sulfide	caa	2070	240	2051	330
chlorobenzene	pp,caa	740	1341	1483	3980
chloroethane	pp,caa	1288	6744	677	6871
chloroform	pp,caa	772	359	1219	1927
chloromethane	pp,caa	732	6652	1459	9517
<i>m</i> -dichlorobenzene	pp	1581	1266	784	1305
<i>o</i> -dichlorobenzene	pp	749	1428	1462	5142
dichlorodifluoromethane	pp	1161	294	921	303
1,1-dichloroethane	pp,caa	705	2049	1060	3053
1,2-dichloroethane	pp,caa	731	1983	1237	6803
1,1-dichloroethene	pp	869	1241	793	1814
1,2-dichloroethene	pp,caa	864	5024		
dichloromethane	pp,caa	750	1174	1276	4113
1,1-dimethylhydrazine	caa	2775	1962	909	3774
ethylbenzene	pp,caa	2975	2031	697	2277
ethylene oxide	pp,caa	3066	987	872	3327
formaldehyde	caa	1745	1248	2802	2581
hexane	caa	2964	1023	1467	7710
hydrogen chloride	caa	2945	3164	2822	3620
hydrogen fluoride	caa	4038	578	3877	761
hydrogen sulfide	caa	1293	535003		
isooctane	caa	2961	554		
methane	ag	3017	1597	1305	2998
methanol	caa	1033	1249	2982	5933
methylmethacrylate	caa	1169	1199	1748	1341
nitric oxide		1894	4388	1843	6816
nitrobenzene	pp,caa	1553	852	1355	1049
nitrogen dioxide	cp	1629	540	1599	742
nitrous oxide	ag	2213	932	1300	3946
ozone	cp	1054	2533	1040	3971
phosgene	caa	849	318	1832	667
phosphine	caa	2326	7699	992	12468
propionaldehyde	caa	1762	2305	2992	4107
propylene oxide	caa	3001	2838	837	4549
styrene	caa	695	1720	909	2908
sulfur dioxide	cp	1377	372		
sulfur hexafluoride	tracer	947	42	615	420
tetrachloroethene	pp,caa	915	708	781	2654
toluene	pp,caa	728	1632	3018	3583
1,1,1-trichloroethane	pp,caa	725	533	1088	1183
1,1,2-trichloroethane	pp,caa	742	1615	941	7933



**TABLE 6-1. Estimated Method Detection Limits (MDLs) for Selected Gases<sup>†</sup>**

Compound	Class <sup>a</sup>	$\nu_{\max}^b$ ( $\text{cm}^{-1}$ )	MDL <sup>b</sup> (ppb-m)	$\nu_{\max}^c$ ( $\text{cm}^{-1}$ )	MDL <sup>c</sup> (ppb-m)
trichloroethene	pp,caa	849	1173	944	1578
trichlorofluoromethane	pp	846	178	1084	634
vinyl acetate	caa	1225	688	1790	1327
vinyl chloride	pp,caa	942	2824	1620	3643
vinylidene chloride	caa	868	1669	1086	2501
<i>m</i> -xylene	pp,caa	768	1601	690	3825
<i>o</i> -xylene	pp,caa	741	1070	2949	5797
<i>p</i> -xylene	pp,caa	795	1765	2936	3340

<sup>†</sup>The MDLs were estimated by using values of the absorptivity calculated from  $1\text{-cm}^{-1}$  reference spectra with triangular apodization from a commercially available spectral library and a minimum detectable absorbance of  $1 \times 10^{-3}$ .

<sup>a</sup>Pollutant classification: priority pollutant (pp); criteria pollutant (cp); hazardous air pollutant from the 1990 Clean Air Act Amendment (caa); atmospheric gas (ag).

<sup>b</sup>Peak position and MDL for the most intense absorption band.

<sup>c</sup>Peak position and MDL for the second most intense absorption band in a different spectral region.

### 6.2.1 The Longest Path

It is possible to determine the maximum usable path in several ways. One is to use the noise equivalent power of the detector as the minimum signal that can be recorded. Another is to use a minimum S/N that the operator is willing to accept. Then if either the noise equivalent power (NEP) signal or the S/N is known at one distance and the energy falls off as the inverse square of the distance, the maximum possible path can be calculated. Any attempt to actually do this calculation results in the conclusion that the maximum path is essentially infinite.

In a practical sense the absorption due to water vapor will limit the usable path long before the theoretical limit calculated above can be reached. The water vapor line at  $1014.2\text{ cm}^{-1}$  has an absorbance of 0.01 at a total path length of about 30 m when the water vapor partial pressure is 10 torr. If an absorbance of 1 is considered the maximum

allowable for this line, then the maximum usable total path is about 3 km.

The companion to this document (Russwurm 1997) describes a method for determining the minimum detection limit for open-path FTIR systems. It has recently been shown by investigators in Germany (Dovard et al. 1997) that this detection limit does not vary with path length as is predicted by Beer's law. This is probably caused by the variability in the atmospheric constituents themselves. At any rate, the work by Dovard et al. implies that a maximum usable path is more on the order of 400–500 m.

### 6.2.2 Shortest Path Requirements

The shortest path for various gases can be calculated from the absorbance measured in the reference spectra, a knowledge of the minimum measurable absorbance, and the assumption that reciprocity holds. To make this calculation, the operator must have chosen the wave number region that will be

used for analysis and obtained the absorbance of the gas from the reference spectrum over that region. The operator must also choose a minimum concentration that is to be measured. Then, by using the minimum detectable absorbance, the minimum path can be calculated as follows.

1. Measure the absorbance at the appropriate wave number for the target gas from the reference spectrum. Record the concentration path length product at which this spectrum was taken.
2. Calculate the absorption coefficient  $\alpha$  for this gas by using the following formula.

$$\alpha = A_r / C_r L_r$$

where  $A$  is the absorbance and  $CL$  is the concentration-path length product. The subscript  $r$  refers to the reference spectrum.

3. Assume a minimum concentration that will be measured, and set the minimum detectable absorbance at 3 times the RMS baseline noise as measured under normal operating conditions, for example,  $3 \times 10^{-4}$ .
4. Calculate the minimum usable path ( $L_m$ ) from

$$L_m = A_m / \alpha C_m$$

where  $A_m$  is the minimum absorbance ( $3 \times 10^{-4}$ ) and  $C_m$  is the minimum concentration assumed in Step 3, and  $\alpha$  is the absorption coefficient calculated in Step 2.

The results of the above calculations for four different gases are given in Table 6-2.

### 6.2.3 Short Path Versus Long Path

As shown in the previous section, the selection of the path length begins by calculating the minimum usable length from Beer's law. If a retroreflector is used, the physical path can be half the optical path determined above. This is advantageous when plumes of finite size are being measured because the path length may be chosen close to the physical extent of the plume.

The length of the path must be chosen to be the minimum length that will allow the measurement to be made with a meaningful statistical accuracy. For the calculations above, this distance was determined by using a minimum absorbance of  $3 \times 10^{-4}$ , or about 3 times the best detection limit that is achievable at the present time. For homogeneously distributed gases, the path can be made longer with some advantage. But for plumes of finite extent, making the path longer than the plume is wide would be a detriment and should not be done. This is because the measurement actually determines the path average concentration, and if a portion of the path has zero concentration, there is a dilution effect. Another reason for choosing a path that is as short as possible is that the effects of spectral interferences will be minimized.

**Table 6-2. Minimum Usable Path Lengths\***

Gas	Wave Number (cm <sup>-1</sup> )	A <sub>r</sub>	C <sub>r</sub> L <sub>r</sub> (ppm-m)	α	C <sub>m</sub> (ppb)	L <sub>m</sub> (m)
p-dichlorobenzene	822	0.085	500	1.7 x 10 <sup>-4</sup>	10	176
chlorobenzene	1025	0.0227	170	1.34 x 10 <sup>-4</sup>	10	223
toluene	1031	0.0203	496	4.09 x 10 <sup>-5</sup>	10	734
benzene	1038	0.0027	27	1.0 x 10 <sup>-4</sup>	10	300

\*A<sub>r</sub> = absorbance of the reference spectrum, C<sub>r</sub>L<sub>r</sub> = concentration-path length product at which the reference spectrum was taken, α = absorption coefficient, C<sub>m</sub> = minimum concentration, L<sub>m</sub> = minimum usable path length.

A different example can be described as follows. There are times when a release of a tracer gas such as SF<sub>6</sub> is desirable. The question is how much must be in the path if it is to be detected. From Figure 6-1, it is seen that the absorbance of SF<sub>6</sub> at 947 cm<sup>-1</sup> is 1.56. The concentration path length is 66 ppm · m. Thus for a working detection limit of 3 × 10<sup>-4</sup> absorbance units and a path length of 50 m, the minimum average concentration in the path must be C = A/αL. The absorption coefficient α is obtained from α = A/CL = 1.56/66. Thus C = (3 × 10<sup>-4</sup> × 66)/(1.56 × 50) ≈ 0.25 ppb. It is clearly seen in this example that because of its large absorption coefficient, not much SF<sub>6</sub> is required for detection.

There is no distance with any of the available instruments that will reduce the absorption due to water vapor and carbon dioxide below the detection limits. In fact, in the wave number region of strongest absorbance for these gases the atmosphere is generally totally opaque. That is, there is

so much light being absorbed that none returns to the detector. These regions are not usable for data analysis with the FT-IR systems.

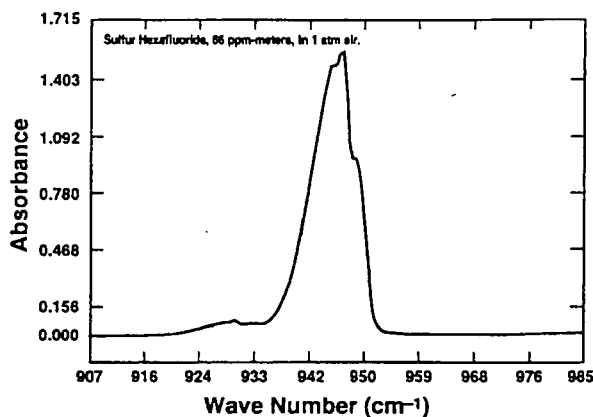


**Figure 6-1. Sulfur Hexafluoride Reference Spectrum.** (Used with permission of P.L. Hanst)

For long-term monitoring programs with permanent installations, the only real option is to place retroreflectors or light sources (depending on the instrument configuration) at various distances and switch from one to the other periodically or

on some predetermined schedule. A scanning system is available with some versions of open-path FT-IR monitors that facilitates this. Currently, almost no work has been done to define various lengths for various conditions. Thus, this chore must be individually repeated for each monitoring program.

#### **6.2.4 Prevailing Winds**

When using the FT-IR long-path technique, the operator depends on the wind to deliver the gases being emitted by a source to the infrared beam. Knowledge of the prevailing winds is important when setting up the path for long-term monitoring programs, but may be much less important for short-term programs. Most operators of open-path monitors have been concerned with short-term programs and know that the wind almost never comes from where the prevailing wind rose predicts. The short-term program usually demands that the operator be prepared to change the path configuration when the wind changes. For either the long-term or the short-term program, the ideal situation is to have more than one retroreflector or light source. This allows the path direction and length to be changed as the requirements of the program dictate without having to transport the instrument itself.

When emission rates need to be calculated from data taken with an FT-IR instrument, the wind direction and speed must be known. The direction of the path with respect to the wind must also be

known. A knowledge of the historical prevailing winds is of little use for this task. When emission rates are required, the wind field at the path must be measured directly.

#### **6.2.5 Slant Path Versus Horizontal Path**

Path orientation is important because the wind is the primary mode of transportation of the gases being monitored. Wind speed and direction can change dramatically over small regions when measured close to the ground. This is true not only because of the changing terrain but also because the motion of the air (a wind) must at least approach zero at the surface. There is some indication that the concentration contours of gases become very complex with altitude, at least in part because of turbulence. There are no data in the FT-IR literature that describe the variation of concentration with altitude. Because of these uncertainties, a comparison of the use of a slant path and a horizontal path cannot be made.

#### **6.3 Changing the Path**

The beginning of this chapter included a discussion of some of the ramifications of path selection. The question here is when should the path length or direction be changed? Obviously, if the plume from a point source or an area source is being monitored and the wind changes direction, the path should be changed. Changing the path, however, should be done in accordance with some plan. Items that need to be covered in the plan include the conditions

that make a change necessary, as described above. They should also consider the ramifications of the change, both the advantages and the disadvantages. For example, if the concentrations of gases crossing a fence line are being monitored, there is little point in changing the direction of the path.

Change in the length of the path should be considered only for purposes of taking a background spectrum or when spectral interferences from compounds like water vapor become so strong that the absorption due to the target compounds is overwhelmed. Whether any accurate monitoring can be done under that condition has not been studied. Certainly, it makes no sense to reduce the path length to the point where the target compounds cannot be monitored.

#### **6.4 Ancillary Measurements**

There are several reasons why some ancillary measurements must be made when taking data with an FT-IR open-path sensor. One is the requirement to take data that can be used for quality control and quality assurance purposes. (See Chapter 10 for a discussion of quality control and quality assurance procedures.) Another is that many programs will require ancillary data such as wind speed and direction. Also, for the foreseeable future, the amount of water vapor in the atmosphere should be monitored because too many unanswered questions about water vapor exist. By far, water vapor represents the strongest spectral

interference, and unless it is measured separately, problems may arise when the data are analyzed. It should be noted that a measurement of relative humidity is not satisfactory for this work. The actual partial pressure of water vapor must be found, and if relative humidity is measured, then the temperature must also be measured. The ambient pressure should also be recorded. At any one monitoring location operators can expect to experience a small change in ambient atmospheric pressure. In some cases, the data may have to be corrected for these changes. However, when acquiring data in places of high altitude, such as Denver, CO, a substantial change in pressure can be expected when compared to sea level. The operator must determine whether his experiment demands that these changes be accounted for in the data.

Guidance for selecting and setting up the instruments for making meteorological measurements can be found in a government handbook (U.S. Environmental Protection Agency 1989). Although this document does not directly address the long-path measurements, it does present useful information about meteorological instrumentation and measurements. For the long-path situation, the only measurements that should be obtained are probably those at or along the path itself.

#### **6.5 A Specific Case**

The literature offers very little information about procedures for selecting the path at any given site. The task is again

divided into two parts: (1) selecting a path or set of paths for long-term monitoring at a fixed installation and (2) selecting a usable path for short-term intensive studies. For this document, we will discuss the latter case only and do so by presenting a real case.

Figure 6-2 is an aerial photograph of a Superfund site undergoing remediation. The active region of the site is at the middle left of the photograph. Two large repository pits can be seen, one in the top middle of the photograph and the other in the top right. The former pit has been filled and capped with dirt while the latter is open and in the process of being lined. To gauge the size of the site, note that the vehicles immediately to the left of the FT-IR monitor are D8 bulldozers.

The site lies between two ridges (not shown), and the prevailing winds blow along the valley through the site from upper left to lower right. The first pit rises sharply from the active area for about 50 ft, and then the terrain falls off about 20 ft to the second pit. The road in front of the FT-IR monitor rises sharply in front of the second pit. The surrounding terrain is forest, with the trees rising about 40 ft above the ground level. Permission had been obtained to make measurements with the FT-IR monitor with the proviso that there would be no interference with the ongoing remediation. The FT-IR operators were not given access to the active area, which was defined as starting at the buildings in the foreground and extending to the forested region to the left of

and behind the capped pit. The remediation operation entailed digging soil from the active area, repacking it in metal drums, and moving it to the lined pit areas. Fluids that were encountered in the active area or in old drums were brought to the settling tanks seen in the middle of the photograph. The predominant chemical in the site was the herbicide Dicamba. Dicamba has a very low vapor pressure, but two by-products were thought to be present. They were benzonitrile and benzaldehyde, and the goal of the FT-IR study was specifically to measure these two compounds. Funding had been allocated for one week of field work. Although the proposed amendments to 40 CFR Part 58 were not available at the time of this study, they were almost exactly followed.

Benzonitrile has a single usable absorption band at  $757 \text{ cm}^{-1}$ . The absorbance of this band is 0.0346 when the concentration-path length product is 186 ppm-m. Repeating the calculation described above for the absorption coefficient gives  $\alpha = 0.0346/186 = 1.9 \times 10^{-4}$ . It was thought that benzonitrile would have a concentration of about 10 ppb. At the time of this study, the FT-IR instrument had a minimum detection limit of about  $1 \times 10^{-3}$  absorbance units. The minimum usable path is calculated as follows.

$$\begin{aligned} L_m &= 1 \times 10^{-3} / (1.9 \times 10^{-4} * 10 \times 10^{-3}) \\ &= 525 \text{ m} \end{aligned} \tag{Eq. 6-1}$$

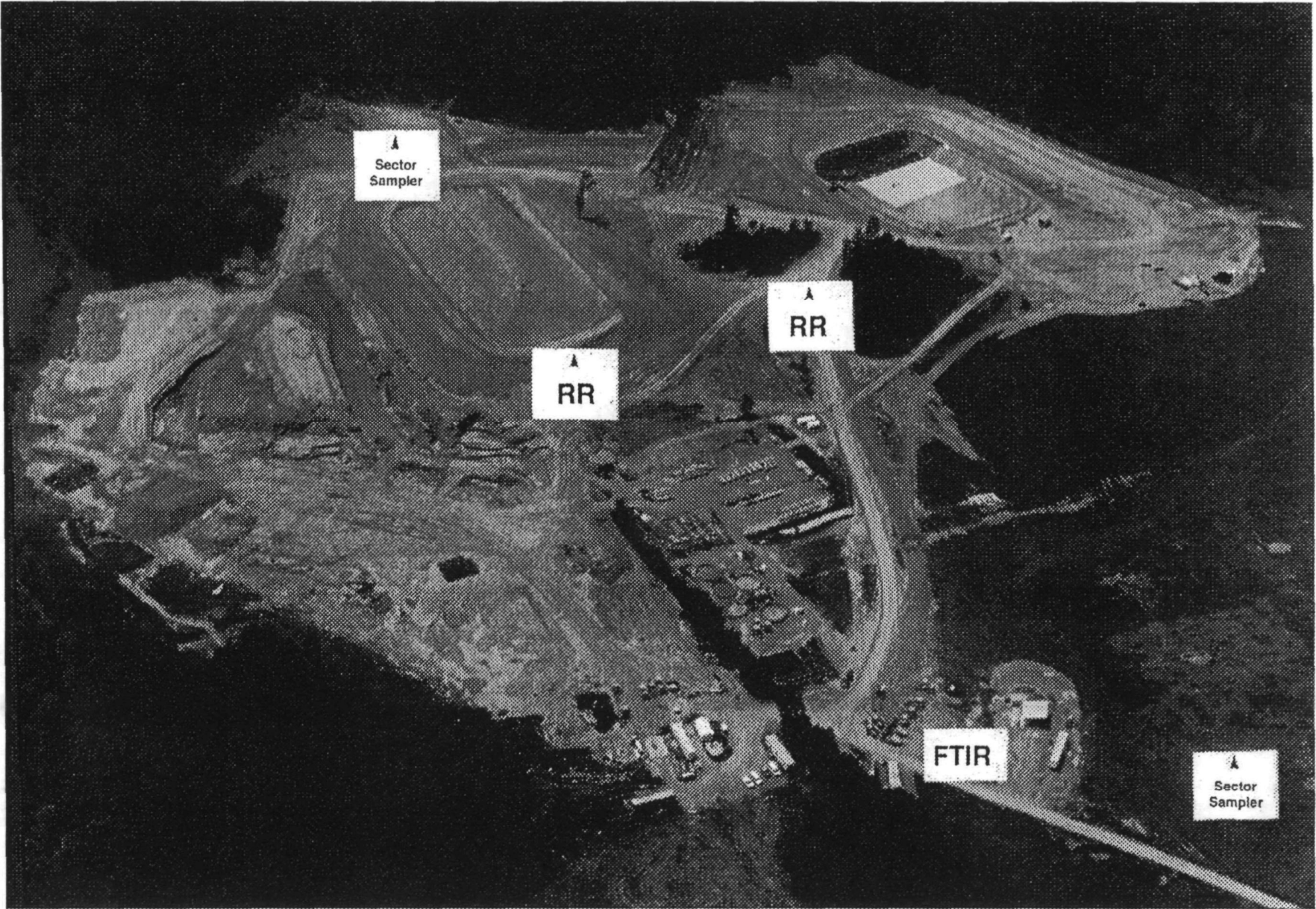


Figure 6-2. Aerial Photograph of a Superfund Site Undergoing Remediation.

The problem is somewhat more complicated than this because there is a weak interfering carbon dioxide peak at  $757\text{ cm}^{-1}$ . The task was then to site the instrument so that the retroreflector could be placed 250 m away while adhering to the constraints imposed by the remediation process. To obtain electrical power without the use of a generator, the only logical place to put the FT-IR monitor was at the main entrance to the site, as it is shown in the Figure 6-2 photograph. From there, only two possible paths of 250 m were available. They are shown in the photograph at the RR positions. The path that extends from the FT-IR monitor to the right RR position in the photograph was selected as the primary path because this would encompass the entire plume coming from the active area according to the prevailing winds. The secondary path, extending from the FT-IR monitor to the bottom of the capped repository pit (at the left RR position), was not really satisfactory because it rose too high above the ground level and went directly over the settling tanks. A path that is too high above the active area would leave the possibility that the plume might go under the beam. If the beam were to go directly over the settling tanks, flux calculations would be virtually impossible.

As an aside, during the week-long field program the remediation process was

halted because of a problem with the lining of the second pit. Also, during this time, the wind never blew more than 0.5 mph, and its direction was almost always from the bottom to the top of the photograph, contrary to expectation.

## 6.6 References

Douard, M., J. Zentzius-Reitz, T. Lamp, A. Ropertz, and K. Weber. 1997. Quality Assurance Procedures and Measurements for Open Path FTIR Spectroscopy Europto Series. *Proceedings of the EnviroSense '97 Meeting in Munich, Germany*. SPIE 3107:114-125.

Russwurm, G.M. 1997. Compendium Method TO-16. Long-Path Open-Path Fourier Transform Infrared Monitoring of Atmospheric Gases. In *Compendium of Methods for the Determination of Toxic Organic Compounds in Ambient Air, Second Edition*, EPA/625/R-96/010b, U.S. Environmental Protection Agency, Research Triangle Park, NC.

U.S. Environmental Protection Agency. 1989. *Quality Assurance Handbook for Air Pollution Measurement Systems, Vol. IV - Meteorological Measurements*. U.S. Environmental Protection Agency, Research Triangle Park, NC.

U.S. Environmental Protection Agency. 1994. Ambient air quality surveillance siting criteria for open path analyzers (proposed rule). *Fed. Reg.* 59(159):42541-42552.



## Chapter 7

### Resolution Considerations in FT-IR Long-Path, Open-Path Spectrometry

#### SUMMARY

The topics and specific points of emphasis discussed in this chapter include the following.

- The definition of resolution in FT-IR spectrometry
- The trading rules between resolution, the signal-to-noise (S/N) ratio, and measurement time
- Example spectra of atmospheric constituents and selected VOCs that illustrate the following effects.
  - Effect of resolution on peak shape and intensity
  - Effect of apodization and zero filling on peak shape and intensity
- A discussion of the effect of resolution on quantitative analysis
- A case study illustrating the effects of resolution, zero filling, and baseline noise on the CLS analysis of multicomponent mixtures

#### 7.1 Introduction and Overview

One important issue regarding the use of long-path, open-path FT-IR systems for monitoring hazardous air pollutants is the appropriate spectral resolution to be used during data acquisition. A resolution should be chosen to maximize the ability to resolve spectral overlap while maintaining a balance between the S/N, analysis time, and data storage requirements. Several factors must be considered when determining the optimum resolution for measuring the IR spectra of atmospheric constituents along an open long path. These factors include (1) the ability to

distinguish between the spectral features of target analytes and those of ambient interfering species in the atmosphere, such as water vapor and CO<sub>2</sub>; (2) the trade-offs between resolution, IR peak absorbance, and S/N; and (3) practical considerations, such as measurement time, computational time to process the interferogram, and the size of the interferogram file for data storage. The use of an inadequate instrumental resolution can distort the true absorption spectrum, affect the quantitative relationship between absorbance and concentration, and diminish the ability to resolve spectral overlap. Resolutions ranging

from 0.25 to 2  $\text{cm}^{-1}$  have been suggested for use in FT-IR monitoring, but there currently is no consensus as to what resolution is generally applicable. The nonlinear response caused by the apodization function discussed in Chapter 8 strongly indicates that higher resolution improves the accuracy of the data.

This chapter describes the fundamental aspects of resolution in FT-IR spectrometry and illustrates the effects of resolution and related instrumental parameters on the measured spectrum. The trading rules that determine the balance between resolution and S/N are discussed. Test spectra were obtained in the laboratory and along an open path to illustrate the effects of resolution, apodization, and zero filling on the IR spectra of  $\text{CO}_2$  and water vapor, common atmospheric species that can interfere with analytical measurements, and selected gases and VOCs. Studies from the literature that address resolution requirements in long-path FT-IR monitoring are discussed. A case study illustrating the effects of resolution, zero filling, and baseline noise on the CLS analysis of multicomponent mixtures is also presented.

In FT-IR spectrometry, the minimum separation in wave numbers ( $\text{cm}^{-1}$ ) of two spectral features that can be just resolved is inversely related to the maximum optical path difference in centimeters of the two mirrors employed in the Michelson interferometer. If the desired resolution is increased by a factor of 2, for example, from 1- to 0.5- $\text{cm}^{-1}$  resolution, the moving mirror in the interferometer must travel twice as far. In

practical terms this means that the scan time will be approximately twice as long, the interferogram file will be approximately twice the size for data storage, and the time required to process the interferogram will be longer for the higher resolution measurement.

The instrumental resolution also affects the S/N. In general, if the size of the aperture, or Jacquinot stop, in the interferometer is held constant, the baseline noise in an FT-IR spectrum is directly proportional to the resolution of the interferometer for measurements made in equal times. For example, changing the resolution from 1- to 0.5- $\text{cm}^{-1}$  increases the noise level by a factor of 2 for equal measurement times. Therefore, to obtain the same baseline noise level for the 0.5- $\text{cm}^{-1}$  spectrum as was measured for the 1- $\text{cm}^{-1}$  spectrum, the measurement time would have to be quadrupled (because the S/N is proportional to the square root of the measurement time).

As described in Chapter 8, resolution also affects the peak absorbance of the bands being measured. For narrow spectral features, the peak absorbance will only approximately double on halving the resolution. In this case, the S/N is nearly the same for the spectra acquired at the higher and lower resolution settings, provided the measurement time is equal. For broad spectral features whose peak absorbance does not change appreciably as a function of resolution, the lower resolution

measurement is preferable. For strongly absorbing bands, whether they are broad or narrow, calibration curves of absorbance values measured at different resolutions and plotted versus concentration must be developed to ascertain the optimum resolution to be used. In light of the work outlined in Chapter 8 it seems to be better to use the highest resolution at which the instrument can operate.

In general, the minimum limit of detection (LOD) should be found for measurements made at the lowest possible resolution that adequately resolves the spectral features of the analyte from those of interfering species. The use of an inadequate resolution can distort the true absorption spectrum, affect the quantitative relationship between absorbance and concentration, and diminish the ability to resolve spectral overlap. Conversely, the use of a higher resolution than is required can result in a poorer S/N and an unnecessary increase in measurement time, processing time, and data storage requirements.

There is currently no consensus as to what resolution and related parameters are generally applicable in long-path, open-path FT-IR monitoring. Most likely, the optimum resolution will need to be determined on a case-by-case basis, depending on the spectral characteristics of the target compounds and their concentration, the path length, and the presence of interfering species. In field measurements, a qualified judgement must be made taking into account these factors in addition to the practical

considerations discussed above and in Chapter 8.

## 7.2 Definition of Resolution

An understanding of the resolution requirements in FT-IR long-path, open-path monitoring requires an understanding of the basic principles involved in generating an interferogram and the operations performed on the interferogram prior to converting it to a spectrum. The following discussion is an attempt to describe these basic principles in a way that will be of general use to analysts in FT-IR monitoring. For a more rigorous treatment of the fundamentals in FT-IR spectrometry, the reader is referred to the definitive text by Griffiths and de Haseth (1986) or several other excellent references (Horlick 1968; Bell 1972; Herres and Gronholz 1984) and Section 2.4.2 of this document.

As shown in Section 2.4.2, the minimum separation in wave numbers of two spectral features that can be resolved is inversely related to the maximum optical path difference, in centimeters, of the two interferometer mirrors employed in the Michelson interferometer. The closer the separation of the two spectral features, the greater the optical path difference must be before the spectral features can be resolved.

In terms of the measured spectrum, resolution can be defined as the minimum separation that two spectral features can have and still be distinguished from one another. A commonly used requirement for

two spectral features to be considered resolved is the Raleigh criterion. This criterion states that two bands that have identical intensity, band shape, and peak width are resolved when the minimum of one band falls on the maximum of the other. When this is the case, there is a dip corresponding to approximately 20% of the absorption maxima between the two overlapping spectral features. It should be noted that this criterion is valid only for a sinc<sup>2</sup> instrument line shape, such as that found in a dispersive spectrometer or an FT-IR instrument using triangular apodization.

The actual spectral resolution in the frequency domain that can be obtained by an interferometer is also affected by the truncation of the interferogram and the application of various apodization functions. The apodization functions can increase the bandwidth and also change the line shape. Apodization is discussed further in Section 7.3.3 and in Chapter 8.

### 7.3 Trading Rules in FT-IR Spectrometry

The quantitative relationships between the S/N, resolution, and measurement time in FT-IR spectrometry are referred to as "trading rules". The factors that affect the S/N and dictate the trading rules are expressed in Equation 7-1, which gives the S/N of a spectrum measured with a rapid-scanning Michelson interferometer. (The derivation of Equation 7-1 is given by Griffiths and de Haseth [1986].)

$$\frac{S}{N} = \frac{U_\nu(T)\theta\Delta\nu t^{1/2}\xi D^*}{(A_D)^{1/2}} \quad (\text{Eq. 7-1})$$

where  $U_\nu(T)$  = the spectral energy density at wave number  $\nu$  from a blackbody source at a temperature  $T$

$\theta$  = the optical throughput of the spectrometric system

$\Delta\nu$  = is the resolution of the interferometer

$t$  = is the measurement time in seconds

$\xi$  = the efficiency of the interferometer

$D^*$  = the specific detectivity, a measure of the sensitivity of the detector

$A_D$  = the area of the detector element

As shown in Equation 7-1, the S/N of a spectrum is proportional to the square root of the measurement time ( $t^{1/2}$ ). For measurements made with a rapid scanning interferometer operating at a constant mirror velocity at a given resolution, as would most likely be the case in FT-IR monitoring applications, the S/N increases with the square root of the number of scans being averaged.

The relationship between the S/N and resolution is not as straightforward as implied in Equation 7-1. If the physical parameters of the spectrometric system,

such as the measurement time, optical throughput, and the interferometer efficiency, are assumed to be constant for measurements made at both high and low resolution, the S/N will be halved on doubling the maximum retardation of the interferometer ( $\Delta_{\max}$ ) or halving the resolution ( $\Delta\nu/2$ ). Because the S/N is proportional to the square root of the measurement time, the measurement time required to maintain the original baseline noise level must be increased by a factor of 4 each time  $\Delta_{\max}$  is doubled, or  $\Delta\nu$  is halved, for measurements made at a constant optical throughput.

The optical throughput does not necessarily remain constant throughout the range of resolutions that could be used to measure atmospheric gases. In low-resolution measurements, a large optical throughput is allowed for the interferometer, and the throughput is limited by the area of the detector element or the detector foreoptics. Most commercial low-resolution FT-IR spectrometers operate with a constant throughput for all resolution settings.

Instruments capable of high-resolution measurements are equipped with adjustable or interchangeable aperture (Jacquinot) stops installed in the source optics that reduce the solid angle of the beam passing through the interferometer. Spectra collected at high resolutions are generally measured with a variable throughput, which decreases as the spectral resolution increases.

In high-resolution measurements made under variable throughput conditions, the

throughput is halved as  $\Delta_{\max}$  is doubled. This results in an additional decrease in the S/N by one-half, which requires increasing the number of co-averaged scans by another factor of 4 to obtain the original S/N. Thus, for high-resolution FT-IR spectrometers operating under variable throughput conditions, the total measurement time is increased by a factor of 16 when  $\Delta_{\max}$  is doubled, if the S/N ratio is to stay the same.

The above discussions apply only to the effect of resolution on the baseline noise level. Resolution may also affect the peak absorbance of the bands being measured. For a narrow spectral feature whose full width at half height (FWHH) is much less than the instrumental resolution, the peak absorbance will only approximately double on doubling  $\Delta_{\max}$ . Assuming this band was measured under constant-throughput conditions, its S/N would be the same for measurements taken at the higher and lower resolution settings, provided the measurement times are equal. However, the degree of overlap by nearby spectral features will be reduced when the measurement is taken at a higher resolution. Therefore, in this case the higher resolution measurement is preferred.

For weak, broad spectral features whose peak absorbance does not change as a function of resolution, the lower resolution measurement is preferable when the optical throughput is constant. For strongly absorbing bands, whether they are broad or narrow, calibration curves of absorbance values measured at different resolutions and

plotted versus concentration must be developed to ascertain the optimum resolution to be used.

In general, the minimum LOD should be found for measurements made at the lowest possible resolution that adequately resolves the spectral features of the analyte from those of interfering species. Increasing the resolution beyond this point degrades the S/N. In FT-IR monitoring, the optimum resolution will be determined by the band widths of the absorption lines in the spectra of the target compounds, the presence of interfering species, and the S/N of the system. The optimum resolution will most likely vary with respect to specific analytes and measurement conditions.

#### 7.4 Example Spectra of CO<sub>2</sub> and Water Vapor

Water vapor and CO<sub>2</sub> have IR absorption bands with theoretical bandwidths

as narrow as 0.1 cm<sup>-1</sup>, according to the USF HITRAN-PC database (University of South Florida 1993). To fully characterize the IR spectra of these compounds, which have absorption bands that may overlap with those of target compounds, an FT-IR spectrometer capable of high-resolution measurements must be employed.

A series of experiments was conducted on a benchtop FT-IR spectrometer in the laboratory and with a transportable FT-IR monitor in the field to illustrate the effects of resolution on the IR spectra of CO<sub>2</sub> and water vapor. Three separate series of experiments were performed. In the first set of experiments, single-beam sample and background spectra were collected at various instrumental resolution settings with the benchtop spectrometer purged with nitrogen. These spectra were used to generate the data given below in Section 7.4.1.1 (Table 7-1).

Table 7-1. Resolution Test Data

Resolution (cm <sup>-1</sup> )	Fourier Transform Points	File Size (bytes)	Scan Time (s)*	Process Time (s)	RMS Noise 2150-2100 cm <sup>-1</sup> (10 <sup>-3</sup> Abs)**
0.25	131072	300268	194	249	1.5115
0.50	65536	168268	112	119	0.9007
1.0	32768	100267	69	60	0.4504
2.0	16384	67803	49	32	0.2347
4.0	8192	35034	28	16	0.1102
8.0	4096	18650	18	10	0.0590
16.0	2048	10266	13	8	0.0225

\* Time to collect 100 scans.

\*\* RMS noise for 1-min measurement times.

In the second set of experiments, a background interferogram was collected at  $0.125\text{ cm}^{-1}$  with the spectrometer purged, and a sample interferogram was collected with the sample compartment open to the laboratory air. These interferograms were used to generate lower resolution spectra by reducing the number of data points used for the Fourier transform. These spectra are shown in Figures 7-1 and 7-2. In the third set of experiments, single-beam spectra were collected along an open path of 150 m at  $0.5$ -,  $1.0$ -, and  $2.0\text{-cm}^{-1}$  resolution with a transportable FT-IR monitor. These spectra are shown in Figure 7-3.

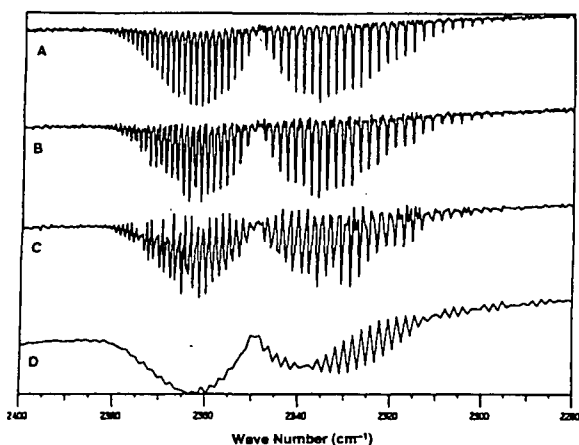


**Figure 7-1. Single-Beam IR Spectra of  $\text{CO}_2$  Measured at (A)  $0.25\text{-cm}^{-1}$ , (B)  $0.50\text{-cm}^{-1}$ , (C)  $1.0\text{-cm}^{-1}$ , and (D)  $2.0\text{-cm}^{-1}$  Resolution with No Apodization and No Additional Zero Filling.**

All laboratory spectra were collected on a benchtop FT-IR spectrometer, which has a nominal instrumental resolution selectable to  $0.125\text{ cm}^{-1}$ . The data system uses two 68000 data processors and contains 2 megabytes of RAM. The long-path spectra

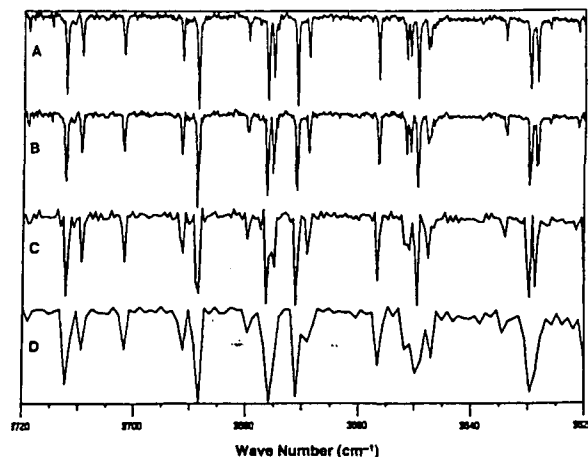


**Figure 7-2. Single-Beam IR Spectra of Water Vapor Measured at (A)  $0.25\text{-cm}^{-1}$ , (B)  $0.50\text{-cm}^{-1}$ , (C)  $1.0\text{-cm}^{-1}$ , and (D)  $2.0\text{-cm}^{-1}$  Resolution with No Apodization and No Additional Zero Filling.**

of water vapor were obtained on a portable FT-IR spectrometer with resolutions selectable to a nominal  $0.5\text{ cm}^{-1}$ . Data acquisition and manipulations were carried out by using a commercial software package on a 486/33-MHz personal computer with 8 megabytes of RAM.

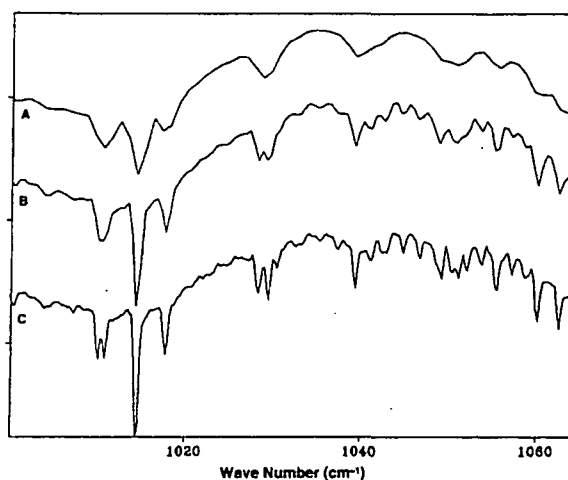


**Figure 7-3. Single-Beam IR Spectra of Water Vapor Measured at (A)  $2\text{-cm}^{-1}$ , (B)  $1\text{-cm}^{-1}$ , and (C)  $0.5\text{-cm}^{-1}$  Resolution over a 150-m Path.**

### 7.4.1 Resolution Effects

The effects of resolution on the IR spectra of CO<sub>2</sub> and water vapor obtained from laboratory measurements and long-path measurements are addressed in this section. The laboratory measurements illustrate the relationship between resolution and scan time, data processing time, data storage requirements, spectral definition, and S/N. The long-path measurements are used to characterize the water vapor spectrum in a region in which it interferes with the analysis of an example target compound, toluene.

#### 7.4.1.1 Laboratory Measurements

Single-beam spectra of the p- and r-branch of CO<sub>2</sub> were recorded at resolutions ranging from 0.25 to 2 cm<sup>-1</sup> as shown in Figure 7-1. No apodization or additional zero filling was applied to the interferograms prior to performing the Fourier transform. When plotted on the scale from 2400 to 2280 cm<sup>-1</sup>, the spectral features of the CO<sub>2</sub> bands appear to be defined equally well at 0.25- and 0.5-cm<sup>-1</sup> resolution, although slight differences were observed in the FWHH measurements. In the spectrum measured at 1-cm<sup>-1</sup> resolution, there is a more noticeable degradation of the rotational fine structure. This structure is completely lost in the spectrum measured at 2-cm<sup>-1</sup> resolution, and the r-branch appears as a broad continuum. The absorption bands that make up the rotational fine structure of CO<sub>2</sub> have bandwidths of approximately 0.2 cm<sup>-1</sup>, according to the USF HITRAN-PC database (University of South Florida 1993). Thus,

these bands are not fully resolved, even at 0.25-cm<sup>-1</sup> resolution, and a resolution of 0.125 cm<sup>-1</sup> is required to fully characterize these bands.

Similar results were observed in spectra of water vapor measured at resolutions of 0.25, 0.5, 1, and 2 cm<sup>-1</sup> with no apodization or additional zero filling (Figure 7-2). The single-beam spectrum of water vapor between 3720 and 3620 cm<sup>-1</sup> exhibits several isolated, sharp features as well as overlapping features that are nearly baseline resolved in the spectrum measured at 0.25-cm<sup>-1</sup> resolution. The spectrum measured at 0.5-cm<sup>-1</sup> resolution exhibits a slight degradation in spectral definition as compared to the 0.25-cm<sup>-1</sup> spectrum, although the general characteristics of the bands are retained. The overall band structure is still present in the spectrum measured at 1-cm<sup>-1</sup> resolution; however, the distinction between some of the closely spaced, weaker bands is lost. In the spectrum measured at 2-cm<sup>-1</sup> resolution, there is no longer any evidence of the spectral definition exhibited in the previous spectra, and the bands are significantly broader.

The effect of resolution on scan time, data processing time, data storage requirements, and baseline noise levels was also determined. For these tests, single-beam sample and background spectra were measured independently at each resolution setting, while holding the Jacquinot stop constant. The number of scans for each spectrum was 100. The RMS noise levels



were calculated from spectra with a 1-min measurement time. The results from this test are presented in Table 7-1.

As shown in Table 7-1, the time required to collect 100 scans increases significantly upon acquiring data at higher resolutions. This is because the moving mirror in the interferometer must travel a greater distance as  $\Delta_{\max}$  is increased for higher resolution scans. On average, the total scan time for 100 scans for this particular instrument increased by a factor of 1.6 each time  $\Delta_{\max}$  was doubled, indicating the poor duty cycle efficiency.

The time required to process the interferogram also increases as  $\Delta_{\max}$  (and as the number of data points collected for the interferogram) increases. In these examples, the processing time is that required to perform the Fourier transform and related operations on both the background and sample interferograms and to calculate the absorption spectrum. The time required to process the interferogram increased on average 1.8 times each time  $\Delta_{\max}$  was doubled. It should be noted that these data were processed on a relatively old data system using a 68000 processor chip. With newer and faster computers the time required to perform the Fourier transform is not as much of a factor. For example, on a 486/33MHz machine with 8 megabytes of RAM, the time required to perform the Fourier transform and plot a single-beam spectrum is 1.65, 3.23, and 7.74 s for 2-, 1-, and 0.5-cm<sup>-1</sup>-resolution interferograms, respectively. However, if time resolution is an

important parameter in a specific FT-IR monitoring application, then the combination of scan time and processing time should be considered, or the interferograms should be stored for post-run processing.

The amount of disk space required for data storage increases almost by a factor of 2 each time the resolution is increased by a factor of 2. For 3.5-in floppy disks with 1.4 megabytes of storage capacity, this means that, for example, 14 interferograms collected at 1-cm<sup>-1</sup> resolution could be stored on one disk, whereas only eight 0.5-cm<sup>-1</sup> interferograms could be stored on one disk at a time. The newer data acquisition software packages and data stations make more efficient use of disk space. For example, 21 interferograms collected at 1-cm<sup>-1</sup> resolution on a newer system could be stored on one 3.5-in. floppy disk. If large amounts of data are expected to be collected, such as might be the case in routine FT-IR monitoring studies, data storage requirements could be an important consideration.

The RMS noise measured between 2200 and 2100 cm<sup>-1</sup> increases as  $\Delta_{\max}$  increases. The data in Table 7-1 were taken from absorption spectra created from background and sample spectra collected over a 1-min scan time with a constant aperture at each resolution setting. These data follow closely the twofold increases in baseline noise expected each time the resolution is increased by a factor of 2. It should be noted that only the baseline noise level was measured in this experiment. Resolution may also affect the peak

absorbance of the bands being measured. For example, for a weak spectral feature whose FWHH is much less than the instrumental resolution, the peak absorbance will approximately double on increasing the resolution by a factor of 2. Therefore, the S/N would be the same for measurements taken at the higher and lower resolution settings, provided the measurement times are equal. For broad bands, the peak absorbance will not be affected by changes in resolution, and the lower resolution measurement would be preferred.

#### **7.4.1.2 Long-Path Measurements**

The laboratory measurements described above illustrate some of the trade-offs encountered between resolution and other experimental parameters. However, the path length used in those studies was insufficient to detect many of the water vapor bands that interfere with bands of target pollutants, such as toluene. Russwurm (1992) has addressed the limitations that the presence of overlapping water vapor bands impose on the ability to detect and quantify toluene by long-path FT-IR spectrometry. With a CLS analysis of the toluene band at  $1031\text{ cm}^{-1}$ , the detection limit for toluene in the presence of 10.5 torr of water vapor was estimated to be approximately 1 ppm. In this spectral region over a path length of 420 m, the absorbance due to water vapor was found to be strong compared to that of toluene. These data clearly indicate that to optimize the detection limits of FT-IR monitors for difficult target

compounds, such as toluene, the water vapor spectrum must be well characterized.

Single-beam spectra measured at 2-, 1-, and  $0.5\text{-cm}^{-1}$  over a 150-m path length are shown in Figure 7-3. The interferograms were processed with triangular apodization and no additional zero filling. The spectra are plotted over the wave number region used to quantify toluene. As expected, the FWHHs of the water vapor absorption bands between  $1000$  and  $1060\text{ cm}^{-1}$  are narrower in the  $0.5\text{-cm}^{-1}$  resolution spectrum as compared to the 1- and  $2\text{-cm}^{-1}$  resolution spectra. In addition, spectral features are resolved in the  $0.5\text{-cm}^{-1}$  spectrum that appear as a single band in the other two spectra. For example, the band at  $1010\text{ cm}^{-1}$  in the  $1\text{-cm}^{-1}$  spectrum is resolved into a doublet at  $1010$  and  $1010.7\text{ cm}^{-1}$  in the  $0.5\text{-cm}^{-1}$  spectrum. Also, bands appearing at  $1028.3$  and  $1029.5\text{ cm}^{-1}$  are much better resolved in the  $0.5\text{-cm}^{-1}$  spectrum. In fact, they are not resolved at all in the  $2\text{-cm}^{-1}$  spectrum.

To completely resolve all of the overlapping bands in the spectrum of water vapor over this wave number region, the spectrum must be recorded at  $0.125\text{-cm}^{-1}$  resolution. The theoretical spectrum of water vapor from the USF HITRAN-PC database is shown in Figure 7-4A.

A  $0.125\text{-cm}^{-1}$  resolution spectrum of water vapor recorded on the ROSE system (Herget 1992) is shown in Figure 7-4B. In these spectra the band at  $1018\text{ cm}^{-1}$  can be resolved into two components, and the bands at  $1010$  and  $1010.7\text{ cm}^{-1}$  are

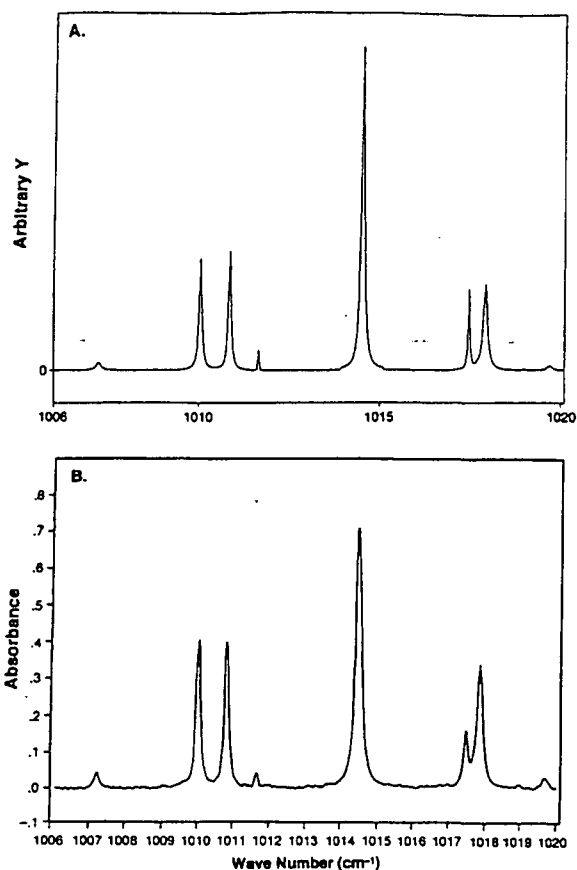


**Figure 7-4. IR Spectra of Water.** (A) 10 torr of water vapor over a 300-m path, from the USF HITRAN-PC database (University of South Florida 1993). (B) Water vapor recorded at 0.125-cm<sup>-1</sup> resolution of the ROSE system (reproduced with permission from W.F. Herget).

completely baseline resolved. Whether or not measuring ambient spectra at 0.125-cm<sup>-1</sup> resolution improves the results of quantitative analyses for difficult target compounds, such as toluene, has not yet been fully investigated.

#### 7.4.2 Zero-Filling Effects

When the interferogram contains frequencies that do not coincide with the frequency sample points, the spectrum

resembles a "picket fence" (Herres and Gronholz 1984). An example of this effect is shown in Figure 7-5 in the spectrum of CO<sub>2</sub> measured on a benchtop FT-IR instrument. In this example, the spectrum of CO<sub>2</sub> measured at 0.25-cm<sup>-1</sup> resolution with no apodization and a zero-filling factor of 1 (Figure 7-5A) exhibits excellent peak shape. However, in the spectrum measured at 0.5 cm<sup>-1</sup> with no additional zero filling (Figure 7-5B), the peaks of several absorption bands are squared off. This effect can be overcome by adding zeros to the end of the interferogram before the Fourier transform is performed. This operation is referred to as zero filling. Zero filling increases the number of points per wave number in the spectrum, and, in effect, interpolates the spectrum. Normally, some multiple (e.g., 2, 4, etc.) of the original number of data points is added to the interferogram. This improves the photometric accuracy of the FT-IR spectrum

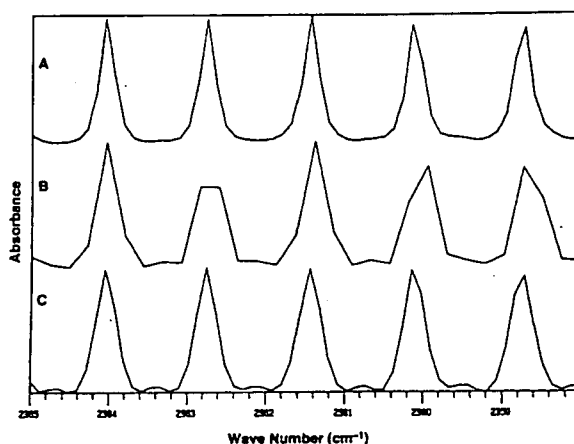


**Figure 7-5. Absorption Spectra of CO<sub>2</sub>** Measured at (A) 0.25 cm<sup>-1</sup> with a Zero-Filling Factor of 1, (B) 0.5 cm<sup>-1</sup> with No Zero Filling, and (C) 0.5 cm<sup>-1</sup> with a Zero-Filling Factor of 2.

and increases the digital resolution. As shown in Figure 7-5C, zero filling the interferogram measured at  $0.5\text{ cm}^{-1}$  by an additional factor of 2 eliminated the picket fence effect.

It should be noted that zero filling improves only the digital resolution, and not the resolution of the FT-IR spectrum. An example of this is illustrated in Figure 7-6 for spectra of water vapor measured at  $0.25\text{-cm}^{-1}$ ,  $0.5\text{-cm}^{-1}$ , and  $1\text{-cm}^{-1}$  resolution. The spectrum measured at  $0.25\text{-cm}^{-1}$  resolution was zero filled by a factor of 1, the  $0.5\text{-cm}^{-1}$  spectrum was zero filled by a factor of 2, and the  $1\text{-cm}^{-1}$  spectrum by a factor of 4. In this case, each of the interferograms contained the same number of data points after being zero filled. Even with additional zero filling, the  $0.5\text{-cm}^{-1}$  spectrum does not match the spectral definition of the spectrum obtained at  $0.25\text{-cm}^{-1}$  resolution. (Compare Spectra A

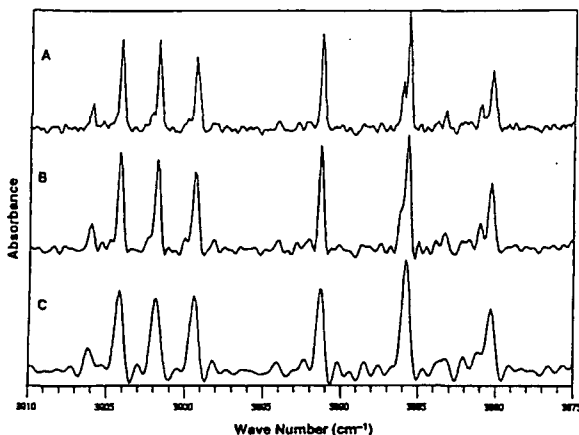


**Figure 7-6. Absorption Spectra of Water Vapor Measured at (A)  $0.25\text{-cm}^{-1}$  Resolution with a Zero-Filling Factor of 1, (B)  $0.5\text{-cm}^{-1}$  Resolution with a Zero-Filling Factor of 2, and (C)  $1\text{-cm}^{-1}$  Resolution with a Zero-Filling Factor of 4.**

and B in Figure 7-6.) The loss of spectral features is more dramatic in the zero-filled  $1\text{-cm}^{-1}$  spectrum. For example, shoulders at  $3905$  and  $3884\text{ cm}^{-1}$  that are detectable in the  $0.25\text{-cm}^{-1}$  and  $0.5\text{-cm}^{-1}$  spectra were not observed in the  $1\text{-cm}^{-1}$  spectrum. Also, side lobes appear in the  $1\text{-cm}^{-1}$  spectrum that was zero filled by a factor of 4 (Figure 7-6, Spectrum C). These side lobes are also present, but are not as severe, in the  $0.5\text{-cm}^{-1}$  spectrum zero filled by a factor of 2 (Spectrum B in Figure 7-6).

The picket fence effect is less extreme if the spectral components are broad enough to be spread over several sampling positions. As a rule of thumb, the original interferogram size should be doubled by zero filling by an additional factor of 2. When a CLS analysis of the spectral data is performed, in general it has been found that one order of zero filling (which is 2 times the original number of data points used in the Fourier transform) yields a factor of 2 lower error than that with no additional zero filling. An example of this is given in Section 7.5.2.2.1. It should be noted that zero filling does increase the file size and the time required for data processing.

### 7.4.3 Apodization Effects

As shown in Chapter 2, the Fourier transform integral has infinite limits for the optical path difference. Thus, to measure the true spectrum of the source, the interferometer must scan infinite distances. However, because the mirror can move only a finite distance, the exact reconstruction of

the spectrum is impossible. The finite movement of the interferometer mirror truncates, or cuts off, the interferogram. This, in effect, multiplies the interferogram by a boxcar truncation function. This function may cause the appearance of side lobes on both sides of the absorption band. The corrective procedure for eliminating these side lobes is called apodization. (For an in-depth discussion of the effects of apodization, see Chapter 8). Apodization is performed by multiplying the measured interferogram by a mathematical function. Typical apodization functions include triangular, Happ-Genzel, and Norton-Beer functions. An example of the effect of these apodization functions on the FT-IR spectrum of CO is shown in Figure 7-7.

Apodization affects the effective spectral resolution, the apparent peak absorbance, and the noise of any FT-IR spectrum. The apparent absorbance of narrow bands will be most affected by the

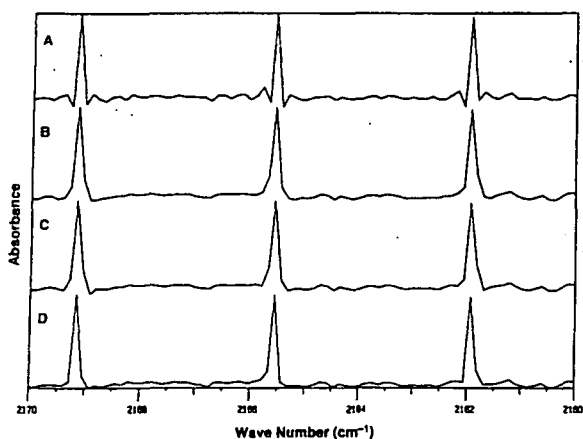


**Figure 7-7. Absorption Spectra of CO Measured at a Nominal  $0.125\text{-cm}^{-1}$  Resolution with (A) No, (B) Triangular, (C) Happ-Genzel, and (D) Norton-Beer-Medium Apodization Functions.**

choice of apodization function. In general, the bands in a spectrum computed with no apodization will be more intense than bands in the spectrum of the same sample computed from the same interferogram after applying an apodization function.

Apodization also degrades resolution. An example of this is illustrated by the spectra of water vapor in Figure 7-8. In this case, subtle differences are observed, for example, at  $3948$  and  $3947\text{ cm}^{-1}$  and  $3924.4\text{ cm}^{-1}$ , in the spectrum generated with no apodization (Figure 7-8A) and the spectra generated by using the three types of apodization functions.

In general, to obtain the optimum S/N for spectra of small molecules with resolvable fine structure, the use of no apodization is preferable if side lobes from neighboring intense lines do not present an interference. If side lobes are present and

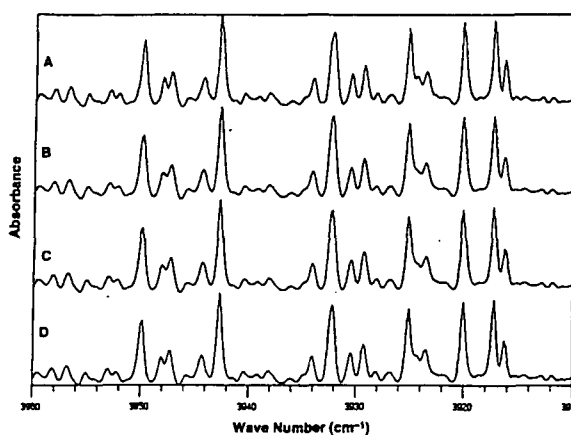


**Figure 7-8. Absorption Spectra of Water Vapor Measured at  $0.5\text{-cm}^{-1}$  Resolution with an Additional Zero-Filling Factor of 2 and with (A) No, (B) Triangular, (C) Happ-Genzel, and (D) Norton-Beer-Medium Apodization Functions.**

interfere with either qualitative or quantitative analyses, apodization becomes necessary. However, when classical least squares is performed, the field spectra must be processed by using the same apodization function that was used for the reference spectra. For broad absorption bands, the measured absorbance is about the same in apodized and unapodized spectra. This can pose some problem in the analysis using classical least squares. Gases that exhibit broadband features in the P and the R branches, but also have a sharp Q branch like that of the gas toluene, will exhibit a different response in these branches because of the apodization function. Overall, the greatest noise suppression will be obtained with the strongest apodization function, but the spectral resolution and band intensities will be greatest for weaker apodization functions (Griffiths and de Haseth 1986). The optimum apodization function has yet to be determined for general use in long-path FT-IR monitoring. In general, there is a reciprocal relation between the suppression of the side lobes and the broadening of the absorption feature for any of the apodization functions. That is, as the side lobes became smaller relative to the peak, the feature becomes broader compared to the unapodized feature.

Triangular and Happ-Genzel apodization functions are commonly used in OP/FT-IR monitoring, although Griffiths et al. (1995) have indicated that a Norton-Beer medium function actually gives a better representation of the true absorbance. In all cases, however, the same parameters should

be used to collect the field spectra that were used to record the reference spectra. The choice of apodization function may be limited by this requirement. If spectra from a commercial or user-generated library are to be the reference spectra for quantitative analysis, then the parameters that were used to generate those reference spectra should be used to collect the field spectra. Otherwise, errors in the concentration measurement will occur.

### **7.5 Effect of Resolution on Quantitative Analyses**

The determination of analyte concentrations by FT-IR spectrometry depends on the linear relationship between IR absorbance and concentration as described by Beer's law. The discussion in Chapter 8 shows that this seems never to be true if an apodization function is used, particularly at low resolution. If the FWHH of the band is narrower than the instrumental resolution, the measured spectrum is actually a convolution of the instrument line shape and true band shape. As a result, the measured absorbance will be only approximately linear with concentration. The higher the resolution for the spectral features of the IR band chosen for quantification, the better the approximation. The apodization function also has an effect on linearity. This section describes studies from the literature that have addressed the effects of resolution and related parameters on quantitative analyses.

### 7.5.1 Studies from the Literature

Strang et al. (1989) designed and evaluated an FT-IR system for monitoring toxic emissions from semiconductor manufacturing processes. This system was used to analyze part-per-billion levels of organic vapors and metal hydrides such as arsine, phosphine, and diborane in simulated workplace environments. The optimal wave number region for quantification and the effects of resolution and spectral overlap on the accuracy of quantitative results were studied. Spectral measurements were taken at resolutions ranging from 0.5 to 8  $\text{cm}^{-1}$  to determine the optimum balance between (1) analysis time, (2) data storage space, (3) S/N, (4) accuracy of quantitative analyses using a CLS program, and (5) the ability to differentiate compounds with overlapping spectra. It should be noted that these data were acquired over a 20.25-m path in a multipass cell. Therefore, findings from this study may not be applicable to long, open-path measurements. Discussion of this study is included in this text because of the interest in workplace monitoring. Also, the methodology used to determine the optimum resolution for the short-path measurements can also be applied to longer path measurements.

The authors specified the following four issues that must be resolved for a CLS analysis at a given resolution to be acceptable.

1. Whether the CLS result varies by more than 50% of the theoretical value
2. Whether false positives or false negatives develop as a result of degraded resolution
3. Whether the amount of error in the measurement will cause potentially toxic concentrations of the target analyte in air to be measured incorrectly
4. Whether the detection limit obtained with the CLS program changes as a function of resolution

Using these criteria, the authors determined the minimum allowable resolution for the target compounds. The results are summarized below in Table 7-2.

In this study, the higher resolutions required for the metal hydrides arsine, diborane, and phosphine were a result of spectral overlap with other target analytes and with interfering atmospheric compounds. For example, phosphine overlaps with  $\text{CO}_2$  and arsine overlaps with water vapor. The authors also determined the effects of decreased resolution on the accuracy of the quantitative results. In the case of diborane, only the 0.5- $\text{cm}^{-1}$  resolution measurements exhibited a linear relationship for all concentrations. Measurements taken at 2- and 4- $\text{cm}^{-1}$  resolution deviated from linearity as the concentration decreased.

The effect of resolution on the ability to quantify overlapping compounds by the CLS analysis was investigated by using mixtures of Freons 11, 13B1, and 22. These

Table 7-2. Optimal Wave Number Region and Minimum Resolution\*

Compound	Wave Number Region ( $\text{cm}^{-1}$ )	Minimum Resolution ( $\text{cm}^{-1}$ )
Acetone	1287-1167	8
Arsine	2132-2106	2
Diborane	2522-2515	0.5
<i>o</i> -Dichlorobenzene	1060-1002	8
2-Ethoxyethanol	1192-984	8
Freon 11	876-813	8
Freon 13B1	1137-1031	8
Freon 22	1193-1063	8
Nitrogen trifluoride	960-833	8
Phosphine	2440-2390	4
Sulfur hexafluoride	965-915	8

\*From Strang et al. (1989). These data are applicable to a 20.25-m path.

compounds have relatively broad spectral features that overlap. The mixtures were analyzed at 0.5-, 2-, 4-, and 8- $\text{cm}^{-1}$  resolution. Each of the individual compounds could be quantified accurately at each resolution in a 1:1:1 mixture at concentrations of 10, 1, and 0.1 ppm.

Strang and Levine (1989) have also determined the LODs for the same target compounds in the previous study as a function of resolution. For most compounds, there was very little difference in the LODs estimated at resolutions of 0.5, 2, 4, and 8  $\text{cm}^{-1}$ . However, for diborane and phosphine the LOD was difficult or impossible to measure at 8  $\text{cm}^{-1}$  resolution. In the case of diborane, the peak selected for quantification had a FWHH of 7  $\text{cm}^{-1}$ . At 8- $\text{cm}^{-1}$  resolution there are only two data points every 8  $\text{cm}^{-1}$ , so a peak 7  $\text{cm}^{-1}$  in width is not

defined well enough to be quantified by the CLS program. For phosphine, the peak shape is severely degraded at 8  $\text{cm}^{-1}$ . Although the CLS program could quantify the peak, the LOD was significantly higher (0.7 ppm-v/v) for spectra measured at 8  $\text{cm}^{-1}$  resolution as compared to those measured at 0.5  $\text{cm}^{-1}$  resolution (0.07 ppm-v/v). This example also illustrates one of the advantages of the CLS program over single peak absorbance measurements in quantitative analysis. The single peak absorbance measurement is difficult to make for broad bands, whereas the CLS program uses multiple data points over the entire spectral range of the broad band.

Spellicy et al. (1991) addressed several issues regarding spectroscopic remote sensing with respect to the Clean Air Act. One issue that was addressed was the



optimum resolution for remote sensing FT-IR applications. The authors presented theoretical calculations describing the relationship between absorbance and concentration for a single Lorentzian line with a half-width of  $0.1 \text{ cm}^{-1}$  measured at resolutions from  $0.01$  to  $0.1 \text{ cm}^{-1}$ . Under these conditions, linearity was observed only at a highest resolution case and at the lowest concentrations. The deviation from linearity most likely would be observed in small molecules such as HCl, CO,  $\text{CO}_2$ , and  $\text{H}_2\text{O}$ , which have sharp spectral features. For larger compounds, such as heavy hydrocarbons that exhibit broader IR bands, the linear relationship between absorbance and concentration is more likely to be followed.

More recently, Marshall et al. (1994) conducted a laboratory study to determine the effect of resolution on the multicomponent analysis of VOCs with a CLS program. When they analyzed for target VOCs, such as acetone, chloroform, toluene, methanol, 1,1,1-trichloroethane, methyl ethyl ketone, carbon tetrachloride, and the xylene isomers, over a short path, resolutions lower than  $4 \text{ cm}^{-1}$  had an adverse effect on the multicomponent analysis. Resolutions of 1 to  $2 \text{ cm}^{-1}$  were found to be adequate for these target compounds when the CLS program was used.

Griffiths et al. (1993) reported the advantages and disadvantages of using low-resolution measurements in long-path FT-IR monitoring. Among the advantages cited were the smaller size and greater portability

of the instrument, an improved S/N, and a lower cost. The disadvantages included a greater difficulty in visualizing the IR bands of the target compounds and potential deviations from Beer's law. A test case of measuring the xylene isomers at resolutions of 2, 4, 8, and  $16 \text{ cm}^{-1}$  was presented. By using a partial least squares (PLS) program, good quantitative results were obtained at the relatively low resolution measurements. These results also indicated that the PLS program might be better than the CLS program for distinguishing and quantifying target compounds with overlapping features.

Bittner et al. (1994) have reported on high-resolution FT-IR measurements of VOCs at a variety of monitoring sites. By recording spectra at  $0.125\text{-cm}^{-1}$  resolution, detection limits for benzene of 0.5 ppm-m were achieved at path lengths between 60 and 100 m at a fuel storage area. The high-resolution measurements allowed the narrow benzene band at  $674 \text{ cm}^{-1}$  to be separated from the strong  $\text{CO}_2$  absorption bands in that spectral region.

#### **7.5.2 Case Study: The Effect of Resolution and Related Parameters on the CLS Analysis of Multicomponent Mixtures**

A study using laboratory-generated spectral mixtures that have overlapping features was conducted to investigate the effect of instrumental resolution and related parameters on the CLS analysis results (Childers and Thompson 1994). The study was designed to simulate conditions that might be encountered in long-path

measurements. The results from three separate cases are discussed.

1. Analytes with narrow bands that overlap, such as those for CO and  $^{13}\text{C}$ -labeled CO
2. Analytes with broad bands that overlap, such as those for acetone, methylene chloride, and ethanol
3. Analytes with narrow and broad bands that overlap, such as those for nitrous oxide and methylene chloride.

The effect of the number of data points and the noise level on the CLS analysis is also illustrated. Because the mixtures analyzed in this study were created from a linear combination of reference spectra, the effect of resolution on the relationship between concentration and absorbance is not addressed.

The spectra were collected on a research-grade, benchtop FT-IR spectrometer equipped with an MCT detector. A gas cell, 50 mm long and 32 mm in diameter, was used to obtain reference spectra of CO,  $^{13}\text{CO}$ , acetone, methylene chloride, ethanol, and nitrous oxide at room temperature and atmospheric pressure. The reference spectra were acquired at resolution settings of 0.125 and 1  $\text{cm}^{-1}$ . The original interferograms were processed by using the appropriate number of data points to yield spectra with nominal resolutions ranging from 0.25 to 8  $\text{cm}^{-1}$ . No additional zero filling was used on the 0.25- $\text{cm}^{-1}$  spectra because of memory limitations in the data system. The 0.5- $\text{cm}^{-1}$  spectra were zero filled by an additional

factor of 2, and the 1.0- $\text{cm}^{-1}$  spectra were zero filled by an additional factor of 4. As a result, the 0.25-, 0.5-, and 1.0- $\text{cm}^{-1}$ -resolution spectra had the same number of data points, that is 131,072. The 2-, 4-, and 8- $\text{cm}^{-1}$  spectra were generated from interferograms that contained 16,384, 8192, and 4096 data points, respectively. No additional zero filling was performed on these interferograms. A triangular apodization function was applied to each interferogram prior to performing the fast Fourier transform.

The concentrations of the individual analytes in the gas cell were determined by comparing the maximum absorbance values of the 0.5- $\text{cm}^{-1}$  spectra to those of reference spectra in a commercial spectral library. The absorbance values of the reference spectra were then normalized to values corresponding to a concentration of 100 ppm. These spectra were added mathematically to produce synthetic mixtures with varying concentrations of each analyte. Synthetic noise corresponding to an amplitude of 1, 5, 10, and 25% of the most intense peak in each spectrum was added to the mixtures. Mixtures with 10% noise added were then analyzed by using a CLS algorithm.

#### 7.5.2.1 *Mixtures of CO and $^{13}\text{CO}$*

Synthetic mixtures of CO and  $^{13}\text{CO}$  were generated by adding reference spectra of CO corresponding to concentrations of 150, 300, 450, and 600 ppm to reference spectra of 100 ppm  $^{13}\text{CO}$ . The 0.25- $\text{cm}^{-1}$

reference spectra and the spectra of the synthetic mixtures corresponding to 150 ppm of CO and 100 ppm of  $^{13}\text{CO}$  recorded at 0.25, 0.5, 1.0, and 2.0  $\text{cm}^{-1}$  resolution are shown in Figure 7-9. CO and  $^{13}\text{CO}$  have several bands that overlap or nearly overlap in the spectral region between 2118 and 2137  $\text{cm}^{-1}$ . For example, overlapping bands at 2123.6 and 2124.2  $\text{cm}^{-1}$  and at 2131.0 and 2131.6  $\text{cm}^{-1}$  are nearly baseline resolved in the 0.25  $\text{cm}^{-1}$  spectrum. These bands can

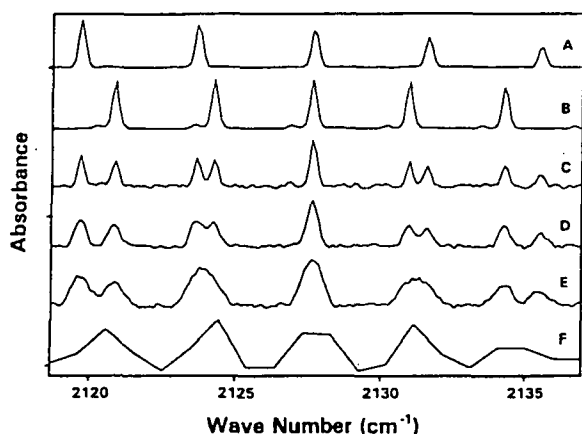


Figure 7-9. Reference 0.25- $\text{cm}^{-1}$  Spectra of (A)  $^{13}\text{CO}$  and (B) CO and Spectra of Synthetic Mixtures of 150 ppm CO and 100 ppm  $^{13}\text{CO}$  Measured at (C) 0.25-, (D) 0.5-, (E) 1.0-, and (F) 2.0- $\text{cm}^{-1}$  Resolution.

still be distinguished at a resolution of 0.5  $\text{cm}^{-1}$ , but appear as only one band in the 1.0- and 2.0- $\text{cm}^{-1}$  spectra. Even though these bands are not resolved at 1.0- and 2.0- $\text{cm}^{-1}$  resolution, the CLS analysis accurately determined the concentration of CO in the mixture when it was analyzed for both CO and  $^{13}\text{CO}$ . Plots of the calculated concentration versus the known concentration of CO were linear over the range of 0 to 600 ppm of CO in the presence

of 100 ppm  $^{13}\text{CO}$ . When the mixtures were analyzed for only CO, a positive bias and an increase in the magnitude of the errors in the measurements were observed. Although the bias was relatively constant, the error increased as the resolution decreased from 0.25 to 1.0  $\text{cm}^{-1}$ . In the case of the 2- $\text{cm}^{-1}$  measurements, CO could not be detected at 150 ppm in the mixture if  $^{13}\text{CO}$  was excluded from the analysis. (See Figure 7-10.)

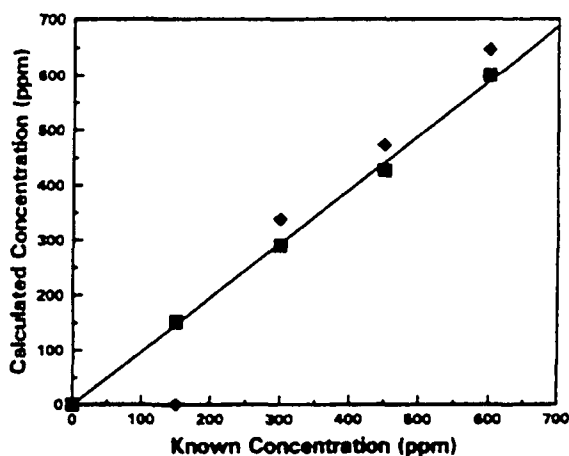


Figure 7-10. Concentration Calculated from CLS Analysis vs. Known Concentration for  $^{13}\text{CO}/\text{CO}$  Mixtures Measured at 2- $\text{cm}^{-1}$  Resolution. The (■) represents a value obtained during analysis for both  $^{13}\text{CO}$  and CO, and the (◆) represents a value obtained during analysis for CO only.

### 7.5.2.2 Mixtures of Acetone, Methylene Chloride, and Ethanol

Synthetic mixtures of acetone, methylene chloride, and ethanol were generated by adding reference spectra of ethanol corresponding to concentrations of 125, 250, 375, and 500 ppm to reference spectra of 100 ppm each of acetone and methylene chloride. The 0.25- $\text{cm}^{-1}$  reference

spectra and the spectra of the synthetic mixtures corresponding to 500 ppm of ethanol and 100 ppm each of acetone and methylene chloride recorded at 1.0-, 2.0-, and 4.0-cm<sup>-1</sup> resolution are shown in Figure 7-11. In this case, the spectrum of each analyte could be adequately measured at 1.0-cm<sup>-1</sup> resolution. At 4-cm<sup>-1</sup> resolution, the Q-branches of these compounds were no longer detected. However, this did not diminish the ability to quantify ethanol in these mixtures with the CLS algorithm. Plots of the calculated concentration versus the known concentration of ethanol were linear over the entire range from 0 to 500 ppm ethanol in the presence of 100 ppm of acetone and 100 ppm of methylene chloride for each resolution setting. Although the concentration of ethanol could be determined in the low-resolution measurements, the errors in the CLS analysis increased with decreasing spectral resolution. The high-

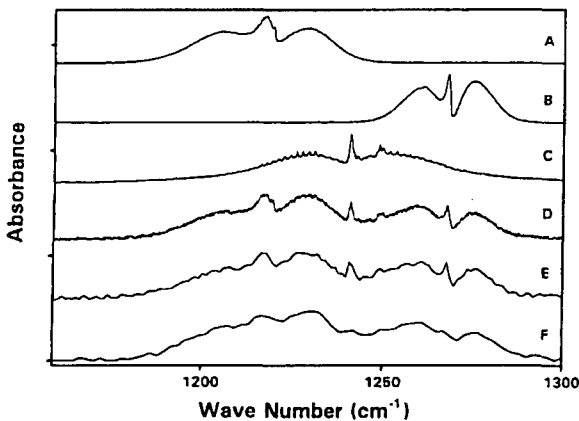


Figure 7-11. Reference 0.25-cm<sup>-1</sup> Spectra of (A) Acetone, (B) Methylene Chloride, and (C) Ethanol and Spectra of Synthetic Mixtures of 100 ppm Acetone, 100 ppm Methylene Chloride, and 500 ppm Ethanol Measured at (D) 1.0-, (E) 2.0-, and (F) 4.0-cm<sup>-1</sup> Resolution.

resolution spectra contain more data points per wave number than do the low-resolution measurements. To determine if this contributed to the increase in the magnitude of the errors, the effect of the number of data points on the CLS analysis was investigated. The effect of S/N on CLS was also investigated.

#### 7.5.2.2.1 Effect of the Number of Data Points on the CLS Analysis

The average error in the CLS analysis for ethanol in the acetone, methylene chloride, ethanol synthetic mixtures for each resolution setting is shown in Table 7-3.

For the 0.25-, 0.5-, and 1.0-cm<sup>-1</sup> measurements, in which additional zero filling was used to keep the number of data points the same, the average error was relatively constant at approximately 9%. However, for the 2.0-, 4.0-, and 8.0-cm<sup>-1</sup> measurements, in which no additional zero filling was used, the average error increased with a decrease in the number of data points. (Note that the 0.25-, 0.5-, and 1.0-cm<sup>-1</sup> spectra were generated from an original interferogram collected at 0.125-cm<sup>-1</sup> resolution, whereas the 2.0-, 4.0-, and 8.0-cm<sup>-1</sup> spectra were generated from an original interferogram collected at 1.0-cm<sup>-1</sup> resolution.)

To show that the increase in error is related to the number of data points per wave number, and is not necessarily a direct result of degrading the spectral resolution, spectral mixtures of acetone, methylene

**Table 7-3. Effect of The Number of Data Points on the CLS Analysis**

Resolution (cm <sup>-1</sup> )	Additional Zero Filling	Data Points	Average Error
0.25	None	131072	9.13
0.5	2 ×	131072	8.93
1.0	4 ×	131072	9.55
2.0	None	16384	24.54
4.0	None	8192	32.73
8.0	None	4096	42.27

chloride, and ethanol obtained at 1-cm<sup>-1</sup> resolution were processed by using no additional zero filling, an additional zero filling factor of 2, and an additional zero filling factor of 4. This resulted in interferograms having 32,768, 65,536, and 131,072 data points, respectively. These results were also compared to those obtained for spectra measured at 2 cm<sup>-1</sup>, which were generated from interferograms containing 16,384 data points.

As can be seen in Table 7-4, the accuracy of the measurements was not affected by the number of data points per spectral element. However, the magnitude of the error in the measurements was related to the number of interferogram data points used to generate the spectra. On average, the error in the CLS analysis decreased by a factor of 1.4 each time the number of data points used to process the interferogram was doubled.

**Table 7-4. The Effect of Zero Filling on the CLS Analysis**

Conc. (ppm)	1-cm <sup>-1</sup>	1-cm <sup>-1</sup>	1-cm <sup>-1</sup>	2-cm <sup>-1</sup>
	Resolution 4 × Zero Fill	Resolution 2 × Zero Fill	Resolution No Zero Fill	Resolution No Zero Fill
0	Below MDL	Below MDL	Below MDL	Below MDL
125	121.40 (8.49)	119.65 (11.89)	124.53 (17.24)	119.85 (22.47)
250	248.33 (9.35)	248.87 (12.87)	252.07 (18.15)	252.18 (22.53)
375	379.85 (9.58)	368.40 (13.83)	380.78 (17.94)	373.87 (24.27)
500	500.81 (10.29)	509.94 (14.73)	492.42 (20.83)	509.24 (28.90)

**7.5.2.2 Effect of S/N on the CLS Analysis**

Synthetic noise was added to 1-cm<sup>-1</sup> spectral mixtures containing 100 ppm acetone, 100 ppm methylene chloride, and 0 to 500 ppm ethanol at levels corresponding to 1, 5, 10, and 25% of the maximum absorbance value in each spectrum.

Spectral mixtures containing 100 ppm acetone, 100 ppm methylene chloride, and 500 ppm ethanol at each noise level are shown in Figure 7-12. In these mixtures, the average error in the CLS analysis was found to be directly proportional to the percentage of noise added to the spectrum. (See Table 7-5.)

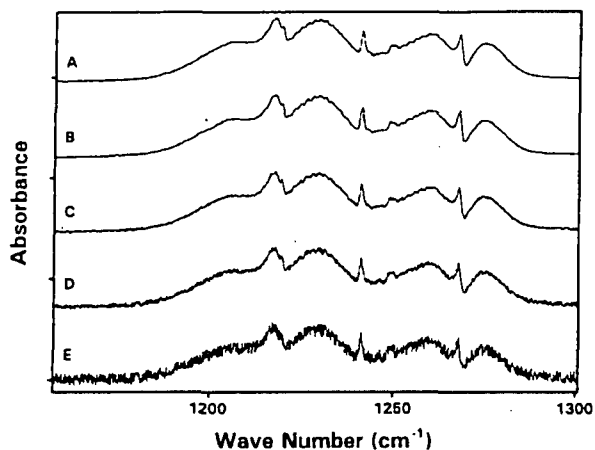


Figure 7-12. Spectra of Synthetic Mixtures of 100 ppm Acetone, 100 ppm Methylene Chloride, and 500 ppm Ethanol Measured at 1-cm<sup>-1</sup> Resolution with (A) 0, (B) 1, (C) 5, (D) 10, and (E) 25% Noise Added.

Table 7-5. Effect of Noise on the CLS Analysis

% Noise	Average Error
0	0.07
1	0.96
5	4.78
10	9.55
25	23.89

**7.5.2.3 Mixtures of Methylene Chloride and Nitrous Oxide**

Synthetic mixtures of methylene chloride and nitrous oxide were generated by adding reference spectra of nitrous oxide corresponding to concentrations of 12.5, 25, 37.5, 50, 75, and 100 ppm to reference spectra of 100 ppm methylene chloride. The 0.25-cm<sup>-1</sup> reference spectra and the spectra of the synthetic mixtures corresponding to 50 ppm of nitrous oxide with both 0 and 100 ppm of methylene chloride recorded at 0.25-, 0.5-, and 1.0-cm<sup>-1</sup> resolution are shown in Figure 7-13.

The spectrum of nitrous oxide exhibits sharp bands that are resolved at 0.25 cm<sup>-1</sup>, but are not as well resolved at 0.5-cm<sup>-1</sup> resolution. These bands become a broad continuum in the 1.0-cm<sup>-1</sup> spectrum. At first glance, one would expect the CLS analysis to perform better for the 0.25-cm<sup>-1</sup> spectra, in which the N<sub>2</sub>O bands are fully resolved. However, this is not the case in these mixtures. When analyses are performed for N<sub>2</sub>O over the entire band envelope from 1231 to 1329 cm<sup>-1</sup>, N<sub>2</sub>O is not detected at concentrations less than 75 ppm in the 0.25-cm<sup>-1</sup> spectra. (See Figure 7-14.)

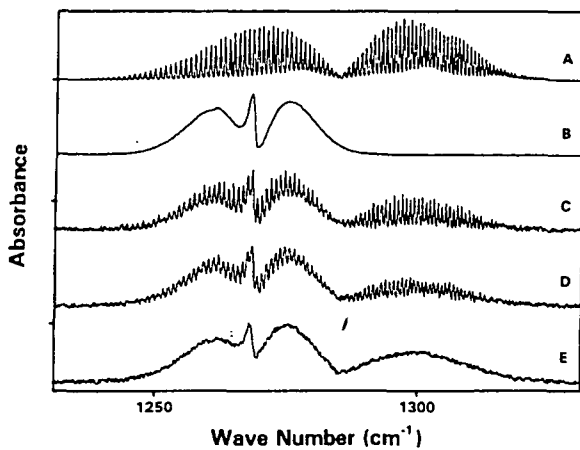


Figure 7-13. Reference 0.25-cm<sup>-1</sup> Spectra of (A) N<sub>2</sub>O and (B) Methylene Chloride and Spectra of Synthetic Mixtures of 50 ppm N<sub>2</sub>O and 100 ppm Methylene Chloride Measured at (C) 0.25-, (D) 0.5-, and (E) 1.0-cm<sup>-1</sup> Resolution.

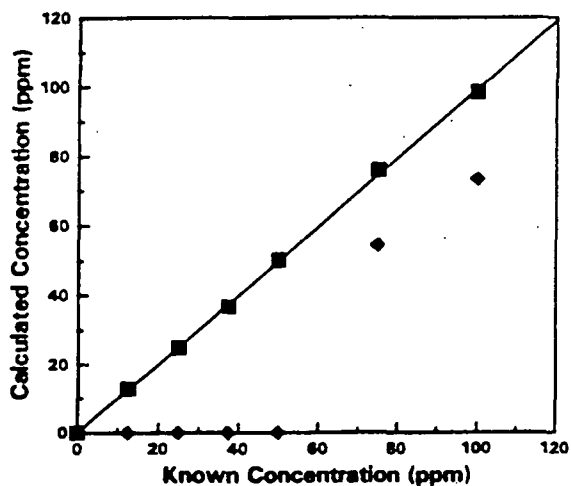


Figure 7-14. Concentration Calculated from CLS Analysis vs. Known Concentration for N<sub>2</sub>O/ Methylene Chloride Mixtures Measured at 0.25-cm<sup>-1</sup> Resolution. The (■) represents a value obtained during analysis over the methylene chloride region, and the (◆) represents a value obtained during analysis over the N<sub>2</sub>O region.

However, when the mixture was analyzed for N<sub>2</sub>O by using the methylene chloride region from 1243 to 1292 cm<sup>-1</sup>, N<sub>2</sub>O was accurately quantified with a high precision. Similar results were obtained for the 0.5-cm<sup>-1</sup> resolution spectra. In contrast, the mixtures recorded at 1.0-cm<sup>-1</sup> resolution could be analyzed successfully over both regions. At 2-cm<sup>-1</sup> resolution, the CLS analysis performed best over the N<sub>2</sub>O region. Apparently, in multicomponent mixtures, the CLS algorithm does not perform well in regions where one or more components exhibit only baseline noise.

This effect seems to be amplified in higher resolution measurements of compounds with sharp spectral features, such as N<sub>2</sub>O. These results indicate that for spectra with sharp features the CLS should be performed over a narrow range that contains absorbing features.

#### 7.5.2.4 Conclusions and Recommendations Based on Case Study

The following conclusions regarding resolution requirements in long-path FT-IR monitoring can be drawn from this simulated study using well-characterized spectral data sets.

In spectra with overlapping sharp features, the CLS algorithm can accurately quantify target analytes, even when the bands used for analysis are not fully resolved. However, a failure to identify all of the overlapping components in a mixture can result in a bias and an increase in the error in

the CLS analysis. Thus, the real value in performing higher resolution measurements might be to facilitate identifying the species present to be included in the CLS analysis set.

In the case of spectra with overlapping broad features, such as those found in acetone, methylene chloride, and ethanol, the accuracy of the CLS analysis is not affected by the resolution setting. However, the magnitude of the errors in the CLS analysis is related to the number of data points per wave number in the analyte spectrum. Therefore, the errors in the CLS analysis will increase with decreasing resolution unless additional zero filling, or some other means, is used to increase the number of data points in the spectrum. However, the use of zero filling or interpolation to indiscriminately increase the number of data points in the spectrum is not recommended, because interpolated data points do not contain independent information. In these mixtures, the errors in the CLS analyses were also found to increase proportionally with increases in the noise level.

The results from the CLS analysis of spectral mixtures with overlapping broad and sharp bands, as was the case with methylene chloride and nitrous oxide, were not as straightforward to interpret. When analyzing for nitrous oxide in spectral regions where methylene chloride did not exhibit any absorption bands, the CLS algorithm performed better at lower resolutions. In regions where the two compounds exhibited

overlapping spectral features, comparable results were obtained for measurements taken at 0.25-, 0.5-, and 1.0-cm<sup>-1</sup> resolution.

In summary, resolution requirements will vary for different target compounds and sampling conditions. In field measurements these requirements will depend on several factors, such as path length, concentration of the target compounds, and the presence of interfering species. Although the simulated studies described here do not provide a definitive answer regarding the resolution question, similar studies using target analytes and possible interfering species should be performed prior to field studies to establish guidelines for data acquisition and analysis.

## 7.6 General Conclusions and Recommendations

As stated in the introduction of this chapter, there is currently no consensus as to what resolution is generally applicable in FT-IR long-path, open-path monitoring. A spectral resolution of 0.125 cm<sup>-1</sup> is required to fully characterize the spectra of atmospheric CO<sub>2</sub> and water vapor. Spectra taken along a 150-m path show that there are significant differences in the water vapor spectra measured at nominal resolutions of 2, 1, and 0.5 cm<sup>-1</sup>. The effect of these differences on the computer-assisted quantitative analyses for target pollutants has not, however, been fully examined for long-path FT-IR measurements. In previous studies, Strang et al. (1989) have shown that for several organic vapors a resolution of



8  $\text{cm}^{-1}$  is sufficient to obtain quantitative results over a short path if a CLS program is used. In contrast, Spellicy et al. (1991) have presented theoretical results that suggest that the FT-IR spectra of small molecules with very fine spectral features will obey Beer's law at only high resolution ( $0.01 \text{ cm}^{-1}$ ) and at very-low concentrations. Recently, Marshall et al. (1994) and Griffiths et al. (1995) have indicated that 1- to  $4\text{-cm}^{-1}$  resolution, or possibly a lower resolution, is adequate for measuring certain VOCs using CLS and PLS multicomponent analysis programs.

Clearly, there is much fundamental research that must be done to "resolve" the resolution question. Experiments similar to those done by Strang et al. (1989), Strang and Levine (1989), Marshall et al. (1993), and Griffiths et al. (1993) should be conducted over a long, open path for the hazardous air pollutants stipulated under the Clean Air Act Amendments of 1990. Measurements of these compounds should be taken at different resolutions, concentrations, and path lengths to determine the optimum experimental conditions for obtaining the best S/N and detection limits. Most likely, the optimum resolution will be different for the various compounds. However, at least minimum resolution requirements could be determined.

Although the question of what resolution should be used in FT-IR long-path, open-path monitoring has not been answered, the reader should have an appreciation for the factors related to

resolution that affect spectral measurements. Instrument manufacturers and software vendors have made great strides in simplifying the use of FT-IR instruments. Most FT-IR software is menu driven and some instruments can be operated at the push of a button. Although these developments facilitate the collection of FT-IR data, they also allow data to be collected without a knowledge of the principles behind the measurement. Analysts working in this field must be aware of the effects of different instrumental parameters on the measured spectrum. Grasselli et al. (1982) have published criteria for presenting spectra from computerized IR instruments, with an emphasis on FT-IR measurements. The authors established recommendations and guidelines for reporting experimental conditions, instrumental parameters, and other pertinent information describing the acquisition of FT-IR spectra. These guidelines should be followed when reporting FT-IR data.

### **7.7 Guidance for Selecting Resolution and Related Parameters**

In this section, general criteria and guidelines are suggested for choosing the optimum resolution for acquiring spectral data. The choice of resolution and related parameters, such as apodization and zero filling, to be used for data collection will be determined by several factors. As stated before, there is no consensus as to what the optimum parameters should be. The parameters need to be optimized for the specific experiments planned, taking into

consideration the goals of the monitoring study. The following guidelines should be taken into account when choosing the optimum instrumental parameters.

**1. Consider the bandwidths of the absorption features used to analyze for specific target compounds.**

If the absorption bands of the target compounds are relatively broad, there may be no need to acquire high-resolution spectra. When this is the case, no additional information will be gained, and the measurements will have a poorer S/N and will require longer data collection, computational times, and larger data storage space. The analyst must be aware, however, that the spectral features of atmospheric constituents such as CO<sub>2</sub>, H<sub>2</sub>O, and CH<sub>4</sub> can be completely resolved only at a resolution of 0.125 cm<sup>-1</sup>. Because these compounds are in every long-path spectrum and often overlap with the target analyte, access to high-resolution data may be required to develop the analysis method. There is some thought that the real advantage of high-resolution spectral data is the ability to visualize the spectral features and to identify interfering species. This information can then be used in developing the analysis method.

**2. Determine if interfering species are present.**

If the comparison method or scaled subtraction is used for quantitative analysis, the resolution should be sufficient to separate spectral features of the target compounds from those of interfering species. For example, in the case of toluene the absorption band used for analysis at

1031 cm<sup>-1</sup> is relatively broad. At first, this would indicate that a low-resolution measurement would be sufficient. However, this band overlaps with bands due to atmospheric water vapor and CO<sub>2</sub>. Therefore, a higher resolution measurement is required to separate the toluene from those of interfering species.

**3. Acquire reference spectra of the target compounds.**

If the specific target compounds are known prior to beginning the monitoring study, reference spectra of the compounds of interest should be recorded at various resolutions. This can be accomplished by collecting a reference spectrum at the highest resolution setting on the instrument, and then processing the data by using the required number of Fourier transform data points for each desired resolution. When this method is used, only one spectrum has to be collected. By comparing the spectra processed at different resolutions, the operator can determine the lowest resolution measurement that still resolves the spectral features of interest. This resolution setting should be used as a starting point for future measurements. If this is not possible, the operator should consult reference libraries to help determine the optimum resolution setting required to characterize the target analyte.

**4. Develop calibration curves of the target compounds.**

If an inadequate resolution is used, the relationship between absorbance and concentration will not be linear. This relationship is also affected by the apodization function. Calibration curves

covering the concentration range of the target compounds expected in the ambient measurements must be developed at different resolutions and with the use of different apodization functions to determine the optimum settings. If the compound of interest does not respond linearly with respect to concentration, a correction curve will need to be fitted to the data and used in the quantitative analysis package.

**5. Use the same parameters to collect field spectra as were used to record the reference spectra.** If spectra from a commercial or user-generated library are to be the reference spectra for quantitative analysis, then the parameters that were used to generate those reference spectra should be used to collect the field spectra. Otherwise, errors in the measurement will occur.

**6. Determine that the instrument is producing data at the specified resolution.** The following factors should be considered here: (a) that the operator has selected the proper parameters, and (b) that the instrument is operating to the manufacturer's specifications and that the manufacturer's specifications are a true indication of the capabilities of the instrument.

a. Most software packages allow the resolution to be selected from a menu. The software then automatically sets the proper parameters to collect data at the selected resolution. Therefore, there is very little opportunity for operator error. In older versions of software that are not menu driven, but instead require entering

line commands, many of the parameters affecting resolution, such as the number of data points used for the Fourier transform, must be entered manually. In this case, the operator must know, and enter correctly, all of the proper parameters, and there is a greater chance of error.

b. If the instrument is not producing data of the selected resolution, it is also possible that the instrument is malfunctioning or that the manufacturer overstated the capabilities of the instrument. The following procedure can be used to determine if the instrument is producing data at the specified resolution. There is a cluster of absorption bands between 1008 and 1020  $\text{cm}^{-1}$  due to water vapor that can be used to verify the resolution of the FT-IR monitor. There is a doublet centered at 1010.5  $\text{cm}^{-1}$ , a single band at 1014.2  $\text{cm}^{-1}$ , and a pair of bands at 1017.5 and 1018  $\text{cm}^{-1}$ . The singlet at 1014.2  $\text{cm}^{-1}$  has a theoretical bandwidth of approximately 0.3  $\text{cm}^{-1}$  (USF HITRAN-PC [University of South Florida 1993]). This band is a good reference band for determining the actual resolution measured by a medium- or low-resolution spectrometer. For example, if this band is measured at an instrument setting of 0.5  $\text{cm}^{-1}$ , the FWHH should be 0.5  $\text{cm}^{-1}$ . If measured with an instrument capable of achieving a higher resolution, for example 0.25  $\text{cm}^{-1}$ , the FWHH should be the theoretical value of 0.3  $\text{cm}^{-1}$ . The doublet centered at 1010.5  $\text{cm}^{-1}$  is just

resolved at  $0.5\text{-cm}^{-1}$  resolution, but is not resolved at  $1\text{-cm}^{-1}$  resolution. The theoretical bandwidth of each of these two absorption bands is approximately  $0.1\text{ cm}^{-1}$  (USF HITRAN-PC), which makes them good reference peaks for instruments capable of measuring at a resolution of  $0.125\text{ cm}^{-1}$ . The two peaks at  $1017.5$  and  $1018\text{ cm}^{-1}$  are resolved at  $0.125\text{ cm}^{-1}$ , but not at lower resolutions. If the instrument is not performing to specifications, there is most likely an alignment problem with the interferometer or source optics. Unless the operator is trained to perform this alignment, a representative from the manufacturer must service the instrument.

The bands centered at  $1014.2\text{ cm}^{-1}$  are a good test of resolution, but they are not as sensitive to misalignment in the interferometer. Other bands that may also be used are the  $2169\text{-cm}^{-1}$  band of CO and the HDO doublet centered at approximately  $2720\text{ cm}^{-1}$ . These bands at shorter wavelength (higher wave number) are more sensitive to interferometer misalignment and can also be used to determine the stability of the interferometer.

These are general guidelines to be used when choosing instrumental parameters to collect data. In reality, the user's choice of parameters that can be actually used may be limited by either the specifications of the spectrometer or by the software. For example, one software package supplied

with FT-IR long-path, open-path systems allows only triangular apodization with no additional zero filling for processing the interferogram with the menu-driven commands. These parameters cannot be changed unless the user has the capability of editing the software code. As the resolution requirements of long-path, open-path FT-IR monitors become better defined, the manufacturers will most likely produce instruments and software to meet those needs.

## 7.8 References

Bell, R.J. 1972. *Introductory Fourier Transform Spectroscopy*. Academic Press, New York.

Bittner, H., T. Eisenmann, H. Mosebach, M. Erhard, and M. Resch. 1994. Measurements of Diffuse Emissions of Volatile Organic Compounds by High Resolution FTIR Remote Sensing. *SP-89 Optical Sensing for Environmental Monitoring*, Air & Waste Management Association, Pittsburgh, PA, pp. 443-454.

Childers, J.W., and E.L. Thompson, Jr. 1994. Resolution Requirements in Long-Path FT-IR Spectrometry, *SP-89 Optical Sensing for Environmental Monitoring*, Air & Waste Management Association, Pittsburgh, PA, pp. 38-46.

Grasselli, J.G., P.R. Griffiths, and R.W. Hannah. 1982. Criteria for Presentation of Spectra from Computerized IR Instruments. *Appl. Spectrosc.* 36:87-91.

Griffiths, P.R., and J.A. de Haseth. 1986. *Fourier Transform Infrared Spectrometry*. John Wiley and Sons, New York.

Griffiths, P.R., D. Qin, R.L. Richardson, and C. Zhu. 1993. Atmospheric Monitoring with FT-IR Spectrometry: Strengths and Weaknesses of Measurement at Low Resolution. Presented at the 44th Pittsburgh Conference and Exposition on Analytical Chemistry and Applied Spectroscopy, Atlanta, GA, March 7-12, paper no. 1142.

Griffiths, P.R., Richardson, R.L., Qin, D., and Zhu, C. 1995. Open-Path Atmospheric Monitoring with a Low-resolution FT-IR Spectrometer. *Proceedings of Optical Sensing for Environmental and Process Monitoring*, O.A. Simpson, Ed., VIP-37, Air & Waste Management Association, Pittsburgh, PA, pp. 274-284.

Herres, W., and J. Gronholz. 1984. Understanding FT-IR data Processing Part 1: Data Acquisition and Fourier Transformation. *Computer Applications in the Laboratory* 4:216-220.

Horlick, G. 1968. Introduction to Fourier Transform Spectroscopy. *Appl. Spectrosc.* 22:617-626.

Marshall, T.M., C.T. Chaffin, V.S. Makepeace, R.M. Hoffman, R.M. Hammaker, W.G. Fateley, et al. 1994. Investigation of the Effects of Resolution on the Performance of Classical Least-Squares (CLS) Spectral Interpretation Programs When Applied to Volatile Organic Compounds (VOCs) of

Interest in Remote Sensing Using Open-Air Long-Path Fourier Transform Infrared (FT-IR) Spectrometry. *J. Mol. Structure* 324:19.

Russwurm, G.M. 1992. Quality Assurance, Water Vapor, and Analysis of FTIR Data, Presented at the Air & Waste Management Association Annual Meeting, Kansas City, MO, June.

Spellicy, R.L., W.L. Crow, J.A. Draves, W.F. Buchholtz, and W.F. Herget. 1991. Spectroscopic Remote Sensing: Addressing Requirements of the Clean Air Act. *Spectroscopy* 6:24-34.

Strang, C.R., and S.P. Levine. 1989. The Limits of Detection for the Monitoring of Semiconductor Manufacturing Gas and Vapor Emissions by Fourier Transform Infrared (FTIR) Spectroscopy. *Am. Ind. Hyg. Assoc. J.* 50:78-84.

Strang, C.R., S.P. Levine, and W.F. Herget. 1989. A Preliminary Evaluation of the Fourier Transform Infrared (FTIR) Spectrometer as a Quantitative Air Monitor for Semiconductor Manufacturing Process Emissions. *Am. Ind. Hyg. Assoc. J.* 50:70-77.

University of South Florida. 1993. USF HITRAN-PC, University of South Florida, Tampa, FL.

## Chapter 8

### Nonlinear Response Caused by Apodization Functions and Its Effect on FT-IR Data

#### SUMMARY

This chapter discusses the effects of apodization and temperature on the accuracy of the FT-IR data. It places special emphasis on the following.

- Why apodization causes the FT-IR response to be nonlinear and how this response is affected by resolution.
- The FT-IR response to absorption of water, methane, and ammonia as functions of concentration, temperature, and resolution.
- The errors incurred by using classical least squares and assuming a linear response.

This chapter uses a set of spectra calculated by using the HITRAN database over a 207-m path at various concentrations and temperatures.

#### 8.1 Introduction and Overview

The technique of using an FT-IR system over a long, open atmospheric path to monitor atmospheric pollutants has undergone a vigorous development over the past several years. However, an in-depth analysis of the error associated with the data has never been reported. One source of error in an FT-IR measurement is the application of an apodization function to the interferogram, causing a nonlinear response to changes in gas concentration.

In an FT-IR instrument, the moving mirror of the interferometer must travel a certain distance in order to achieve a specific resolution. At the end of the travel, the

mirror returns to its original position and repeats the movement. The abrupt cutting off of the interferogram at the end of the mirror travel is called truncation. When the Fourier transform of the truncated interferogram is performed, an exact spectrum is not reproduced, and there are spurious oscillations in the reproduced spectrum. These oscillations distort the shape of the spectral features, both in the bandwidth and in the amplitude of the various spectral peaks. A graph of an unapodized (boxcar) water spectrum is shown in Figure 8-1a. The graph in Figure 8-1b is the same portion of the water spectrum, but it has been processed with triangular apodization. Both spectra are at  $0.25\text{-cm}^{-1}$  resolution and are calculated for a

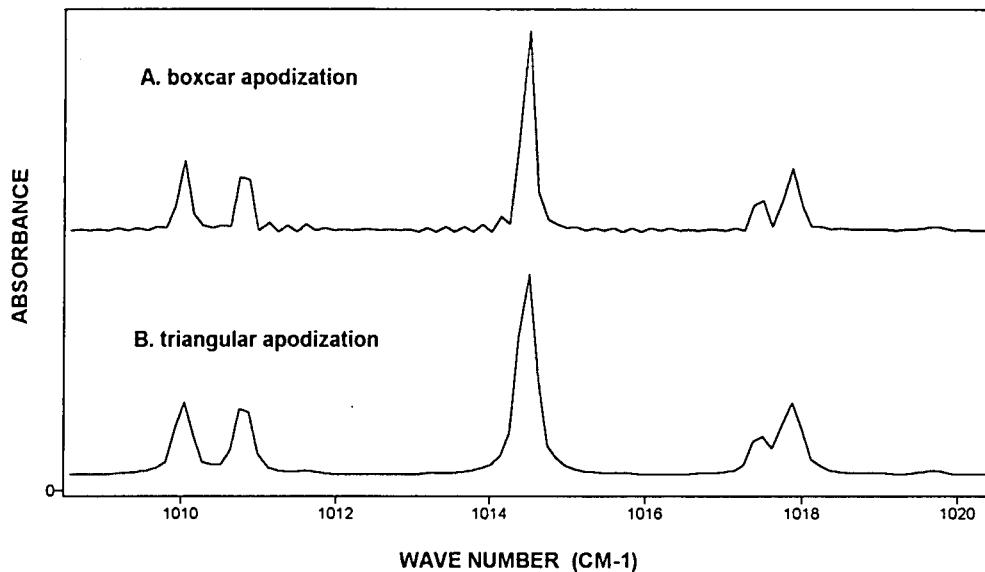


**Figure 8-1. A Portion of a Water Spectrum Using (A) Boxcar Apodization and (B) Triangular Apodization.**

path length of 207 m and a partial pressure of water of 15 torr. The spurious oscillations are clearly visible in the upper curve.

To reduce the magnitude of these oscillations, various apodization functions can be applied to the interferogram before the transform is performed. Many mathematical forms of the apodization functions have been investigated (Happ and Genzel 1961; Filler 1964; Norton and Beer 1976; Kauppinen et al. 1981) and are available for use by the operator. In general, these apodization functions create a broader line width than is available in the unapodized spectrum and are also partly responsible for a nonlinear response of the instrument to

changes in absorbance. This is separate from the detector's nonlinearity, which has not been considered in this discussion.

The FT-IR instruments commercially available for remote sensing generally do not provide a large selection of apodization functions for the operator, and triangular apodization is commonly used. This means that the interferogram is multiplied by a triangular mathematical function with the peak at the so-called center burst before the Fourier transform is performed.

The analysis of the spectra for concentration is generally done by using the method of classical least squares and using

reference spectra of known concentration-path length products, and these spectra have also been processed with triangular apodization. Included in these reference spectra is a water vapor reference that is generally manufactured by the operator (Russwurm 1996) from a field spectrum taken during an actual monitoring program. Generally, there is only one reference spectrum per gas, and it has been acquired for a single concentration-path length product at a specific temperature, although the temperature information is normally not supplied with the spectrum.

The procedure is usually set up so that the least squares calculation is performed over a range of wave numbers that encompasses a major absorption peak of the target gas and generally accounts for all known spectral interferences. The ensuing mathematical analysis process assumes a linear relation between absorbance and concentration, as described by Beer's law. Since the apodization function produces a nonlinear instrument response with concentration but the mathematical data process, usually classical least squares, assumes linearity, an error in the data occurs.

How this manifests itself is shown schematically in Figure 8-2. The linear curve in Figure 8-2 represents the assumed change in absorbance with concentration-path length product while the quadratic curve represents the actual response expected in the field

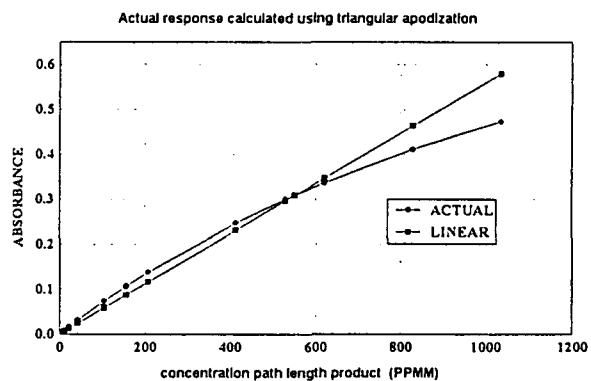


Figure 8-2. Schematic of Actual and Assumed FT-IR Responses.

spectra. While Figure 8-2 is intended to be indicative of the instrument response, the actual curve is the response for methane at  $2927\text{ cm}^{-1}$ . The point where the two curves cross is the concentration-path length product of the reference spectrum. From Figure 8-2 it is seen that if the concentration-path length product of the field spectrum is less than that of the reference, the actual concentration is overestimated, and the actual concentration is underestimated when the concentration-path length product of the field spectrum is greater than that of the reference. Evidently, triangular apodization creates a broader final absorption feature (Marshall and Verdun 1990) than most of the other commonly used functions and therefore a more pronounced nonlinear response. Triangular apodization has been used exclusively throughout the remainder of this chapter because use of this apodization function is considered a worst case.



This chapter examines the magnitude of the error in several ways—by examining the error for a single line in a pure gas, then considering the effects of the spectral interference created by water vapor, and finally examining the error created when a range of wavelengths is used with the classical least-squares technique.

## 8.2 Procedure and Theoretical Basis

The primary data used in this chapter is a set of spectra calculated from the HITRAN database.<sup>1</sup> The three gases used are ammonia, methane, and water vapor. These three gases were chosen because absorbance due to ammonia is not heavily impacted by water, and the absorbance due to methane is strongly affected by water. Water is the primary interfering species, and it perhaps presents the largest problem in the atmospheric spectroscopy of the mid-infrared region. Indeed, the spectrum obtained from the open atmosphere is primarily a water vapor and carbon dioxide spectrum, and the gases of interest (the target gases) represent only small perturbations to that spectrum. The HITRAN database was used to calculate Lorentzian absorption lines over a 207-m path at a total pressure of one atmosphere and with varying concentrations and temperatures. Following that calculation, the spectra were reprocessed with an algorithm that allows an apodization function to be

applied to the spectra and also allows changing the resolution to some other desired resolution. To match the wanted resolution and to apply the apodization function, the following mathematical procedure has been used.

- Calculate an unapodized high-resolution spectrum  $T$  from HITRAN.
- Calculate the inverse Fourier transform of the spectrum  $T$ .
- Multiply this inverse transform by the apodization function.
- Calculate the Fourier transform of the product spectrum from the step above.

The mathematical justification for this procedure is straightforward and is described as follows. The spectrum actually measured by an FT-IR instrument,  $T_r(\omega)$ , is given by the convolution of the true spectrum  $T(\omega)$  and the instrument line function  $S(\omega)$  as

$$T_r(\omega) = \int T(\omega - x)S(x)dx \quad (8-1)$$

However, the instrument line function for an FT-IR instrument is the Fourier transform of the apodization function  $A(\delta)$ , where  $\delta$  is the optical path difference in the two legs of the interferometer. That is,  $S(\omega) = F[A(\delta)]$ , or  $A(\delta) = F^{-1}[S(\omega)]$ . Therefore, Equation (8-1) can be rewritten as

$$T_r(\omega) = \int T(\omega - x)F[A(x)]dx \quad (8-2)$$

---

<sup>1</sup>The AFGL HITRAN molecular absorption parameters database. See, for example, Rothman et al. (1987).

Application of the inverse transform followed by the forward transform to the right-hand side of Equation (8-2) yields

$$T_r(\omega) = F[F^{-1}[\int T(\omega-x)F[A(x)]dx]] \quad (8-3)$$

The convolution theorem for Fourier transforms states that the Fourier transform (or inverse) of the convolution of two functions is equal to the product of their Fourier transforms (or inverses). Applying this theorem to Equation (8-3) gives the final expression that

$$T_r(\omega) = F[F^{-1}[T(\omega)]A(\omega)] \quad (8-4)$$

and all the spectra that were calculated from HITRAN and FASCODE and used for this effort were processed in this manner.

It is convenient to discuss here two other points about the linearity of the response of the FT-IR instrument to changes in concentration of the atmospheric gases. These points consider what concentration levels must be exceeded to make the response nonlinear and what resolution will make the response nonlinear. To evaluate these points, note that the intensity  $I(\omega)$  that is measured by a Fourier transform spectrometer is proportional to the convolution of the incident intensity and the Fourier transform of the instrument line function  $S(\omega)$ . But the function  $S(\omega)$  is a function of the resolution, which in turn is dependent upon the maximum optical path difference between the two mirrors of the

interferometer. The measured intensity can be written as

$$I_m(\omega) = D(\omega) \int I(\omega+\delta)S(\delta,R)d\delta$$

In keeping with Beer's law, the measured background intensity is given as

$$I_{mo}(\omega) = D(\omega) \int I_o(\omega+\delta)S(\delta,R)d\delta$$

where  $D(\omega)$  is the response of the instrument optics and the electronics. The actual transmission  $T(\omega)$  through the absorbing medium can be written (from Beer's law) as

$$I(\omega) = I_o(\omega)T(\omega)$$

and for a single gas component  $T(\omega) = \exp(-c\alpha(\omega))$ . Here  $c$  is the concentration-path length product (with units of ppm·m) and  $\alpha(\omega)$  is a unity absorbance based on 1 ppm. The transmission actually recorded by the FT-IR,  $T_r(\omega)$ , can then be written as

$$T_r(\omega) = \frac{I_m(\omega)}{I_{mo}(\omega)} = \frac{D(\omega) \int I_o(\omega+\delta)T(\omega+\delta)S(\delta,R)d\delta}{D(\omega) \int I_o(\omega+\delta)S(\delta,R)d\delta}$$

If the background intensity is a slowly varying function over the instrument line function  $S$ , then it can be taken outside the integral sign, and the measured transmission,  $T_r(\omega)$ , can be rewritten as

$$T_r(\omega) = \frac{\int T(\omega+\delta)S(\delta,R)d\delta}{\int S(\delta,R)d\delta}$$

Because the instrument line function has a unity normalized integral ( $\int S(\delta,R)d\delta = 1$ ), the measured transmission  $T_r$  can simply be written as

$$T_r(\omega) = \int T(\omega + \delta) S(\delta, R) d\delta \quad (8-5)$$

The measured absorbance can be obtained by taking the negative logarithm of Equation (8-5). Substituting for  $T$  from Beer's law, the expression

$$A_m(\omega) = -\log[\int \exp(-c\alpha(\omega + \delta)) S(\delta, R) d\delta] \quad (8-6)$$

is obtained. From Equation (8-6), the above two points can be examined. If the exponent  $c\alpha(\omega)$  is small, only the first two terms of the expanded exponential term can be retained, and the expression can be written as

$$A_m(\omega) \approx -\log\{\int [1 - c\alpha(\omega + \delta)] S(\delta, R) d\delta\}$$

Then, making use of the unity integral of  $S$  and the fact that  $\log(1 - x) \approx -x$  for small  $x$ , the measured absorbance can be written as

$$A_m(\omega) = c \int \alpha(\omega + \delta) S(\delta, R) d\delta$$

and this expression is linear with concentration. The assumption that is important here is that the product  $c\alpha$  must be small, at least compared to the quadratic term in the expansion of the exponential.

Another limiting case is that of high spectral resolution; that is, the instrument line function should be small compared to the half width of the gas absorption features. With that assumption, the transmission function is a slowly varying term in comparison with the instrument line function and can be brought outside the integral.

Then, again using the unity normal integral of  $S$ , the absorbance  $A$  can simply be written as

$$A_m(\omega) = -\log[\exp(-c\alpha(\omega))] = c\alpha(\omega)$$

which is again linear with concentration.

The predominant absorption features in spectra taken over an open path come from water vapor in the atmosphere, and these features have a FWHH of about  $0.1-0.2 \text{ cm}^{-1}$ . Therefore, the assumption above implies that the instrument resolution should be about  $0.05 \text{ cm}^{-1}$ . However, this requirement is not satisfied at present by any of the commercially available instruments for OP/FT-IR monitoring. Therefore, the response of the instruments that are available should be expected to be nonlinear, at least for water.

It is not easy to verify experimentally the nonlinear response of an FT-IR instrument since the concentrations normally present in the open air do not encompass a large enough range. The nonlinear response has been verified experimentally for methane by Ropertz (1997), and a copy of a portion of his data is shown in Figure 8-3. Additionally, reference spectra made from known concentrations of pure gases are available commercially. One ammonia reference that is commonly used has a concentration-path length product of  $550 \text{ ppm}\cdot\text{m}$ . When the absorption of that spectrum is compared to the absorption of the calculated spectrum at the same concentration-path length product, the agreement is within about 7%.

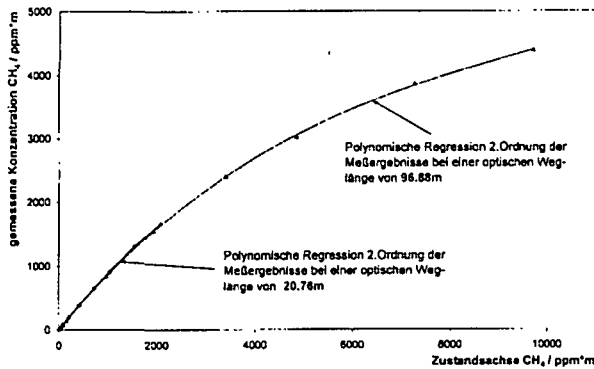


Figure 8-3. Measured Concentration of Methane vs. the Experimental Response of the FT-IR (reprinted with permission of A. Ropertz).

### 8.3 Results of Calculations

The effect of the nonlinear response has been studied for three gases: methane, ammonia, and water vapor. All the absorbances were calculated for a range of concentration-path length products at specific wavelengths and then fit to a polynomial of order 2, since this seemed to be the best fit. In one case (an ammonia line at  $1046\text{ cm}^{-1}$ ), the quadratic fit was not really satisfactory. The absorbance at that ammonia line was best fit with a linear approximation over a portion of the data and a quadratic approximation over the remainder. This is a clear indication that the functions describing the absorbance at various wave numbers are different. The absorbance was also calculated as a function of temperature and for the four resolutions  $0.25, 0.5, 1.0,$  and  $4.0\text{ cm}^{-1}$ .

The coefficients for the various polynomials were calculated by using

nonlinear regression. It was then possible to determine the maximum value of either the concentration-path length product or the temperature that can be used before the response must be considered nonlinear. To do that, the ratio of the quadratic to linear terms of the polynomial fit should be small, and this ratio was arbitrarily set equal to 0.1. This is equivalent to requiring that the concentration-path length product or the temperature be less than the term  $0.1c_l/c_q$ , where the  $c_l$  and the  $c_q$  are the linear and the quadratic coefficients, respectively.

The methane absorbance was measured at various points in the  $2900\text{--}3000\text{-cm}^{-1}$  region because that is the region most commonly used for the analysis. Within this region the absorbance was calculated for the concentration-path length product range from 300 to 2100 ppm·m. This corresponds to a path length of 200 m and a range of concentrations from 1.5 to 10 ppm. This range was selected because it covers the range from slightly below accepted ambient levels to slightly above the levels that could be expected at coal mines, landfills, or hog farms.

The ammonia absorbance was measured at various points in the  $850\text{--}1050\text{-cm}^{-1}$  region and covering the range from essentially 0 to 1100 ppm·m. For a 200-m path length, this range covers the concentration from the ambient levels to 5 ppm, or that concentration seen at hog farms.

The water spectra were calculated over the wavelength ranges of methane and ammonia since the absorbance due to water is the predominant interfering absorbance in the mid-infrared atmospheric spectrum. The water vapor absorbance was calculated in terms of the partial pressure of water from 0.5 to 35 torr, or from slightly below to slightly above that range seen here at Research Triangle Park (RTP), North Carolina, over a year. The various graphs for water that follow are plotted with the partial pressure in torr along the abscissa. The water absorbances were calculated for a path length of 207 m, which is the path length used when we take measurements at RTP.

All the absorbances were calculated over the temperature range from 250 K to 310 K in 5-K increments. This range was chosen because it covers the yearly range normally seen at RTP. This range is appropriate also in that it encompasses the temperature range over which the commercially available instruments can work. Finally, all the spectra were calculated for the following four resolutions: 0.25, 0.5, 1.0, and 4.0  $\text{cm}^{-1}$ .

Figures 8-4, 8-5, and 8-6 show the overall absorbance due to methane at 2927  $\text{cm}^{-1}$ , ammonia at 967  $\text{cm}^{-1}$ , and water at 1014.5  $\text{cm}^{-1}$ , respectively. The plots for methane and ammonia show the absorbance as a function of the concentration-path length product and the temperature. The

water absorbance is shown as a function of the partial pressure of water and temperature, with the absorbance being calculated for a path length of 207 m.

Figures 8-7 and 8-8 show, respectively, the absorbance for methane and ammonia as a function of concentration-path length product at a constant temperature of 295 K. Figure 8-9 shows the absorbance due to water as a function of the partial pressure of water, also at a constant temperature of 295 K. These graphs also contain the second-order polynomial that best describes the curvature of the absorbance.

As stated above, the dependence of the absorbance on temperature was also calculated for these three gases. The change in absorbance as a function of temperature for methane and ammonia is not very strong, as is depicted in Figures 8-4 and 8-5, but that is not the case for water. The change in absorbance with temperature for water is shown in more detail in Figures 8-10 and 8-11. Figure 8-10 shows the dependence of water absorbance on temperature at a partial pressure of 0.5 torr, and Figure 8-11 shows this dependence at a partial pressure of 35 torr.

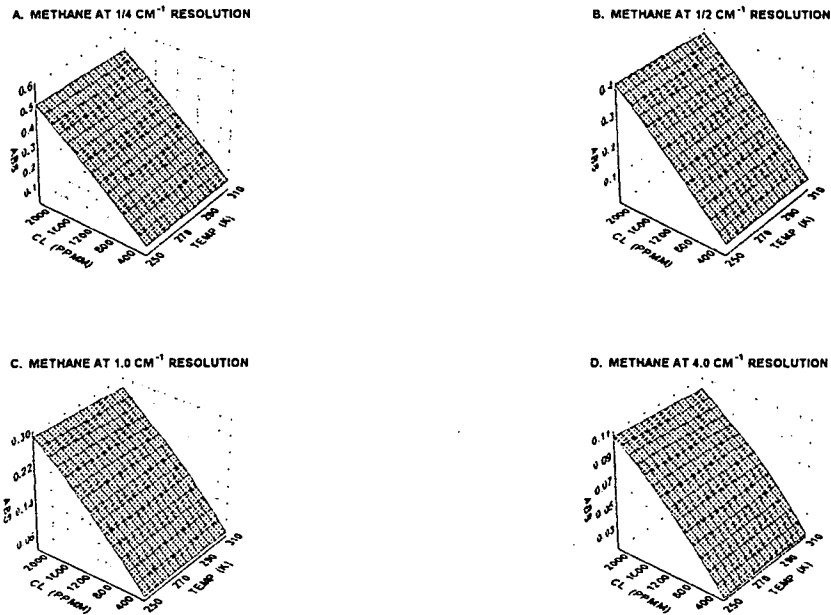


Figure 8-4. Methane Absorbance at 2927  $\text{cm}^{-1}$ .

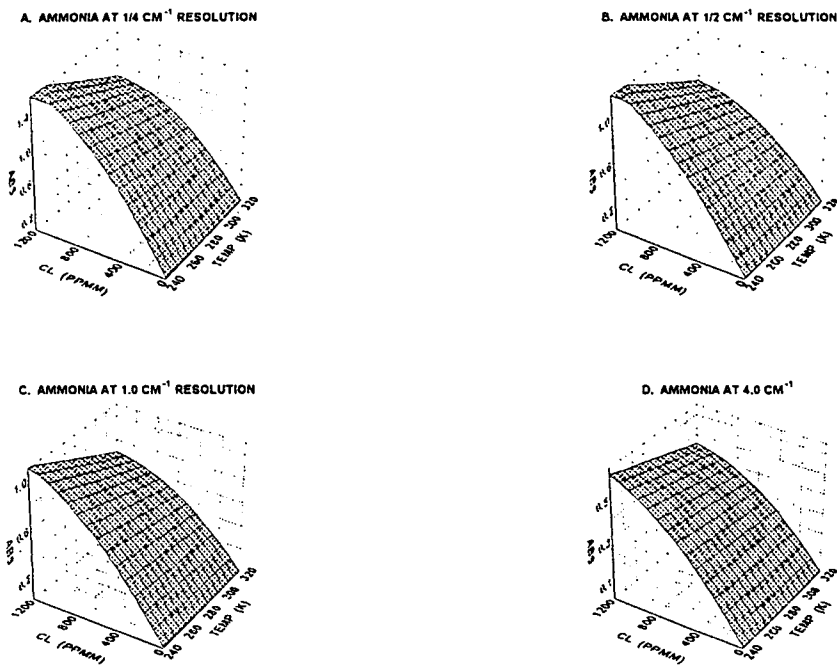


Figure 8-5. Ammonia Absorbance at 967  $\text{cm}^{-1}$ .

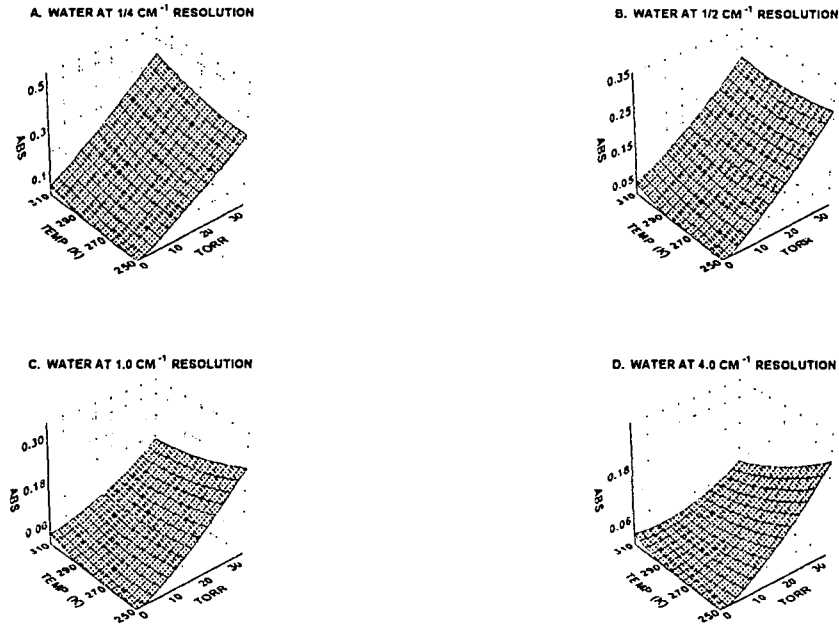


Figure 8-6. Water Absorbance at 1014.5 cm<sup>-1</sup>.

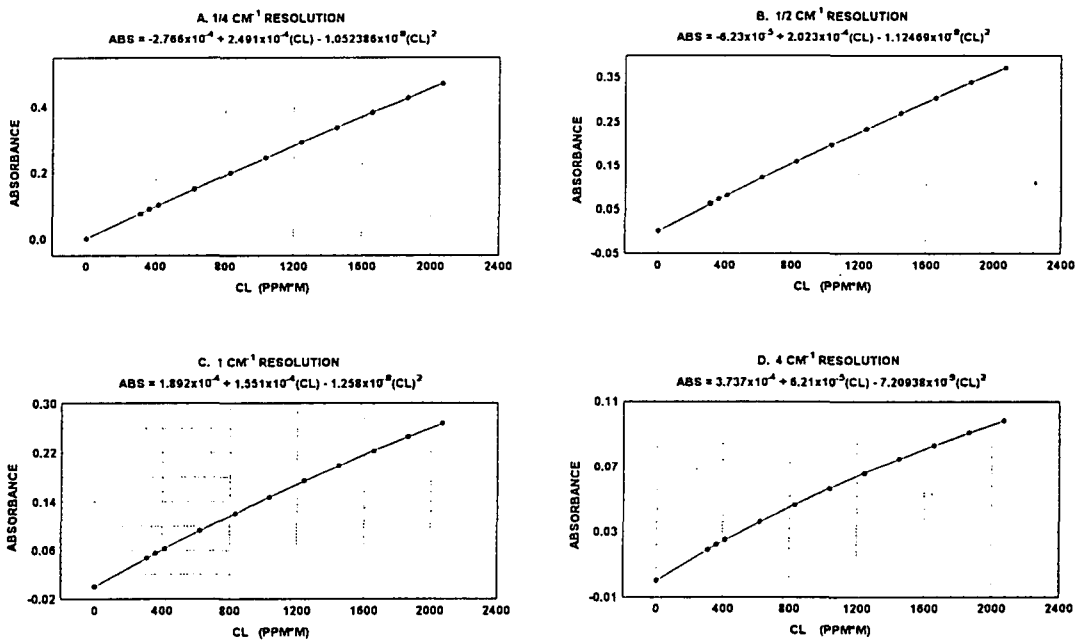


Figure 8-7. Methane Absorbance vs. CL at 2927 cm<sup>-1</sup>.

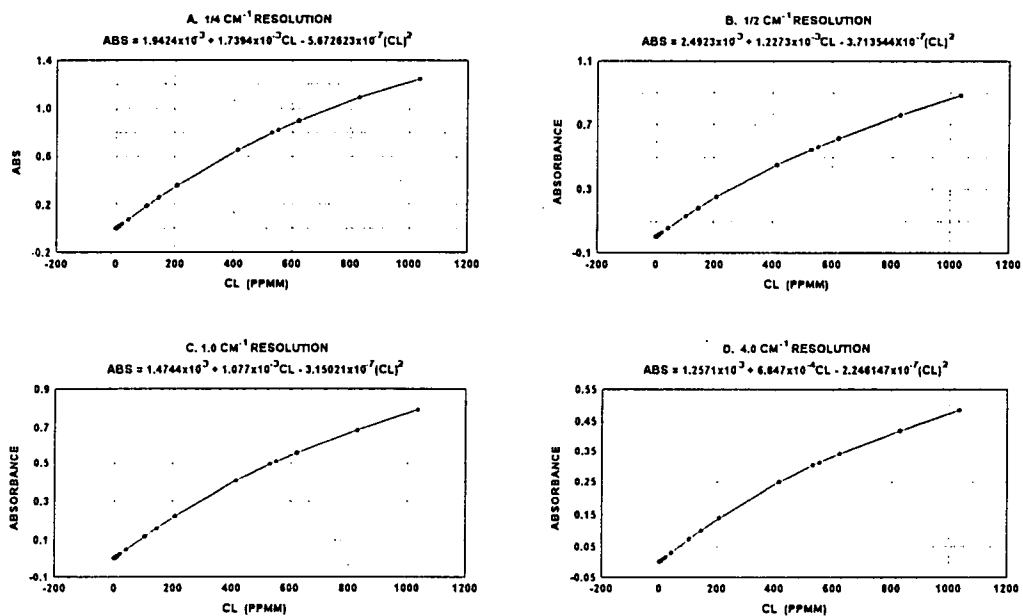


Figure 8-8. Ammonia Absorbance vs. *CL* at 967 cm<sup>-1</sup>.

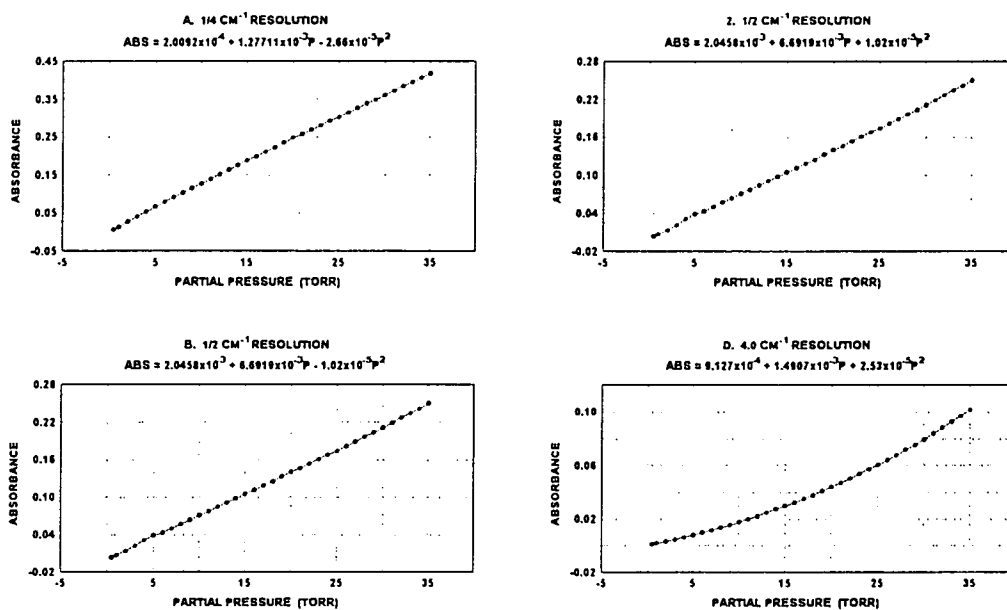


Figure 8-9. Water Absorbance vs. *P* at 1014.5 cm<sup>-1</sup>.



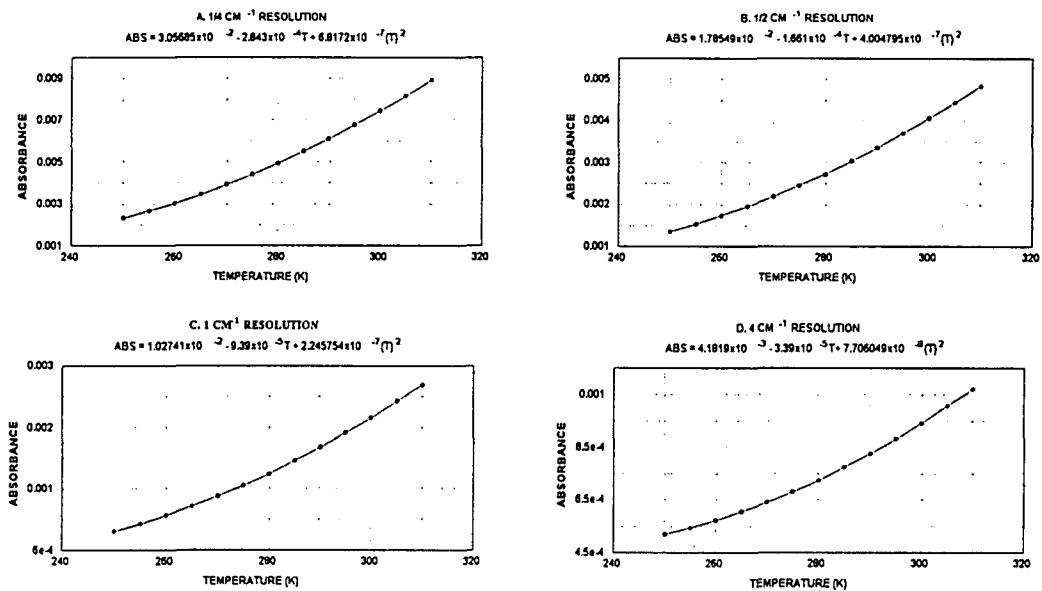


Figure 8-10. Water Absorbance for 0.5 torr at 1014.5 cm<sup>-1</sup>.

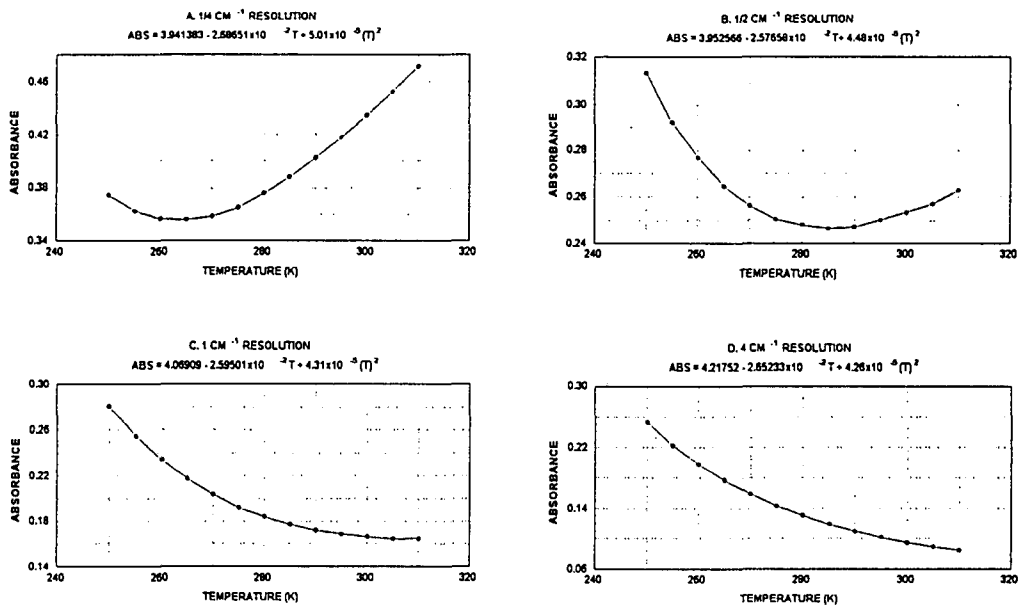


Figure 8-11. Water Absorbance for 35 torr at 1014.5 cm<sup>-1</sup>.

## 8.4 Analysis

Once the absorbance function is determined, it is instructive to find the maximum value in concentration for which the absorbance can be considered linear. This can be done by requiring that the quadratic term in the polynomial representing the absorbance be small in comparison with the linear term. That is, if the absorbance is represented by the polynomial  $ABS = a_0 + a_1X + a_2X^2$ , then for the absorbance to be considered linear, the ratio  $a_2X^2/a_1X$  must be small. The value of  $X$  can be found by requiring that this ratio be less than some value  $k$ , which is equivalent to requiring that the independent variable  $X$  must be less than the quantity  $a_1k/a_2$ . These values have been calculated for a  $k$  value of 0.1 and a temperature of 295 K and are shown for methane and ammonia in column 4 of Table 8-1.

Next, the error is estimated. The error made when a linear response is assumed depends on how far removed the

concentration-path length product of the field spectrum (the actual measurement) is from the concentration-path length product of the reference spectrum. (See Figure 8-2.) Column 5 of Table 8-1 shows the predicted error at the calculated maximum values  $X_{max}$  when references at 81 and 550 ppm·m are used for methane and ammonia, respectively. These reference values come from two commercial sources that are commonly used by the instrument users. The errors have been calculated in the following way. The linear response is simply based on the assumption that the absorbance goes through the 0 and the reference absorbance at the concentration-path length product listed. Thus the linear response is given by the expression  $ABS_L = (ABS_{REF})(CL)/CL_{REF}$ , where the  $(CL)_{REF}$  is the concentration-path length product of the reference spectrum. The absorbances for both the linear response and the quadratic response can be calculated for the same  $CL$  and the error found from  $\%E = (ABS_Q - ABS_L)/ABS_Q$ . The results of these calculations are given in Table 8-1.

**Table 8-1. Maximum Values Over Which Response Can Be Considered Linear and Associated Errors**

Gas	$\nu$ (cm <sup>-1</sup> )	Resolution (cm <sup>-1</sup> )	$X_{max}$ (ppm·m)	% Error at $X_{max}$
Methane	2927	0.25	2367	-9.3, Ref. at 81 ppm·m
		0.5	1799	-10.2
		1.0	1232	-11.9
		4.0	861	-17.4
Ammonia	967	0.25	307	+8.9, Ref. at 550 ppm·m
		0.5	330	+7.6
		1.0	342	+6.9
		4.0	305	+9.2

Similar calculations can be carried out for water, but in that case it is found that the absorbance is not linear for resolutions poorer than  $0.5 \text{ cm}^{-1}$  throughout the entire range of partial pressures for which the absorbances were calculated. This is also true for the water absorbance as a function of temperature. The water absorbance was also examined at  $1012.4 \text{ cm}^{-1}$ , which is considered to be at the baseline between peaks. As the partial pressure of water rises and the absorbance increases, the wings of the individual peaks merge to become a continuum, which then forms the spectral baseline. This is particularly troublesome for the least-squares analysis because the absorbance at the baseline changes in a nonlinear way over the entire range of partial pressures for which the calculations were done.

While the actual concentration of water is of little interest as an atmospheric pollutant and water is seldom a target compound, it must almost always be included in the least-squares analysis as an interfering species. One question that this work set out to answer is how to overcome the difficulty with matching the water vapor reference to the actual water in the field spectrum. The concentration of water can and does change rapidly and dramatically in the atmosphere. Therefore, it was instructive to look at the case where the water vapor reference was obtained from a spectrum that was taken when the partial pressure was 10 torr but the actual partial pressure of

water for the spectra being analyzed was 20 torr.

Figure 8-12 is a plot of the water absorbance in the  $1014.5\text{-cm}^{-1}$  region. The solid curve is a water spectrum calculated for 20 torr of water at 207 m. The dotted curve is a 10 torr spectrum that has been normalized to the 20 torr spectrum at  $1014.5 \text{ cm}^{-1}$ . Note that the only place where the curves seem to match is at that peak, and there is a particularly large discrepancy in the baseline. But this kind of normalization is not exactly what classical least squares does. The mathematics of classical least squares adjusts the curves, one to the other, so that the sum of the differences between them squared is a minimum. It does that by calculating a slope as the single coefficient by which to multiply the entire curve (in this case the 10 torr spectrum) and by adding some constant value to the result. However, because of the nonlinear response of the instrument and the fact that the polynomials describing the absorbance seem to be

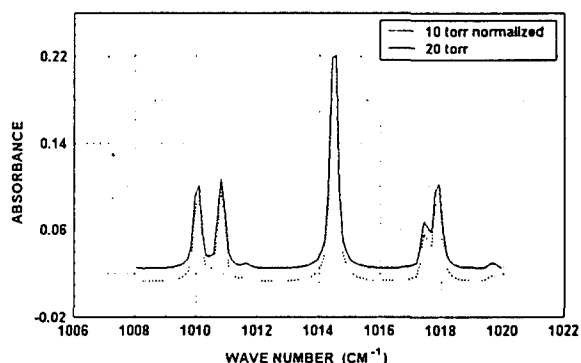


**Figure 8-12. Match of Water Absorbance at  $1014.5 \text{ cm}^{-1}$ .**

different for different wave numbers, no such process can really match the curves.

All the above analysis describes what error would be made if the analysis for concentration were done at a single wave number using a single reference. However, the classical least squares analysis uses a range of wave numbers for the calculation. In the remainder of this Analysis section, the classical least-squares technique is applied to this data to determine the actual error involved with this procedure in light of the nonlinearities discussed above.

To explore the effect of a reference spectrum whose concentration-path length product is not at the concentration-path length product of the field spectrum, a methane spectrum calculated for 6 ppm of methane at 295 K was used as a "field" spectrum. The spectra used as references were all at 295 K, but the concentrations were allowed to vary from 1.5 ppm to 10 ppm. The results for these calculations are shown in Figures 8-13 and 8-14. Figure 8-13 is a plot of the analyzed concentrations of methane over the wave number range 2915–2929  $\text{cm}^{-1}$ . This region was chosen for this analysis because there are two methane lines that are not strongly impacted by the interfering species water. In Figure 8-14, the analysis region has been expanded to cover the region from 2900 to 3000  $\text{cm}^{-1}$ . These plots clearly indicate that the best accuracy is at the higher resolution, and also that the smaller analysis region

seems to also have better accuracy. This must indicate that the least-squares technique is less efficient at matching the two spectra when the analysis region is large.

To explore the effect of water as an interfering species, a "field" spectrum of methane and water was calculated from HITRAN and then analyzed by classical least squares. The field spectrum used a concentration of 6 ppm for methane and a partial pressure of water of 15 torr, all at a temperature of 295 K. The partial pressure of the spectra used as water references was allowed to range from 10 to 20 torr at 295 K. Figure 8-15 shows the results from classical least-squares analysis for methane for the two wave number regions 2915–2929  $\text{cm}^{-1}$  and 2900–3000  $\text{cm}^{-1}$ . The data points for the two regions have been shifted slightly for clarity. These results indicate that the methane concentration is not strongly impacted by the presence of water. There does seem to be a bias of a few percent for each region from the true value, and the magnitude of the error bars is larger for the larger region. It is not clear why the small but definite biases in these graphs are present. A possible reason is that in the presence of water, because of its high concentration-path length product, the resulting absorption spectrum is not simply a linear combination of the absorbances from methane and water.

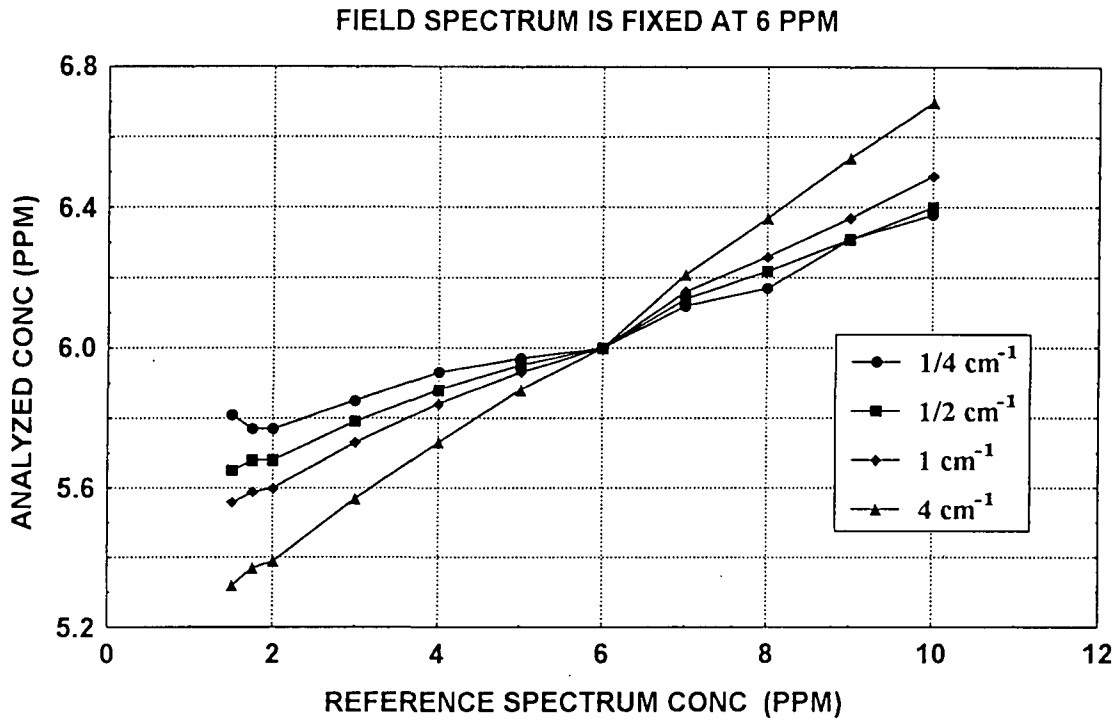


Figure 8-13. Analysis Results for Methane from 2915 to 2929 cm<sup>-1</sup>.

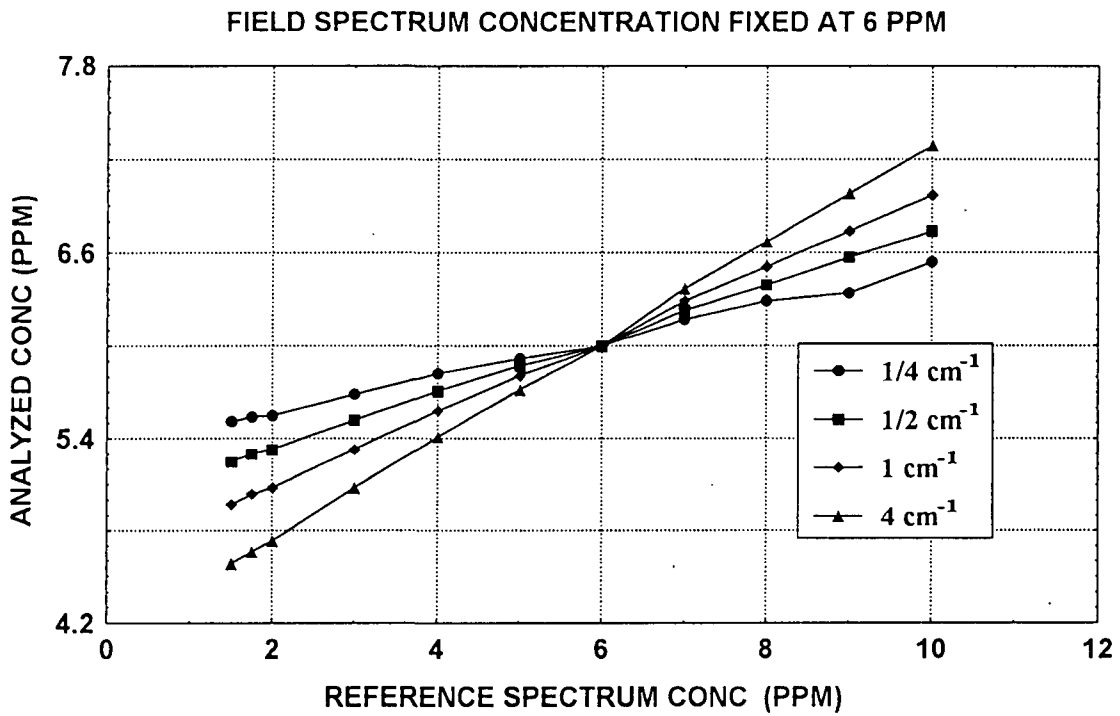
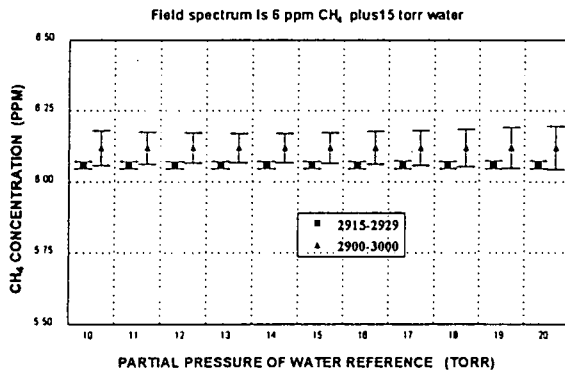


Figure 8-14. Analysis Results for Methane from 2900 to 3000 cm<sup>-1</sup>.



**Figure 8-15. Methane Analysis Allowing the Water Reference Concentration to Vary.**

Some further study has shown that as the resolution gets poorer, the errors for the above calculations also get worse (data not shown). The reason for water as an interfering species to not strongly impact the methane analysis, although somewhat surprising, is clear. The mathematical procedure of classical least squares adjusts the spectra so that for the individual components most of the variability of the absorbance in the field spectrum is accounted for. It makes that adjustment by minimizing the sum of the squares of the residuals. But, in the case of water—just as with methane, the calculated concentration is not the correct value unless the water reference has the same partial pressure and was taken at the same temperature as the water in the field spectrum. Nonetheless, because the residuals have been minimized, classical least squares accounts for most of the variability in the absorbance of the water and also minimizes the effect of water on the analysis of methane.

## 8.5 Discussion

The calculated spectra have been analyzed to determine the magnitude of the error when a linear function is assumed for the response of the FT-IR instrument. From Figure 8-2 it is seen that for a measured absorbance the concentration is overestimated when the concentration-path length product of the field spectrum is less than that of the reference spectrum. Conversely, the concentration is underestimated when the concentration-path length product of the field spectrum is high in comparison with the reference. It is also shown here that the magnitude of the error is larger with poorer resolution.

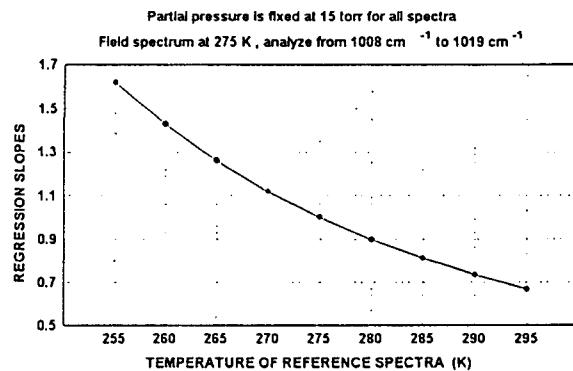
At present there seems to be no simple correction that can be applied to the calculated concentration-path length product to account for the error. In the cases presented here, the spectra could be calculated from the HITRAN database, but the number of gases available in HITRAN is quite limited to the predominant atmospheric species. What must be made available is either a set of references for each gas that encompasses a large range of concentration-path length products or a set of high-resolution spectra that can be modified through the mathematics shown here to account for the nonlinear response. Then the analysis should proceed by using a polynomial fit to the absorbance versus concentration.

Even with a reasonable estimate of the maximum concentration-path length product that can be used with some assurance that the errors will not be very large, the implied maximum allowable concentrations in terms of parts per million over the 207-m path are fairly small. For example, Table 8-1 shows that at a resolution of  $4\text{ cm}^{-1}$  the maximum allowable concentration would not really encompass the methane concentration variability normally seen in the atmosphere. While the higher resolutions imply higher maximum values, measurements at coal mines might have high unexpected errors that are not reported at all by the classical least-squares technique. The criterion used to arrive at the values in this paper was that the ratio of the quadratic term to the linear term should be less than 0.1. It is felt that this is not a stringent criterion, and that implies that higher reported values of methane, even at normal atmospheric concentrations, probably have some unexpected and unreported error associated with them. The magnitude of such errors is probably unknown to the experimenter.

The results for ammonia are similar to those of methane except that at the  $967\text{-cm}^{-1}$  peak there does not seem to be as much effect due to changing resolution.

Water presents an entirely different problem to the analysis of FT-IR data. The absolute value of the concentration of water is rarely, if ever, calculated, and the

important concern seems to be whether the absorbance due to water is adequately accounted for. This evaluation indicates that analyzing for an actual value for the concentration of water may be difficult but that this may not make much difference since the variability of the absorbance due to water seems to be accounted for almost entirely. Figures 8-15 and 8-16 tend to corroborate these assumptions. Figure 8-16 plots the value of the linear regression slope when the dependent variable is a water spectrum at a partial pressure of 15 torr and a temperature of 275 K. The independent variables were a set of water spectra whose partial pressures were all 15 torr but whose temperatures varied from 255 to 295 K. The expected value of all the slopes was 1.00. This curve implies that the temperature difference plays a major role in the error of the analysis. If, for example, the calculations are repeated for a set of independent variables, all at the same temperature but at changing partial pressure, the regression slopes are all within a few percent of the expected values.



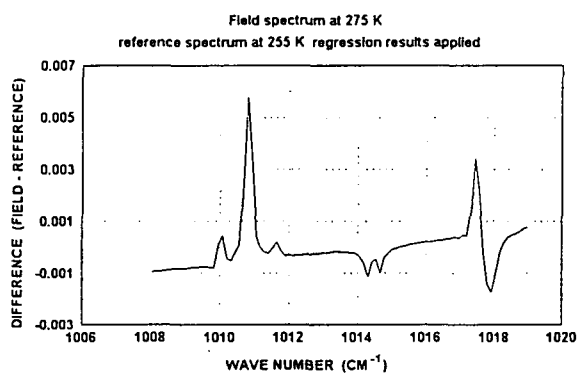
**Figure 8-16. Plot of Regression Slopes Vs. Temperature.**

Figure 8-17 is a plot of the difference of two spectra. One is the original field spectrum where the partial pressure of water is 15 torr at 275 K. The reference spectrum was at 15 torr but at a temperature of 255 K. To obtain the plot in Figure 8-17, the difference was found between the field spectrum and the reference spectrum to which the regression results had been applied. These results show that the difference is less than 10% of the original, thereby accounting for at least most of the absorbance due to water. Figure 8-17 also shows a number of other curious results. The two spectra were aligned at the 1014.5-cm<sup>-1</sup> line, but the difference clearly shows that the reference spectrum was somewhat broader than the field spectrum because of the "W" shape of the curve. The line at 1017 cm<sup>-1</sup> clearly shows that these two spectra were not properly aligned, although they were at 1014.5 cm<sup>-1</sup>. At the 1010.7-cm<sup>-1</sup> line, the difference indicates both a misalignment and a difference in the widths of the two lines. The discussion of this chapter does not speculate on why

that happens, but most workers in the field of open-path FT-IR measurements have seen this occur on many occasions.

## 8.6 Conclusions and Recommendations

The work that has been carried out here has been restricted to molecules that have fairly narrow absorption features, and broadband features have yet to be studied. It is likely that whenever the instrument line function (or slit function) is broad in comparison with the absorption feature, the results presented here will be noticeable. Because the response of the FT-IR instrument is inherently nonlinear but the most commonly used analysis technique assumes it to be linear, errors of an unknown magnitude can occur in the data. These errors occur for two primary reasons: First, the reference spectra that are commonly used by workers with the FT-IR instrument have not been taken at the same concentration-path length product or at the same temperature as existed during the field spectra acquisition phase. Second, the differences in the temperatures at which the reference and the field spectra were acquired seem to be more important than was at first thought. This is clearly true for water.



**Figure 8-17. Difference After Regression Coefficients Have Been Applied.**

From this work, the conclusions that can be drawn are as follows.

- Errors of unknown magnitude occur in the FT-IR data whenever the reference spectrum of the target gas does not have the same concentration-path length product as the field spectrum. There is probably at least a 10% error



whenever the reference and the field spectrum differ in concentration–path length product by a factor of 2.

- Differences in temperature cause some further error.
- In all the cases studied here, higher resolution indicated lower predicted errors.
- Water, when used as an interfering species, does not strongly impact the analysis, even when the difference in concentration–path length product is large. It is anticipated that this is true for all interfering species.
- The analysis for water directly is limited by the same difficulty as analysis for any other target gas.
- It is essentially impossible to determine the absolute error in concentration calculated for any one field spectrum. This is because the magnitude of the error depends on the magnitude of the difference in the concentration–path length product of the reference and the field spectra.

Although this may seem to be a formidable problem for the analysis of FT-IR data when the response is assumed to be linear, there are some ways to overcome it. The recommendations are as follows.

- The use of high resolution ( $0.25 \text{ cm}^{-1}$ ) makes the errors smaller and manageable.

- The combination of high resolution and boxcar apodization (or unapodized spectra) seems to create the most linear response. Because it is likely that at present few reference spectra using boxcar apodization exist, they must be manufactured.
- A new mathematical analysis approach that accounts for the nonlinear response directly during the analysis should be developed.
- Future databases like the NIST database should incorporate high-resolution spectra, along with the capability to create apodized, lower resolution spectra that account for the inherent nonlinearity created by the instrument line function.

## 8.7 References

Filler, A.S. 1964. Apodization and Interpolation in Fourier-Transform Spectroscopy. *J. Opt. Soc. Am.* 54:762–767.

Happ, H., and L. Genzel. 1961. Interferenz-Modulation Mit Monochromatischen Millimeterwellen. *Infrared Phys.* 1:39–48.

Norton, R.H., and R. Beer. 1976. New Apodizing Functions for Fourier spectrometry. *J. Opt. Soc. Am.* 66:259–264.

Kauppinen, J.K., D. J. Moffatt, D.G. Cameron, and H.H. Mantsch. 1981. Noise in Fourier Self-Deconvolution. *Appl. Opt.* 20:1866–1879.

Marshall, A.G. and F.R. Verdun. 1990. *Fourier Transforms in NMR, Optical, and Mass Spectrometry*, Elsevier, Amsterdam.

Ropertz, A. 1997. Kalibrierung Eines FT-IR Langwegabsorptionsspektrometers in Verbindung Mit Einer Einstelbaren Infrarot-multi-reflexionsgaszelle Und Validerung Der Ergebnisse Wahrend Einer Messkampagne Bei Einer Raffinerie. Diplomarbeit im Fachbereich Maschinen und Verfahrenstechnik an der Fachhochschule Dusseldorf, Matrikel-Nr 240415, Dusseldorf.

Rothman, L.S., R.R. Gamache, A. Goldman, R.A. Toth, H.M. Pickett, R.L. Poynter, J.M. Flaud, C. Camy-Peyret, A. Barbe, N. Hussen, C.P. Rinsland, and M.A.H. Smith. 1987. The HITRAN Database: 1986 Edition. *Appl. Opt.* 26:4058-4096.

Russwurm, G.M. 1996. Long-Path Open-Path Fourier Transform Infrared Method Monitoring of Atmospheric Gases. *Compendium of Methods for the Determination of Toxic Organic Compounds in Ambient Air—Compendium Method TO-16*, EPA/625/R-96/010b, U.S. Environmental Protection Agency, Research Triangle Park, NC.

## Chapter 9

### The Technique of Classical Least Squares

#### SUMMARY

This chapter can be considered a tutorial on the use of classical least squares analysis as applied to the FT-IR data. The following specific points are addressed.

- Least squares analysis for one dependent and one independent variable or simply regression analysis
- Development of the least squares techniques in matrix terms
- Using more than one reference gas
- Expansion of the technique to include the quadratic terms
- Discussion of the errors as calculated by this technique

#### 9.1 Introduction and Overview

At the time of this writing the preferred technique for data analysis of the FT-IR spectra is the method of least squares. In order for this technique to be used, a set of reference spectra must be available to the operator. These spectra are acquired by using pure samples of gas under controlled conditions of pressure and temperature. They are generally acquired with the gas in an enclosed cell in a laboratory. Once the absolute pressure of the target gas in the cell is adjusted, the cell is backfilled to a total pressure of one atmosphere by using a nonabsorbing gas such as nitrogen, and the spectrum is acquired. In order to accurately analyze a so-called field spectrum there has to be one reference spectrum for each gas whose absorbance is contained in the field spectrum.

This chapter describes in some detail the process of the analysis itself, and this description is by necessity somewhat mathematical. Section 9.2 of this chapter considers the case where there is one gas in the field spectrum and only one gas is used as a reference. The result of this is to derive the general expressions for the linear least-squares fit, or what is generally referred to as linear regression. Section 9.3 introduces matrix terminology and describes how the analysis is generalized to several gases. Section 9.4 describes those changes in the matrix terminology that are necessary to include a quadratic term in the equations so that a nonlinear response can be accounted for.

#### 9.2 Least Squares Analysis for One Gas

The least squares technique has been developed for many years and is amply

described in many texts (Sokolnikoff and Redheffer 1966; Draper and Smith 1966). As applied here, it consists of trying to fit the absorbance of a reference spectrum to the absorbance measured in a field spectrum in some so-called best way. The assumption is that at each wave number of the spectra there is a linear relation between the field spectrum absorbance and the absorbance of the reference spectrum. This assumption arises naturally from Beer's law, which implies that there is a linear relation between the absorbance and the concentration-path length product from which the spectrum was obtained. Mathematically, this linear relation is written as  $A = \alpha CL$ , where  $CL$  is the concentration-path length product and the constant of proportionality is  $\alpha$ , the absorption coefficient of the gas. This implies that for a fixed path length  $L$  the absorbance is a linear function of the concentration  $C$ . Thus at each wave number there is a linear relation between the absorbance of the field spectrum and the absorbance of the

reference spectrum. If the absorbance of the field spectrum is considered to be the dependent variable  $Y$  and the absorbance of the reference the independent variable  $X$ , then at each wave number a relation of the form  $Y = mX + b$  should exist. The problem then becomes a mathematical one of determining the slope  $m$  and the intercept  $b$ . As an illustration, consider the situation where there is a single gas in the field spectrum, and therefore only one gas is necessary in the reference set. If the instrument is operating at a resolution of  $0.5 \text{ cm}^{-1}$ , then there is a data point at every  $0.25 \text{ cm}^{-1}$ . A partial tabular listing of the absorbance data looks like that given in Table 9-1 below.

The data in this table shows that the baseline for both the field spectrum and the reference spectrum is at an absorbance (abs) of 0.001 and that an absorbance peak exists at  $1000.75 \text{ cm}^{-1}$ . If a graph of these absorbances is plotted with abs (field) along

**Table 9-1. Partial Listing of Spectral Absorbance (abs) Data**

Wave Number	abs (field)	abs (reference)
1000.00	0.001	0.001
1000.25	0.050	0.010
1000.50	0.085	0.017
1000.75	0.100	0.020
1001.00	0.090	0.018
1001.50	0.055	0.011
1001.75	0.030	0.006
•	•	•
•	•	•
•	•	•

the Y-axis (dependent variable) and the abs (reference) along the X-axis (independent variable), then the linear relation becomes apparent. In the absence of noise in the spectra, the intercept should be 0 according to Beer's law, but because of noise it is not, and the individual data points do not lie precisely on a straight line.

The question then becomes what is the "best" straight line that can be fit to the data points. The classical least squares technique defines what is meant by the term *best*, in that it requires that the sum of the squares of the residuals be a minimum. Once the slope and the intercept are determined, then a  $Y$  value can be calculated for any point  $X$  from  $Y = mX + b$ . The  $X$  values are chosen to coincide with the actual data points along the X-axis, and then the difference between the calculated  $Y$  and the actual  $Y$  data value is found. This difference is the residual. The individual residuals are squared and then summed, and the best fit is found when this sum is a minimum.

This procedure gives rise to the term *least squares*. The minimization process is completely transparent to the user, and he does not have to make small adjustments to the line and recalculate the sum of the residuals squared and then select the one slope and intercept that gives a minimum result. The process does that automatically because the equations used already make the sum a minimum.

The situation is shown schematically in Figure 9-1. The original data points are

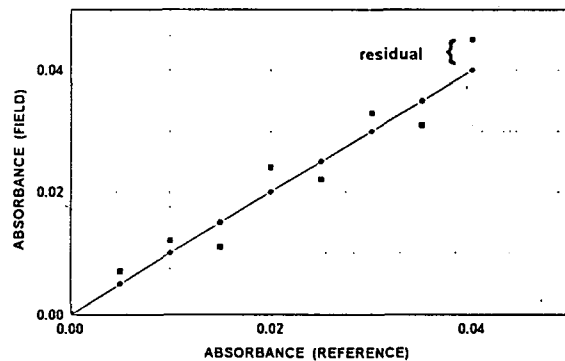


**Figure 9-1. Least Squares Fit of a Data Set.** The squares represent actual data but do not fall on the regression line.

shown as squares in the figure along with the best fit line. The residual at one data point (0.04,0.045) is also depicted.

As a demonstration of how the usual least squares equations for this simplified case arise, consider the following. Suppose that a field spectrum has been acquired and that the analysis region covers a range of discrete data points (total  $M$ ) along the wave number axis. The reference spectrum has the same number  $N$  of data points along the wave number axis. A plot similar to that in Figure 9-1 is made, and the problem is to determine the slope  $m$  and the intercept  $b$  for the best fit straight line between the two sets of spectral data. Let the equation of the best fit line be given as  $y = mX + b$  and let the original data points in the field spectrum be at  $(X_i, Y_i)$ . At each data point  $(X_i, Y_i)$ , calculate a new  $y$  from the equation such that  $y_i = mX_i + b$ . Then form the residuals at each point such that  $R_i = Y_i - y_i = Y_i - (mX_i + b)$ . The individual residuals are then squared and summed over all the data points. This leads to the expression

$$S = \sum R_i^2 = \sum [Y_i - (mX_i + b)]^2 \quad (9-1)$$

where the sum is taken over all the data points from 1 to  $N$ . In order to minimize  $S$ , the derivative of  $S$  with respect to both  $m$  and  $b$  must be found and each set equal to 0. The derivatives are each given below.

$$\frac{\partial S}{\partial m} = 2 \sum [Y_i - (mX_i + b)] X_i = 0 \quad (9-2)$$

and

$$\frac{\partial S}{\partial b} = 2 \sum [Y_i - (mX_i + b)] = 0 \quad (9-3)$$

Equations 9-2 and 9-3 are a set of simultaneous equations that can be solved for  $m$  the slope and  $b$  the intercept. These expressions can be rewritten as

$$m \sum X_i^2 + \sum X_i b = \sum X_i Y_i \quad (9-4)$$

and

$$m \sum X_i + \sum b = \sum Y_i \quad (9-5)$$

The term  $\sum b$  is equal to  $Nb$ , where  $N$  is the total number of data points, so Equation 9-4 can be solved for  $b$  as

$$b = \frac{1}{N} (\sum Y_i - m \sum X_i) \quad (9-6)$$

This expression for  $b$  can be substituted into Equation 9-3, which can then be solved for  $m$  to get

$$m = \frac{\sum X_i Y_i - \frac{1}{N} \sum X_i \sum Y_i}{\sum X_i^2 - \frac{1}{N} (\sum X_i)^2} \quad (9-7)$$

It should be noted that in Equation 9-6 the terms

$$\frac{1}{N} \sum X_i$$

and

$$\frac{1}{N} \sum Y_i$$

are just the average values of the  $X$ 's and the  $Y$ 's, so Equation 9-5 becomes

$$b = \bar{Y} - m \bar{X} \quad (9-8)$$

Equations 9-6, 9-7, and 9-8 are the usual equations that are used for doing a linear regression between two data sets. As applied to the spectral data from the FT-IR, the  $X$ 's in these equations are the absorbances at the various wave numbers for the reference spectrum, and the  $Y$ 's are the absorbances of the field spectrum.

As a numerical example, the data in Table 9-1 can be used. There are a total of seven data points, so  $N = 7$ . There are really

only four quantities that have to be calculated. They are the sum of the  $X$ 's, the sum of the  $Y$ 's, the sum of  $XY$  products and the sum of the  $X$ 's squared. From the data in Table 9-1, these quantities are:  $\sum X = 0.083$ ,  $\sum Y = 0.411$ ,  $\sum XY = 0.006351$ , and  $\sum (X)^2 = 0.001271$ . Substituting these values into Equation 9-7, the slope is obtained as

$$m = \frac{\sum XY - \frac{1}{N} \sum X \sum Y}{\sum X^2 - \frac{1}{N} (\sum X)^2} =$$

$$\frac{0.006351 - \frac{(0.083)(0.411)}{7}}{0.001271 - \frac{(0.083)(0.083)}{7}} = 5.151$$

The intercept can be calculated next from Equation 9-8. From the above data the intercept is

$$b = \frac{1}{N} \sum Y - \frac{m}{N} \sum X =$$

$$\frac{0.411}{7} - \frac{(5.151)(0.083)}{7} = -0.002367$$

When the results of this calculation are applied to the original data to determine the atmospheric concentration of the gas, the concentration product of the reference is multiplied by the slope and then divided by the actual path length used to acquire the field spectrum. So if the reference concentration-path length product is 20 ppm·m and the actual path length used was 200 m, then the atmospheric concentration is  $20 * 5.15 / 200 = 515$  ppb.

### 9.3 Matrices

The technique outlined above is limited to a single gas in the field spectrum and therefore uses a single reference. Continuing on to the more realistic case of several gases and several interfering species is a tedious if not impossible task in the method described above, and some other method of describing the process has to be found. Fortunately, there is such a method, and it involves the use of matrices. Thus a short tutorial session on the description and manipulation of matrices is presented next. Many excellent texts (Hohn 1964; Belman 1970) cover the mathematics of matrices, and the interested reader should consult them for more in-depth descriptions of the use of matrices.

#### 9.3.1 Matrix Types

A matrix is simply an array of numbers. The array can have  $i$  rows and  $j$  columns. If the number of rows  $i$  equals the number of columns  $j$ , the matrix is said to be square. The convention used in this tutorial will be to designate a matrix by an italicized bold letter. A square matrix  $A$  that has 3 rows and 3 columns is shown below

$$A = \begin{bmatrix} a_{11} & a_{12} & a_{13} \\ a_{21} & a_{22} & a_{23} \\ a_{31} & a_{32} & a_{33} \end{bmatrix}$$

where the elements of the matrix are designated by the subscripts  $ij$ . The element  $a_{11}$  is the element in the first row and the first column, while the element  $a_{32}$  is the

element in the third row and the second column. The numerical elements of a matrix will always be enclosed by the square brackets as shown. A matrix can have only 1 row as  $A = [a_{11} \ a_{12} \ a_{13} \ \dots \ a_{1j}]$  or it can have only 1 column as

$$A = \begin{bmatrix} a_{11} \\ a_{21} \\ a_{31} \\ \vdots \\ a_{i1} \end{bmatrix}$$

In these cases the matrices are called either a row vector or a column vector. A general matrix of  $i$  rows and  $j$  columns can be written as  $A = [a_{ij}]$  or just simply as  $A$ . There are other matrices that are necessary for this work, and they will be introduced at the appropriate time.

Matrices arise naturally in mathematics from the study of the solutions to simultaneous equations, and they represent a concise way to manipulate the coefficients of the equations. For a pair of simultaneous equations

$$\begin{aligned} a_0 X + a_1 Y &= c_1 \\ b_0 X + b_1 Y &= c_2 \end{aligned}$$

there are a number of matrices that can be written to describe these equations. The coefficient matrix is shown below as the [2x2] matrix

$$C = \begin{bmatrix} a_0 & a_1 \\ b_0 & b_1 \end{bmatrix}$$

and the augmented matrix shown below as the [2x3] matrix

$$A = \begin{bmatrix} a_0 & a_1 & c_1 \\ b_0 & b_1 & c_2 \end{bmatrix}$$

### 9.3.2 Some Matrix Properties

Matrices have a number of mathematical properties that allow them to be used for obtaining the solutions of algebraic equations. They can be added and subtracted from one another so that if  $A = [a_{ij}]$  and  $B = [b_{ij}]$ , then  $A \pm B = [a_{ij} \pm b_{ij}]$ . A matrix  $A$  can be multiplied by a scalar  $k$ , (simply a number) such that if  $A = [a_{ij}]$ , then  $kA = [ka_{ij}]$ . These properties are demonstrated with actual numbers below. If

$$A = \begin{bmatrix} 2 & 7 \\ 5 & 12 \end{bmatrix}$$

and

$$B = \begin{bmatrix} 4 & 9 \\ 3 & 8 \end{bmatrix}$$

then

$$A + B = \begin{bmatrix} 6 & 16 \\ 8 & 20 \end{bmatrix}$$

and

$$A - B = \begin{bmatrix} -2 & -2 \\ 2 & 4 \end{bmatrix}$$



Also, for multiplication by a scalar, say  $k = 3$ , then

$$kA = 3A = \begin{bmatrix} 6 & 21 \\ 15 & 36 \end{bmatrix}$$

Division of a matrix by a scalar is also possible.

Multiplication of one matrix by another is allowed, but it is not possible to divide one matrix by another. Multiplication of one matrix by another follows certain mathematical rules, and these are described in the next section.

### 9.3.3 Multiplication of Matrices

The description of matrix multiplication begins with a discussion of how to multiply two square matrices together. Suppose that two matrices,  $A$  and  $B$ , are each  $[2 \times 2]$  matrices and they are to be multiplied as  $C = AB$ . Then if

$$A = \begin{bmatrix} a_{11} & a_{12} \\ a_{21} & a_{22} \end{bmatrix}$$

and

$$B = \begin{bmatrix} b_{11} & b_{12} \\ b_{21} & b_{22} \end{bmatrix}$$

then the product  $C = AB$  is given by

$$C = \begin{bmatrix} a_{11} & a_{12} \\ a_{21} & a_{22} \end{bmatrix} \begin{bmatrix} b_{11} & b_{12} \\ b_{21} & b_{22} \end{bmatrix} =$$

$$\begin{bmatrix} a_{11}b_{11} + a_{12}b_{21} & a_{11}b_{12} + a_{12}b_{22} \\ a_{21}b_{11} + a_{22}b_{21} & a_{21}b_{12} + a_{22}b_{22} \end{bmatrix}$$

The first thing to note here is that each of the elements of the product matrix is made up of a sum of products of the original matrix elements. Each of the product elements is found by multiplying a row element of  $A$  with a corresponding column element of the matrix  $B$  and then summing the individual terms. So, the elements of row 1 of the matrix  $A$  are multiplied by the elements of column 1 of the matrix  $B$ , and then the individual terms are summed to get the element (1,1) of the product matrix  $C$ . The element (1,2) of the product matrix  $C$  is found by using the elements from row 1 of the matrix  $A$  and the elements from column 2 of the matrix  $B$ . Thus the subscripts of the product matrix elements provide the instructions of which row and which column to use from the original matrices. The numerical examples above for the matrices  $A$  and  $B$  can be used to demonstrate this multiplication. Thus

$$C = AB = \begin{bmatrix} 2 & 7 \\ 5 & 12 \end{bmatrix} \begin{bmatrix} 4 & 9 \\ 3 & 8 \end{bmatrix} =$$

$$\begin{bmatrix} 8+21 & 18+56 \\ 20+36 & 45+96 \end{bmatrix} = \begin{bmatrix} 29 & 74 \\ 56 & 141 \end{bmatrix}$$

However, an important point about matrix multiplication is that it is not commutative. That is, the product  $AB$  does not equal the product  $BA$ . This is clearly shown in the example below (again using the same matrices as above).

$$C' = BA = \begin{bmatrix} 4 & 9 \\ 3 & 8 \end{bmatrix} \begin{bmatrix} 2 & 7 \\ 5 & 12 \end{bmatrix} =$$

$$\begin{bmatrix} 8+45 & 28+108 \\ 6+40 & 21+96 \end{bmatrix} = \begin{bmatrix} 53 & 136 \\ 46 & 117 \end{bmatrix}$$

Matrices need not be square in order to multiply them together. For example, a matrix with 3 rows and 2 columns can be multiplied by a matrix that has 2 rows and 3 columns. An example is shown below. Suppose that

$$A = \begin{bmatrix} a_{11} & a_{12} & a_{13} \\ a_{21} & a_{22} & a_{23} \end{bmatrix}$$

and

$$B = \begin{bmatrix} b_{11} & b_{12} \\ b_{21} & b_{22} \\ b_{31} & b_{32} \end{bmatrix}$$

then the result is a [2x2] matrix  $C$  such that

$$C = AB =$$

$$\begin{bmatrix} a_{11}b_{11} + a_{12}b_{21} + a_{13}b_{31} & a_{11}b_{12} + a_{12}b_{22} + a_{13}b_{32} \\ a_{21}b_{11} + a_{22}b_{21} + a_{23}b_{31} & a_{21}b_{12} + a_{22}b_{22} + a_{23}b_{32} \end{bmatrix}$$

If the product  $BA$  is found, then the result is a [3x3] matrix. Thus the order of multiplication is again important, and one generally speaks of either pre-multiplying one matrix by another or post-multiplying one matrix by another. For the product  $AB$ , one says that  $A$  pre-multiplies  $B$ , while for the product  $BA$  the matrix  $A$  post-multiplies the matrix  $B$ . In general a matrix of order  $(i,j)$  (one that has  $i$  rows and  $j$  columns) can pre-multiply a matrix of order  $(k,l)$  only if  $j = k$ . This gives rise to a matrix of order  $(i,l)$  or a matrix with  $i$  rows and  $l$  columns.

To solve the matrix equations that are used for the least squares analysis of FT-IR data, several further definitions are required. They include the identity matrix, the transpose of a matrix, cofactors of matrices or submatrices, and the inverse of a matrix. Also required is a discussion of the determinant of a matrix. Rather than provide a purely mathematical definition of the determinant, several examples are used, which provide the information about them that is required for the present discussion.

### 9.3.4 The Identity Matrix

The identity matrix  $I$  is simply a matrix that has all ones along the principal diagonal of the matrix and zeroes in all other

elements. Thus a [3x3] identity matrix is written as

$$I = \begin{bmatrix} 1 & 0 & 0 \\ 0 & 1 & 0 \\ 0 & 0 & 1 \end{bmatrix}$$

The principal diagonal of a matrix is the diagonal going from the upper left element to the lower right element. The usefulness of this matrix is explained below.

### 9.3.5 The Transpose of a Matrix

The transpose of a matrix  $A$  is written as  $A^T$  and is that matrix formed by interchanging the rows and the columns of the matrix  $A$ . So if the matrix  $A$  is a [3x3] matrix written as

$$A = \begin{bmatrix} a_{11} & a_{12} & a_{13} \\ a_{21} & a_{22} & a_{23} \\ a_{31} & a_{32} & a_{33} \end{bmatrix}$$

then the transpose is also a [3x3] matrix, but the elements are rearranged so that

$$A^T = \begin{bmatrix} a_{11} & a_{21} & a_{31} \\ a_{12} & a_{22} & a_{32} \\ a_{13} & a_{23} & a_{33} \end{bmatrix}$$

A numerical example of a matrix  $A$  and its transpose is given below. Let

$$A = \begin{bmatrix} 7 & 12 & 9 \\ 6 & 22 & -3 \\ 4 & 11 & -1 \end{bmatrix}$$

then the transpose is

$$A^T = \begin{bmatrix} 7 & 6 & 4 \\ 12 & 22 & 11 \\ 9 & -3 & -1 \end{bmatrix}$$

### 9.3.6 The Determinant of a Matrix

The determinant of a matrix is a single number (a scalar) that is determined by multiplying various elements of a matrix together and then adding or subtracting the individual terms. Because the mathematical formulae that describe a determinant are complex, it seems prudent to simply describe the procedure to obtain a determinant by the use of examples. Only a square matrix can have a determinant, and the result can be any number, including zero. The determinant of a diagonal matrix is simply the product of all the elements along the diagonal. A diagonal matrix as used here is a matrix that has zeroes for all elements except along the principal diagonal. Thus if any diagonal element of a diagonal matrix is zero the determinant is also zero. The determinant of the identity matrix as defined above is simply 1 because all the elements along the diagonal are 1. The determinant of a matrix  $A$  will be designated as  $\det(A)$  for this discussion.

The determinant of a [2x2] matrix is found by multiplying the elements of the principal diagonal together and subtracting from that product the result of multiplying the elements of the secondary diagonal. The secondary diagonal of a matrix is that diagonal running from the upper right to the lower left of the matrix. Thus if the [2x2] matrix is given by

$$A = \begin{bmatrix} a_{11} & a_{12} \\ a_{21} & a_{22} \end{bmatrix}$$

the determinant is given by the expression  $\det(A) = a_{11}a_{22} - a_{12}a_{21}$ . A numerical example of this is given below. If the matrix  $A$  is

$$A = \begin{bmatrix} 7 & 4 \\ 8 & 3 \end{bmatrix}$$

then the determinant of the matrix  $A$  is  $\det(A) = (7)(3) - (4)(8) = -11$ .

In order to find the determinant of a larger, say [3x3], square matrix, the problem must always be reduced to one of finding the appropriate [2x2] matrices by using the rules to be discussed. To obtain the proper [2x2] matrices from the original [3x3] matrix, the elements of the top row are each used in turn. The row and the column that element is in is then eliminated from the original matrix. The [2x2] matrix that remains is the one that has to be used. To complicate matters a little, the [2x2] must be multiplied by the matrix element whose row and column were eliminated. So, if the [3x3] matrix is given by

$$A = \begin{bmatrix} a_{11} & a_{12} & a_{13} \\ a_{21} & a_{22} & a_{23} \\ a_{31} & a_{32} & a_{33} \end{bmatrix}$$

then the determinant is given by

$$\begin{aligned} \det(A) = & a_{11}(a_{22}a_{33} - a_{23}a_{32}) \\ & - a_{12}(a_{21}a_{33} - a_{23}a_{31}) \\ & + a_{13}(a_{21}a_{32} - a_{22}a_{31}) \end{aligned}$$

It is important to note the change in sign from a plus to a minus in the second term in the determinant. The first term of the determinant is formed by starting with the element [1,1], then crossing out the first row and the first column and then finding the determinant of the [2x2] cofactor of the element [1,1]. The second term is found by starting with the negative of the element [1,2], then crossing out the first row and the second column and using the determinant of the cofactor of the element [1,2]. The third term is found by starting with the element [1,3] and then crossing out the first row and the third column to get the determinant of the [2x2] cofactor of the element [1,3]. Whether the sign in front of any particular term is positive or negative is found by actually using the expression  $(-1)^{i+j}$  where the  $i$  and the  $j$  are the element subscripts. Thus for the first term the element subscripts are 1,1 and  $1+1 = 2$ ; therefore  $(-1)^2 = 1$ . For the second term, however, the  $i$  and the  $j$  subscripts total 3 and  $(-1)^3 = -1$ . The subscripts for the third term again yield a +1 multiplier. A numerical example of

calculating the determinant for a [3x3] matrix is given below. Let the matrix  $A$  be given by

$$A = \begin{bmatrix} 3 & 9 & 1 \\ 6 & 7 & 5 \\ 12 & 2 & 8 \end{bmatrix}$$

The determinant for this matrix is found following the rules above as

$$\begin{aligned} \det(A) &= 3[(7)(8) - (5)(2)] - \\ & 9[(6)(8) - (5)(12)] + 1[(6)(2) - (7)(12)] \\ &= 3(56 - 10) - 9(48 - 60) + 1[12 - 84] \\ &= 138 + 108 - 72 \\ &= 174 \end{aligned}$$

In general the determinant is found by using all the elements along the top row as described above and then continuing down to the [2x2] matrix level. This procedure becomes very cumbersome very quickly, and for a [4x4] matrix the determinant has four terms that each multiply a [3x3] matrix. Each of these [3x3] matrices have a three-term determinant, so that for a [4x4] matrix there are 12 terms to calculate to obtain the determinant.

### 9.3.7 Cofactors of Matrices

A cofactor of the  $[i,j]$  element of a matrix is the determinant of the matrix that remains after the  $i$ th row and  $j$ th column are removed from the original matrix. Just as for the determinant, each cofactor has to be multiplied by the term  $(-1)^{i+j}$ . There can be as many cofactors as there are elements in

the original matrix. Thus if the matrix  $A$  is given by

$$A = \begin{bmatrix} a_{11} & a_{12} & a_{13} \\ a_{21} & a_{22} & a_{23} \\ a_{31} & a_{32} & a_{33} \end{bmatrix}$$

and the row and the column that contain the element  $a_{11}$  is eliminated from the matrix, the cofactor that remains is the determinant of the [2x2] matrix  $D_{11}$ , given by

$$D_{11} = (-1)^2 \begin{bmatrix} a_{22} & a_{23} \\ a_{32} & a_{33} \end{bmatrix}$$

Or, the cofactor of the element [1,1] is  $\det(D_{11}) = a_{22}a_{33} - a_{23}a_{32}$ .

By using the same procedure, the cofactor of the element  $a_{22}$  is given by  $\det(D_{22})$  and is seen to be

$$\det(D_{22}) = \det \begin{bmatrix} a_{11} & a_{13} \\ a_{31} & a_{33} \end{bmatrix} = a_{11}a_{33} - a_{13}a_{31}$$

where again the -1 multiplier is a plus because  $(-1)^{2+2} = +1$ . These cofactors are important for the discussion of the inverse of a matrix that follows below.

### 9.3.8 The Inverse of a Matrix

Division of one matrix by another is not allowed, but there is a process that is similar to a division, and it is called inversion. The inverse of a matrix  $A$  is simply written as  $A^{-1}$ . The principal property of the inverse is

that the result of multiplying a matrix by its inverse yields the identity matrix. That is, given the matrix  $A$  and its inverse  $A^{-1}$

$$(A)(A^{-1}) = (A^{-1})(A) = I$$

There are two very important properties that a matrix must have in order for an inverse even to exist. First, the matrix must be square; it must have as many rows as it has columns. Second, the determinant of the matrix cannot be equal to zero. In a very loose sense, this merely implies that dividing by zero is not allowed. Nonsquare matrices must first be made into a square matrix before the inverse can be found. This can be accomplished by simply multiplying a matrix by its transform (explained below).

Since this chapter is meant to be a simplified discussion of matrices and how they are applied to the classical least squares analysis of FT-IR data, a definition, without proof, and a numerical example of finding the inverse will be sufficient.

In order to find the inverse of a matrix, one first has to find the determinant of the matrix as defined above. Then for each element of the matrix, the cofactor of that element of the original matrix has to be found. The transform of the matrix formed by the cofactor matrix must then be found by interchanging the rows and the columns. If the cofactor matrix is given by  $C$ , then the transform is given by  $C^T$ , and the inverse  $A^{-1}$  of the [2x2] matrix  $A$  is then given by

$$A^{-1} = \frac{C^T}{\det(A)}$$

Thus for the [2x2] matrix

$$A = \begin{bmatrix} a_{11} & a_{12} \\ a_{21} & a_{22} \end{bmatrix}$$

the cofactor matrix is seen to be

$$C = \begin{bmatrix} a_{22} & -a_{21} \\ -a_{12} & a_{11} \end{bmatrix}$$

The transform of this matrix is given by

$$C^T = \begin{bmatrix} a_{22} & -a_{12} \\ -a_{21} & a_{11} \end{bmatrix}$$

and the inverse of the matrix  $A$  is finally found as

$$A^{-1} = \frac{1}{\det(A)} \begin{bmatrix} a_{22} & -a_{12} \\ -a_{21} & a_{11} \end{bmatrix}$$

For a numerical example, let the matrix  $A$  be

$$A = \begin{bmatrix} 4 & 9 \\ -2 & -5 \end{bmatrix}$$

The cofactor matrix is given by

$$C = \begin{bmatrix} -5 & 2 \\ -9 & 4 \end{bmatrix}$$

and the transform of the cofactor matrix is

$$C^T = \begin{bmatrix} -5 & -9 \\ 2 & 4 \end{bmatrix}$$

The determinant of the matrix  $A$  is easily found to be  $-2$ . Thus the inverse of the matrix  $A$  is given by

$$A^{-1} = \begin{bmatrix} \frac{-5}{-2} & \frac{-9}{-2} \\ \frac{2}{-2} & \frac{4}{-2} \end{bmatrix} = \begin{bmatrix} 2.5 & 4.5 \\ -1 & -2 \end{bmatrix}$$

From here it is an easy matter to show that this last matrix is indeed the inverse of  $A$  simply by multiplying  $A$  and  $A^{-1}$  together to get the identity matrix. Thus

$$AA^{-1} = \begin{bmatrix} 4 & 9 \\ -2 & -5 \end{bmatrix} \begin{bmatrix} 2.5 & 4.5 \\ -1 & -2 \end{bmatrix} = \begin{bmatrix} 10-9 & 18-18 \\ -5+5 & -9+10 \end{bmatrix} = \begin{bmatrix} 1 & 0 \\ 0 & 1 \end{bmatrix}$$

At this point all the tools that are required to continue processing the FT-IR spectra data are available in matrix form.

#### 9.4 Matrices and Algebraic Equations

The utility of matrices can easily be demonstrated by considering the solution for a set of simultaneous equations. As an illustration, consider the following set of equations

$$\begin{aligned} aX + bY &= k_0 \\ cX + dY &= k_1 \end{aligned}$$

To solve these equations for  $X$  and  $Y$ , the first equation can be solved for  $X$  to get

$$X = \frac{k_0 - bY}{a}$$

This can be substituted into the second equation to get

$$\frac{ck_0 - cbY}{a} + dY = k_1$$

which when solved for  $Y$  yields

$$Y = \frac{ak_1 - ck_0}{ad - cb}$$

Then by using the expression for  $Y$  and solving for  $X$ , it is seen that

$$X = \frac{dk_0 - bk_1}{ad - cb}$$

To solve these equations by using matrices, the equations are first written in matrix form so that

$$\begin{bmatrix} a & b \\ c & d \end{bmatrix} \begin{bmatrix} X \\ Y \end{bmatrix} = \begin{bmatrix} k_0 \\ k_1 \end{bmatrix}$$

This expression is seen to be a column matrix that is multiplied by the coefficient matrix, and that product is equal to the column matrix of the constant terms. It can

be rewritten in purely matrix format as  $CV = K$ , where the  $C$  represents the coefficient matrix, the  $V$  represents the variable column matrix, and the  $K$  represents the column matrix of the constants. To solve this for the variable matrix, the coefficient matrix must be removed from the left-hand side of the equation. This is easily accomplished by multiplying both sides of the equation by the inverse of the coefficient matrix  $C^{-1}$  to get  $C^{-1}CV = C^{-1}K$ . Then, after noting that a matrix times its inverse is just the identity matrix  $I$ , the final expression for the variable matrix is obtained as  $V = C^{-1}K$ . Thus in order to solve this equation for the  $X$  and the  $Y$ , the inverse of the coefficient matrix must be found. In reviewing the rules for finding the inverse of a matrix given in Section 9.3.8, it is seen that in order to find the inverse of the coefficient matrix, one has to obtain its determinant and then form the transpose of the cofactor matrix. The determinant of the coefficient matrix is just the term  $ad - bc$ . The cofactor matrix is found to be

$$\begin{bmatrix} d & -c \\ -b & a \end{bmatrix}$$

The transpose of this is

$$\begin{bmatrix} d & -b \\ -c & a \end{bmatrix}$$

and the inverse of the coefficient matrix is just this transpose divided by the determinant, or

$$C^{-1} = \frac{1}{ad - bc} \begin{bmatrix} d & -b \\ -c & a \end{bmatrix}$$

Now the final matrix expression becomes

$$\begin{bmatrix} X \\ Y \end{bmatrix} = \frac{1}{ad - bc} \begin{bmatrix} d & -b \\ -c & a \end{bmatrix} \begin{bmatrix} k_0 \\ k_1 \end{bmatrix}$$

By multiplying out the matrix terms on the right-hand side of this equation, the final result is obtained as

$$\begin{bmatrix} X \\ Y \end{bmatrix} = \frac{1}{ad - bc} \begin{bmatrix} dk_0 - bk_1 \\ -ck_0 + ak_1 \end{bmatrix}$$

The  $X$  term is the upper element of the matrix divided by the determinant, and the  $Y$  term is the lower element of the matrix divided by the determinant. These expressions are seen to be identical to the expressions derived above by the algebraic substitution method.

## 9.5 Least Squares and Matrices

The next step in this discussion is to show that the matrix technique allows the same equations for the regression analysis, which was initially presented, to be derived. Note that in that discussion a linear relation was assumed between the absorbance of the field spectrum and the absorbance of the reference spectrum so that at each particular data point (or wave number) an expression of the form  $Y = mX + b$  could be used. In terms



of the spectra, the  $Y$  represents the absorbance of the field spectrum as a function of wave number. Therefore, the matrix that represents this absorbance has one element for each data point over the range of the analysis. It is represented by a column matrix given by

$$A_F = \begin{bmatrix} a_1 \\ a_2 \\ \bullet \\ \bullet \\ \bullet \\ a_N \end{bmatrix}$$

The FT-IR usually acquires data at a rate so that there are two data points per resolution unit. Thus if the instrument is operating at a resolution of  $1 \text{ cm}^{-1}$  there is one data point every half wave number. It is best, for statistical reasons, to use about 80 data points in the analysis, so the matrix above would have 80 elements and  $N = 80$ , and the wave number range for the analysis would cover 40 wave numbers at  $1\text{-cm}^{-1}$  resolution.

In the case of the FT-IR, the variables that are to be calculated are actually the slope  $m$  and the intercept  $b$ . Therefore, the variable matrix  $V$  is given as

$$V = \begin{bmatrix} b \\ m \end{bmatrix}$$

The matrix that is used for the absorbance of the reference spectrum is a two-column matrix that will also have  $N$  rows to match the absorbance of the field spectrum matrix. This matrix is represented by  $A_R$  and is given by

$$A_R = \begin{bmatrix} 1 & a_{R1} \\ 1 & a_{R2} \\ \bullet & \bullet \\ \bullet & \bullet \\ \bullet & \bullet \\ 1 & a_{R(N-1)} \\ 1 & a_{RN} \end{bmatrix}$$

This matrix has one column that is all 1's because of the intercept term  $b$  that arises from the linear fit. The  $a_R$ 's are the absorbances of the reference spectrum at the individual data points. They must be chosen to be at the same wave numbers as the data in the field spectrum, and there must be an equal number of data points  $N$  in each matrix. The fundamental matrix equation that has to be solved is then  $A_F = A_R V + \epsilon$ . The  $\epsilon$  is a matrix that describes the errors in the data. Without the error term all the data would fall on a straight line, and the least squares process has essentially no meaning. The  $\epsilon$  matrix is the matrix that represents the residuals, and that can be solved for and then squared to get the sum of the residuals squared. This gives rise to the expressions below.

$$\begin{aligned} \varepsilon^T \varepsilon &= (A_F - A_R V)^T (A_F - A_R V) \\ &= A_F^T A_F - A_F^T A_R V - (A_R V)^T A_F - \\ &\quad (A_R V)^T A_R V \end{aligned}$$

Although it will not be carried out here, when this expression is differentiated with respect to  $V$  and set equal to zero, and after making use of the fact that

$$(AB)^T = B^T A^T$$

twice the primary matrix equation that must be solved is obtained. That is,

$$A_F = A_R V$$

The terms in the variable matrix  $V$ , namely the intercept  $b$  and the slope  $m$ , are the terms that have to be found and are the best estimates of the slope and the intercept. In order to solve for the  $b$  and the  $m$ , the matrix  $A_R$  must be removed from the right-hand side of the equation. The way to do that is, just as before, to pre-multiply both sides by the inverse of the matrix  $A_R$ . But there is a problem here because only square matrices have inverses, and the matrix  $A_R$  is decidedly not square. It has at least 80 rows but only 2 columns. So the first step is to make the matrix  $A_R$  square by multiplying it by its transpose

$$A_R^T$$

At this point the fundamental matrix equation that needs to be solved is

$$V = (A_R^T A_R)^{-1} A_R^T A_F \quad (9-9)$$

This is, in reality, a fairly simple equation and comprises only two spectra, the measured absorbance spectrum  $A_F$  and the reference spectrum  $A_R$ . The following discussion describes how these two matrices must be manipulated to derive the expressions used for normal linear regression calculations.

The matrix that represents the reference spectrum  $A_R$  requires the most manipulation, and although that chore may seem formidable, it is seen that the task quickly becomes fairly simple. The first step is to multiply the  $A_R$  matrix by its transpose in order to get a square matrix. The transpose of  $A_R$  is given by

$$A_R^T = \begin{bmatrix} 1 & 1 & \cdot & \cdot & \cdot & 1 & 1 \\ a_{R1} & a_{R2} & \cdot & \cdot & \cdot & a_{R(N-1)} & a_{RN} \end{bmatrix}$$

and it has to multiply the  $A_R$  matrix in the following way

$$A_R^T A_R = \begin{bmatrix} 1 & 1 & \cdot & \cdot & \cdot & 1 & 1 \\ a_{R1} & a_{R2} & \cdot & \cdot & \cdot & a_{R(N-1)} & a_{RN} \end{bmatrix} \begin{bmatrix} 1 & a_{R1} \\ 1 & a_{R2} \\ \cdot & \cdot \\ \cdot & \cdot \\ \cdot & \cdot \\ 1 & a_{R(N-1)} \\ 1 & a_{RN} \end{bmatrix}$$

Now, utilizing the rules set out above about the multiplication of matrices, it is seen that this product will result in a [2x2] matrix. Before writing down the result, it is

instructive to first contemplate the individual elements in the product matrix.

- For the element [1,1] it is seen that the first row elements of the transpose matrix must multiply the first column elements of the original matrix and then be summed. But these elements are just all 1's and when summed yield the number  $N$ , the total number of data points.
- To obtain the element [1,2] the first row elements of the transpose matrix must multiply the second column elements of the original. But this just turns into the sum of the absorbances of the individual data points from the reference spectrum.
- The element [2,1] of the product matrix is again the sum of the individual absorbances because it is found by multiplying the elements of row 2 of the transpose by the elements of column 1 of the original (all 1's).
- The fourth and final element of the product matrix (element [2,2]) is found by multiplying the elements from row 2 of the transpose by the elements of column 2 of the original and summing. These individual terms are seen to be the squares of the absorbances at the individual data points, so the element [2,2] becomes the sum of these squares.

The result of multiplying the matrix  $A_R$  by its transpose becomes

$$A_R^T A_R = \begin{bmatrix} N & \sum a_{Ri} \\ \sum a_{Ri} & \sum (a_{Ri})^2 \end{bmatrix}$$

Next, the inverse of this matrix has to be found, and this is done in three steps. The first is to find the cofactor matrix, the second it to take the transpose of that, and the third is to divide the individual elements by the determinant of the original matrix. The cofactor matrix is

$$\text{cofactor}(A_R^T A_R) = \begin{bmatrix} \sum (a_{Ri})^2 & -\sum a_{Ri} \\ -\sum a_{Ri} & N \end{bmatrix}$$

Because the elements [1,2] and [2,1] are identical, the transpose of this matrix is the same as the original. The determinant of the original matrix is found to be

$$\det(A_R^T A_R) = N \sum a_{Ri}^2 - \sum a_{Ri} \sum a_{Ri}$$

The inverse that is required here is just the cofactor transpose divided by the determinant, so that

$$(A_R^T A_R)^{-1} = \frac{1}{N \sum a_{Ri}^2 - \sum a_{Ri} \sum a_{Ri}} \begin{bmatrix} \sum a_{Ri}^2 & -\sum a_{Ri} \\ -\sum a_{Ri} & N \end{bmatrix} \quad (9-10)$$

The next step is to multiply the matrix that represents the absorbance in the field spectrum by the transpose of the reference spectrum matrix, that is, to find the product

$$A_R^T A_R$$

This product is

$$A_R^T A_F = \begin{bmatrix} 1 & 1 & \cdot & \cdot & \cdot & 1 & 1 \\ a_{R1} & a_{R2} & \cdot & \cdot & \cdot & a_{R(N-1)} & a_{RN} \end{bmatrix} \begin{bmatrix} a_{F1} \\ a_{F2} \\ \cdot \\ \cdot \\ \cdot \\ a_{F(N-1)} \\ a_{FN} \end{bmatrix}$$

Here again, a little inspection is helpful. The result of this product will be a column matrix with only two rows. The first element is made by multiplying the first row of the transformed reference matrix by the elements of the field spectrum matrix. But that is just the sum of the absorbances at the individual data points. The second row is obtained by multiplying the second row of the transformed reference matrix by the elements of the field spectrum matrix. This is again a sum, but now the terms to be summed are the products of the two absorbances such that each individual term has the form

$$A_{Rj} A_{Fj}$$

It should be clear now why there is the requirement that the number of data points in the field spectrum must be the same as the number of data points in the reference spectrum. If they were not, then this last matrix multiplication could not be done. At any rate, this product is given by

$$A_R^T A_F = \begin{bmatrix} \sum a_{Fi} \\ \sum a_{Ri} a_{Fi} \end{bmatrix} \quad (9-11)$$

The final step in obtaining the variable matrix is then multiplying the two matrices from Equations 9-10 and 9-11 together. Remember here though that the order of multiplication is important. When this final product is performed, the result is

$$V = \frac{1}{N \sum a_{Ri}^2 - \sum a_{Ri} \sum a_{Ri}} \begin{bmatrix} \sum a_{Ri}^2 & -\sum a_{Ri} \\ -\sum a_{Ri} & N \end{bmatrix} \begin{bmatrix} \sum a_{Fi} \\ \sum a_{Ri} a_{Fi} \end{bmatrix}$$

or

$$V = \begin{bmatrix} b \\ m \end{bmatrix} = \frac{1}{N \sum a_{Ri}^2 - \sum a_{Ri} \sum a_{Ri}} \begin{bmatrix} \sum a_{Fi} \sum a_{Ri}^2 - \sum a_{Ri} \sum a_{Ri} a_{Fi} \\ -\sum a_{Ri} \sum a_{Fi} + N \sum a_{Ri} a_{Fi} \end{bmatrix}$$

When these results for the intercept  $b$  (the element [1,1] of  $V$ ) and the slope  $m$  (the element [2,1] of  $V$ ) are compared to the results derived from an algebraic standpoint, it is seen that the expressions are the same.

## 9.6 Expansion to Many Gases

Once the expressions for the slope and the intercept are obtained as above, it is fairly simple to see how to expand this solution to analyze for several gases simultaneously or to analyze for one gas in the presence of several interfering species. The fundamental matrix equation stays the same. That is, the expression

$$V = (A_R^T A_R)^{-1} A_R^T A_F$$

always stays the same, but the individual matrices  $V$  and  $A_R$  have to change to incorporate more information. In most cases the problem is formulated a bit differently

than was used above, in that the intercepts are actually ignored. When several gases are to be analyzed for, the problem is usually stated by considering the final field absorption spectrum to be a linear combination of the individual reference absorbance spectra. The mathematical statement is that

$$A_F(\nu) = \sum m_i A_{Ri}(\nu)$$

and the problem now becomes one of determining the individual  $m_i$  terms. These  $m_i$ 's are the coefficients for the individual references. In the mathematical equation, they determine the amount of each of the individual references to use to achieve the final result of matching the field spectrum.

Thus the expanded  $A_R$  reference matrix changes from a two-column matrix, with the first column being 1's, to a matrix with  $N$  columns, but there are no 1's. That is,

$$A_R = \begin{bmatrix} a_{11} & a_{21} & \bullet & \bullet & \bullet & a_{j1} \\ a_{12} & a_{22} & \bullet & \bullet & \bullet & a_{j2} \\ \bullet & \bullet & \bullet & \bullet & \bullet & \bullet \\ \bullet & \bullet & \bullet & \bullet & \bullet & \bullet \\ \bullet & \bullet & \bullet & \bullet & \bullet & \bullet \\ a_{1N} & a_{2N} & \bullet & \bullet & \bullet & a_{jN} \end{bmatrix}$$

Here there are  $j$  gases and  $N$  absorbance values for each gas. Typically, there are perhaps six or seven gases that are analyzed

for simultaneously, but there can be many more, and there are cases where as many as 30 have been targeted. The final maximum number of gases that can be used is determined by how large a matrix is allowed by the computer and the algorithm being used. The final variable matrix  $V$  is then a one-column matrix with  $j$  rows that represent the  $m$ 's as given above. That is

$$V = \begin{bmatrix} m_1 \\ m_2 \\ \bullet \\ \bullet \\ \bullet \\ m_j \end{bmatrix}$$

It is now easy to see how to expand the least squares technique even further to account for a quadratic fit such as is indicated by the development in Chapter 8. In that case the  $A_R$  matrix needs to contain terms that are the squares of the absorbances, or

$$a_{Ri}^2$$

and for each addition column in the reference matrix, there has to be one additional  $m$  in the variable matrix that needs to be determined.

Calculating anything but the simple case that is presented above is not really possible, nor would it be overly instructive. However, it is of interest that the absorbance due to water actually contributes to the continuum, and that makes up the baseline as seen in the single beam spectrum. The

water concentration can and does change in time rather dramatically, and therefore there are changes in the baseline. If the water absorbance is measured from the baseline to a peak, an error will occur because of the continuum, which is already at a lower transmission than 100% by a few percent. The work in Chapter 8 indicates that the absorbance in the water continuum actually rises as the square of the partial pressure of water. This seems to indicate that a square term ought to be included in the reference matrix for the water. At the present time none of these considerations have been tested with spectra to determine whether the analysis results are better than the current methods. Also, only two software packages that include that term (the Nicolet Omnic software [Madison, WI] and the MIDAC AutoQuant software [Irvine, CA]) seem to be available at the time of this writing.

### 9.7 Least Squares Errors

Once the coefficients for the individual gaseous components have been determined from the least squares technique, the uncertainties in these coefficients must be examined if the uncertainties in the concentrations are to be understood. The overall derivation of the expressions for the errors and a thorough examination of the errors can be quite involved, and an in-depth discussion is felt to be beyond the scope of this work. The interested reader is directed to two excellent references (Draper and Smith 1966; Bevington 1969) for an in-depth analysis of these questions.

However, it is important to note here that the errors calculated by statistical techniques are associated with only the least squares technique, and they are not indicative of the overall error in the FT-IR data. The expressions for determining the errors are derived from a study of the residuals or the analysis of variance. These errors are related to the amount of the variance in the original field spectrum that is explained by the variance in the sum of the individual reference spectra, and these errors have more to do with how well the sum of the reference spectra match the original field spectrum rather than any absolute error.

While these errors are important to the overall discussion of the FT-IR data, they do not comprise the entire picture of the errors. The errors generally reported by the least squares technique do not take into account the actual magnitude of the real errors in the data because they do not account for several major contributors to the error. These unreported errors are errors like the nonlinear response error produced by the apodization function or the temperature effect on the reference spectra, as described in Chapter 8 of this document. They also do not include any errors in the reference spectra themselves.

Any study of these unreported errors shows that they can be quite large when compared to the errors calculated from the least squares technique. Because of this, it is felt that no claim for accuracy better than about  $\pm 30\%$  can be made for the FT-IR

data, regardless of what the error calculations of the least squares technique produce.

### 9.8 References

Belman, R. *Introduction to Matrix Analysis* 2<sup>nd</sup> ed. McGraw Hill Book Company, 1970.

Bevington, P.R. *Data Reduction and Error Analysis for the Physical Sciences*. McGraw Hill Book Company, 1969.

Draper, N.R. and H. Smith. *Applied Regression Analysis*. John Wiley & Sons Inc, 1966

Hohn, F. E. *Elementary Matrix Algebra* 2<sup>nd</sup> ed. The Macmillan Company, New York, 1964.

Sokolnikoff, I.S., and R.M. Redheffer. 1966. *Mathematics of Physics and Modern Engineering*. McGraw-Hill Book Company, New York.

## Chapter 10

### Quality Assurance and Quality Control

#### SUMMARY

The topics and specific points of emphasis discussed in this chapter include the following.

- The need for a quality assurance (QA) project plan
- QA project plan categories and relevant EPA documents
- A general format for a 16-point QA project plan
- A discussion of specific quality assurance and quality control (QA/QC) issues related to FT-IR long-path, open-path monitoring
- Portions of an approved QA project plan
- A case study presenting QA data collected over a two and one-half month period
- Recommendations of procedures to be included in a QA program

#### 10.1 Introduction and Overview

For open-path FT-IR spectrometry to become an accepted method for environmental monitoring, QA procedures must be established. While QA issues have been addressed (Kricks et al. 1992; Russwurm 1992a,b; Weber et al. 1992; Kagann et al. 1994), there is currently no consensus regarding the proper QA procedures required to validate open-path FT-IR data. In fact, there is very little information in the literature that addresses the quality of the data generated by FT-IR long-path, open-path systems. For example, when error bars are given, they are often merely stated, and no discussion of how they

were derived is supplied. As the FT-IR long-path technique begins to be used for routine monitoring, this approach will not be satisfactory, and a more extensive QA plan must be developed.

The development of and adherence to a QA project plan requires the operator to consider exactly how the data generated by an FT-IR long-path, open-path monitoring program will be obtained, processed, interpreted, and used. When implemented properly, the QA plan will alert the operator if the instrument is not functioning properly or is generating erroneous data, and it will contain recommendations for the corrective action to be taken. The various levels of QA



project plan designs apply to programs ranging from research and development programs to routine monitoring programs that must produce legally defensible data. This chapter covers some of the points that will have to be addressed for any QA program.

The general points that must be addressed for any QA program are given in this chapter. These points are drawn from specific documents that address QA requirements for data obtained for the U.S. Environmental Protection Agency. Points of emphasis discussed in these documents include the following: project description, organization, and responsibilities; QA objectives; site selection and sampling procedures; sample and data custody; calibration procedures and frequency; analytical procedures; data reduction, validation, and reporting; internal quality control checks; performance and systems audits; preventive maintenance; calculation of data quality indicators; corrective action; quality control reports to management; and references.

These, and other, items are addressed with respect to FT-IR long-path, open-path monitoring in this chapter. In addition, portions of the QA project plan for a 1989 Superfund Innovative Technology Evaluation study in Delaware are presented as an example for use in FT-IR long-path, open-path monitoring. Also, a case study involving the acquisition of QA data over a two and one-half month period is presented in Section 10.3, and recommendations for procedures

to be included in a QA program are given in Section 10.4.

## 10.2 Project Plan Categories

The U.S. Environmental Protection Agency has published a document that defines four different categories of QA project plans, as described in Section 10.2.1. The program with the least requirements is a research and development program (Category IV), whereas a program that produces data by routinely monitoring the atmosphere (Category I) has the most. When considering programs that are specifically designed to obtain data for the U.S. Environmental Protection Agency, it is convenient to refer to two documents that describe QA project plans: (1) *Preparing Perfect Project Plans: A Pocket Guide for the Preparation of Quality Assurance Project Plans* and (2) *Preparation Aids for the Development of RREL Quality Assurance Plans* (U.S. Environmental Protection Agency 1989, 1991). Actually, there are four parts to the second document, one for each of the four categories, and each has its own document number.

Some of the features of the items that need to be addressed in the Category I project plans are covered in Sections 10.2.1 and 10.2.2. It is intended that these sections be a paraphrasing of the two documents listed above. People who have to deal with these issues must obtain a copy of the documents and follow the guidance given there. To give some specificity to the various points of a QA project plan, the QA project plan used for a recent program

conducted by EPA is used as an example. The program entailed taking data with an FT-IR open-path monitor in an industrial complex and comparing that data to data obtained by a canister technique according to method TO-14 (Russwurm and McClenny 1990). Funding was allocated for 10 days of measurements with the FT-IR instrument in the field.

### **10.2.1 Category Definitions**

- Category I projects are those that are designed so that their results can be used directly, without additional support for compliance or other litigation. As such, they must be able to withstand legal challenge and therefore have the most rigorous and detailed requirements. These projects are critical to the goals of the U.S. Environmental Protection Agency.
- Category II projects are those whose data complement other projects. When combined with the output from other projects, these data can be used for rule making or policy making.
- Category III projects are those producing data that allow the evaluation and selection of basic options for use in feasibility studies.
- Category IV projects are those that are associated with research and development projects. The results are used to assess the basic or underlying assumptions or suppositions of other

work. Because of the nature of these projects, they have the minimum number of items that need to be addressed in a QA program.

These categories are intended to be fairly general and broad, and any project must fit into one of the four. The number of items that must be addressed for each of the categories is 16, 13, 12, and 6 for Categories I through IV, respectively. The project described above for acquisition of data for comparison purposes and referred to as an example in Sections 10.2.2.1 through 10.2.2.16 was considered to be a research program, and therefore it fell into Category IV.

### **10.2.2 Category I Points to Be Addressed**

The 16 items that must be addressed for the QA project plan in this category are listed below.

1. Project description
2. Project organization and responsibilities
3. QA objectives
4. Site selection and sampling procedures
5. Sample custody
6. Calibration procedures and frequency
7. Analytical procedures
8. Data reduction, validation, and reporting
9. Internal quality control checks
10. Performance and systems audits
11. Preventive maintenance
12. Calculation of data quality indicators

13. Corrective action
14. Quality control reports to management
15. References
16. Other items

These 16 items are discussed briefly below.

#### **10.2.2.1 Project Description**

The most important feature of the project description is that a person who is unfamiliar with the project, but is familiar with the technology, must be able to understand this section.

For the example project, the following items were included in this section.

- *An in-depth discussion of the comparison program.* The primary aspect of this was to relate in detail how the data would be taken. The FT-IR instrument is a long-path monitor, and the canister technique is a point monitor. Thus, it was decided to transport the canister along the path while the FT-IR monitor was acquiring data. Topics that had to be included in the QA project plan were the number of traversals along the path and the number of scans the FT-IR spectrometer would make.
- *A brief description of the FT-IR technique and the canister technique.* The techniques were described, and appropriate documents for each technique were referenced.

#### **10.2.2.2 Project Organization and Responsibilities**

This section must describe the relationships among all of the people connected with the project, including the QA manager, and give their responsibilities. It should be noted that, somewhere in the organization conducting the program, there should be an autonomous QA representative. Most organizations have this function removed from the technical staff and under the jurisdiction of an administrative manager. The primary function of this person is to act as final arbiter for any disputes about the QA aspects of the program. Therefore, he should not be administratively connected with the technical program.

For the project being outlined as an example, the management and administrative staff consisted of U.S. Environmental Protection Agency staff and staff from two contractors. The following descriptions were therefore included in this section.

- All the principal people involved and their duties
- The relationship of one person to the other concerning decision-making responsibilities
- The lines of communication among the project personnel

All lines of communication among the various project personnel, including any sub-contractors, must be described. If no

subcontractors are used, it is sufficient to simply state that fact.

### **10.2.2.3 QA Objectives**

This section of the QA project plan must cover items such as detection limits, precision, accuracy, completeness of the data, representativeness of the data, and comparability of the data. There must be a discussion of the impact of not meeting these objectives and how these indicators will affect the legal defensibility of the data.

Inadequately addressing these items is probably the most frequent cause of the rejection of a QA project plan.

Three items—detection limits, precision, and accuracy—must be numerically defined as QA objectives. Completeness of the data defines what percentage of the total number of possible data points that are available under the sampling schedule are expected to be captured. Representativeness of the data implies how well the acquired data account for the variability of the real situation. Representativeness of the data concerns itself with sampling. Comparability of the data indicates how well the data can be compared to that taken with other instrumentation.

A portion of the example field program (Russwurm and McClenny 1990) was designed to determine how to best make measurements of the detection limits, the accuracy, and the precision. Therefore, no

specific definitions were required. At the present time there are no generally accepted definitions for these quantities for FT-IR open-path monitors.

For the completeness of the data, the following procedure was used. A 10-h working day was assumed, and 2 h were allocated for setup and warm-up time of the instrument. The data-taking period was assumed to be 0.5 h for each spectrum. Therefore, it was anticipated that 16 spectra a day would be taken. During the study, it was noted that the concentration of the gases being monitored was changing at a much higher rate than could be accommodated by the 0.5 h allocated to each data spectrum. Therefore, the sampling schedule was altered to account for the change. It should be noted that this is certainly an appropriate response to changing conditions. The QA plan is a guide for subsequent operations and not something that is unchangeable. All changes must be recorded, and the rationale for the change must be presented.

A large section of the plan concerned itself with the representativeness and comparability of the data. The reason that the canisters had to be transported along the path was precisely to satisfy the requirements of these two items.

### **10.2.2.4 Site Selection and Sampling Procedures**

In addition to a physical description of the site, the rationale for selecting any

individual site must be presented. This discussion must address how the site will allow the data objectives to be met.

The sampling portion of this section must address the scientific and regulatory (if any) objectives that the sampling protocol allows. It must also address how any calibration samples are to be obtained and delivered to the system. In the case of the FT-IR system, if a gas sample cell is to be used, then its preparation and use must be addressed in this section.

Site selection and sampling procedures played an important role in the example study. Several months before the field portion of the example study, a search for suitable sites was started. The general area of the study had been selected, but the individual sites and FT-IR paths needed to be chosen. Therefore, this section of the example QA plan contained the following descriptions for the site selection process and sampling procedures.

- Background information on site selection. During a number of trips to the general area, various land owners were contacted, and several sites were selected as usable for the study.
- Predominant requirements for the site. Proximity to the source, an unobstructed path length of up to 300 m, a path that could be used to transport the canister while the FT-IR monitor was taking data, and a site that was safe for the operators.

- Procedure for using a QA gas cell. A description of using a short cell filled with a high concentration of gas for calibration purposes was described here. The use of this cell was also intended for determining the precision of the instrument.

#### ***10.2.2.5 Sample Custody***

This section must present complete sample custody procedures and personnel responsibilities in handling samples. Because the FT-IR data are stored on disk, all procedures for ensuring the integrity of the data on the disk and the legal defensibility of those procedures must be addressed.

For the example program, no sample custody procedures were required because it was a research program.

#### ***10.2.2.6 Calibration Procedures and Frequency***

The FT-IR open-path monitor is not calibrated in the classical sense. That is, a sample of known concentration is not presented to the instrument for measurement. During FT-IR sampling, the absorbance values in all the spectra obtained at various wave numbers for the specific gases are always compared to the absorbance values of the reference spectra. These reference spectra are made with pure samples of the gas. Production of reference spectra is a formidable task, and few laboratories are equipped for such an undertaking. Because of this, only a limited

number of spectral libraries that can be used for quantitative analysis exist.

Although measurements of the precision can be made by using a short cell filled with a pure sample of the gas, this is not routinely done at the present time. There is currently no agreed-upon procedure for the use of such a cell.

The project being used as an example did not require that the system be calibrated. However, a written procedure for using a short cell to make precision measurements was part of the QA plan.

#### ***10.2.2.7 Analytical Procedures***

For the most part, unless other techniques are to be used along with the FT-IR system, there is nothing to address in this section. The analytical procedures that are to be used to determine the concentrations of any short-cell gas mixtures would have to be addressed here.

In the QA project plan being used as an example, the procedures for preparing the short cell and the gas mixtures were given here. The cells are generally filled with a pure gas sample and then backfilled with nitrogen so that the total pressure is 1 atm. All the apparatus used for this procedure was described in this section.

This section also contained a description of the procedure to be used for the analysis of the canister samples. This was a brief description, but it referenced the

TO-14 procedure manual. The entire QA procedure for that portion of the effort did not have to be presented in the plan, but it had to be referenced. If one had not been available, then it would have had to be written and given in this section.

#### ***10.2.2.8 Data Reduction, Validation, and Reporting***

The data reduction procedures must be discussed in this section. This includes the least-squares regression analysis, or other multicomponent analysis method, if it is to be used. All statistical methodology that is used as an aid to data interpretation must be described here. This section can also include sample calculations. All procedures to be used for flagging the data and removing outliers from the data set must be stated in this section. The flow of data and the procedures that will be used to transfer the data from where it is generated to the end user must also be described.

The QA project plan being used for discussion purposes included an analysis of the spectral data with a classical least squares algorithm. The actual process of recording the interferogram, performing the Fourier transform, and the least-squares analysis was not discussed in detail. The published papers that describe these techniques were referenced. The process of selecting the wave number range for analysis was discussed, and the wave number regions that were used were listed in this section of the QA project plan.

The TO-14 procedure for data reduction also was referenced, but the actual details were not presented in the plan.

The major portion of this section dealt with the comparison of the data which was to be done by regression techniques. At various stages in the program, two canister samples were taken simultaneously, and the comparison procedure for these data was discussed.

Validation of the data was described as the process of reviewing the study logbooks to make sure that no unwanted contamination of the samples had occurred. For example, one sample was invalidated because an automobile had followed the person transporting the canister along the path.

#### ***10.2.2.9 Internal Quality Control Checks***

This section is designed to determine what internal QC checks are to be made. It must also cover why these checks are necessary and how they will help to achieve the data quality objectives. For example, this section would describe the use of control charts that show the peak-to-peak readings of the single-beam spectrum at various path lengths and with varying amounts of water vapor.

At the time of the example study, there were no requirements for internal QC measurements written into the plan. A portion of the study was designed as an

attempt to develop procedures for making these measurements.

#### ***10.2.2.10 Performance and System Audits***

System audits are generally done before any data are taken. They are designed to answer questions about the proposed procedures and sampling protocols to be used in the program. The performance audits are designed to determine whether the instrument is operating as it was described in the other sections of the study's QA project plan. Both of these audits are generally done by people who are not associated with the daily operation of the instrument.

There were no provisions for either system or performance audits for the study being used as an example.

Although it is easy to envision the system audit for the FT-IR instrument, the performance audit of the instrument would be much more difficult to do at this time. This is usually done by using the instrument to measure a known concentration of gas and determining the response. There has been no systematic development of a procedure for doing this for the FT-IR systems to date. Currently, not all commercially available systems have provisions for putting a short cell in the beam.

#### ***10.2.2.11 Preventive Maintenance***

This section requires a description of the preventive maintenance procedures and

the schedule on which they will be performed. The time involved in performing preventive maintenance will affect the total amount of data that can be taken, and this must be accounted for in the description of the completeness requirements.

In the example QA project plan, no preventive maintenance schedule was given because the study was a short-term intensive program. Over the 10-day field program, no maintenance of the instrument was required.

#### ***10.2.2.12 Calculation of Data Quality Indicators***

This section must contain detailed procedures that are to be used for determining the data quality. It must include all the statistical routines that are to be used. Items that must be addressed are precision, accuracy, outliers, etc.

Currently, no generally accepted definitions for precision and accuracy are available for the FT-IR open-path technique.

#### ***10.2.2.13 Corrective Action***

The corrective action portion of the QA project plan is a set of contingency plans that try to address "what if" questions. These corrective action plans serve as a check for the general tendency to want to perform quick fixes of equipment to get as much data as possible. This is certainly the case with short-term field programs, but it is generally better to take the instrument off line and repair or adjust it properly. The

corrective action plans should describe how this is to be done and specifically what criteria will be used to make the judgement as to when to discontinue data collection and shut down the instrument for repair. This section was not a requirement for the example QA project plan.

#### ***10.2.2.14 Quality Control Reports to Management***

This section must state what reports will be transmitted to whom and when they will be transmitted. There should be a description of the contents of each report, and all the QA/QC data that must be included in each report should be stated in this section of the QA project plan.

The QA project plan for the example study did not address this requirement because there was no consistent QA data generated in the program.

#### ***10.2.2.15 References***

When references related to the present program are available, they should be included in the QA project plan. For example, as mentioned in Sections 10.2.2.1 and 10.2.2.7, appropriate documents were referenced for the canister technique used in the example QA project plan.

#### ***10.2.2.16 Other Items***

The QA project plan contains information that the principal investigator will need at various points of the program.



Because of this, it is somewhat personalized, and this section can include any other items that are considered important to the program.

There were no other items included in the QA project plan for the example study.

### **10.3 Case Study: QA Data Collected Over Two and One-Half Months at a Semipermanent Field Site**

The study described here was designed to evaluate the stability of a long-path FT-IR system and to determine the precision and accuracy of the concentration measurements (Thompson et al. 1994). The following criteria were used to assess the stability of the instrument: electronic noise, the magnitude of the return signal, the RMS baseline noise, and the repeatability of the position and full width at half height (FWHH) of selected absorption bands. Ambient concentrations of CH<sub>4</sub>, N<sub>2</sub>O, and CO were measured to test the use of these data for determining the precision and accuracy of the FT-IR open-path monitor. Measurements were made daily over two and one-half months, from November 1993 to mid-January 1994.

Spectral data were acquired by using a monostatic FT-IR monitor. Each spectrum consisted of 64 co-averaged scans recorded at a nominal 1-cm<sup>-1</sup> resolution. Triangular apodization was used. The collection of each spectrum required approximately 5 minutes. A spectrum was taken every 15 minutes. Single-beam spectra were typically acquired over a 7- to 8-h time

period. Absorption spectra were created by ratioing the single-beam spectra to a synthetic background spectrum generated from a 2048-scan single-beam spectrum recorded over the 414-m path. This background spectrum was recorded at the beginning of the experiment and was used throughout the study. The data were analyzed by using a CLS software package and reference spectra from a commercial library.

The site is located near I-40, one of the main traffic arteries for the Research Triangle Park, NC, area. The instrument was kept in a climate-controlled shed, which is heated during the winter months. The total path length was 414 m, and it extended over an open, grassy field and a small parking area with very limited traffic. The beam path rose from about 1.8 m to 12.8 m above the ground as it was directed from the FT-IR spectrometer to the retroreflector array, which was mounted on a tower.

The instrumental electronic noise was measured each morning before the detector was cooled with liquid nitrogen. This signal typically ranged between 600 and 620 counts with the instrument in the single-beam mode. Shortly after the detector was cooled, the instrument was aligned and the maximum return signal was recorded. The return signal was recorded again (without realignment) around noon to check the stability of the signal. On clear days the single-beam return signal ranged from 10,500 to 13,500 counts. (See Figure 10-1.) Certain atmospheric conditions caused the

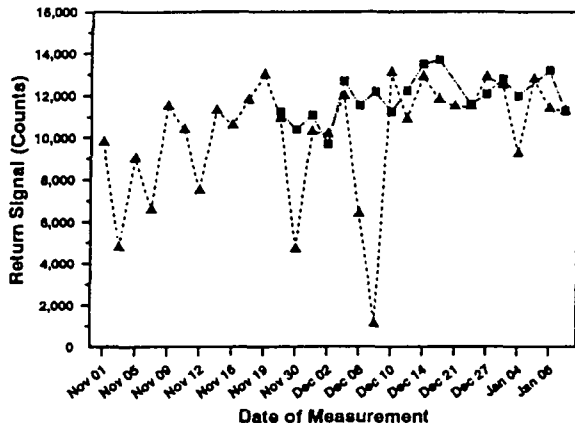


Figure 10-1. Return Signal Magnitude of the FT-IR Monitor Measured Daily at 0700 (▲) and 1200 (■). (The data points have been connected by lines for the convenience of the reader and not to indicate continuous data.)

return signal to vary from day to day. For example, the return signal dropped by 20–30% during fog. On some mornings, when the humidity was close to or below the dew point, condensation or ice formed on the retroreflector, resulting in a lower return signal in the early morning measurement. As the condensation evaporated, an increase in return signal counts was measured. To remedy the problem of condensation, a heat lamp was mounted on the tower and directed at the retroreflector. After the heat lamp was installed on December 10, the noon and early morning return signals were nearly the same. The use of the heat lamp did not cause an increase in noise or detected IR signal.

The RMS baseline noise measured over 26 days is illustrated in Figure 10-2. The baseline noise was determined by collecting two back-to-back, 64-scan, co-

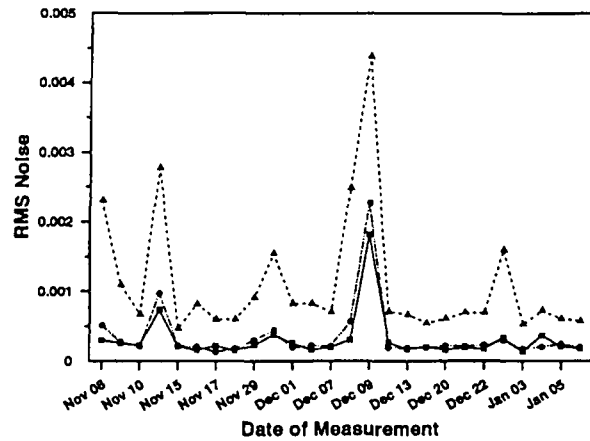


Figure 10-2. The RMS Baseline Noise Measured Between 980 and 1020  $\text{cm}^{-1}$  (■), 2480 and 2520  $\text{cm}^{-1}$  (●), and 4380 and 4420  $\text{cm}^{-1}$  (▲). (The data points have been connected by lines for the convenience of the reader and not to indicate continuous data.)

added spectra. One spectrum was ratioed against the other to obtain an absorption spectrum. The RMS noise (in absorbance units) was calculated over three spectral regions: 980–1020, 2480–2520, and 4380–4420  $\text{cm}^{-1}$ . During operations when condensation did not form on the retroreflector, the baseline noise was on average approximately  $2 \times 10^{-4}$  for the 980–1020- $\text{cm}^{-1}$  region,  $2.5 \times 10^{-4}$  for the 2480–2520- $\text{cm}^{-1}$  region, and  $9 \times 10^{-4}$  for the 4380–4420- $\text{cm}^{-1}$  region. In these measurements, the 980–1020- $\text{cm}^{-1}$  region included water vapor bands. For a true measurement of instrument performance that is not influenced by temporal changes in water vapor concentration, it is recommended that the region from 968 to 1008  $\text{cm}^{-1}$  be used. During measurement periods when condensation formed on the retroreflector, the baseline noise for these

regions increased to  $9.7 \times 10^{-4}$ ,  $5.5 \times 10^{-4}$ , and  $2.9 \times 10^{-3}$ , respectively.

The wave number stability of the instrument was determined by monitoring the peak position and the FWHH of the water vapor singlet at  $1014.2 \text{ cm}^{-1}$ . Band positions typical of data collected at the beginning, in the middle, and near the end of the study are depicted in Figure 10-3. No shift in the frequency was observed during this time period. Also, no shifts were observed in the  $1\text{-cm}^{-1}$  spectra collected under a variety of weather conditions, including rain, freezing rain, sleet, snow, and low (single-digit) temperatures. To determine if the water vapor singlet at  $1014.2 \text{ cm}^{-1}$  broadened, a spectrum collected at the beginning of the experiment was subtracted from a spectrum in the middle and end of the experiment. No broadening was evident during the middle of the experiment; however, a slight broadening for some of the spectra at the end of the

experiment was observed. The FWHH of the water vapor singlet in spectra taken during different atmospheric conditions was also examined. When a clear day spectrum was subtracted from any of these spectra, no broadening was evident. It should be noted that short wavelengths (higher wave numbers) will be more sensitive to spectral shifts and changes in resolution. The HDO doublet centered at  $2720 \text{ cm}^{-1}$ , the CO band at  $2169 \text{ cm}^{-1}$ , or other water vapor bands in the higher wave number region can also be used to test for shifts and changes in resolution.

The feasibility of using ambient gases for accuracy and precision measurements was also investigated. Ambient concentrations of  $\text{N}_2\text{O}$ ,  $\text{CH}_4$ , and CO were measured on a daily basis. Each morning between 0715 and 0930 the concentrations of these gases increased, then steadily decreased during the remainder of the day. However, concentrations of  $\text{N}_2\text{O}$  and  $\text{CH}_4$  remained constant, approximately 250 ppb and 1.7 ppm, respectively. To determine whether the increases in concentration during the first 3 h of operation were due to an instrument effect or to the proximity of the site near a major highway, data were collected continuously for 36 h.

Data were collected from November 17 at 0730 until 1730 on November 18. The  $\text{CH}_4$  concentration data exhibited scatter during an early morning fog episode and decreased steadily during the day. (See Figure 10-4A.) A step in the  $\text{CH}_4$

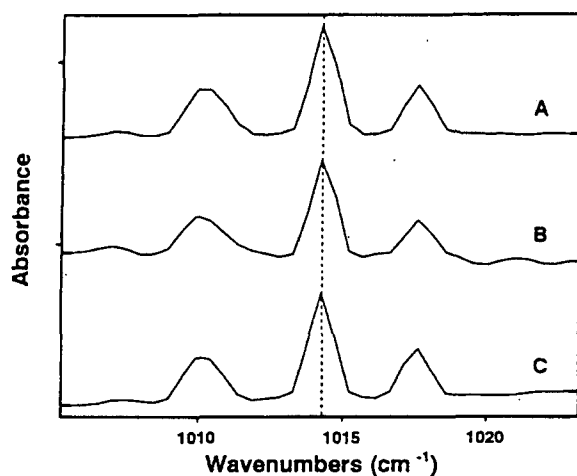


**Figure 10-3. Repeatability of the Position of the Water Vapor Singlet at  $1014.2 \text{ cm}^{-1}$  Measured on (A) November 10, 1993, (B) December 22, 1993, and (C) January 4, 1994.**

concentration measurement was observed when the liquid nitrogen in the detector was depleted at approximately 2345 on November 17. The CH<sub>4</sub> concentration value was 1.70 ppm just before the liquid nitrogen was depleted, increased to 1.9 ppm after liquid nitrogen was refurbished, and remained 10% higher compared to the previous levels. The concentration data for CO showed a similar, stepped increase.

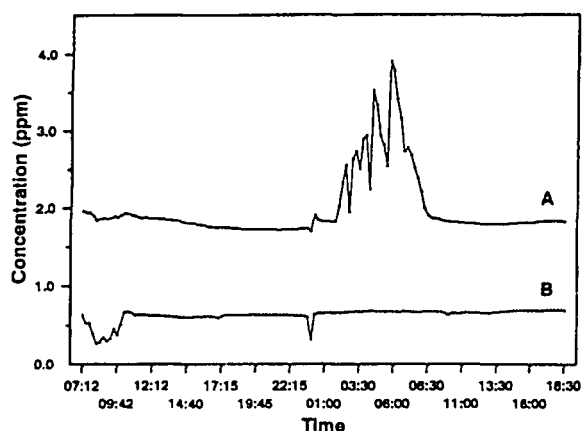


**Figure 10-4. Measurement of (A) Ambient Methane Concentration and (B) Single-Beam Intensity at 987 cm<sup>-1</sup> on November 17 and 18, 1993.**

The CH<sub>4</sub> concentration data exhibited irregular behavior during a 6-h period shortly after the detector Dewar was refilled with liquid nitrogen. To determine if the instrument was operating properly during this time period, the single-beam intensity at 987 cm<sup>-1</sup> was measured from archived spectra. The single-beam spectra had a lower intensity during the fog episode, then leveled off until the detector ran out of coolant. (See Figure 10-4B.) After this sudden drop, the single-beam intensity

returned to its original reading and remained relatively constant throughout the remainder of the experiment. This indicates that the instrument was working properly during the episode of high measured CH<sub>4</sub> levels.

One other observation during this time period concerned the effect of water vapor concentration on CLS analysis for CH<sub>4</sub>. On November 17 a cold front moved through the area in the late evening, and the water vapor pressure dropped rapidly. Because the water vapor spectrum is used as an interfering species in the CLS concentration analysis for CH<sub>4</sub>, the sudden change in water vapor pressure could have had an effect on the CH<sub>4</sub> concentration measurements. The relative concentration of water vapor along the path was determined by measuring the peak area of the absorption band at 1014.2 cm<sup>-1</sup>. Likewise, the relative concentration of CH<sub>4</sub> was determined by measuring the peak area of the absorption band at 2998.8 cm<sup>-1</sup>. This peak was chosen because the water vapor bands do not interfere with it. However, it was later brought to our attention that this CH<sub>4</sub> band actually overlapped nearly exactly with a water vapor band (W.F. Herget, ETG, personal communication). This might explain the dip in the peak area measured at 2998.8 cm<sup>-1</sup> during the time that the water vapor concentration was decreasing rapidly. Therefore, this band is not a good choice for this type of data analysis; the CH<sub>4</sub> bands at 2916.8 and 2927 cm<sup>-1</sup> do not overlap with water vapor and should be used instead. As shown in Figure 10-5, the relative water vapor concentration decreased rapidly when the front moved through the area. The

relative CH<sub>4</sub> concentration increased during this period. Similar trends were observed between plots of the CH<sub>4</sub> peak area and CH<sub>4</sub> concentrations determined by the CLS concentration analysis. This indicates that the change in water vapor concentration did not greatly affect the CLS analysis for CH<sub>4</sub>, and the fluctuations in the CH<sub>4</sub> concentrations were real.

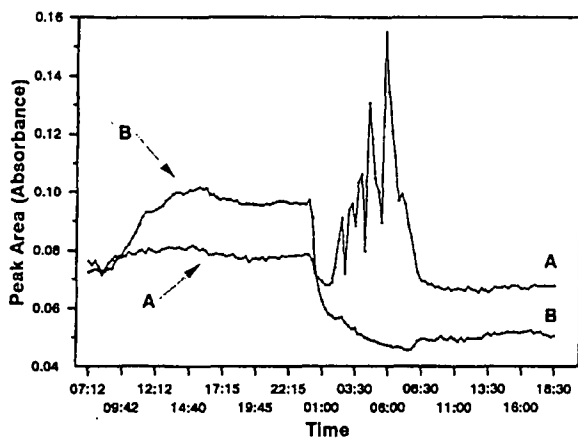


**Figure 10-5. Peak Area of 2998.8-cm<sup>-1</sup> Absorption Band of CH<sub>4</sub> (A) and the 1014.2-cm<sup>-1</sup> Absorption Band of Water Vapor (B) Measured on November 17 and 18, 1993.**

The data collected in this study indicate that for this particular FT-IR monitor the return signal and baseline noise are repeatable and are instrumentally stable over extended periods, but are subject to variations due to weather conditions. The peak positions and the FWHHs of the water vapor singlet at 1014.2 cm<sup>-1</sup> were repeatable from day to day and were not affected by rain, freezing rain, snow, or single-digit temperatures. The variability in the concentrations of CH<sub>4</sub> limits its use in instrument stability studies and for accuracy and precision determinations. A step in the

concentration measurements associated with the depletion and refurbishment of detector coolant is not yet understood. Future experiments with a QA cell and surrogate standards are planned to further investigate this effect.

#### **10.4 Recommendations for Tests to be Included in a QA Program for FT-IR Long-Path Monitors**

We are currently evaluating and developing procedures to determine the quality of data taken with FT-IR monitors. The following is an outline of criteria that we have used in a preliminary QA program to verify the performance of an FT-IR long-path system. Development of a QA plan for FT-IR monitoring should include, but not necessarily be limited to, these types of measurements. These tests are designed to determine that the instrument is operating properly and producing good data. Some of these issues were discussed in Chapter 3 for the initial verification of instrument performance, but can be used for routine QA procedures as well. Other criteria for development of a QA plan, such as siting criteria or data chain-of-custody, should be addressed as warranted, but are not discussed here. These procedures were developed for a research and development program, but factors relevant to routine monitoring programs were also taken into consideration. Bear in mind that two separate issues must be addressed in a QA plan. One is whether or not the instrument is working properly. The other issue is if the

method used for quantitative analysis is producing the correct results.

#### 10.4.1 Noise Measurements

Measurements of two types of noise can be routinely taken, instrumental electronic noise and random baseline noise. Electronic noise is recorded before the detector Dewar is filled with liquid nitrogen. This small signal is indicative of the electronic noise of the system with no detector signal. This should remain relatively constant and typically contributes less than 0.25% of the total return signal. If some electrical component of the system is producing spurious noise, it will become apparent from this measurement.

Random baseline noise is measured by recording back-to-back spectra after the detector has been filled with liquid nitrogen. One spectrum is then ratioed to the other and the absorption spectrum is calculated. The result is a spectrum of the random system noise. The RMS or peak-to-peak noise in absorbance units can then be calculated from these spectra. These spectra should be acquired by using the instrumental parameters to be used during the analytical measurements. The baseline noise measurements should be taken in a spectral region that is devoid of absorption due to water vapor or other atmospheric gases. If not, changes in water vapor concentration over the measurement time will influence the magnitude of the noise calculations. Noise measurements can also be taken over the spectral region chosen for

analysis of a target gas to give an estimate of detection limits.

For the baseline noise measurement it is best to record these two spectra back to back, as passage of time between the two spectra might also include changes in atmospheric conditions or concentrations of species in the path. Spectra taken at longer time intervals during the study can be ratioed in this manner to determine baseline stability or systematic noise.

#### 10.4.2 Stability of Instrument

Several aspects related to the stability of the instruments can be measured. One is the repeatability of the noise measurements described above. These noise measurements should be taken daily and recorded on a control chart to alert the operator of any gross changes or trends in the deterioration of the baseline noise.

Another measurement to be taken daily, or several times during the day, is the return intensity. This can be measured either as the single-beam intensity at a selected wave number region or the magnitude of the interferogram. At this time, the position of the zero peak difference of the interferogram should also be recorded, and the single-beam spectrum should be examined for evidence of system nonlinearity (see Chapter 3, Section 3.4). The single-beam intensity should be measured in different wave number regions to determine if the source characteristics have changed or the interferometer alignment has been altered.

The high wave number (short wavelength) portion of the spectrum will be most sensitive to interferometer misalignment and will show a decrease in intensity relative to the other wave number regions if changes have occurred.

In addition to being dependent on the instrument's performance, the return intensity also depends on atmospheric conditions. For example, fog has a deleterious effect on the return signal. Thus, the atmospheric conditions must be noted when the measurement is taken. As with the noise measurements, the return intensity should also be plotted daily on a control chart. A decrease in return intensity could be related to a drop in the source intensity, misalignment of the external optics, misalignment of the interferometer optics, deterioration of the system optics, or a loss in the detector Dewar hold time.

The positions of selected absorption bands should also be recorded. In long-path measurements the water vapor singlet at  $1014.2\text{ cm}^{-1}$  works well for this purpose. The FWHH of this band can also be measured to determine the repeatability of the resolution of the system. The subtraction technique described by Russwurm (1992b) can be used to detect small frequency shifts or subtle changes in the instrument resolution. If the resolution of the system is deteriorating, and the band becomes broader than a spectrum recorded previously, the subtraction result will appear as an "M". Shifts in frequency will produce a derivative shape in the subtraction result.

Note that the FWHH measurement and the spectral subtractions should be done on an absorption spectrum, and not on a single-beam spectrum or transmission spectrum.

As mentioned previously, bands in higher wave number regions actually may work better for this test, as they will be more sensitive to spectral shifts and changes in resolution. In addition to the water vapor bands centered at  $1014.2\text{ cm}^{-1}$ , the HDO bands centered at  $2920\text{ cm}^{-1}$  can be used for this test.

All of the above measurements should be recorded on at least a daily basis and compared to existing data to establish that the instrument is performing properly.

#### 10.4.3 Accuracy and Precision

The determination of accuracy and precision are not as straightforward as the tests used to determine if the instrument is performing properly. The concentrations of ambient gases, such as  $\text{CH}_4$  or  $\text{N}_2\text{O}$ , can be used to a certain extent for these purposes. This approach has the advantage that certain gases are always present in open-path spectra and no changes have to be made to the instrumental configuration to measure these gases. If the ambient concentrations of these gases are assumed to be constant, precision measurements can be made. For example, we have measured the concentration of  $\text{N}_2\text{O}$  continuously over a five-day period in the late spring to be within  $\pm 3.5\%$  of the mean value. On the other hand, as discussed in Section 10.3, we have

seen CH<sub>4</sub> concentrations increase by a factor of 2.5 in a short time during measurements taken in the late fall. Therefore, care must be taken to account for possible emission sources if ambient gases are used for QA purposes. Ambient gases can also be used to test for frequency shifts or changes in resolution as described above. The use of ambient gases for QA purposes can be used to estimate the precision of the measurement, but this approach does not really address the accuracy of the method.

The alternative approach to using ambient gases for QA data is to insert a short gas cell that contains surrogate standards into the beam. This has the disadvantage of an attenuated IR beam due to the transmitting and reflecting properties of the windows used in the cell. Thus, the performance of the instrument is somewhat degraded. However, this approach does have the advantage of having a known quantity of target gas in the path. Assuming this quantity is accurately known and it remains constant, accuracy and precision measurements can be made with a short cell technique. To date, however, no universally applicable technique using a short cell has been developed.

As discussed in Chapter 3, stray light in the monostatic configuration and background blackbody radiation in the bistatic configuration can affect the quantitative results. The signal due to stray light or background radiation must be subtracted from the sample spectrum prior to quantitative analysis. The stray light in the

spectrometer of a monostatic instrument can be measured by blocking the return beam with some type of opaque and nonreflective material. In our experience the signal due to stray light has been relatively constant, provided no components of the system are changed. The background blackbody radiation of a bistatic system can be measured with the IR source off. This response will vary for different sites and can also change throughout the day. Therefore, this signal must be recorded on a more frequent basis. It is not obvious at this point, however, that simple subtraction adequately compensates for the effects of stray light or background radiation linearly over a range of absorption values. Thus, the accuracy of the system might be affected.

In addition to determining the accuracy and precision of the instrument, the accuracy and precision of the method used for quantitative analysis must also be determined. In most cases, an automated software package, such as one that uses the CLS algorithm, is used to determine the concentrations of the target gases. These procedures can be checked manually by comparing the sample spectra to spectra of reference gases with a known concentration. Interactive subtraction procedures that yield a scaling factor for the reference spectrum can be used to check the concentration measured by the CLS software. In addition, the reference spectra can be scaled to the desired concentration and then added to the sample spectrum. When the composite spectrum is then analyzed, the measured concentration should reflect the amount of



reference gas added. Care must be taken in choosing the spectral regions used to analyze for each target compound. For example, the optimum region for analysis does not always encompass the entire absorption envelope. Possible interfering species must also be accounted for in the analysis method.

The operator should also be aware that any time a concentration spike appears that cannot be immediately attributed to a known source, the actual spectral data should be examined to verify the presence of the compound in question and its concentration. This can be done by first subtracting the appropriate absorption spectra of any interfering species from the sample spectrum. The signature and absorbance values of the resultant spectrum should then be compared to the reference spectrum for proper features and intensities. Also, any time that the concentrations of the target compounds seem to correlate with changes in water vapor concentration, the spectra of the target compounds should be examined to verify that the changes in concentration are real. If the concentrations of the target compounds exhibit either positive or negative inflections with respect to changes in water vapor concentration, the analysis method should be altered to alleviate the problem.

Ultimately, if the instrument is operating properly and a suitable analysis method is developed, the accuracy of the FT-IR technique will be determined by the accuracy of the reference spectra. To date,

no way of validating or certifying these reference spectra exists.

#### **10.4.4 Completeness and Representativeness of Data**

These requirements will vary with specific monitoring applications. Care must be taken to ensure that data points are acquired frequently enough to account for the variability of the target gas concentration. Failure to do this will make it difficult to discern between real changes in the target gas concentration and possible variability in the FT-IR measurements.

#### **10.4.5 Comparability of the Data**

If possible, the FT-IR data should be initially compared to an established method. This can be difficult because the FT-IR produces a path-averaged concentration, whereas most established methods use some type of point monitor. As discussed in Section 10.2.2, some of the FT-IR data have been compared to the canister method. In a current study, we are comparing ozone measurements recorded with the FT-IR monitor to those taken with personal sampling devices and to hourly averages from the state ozone monitoring program. Although not exact, these comparisons can give the operator an idea if the FT-IR measurements are within generally accepted values. If not, corrective action should be taken.

#### 10.4.6 Ancillary Measurements

The type of ancillary measurements required will vary, depending on the type of study being conducted. For any long-path, open-path measurements, the ambient temperature, water vapor concentration, ambient pressure, and wind velocity should be recorded. The operator should also be aware of the effect of changes in altitude on ambient pressure. If the instrument is housed in an enclosed environment, the temperature of that environment should also be recorded. We have also found it useful to record the temperature inside the spectrometer itself, especially in cold weather situations.

#### 10.4.7 Documentation

As with any analytical methodology, a log of instrument usage, downtime, and repairs, as well as notes regarding unusual observations, should be maintained. These notes can prove invaluable for analyzing data that appear to be abnormal. Records should be kept that are appropriate for the type of study being conducted. For example, requirements for a research and development project may be different from those required for legally defensible data.

#### 10.5 References

- Kagann, R.H., J.G. Jolly, D.S. Shoop, M.R. Hankins, and J.M. Jackson. 1994. Validation of Open-Path FTIR Data at Treatment, Storage, and Disposal Facilities. *SP-89 Optical Sensing for Environmental Monitoring*, Air & Waste Management Association, Pittsburgh, PA, pp. 437-442.
- Kricks, R.J., Scotto, R.L., Pritchett, T.H., Russwurm, G.M., Kagann, R.H., and Mickunas, D.B. 1992. Quality Assurance Issues Concerning the Operation of Open-Path FTIR Spectrometers. *Proceedings of Optical Remote Sensing. Applications to Environmental and Industrial Safety Problems*, SP-81, Air & Waste Management Association, Pittsburgh, PA, pp. 224-231.
- Russwurm, G.M. 1992a. Quality Assurance, Water Vapor, and the Analysis of FTIR Data. *Proceedings of the 85th Annual Meeting and Exhibition of the Air & Waste Management Association*. Air & Waste Management Association, Pittsburgh, PA, pp. 92-73.03.
- Russwurm, G.M. 1992b. Quality Assurance and the Effects of Spectral Shifts and Interfering Species in FT-IR Analysis. *Proceedings of Optical Remote Sensing. Applications to Environmental and Industrial Safety Problems*, SP-81, Air & Waste Management Association. Pittsburgh, PA, pp. 105-111.
- Russwurm, G.M. and W.A. McClenny 1990. A Comparison of FTIR Open Path Ambient Data with Method TO-14 Canister Data. *Proceedings of the 1990 U.S. EPA/A&WMA International Symposium on the Measurement of Toxic and Related Air Pollutants*. Air & Waste Management Association, Pittsburgh, PA, pp. 248-253.
- Thompson, E.L, Jr., J.W. Childers, and G.M. Russwurm. 1994. Development of Quality Assurance Procedures in Open-Path FT-IR Monitoring. *Proceedings of the 1994 U.S. EPA/A&WMA International Symposium on Measurement of Toxic and Related Air Pollutants*. Air & Waste Management Association, Pittsburgh, PA, pp. 529-534.

U.S. Environmental Protection Agency. 1989. *Preparing Perfect Project Plans: A Pocket Guide for the Preparation of Quality Assurance Project Plans*. EPA/600/9-89/087. Available from Guy F. Simes, Quality Assurance Manager, U.S. Environmental Protection Agency, Risk Reduction Engineering Laboratory, Cincinnati, OH 45268.

U.S. Environmental Protection Agency. 1991. *Preparation Aids for the Development of RREL Quality Assurance Plans (Category I Project Plans)*. EPA/600/8-91/003. Available from Guy F. Simes, Quality Assurance Manager, U.S. Environmental

Protection Agency, Risk Reduction Engineering Laboratory, Cincinnati, Ohio 45268.

Weber, K., H.J. van de Wiel, A.C.F. Junker, and C. de LaRiva, C. 1992. Definition and Determination of Performance Characteristics of Air Quality Measuring Methods as Given by the International Organization for Standardization (ISO) - Applicability to Optical Remote Sensing. *Proceedings of Optical Remote Sensing. Applications to Environmental and Industrial Safety Problems*, SP-81, Air & Waste Management Association, Pittsburgh, PA, pp. 30-42.

## Chapter 11

### Glossary of Terms for FT-IR Open-Path Remote Sensing

#### 11.1 Introduction and Overview

This chapter contains a glossary of terms for remote sensing, with an emphasis on those terms relevant to FT-IR long-path, open-path monitoring. When possible, definitions of terms have been drawn from authoritative texts or manuscripts in the fields of remote sensing, air pollution monitoring, spectroscopy, optics, and analytical chemistry. In some cases, general definitions have been augmented or streamlined to be more specific to long-path, open-path monitoring applications. These definitions were intended to remain scientifically rigorous and still be generally applicable to a variety of FT-IR open-path remote-sensing issues.

#### 11.2 Terms

**Absorbance:** The negative logarithm of the transmission.  $A = -\ln(I/I_0)$ , where  $I$  is the transmitted intensity of the light and  $I_0$  is the incident intensity. Generally, the logarithm to the base 10 is used, although the quantity  $I$  really diminishes exponentially with  $A$  (Pfeiffer and Liebafsky 1951). If the term "fractional transmission" is used for the ratio  $I/I_0$ , then the implication is that the instrument's slit function (see "Instrument function") is accounted for (Penner 1959).

**Active system:** A system that radiates energy to the surrounding environment (for example, a radio transmitter).

**Apodization:** A mathematical transformation carried out on data received from an interferometer to alter the instrument's response function. There are various types of transformation; the most common are boxcar, triangular, Happ-Genzel, and Beer-Norton functions.

**Average concentration:** For FT-IR or differential absorption spectroscopy systems, this quantity is the result of dividing the integrated concentration (the quantity that is measured) by the path length used for the measurement. It has units of parts per million, parts per billion, micrograms per cubic meter, etc. (McClenny and Russwurm 1978).

**Background spectrum:** 1. With all other conditions being equal, that spectrum taken in the absence of the particular absorbing species of interest. 2. Strictly, that radiant intensity incident on the front plane of the absorbing medium. 3. A spectrum obtained from the ambient black body radiation entering the system. This background must be considered in FT-IR systems, in which the IR beam is not modulated before it is transmitted along the path. For FT-IR systems that do not use a separate source of

infrared energy, the background is the source of infrared energy.

**Band pass filter:** A filtering device that allows the transmission of only a specific band of energies. It can be wide band or narrow band.

**Bandwidth:** The width of a spectral feature as recorded by a spectroscopic instrument. This width is listed as the full width at the half maximum of the feature or as the half width at the half maximum of the spectral feature. This is also referred to as the line width (Lengyel 1971).

**Beer's law:** Beer's law states that the intensity of a monochromatic plane wave incident on an absorbing medium of constant thickness diminishes exponentially with the number of absorbers in the beam. Strictly speaking, Beer's law holds only if the following conditions are met: (1) perfectly monochromatic radiation, (2) no scattering, (3) a beam that is strictly collimated, (4) negligible pressure-broadening effects (Pfeiffer and Liebafsky 1951; Lothian 1963). For an excellent discussion of the derivation of Beer's law, see Penner (1959).

**Bistatic system:** A system in which the receiver is some distance from the transmitter. This term is actually taken from the field of radar technology. For remote sensing, this implies that the light source and the detector are separated and are at the ends of the monitoring path.

**Broad band system:** Any system that admits a broad range of energies into its signal-processing section. Alternatively, a system that has a flat response to a large range of energies.

**Closed path:** The optical path over which the beam travels in a sensor that is entirely enclosed. This is the case when White cells or Harriot cells are used with the system.

**Cooler:** A device into which the detector is placed for maintaining it at a low temperature in an IR system. At a low temperature, the detector provides the high sensitivity that is required for the IR system. The two primary types of coolers are a liquid nitrogen Dewar and a closed-cycle Stirling cycle refrigerator.

**COSPEC:** An acronym for "correlation spectrometer." This is a misnomer for the type of instrument implied. It is really an instrument that uses a diffraction grating either in the active, bistatic or the passive mode. This instrument is more correctly included in the class of instruments using differential absorption spectroscopy techniques. It is used primarily to measure sulfur dioxide and nitrogen oxide.

**DIAL:** An acronym for "differential absorption lidar." This system uses two pulsed frequencies from the same laser or from different lasers to measure the concentration of gas over a path. The two laser lines are at different positions within the absorption feature. The difference of the amount of light backscattered at these two

wavelengths is the quantity used for the measurement.

**DOAS:** An acronym for differential optical absorption spectroscopy. A technique whereby, in principle, any known difference in absorbance is used to determine the concentration of a gas. Generally, the absorption difference is taken between the spectral line center and the wing.

**Electromagnetic spectrum:** The total of all possible frequencies of electromagnetic radiation. Different sources may emit over different frequency regions. All electromagnetic waves travel at the same speed in free space (Halliday and Resnick 1974).

**Fingerprint region:** The region of the absorption spectrum of a molecule that essentially allows its unequivocal identification. This region covers the wave number range from 650 to 1300  $\text{cm}^{-1}$  (Willard et al. 1974).

**Flux:** The number or mass of particles or molecules that pass through a given unit area of surface per unit of time (Calvert 1990).

**Fourier transform:** A mathematical transform that allows an aperiodic function to be expressed as an integral sum over a continuous range of frequencies (Champeny 1973). The Fourier transform of the interferogram produced by the Michelson interferometer in an FT-IR is the intensity as a function of frequency.

**FT-IR:** An abbreviation for "Fourier transform infrared." A spectroscopic instrument using the infrared portion of the electromagnetic spectrum. The working component of this system is a Michelson interferometer. To obtain the absorption spectrum as a function of frequency, a Fourier transform of the output of the interferometer must be performed. For a brief overview of the FT-IR, see the publication by Nicolet (Nicolet Analytical Instruments 1986). For an in-depth description of the FT-IR, see Griffiths and deHaseth (1986).

**GASPEC:** An acronym for "gas filter correlation spectrometer." The earliest of these devices was described by Luft in 1943, and they have been used in various configurations ever since. The primary feature of these devices is a pair of gas cells. One cell contains a carefully selected quantity of the target gas and the other a gas that is spectroscopically inactive. The difference in spectral transmittance of the two cells is an indicator of the concentration of the target gas in the atmosphere (Ward and Zwick 1975).

**Infrared spectrum:** That portion of the electromagnetic spectrum that spans the region from about 10  $\text{cm}^{-1}$  to about 12,500  $\text{cm}^{-1}$ . It is divided (Willard et al. 1974) into (1) the near-infrared region (from 12,500 to 4000  $\text{cm}^{-1}$ ), (2) the mid-infrared region (from 4000 to 650  $\text{cm}^{-1}$ ), and (3) the far-infrared region (from 650 to 10  $\text{cm}^{-1}$ ).

**Instrument function:** The function superimposed on the absorption line shape

by the instrument. This is sometimes referred to as the slit function, a term taken from instruments that use slits to obtain resolution.

**Intensity:** The radiant power per unit solid angle. When the term "spectral intensity" is used, the units are watts per steradian per nanometer. In most spectroscopic literature, the term "intensity" is used to describe the power in a collimated beam of light in terms of power per unit area per unit wavelength. However, in the general literature, this definition is more often used for the term "irradiance," or "normal irradiance" (Calvert 1990; Stone 1963).

**Interference:** The physical effects of superimposing two or more light waves. The principle of superposition states that the total amplitude of the electromagnetic disturbance at a point is the vector sum of the individual electromagnetic components incident there. For a two-component system of collinear beams of the same amplitude, the mathematical description of the result of addition is given by  $I(p) = 2I_0(1 + \cos[A])$ , where  $I_0$  is the intensity of either beam, and  $A$  is the phase difference of the two components. The cosine term is called the "interference term" (Halliday and Resnick 1974; Stone 1963). See also "Spectral Interference."

**Interferogram:** The effects of interference that are detected and recorded by an interferometer; the output of an FT-IR and the primary data that is collected and stored (Stone 1963; Griffiths and deHaseth 1986).

**Interferometer:** Any of several kinds of instruments used to produce interference effects. The Michelson interferometer used in FT-IR instruments is the most famous of a class of interferometers that produce interference by the division of an amplitude (Tolansky 1962).

**Irradiance:** Radiant power per unit projected area of a specified surface. This has units of watts per square centimeter. The term "spectral irradiance" is used to describe the irradiance as a function of wavelength. It has units of watts per square centimeter per nanometer (Calvert 1990).

**Laser:** An acronym for the term "light amplification by stimulated emission of radiation". A source of light that is highly coherent, both spatially and temporally (Lengyel 1971).

**LIDAR:** An acronym for the term "light detection and ranging" (Calvert 1990). A technique for (1) detecting the presence of gases and aerosols by measuring the backscattered portion of a laser beam and (2) determining the range of these gases and aerosols by electronically gating the detected signal and performing a calculation based on the speed of light (about 30 cm/ns).

**Light:** Strictly, light is defined as that portion of the electromagnetic spectrum that causes the sensation of vision. It extends from about 25,000  $\text{cm}^{-1}$  to about 14,300  $\text{cm}^{-1}$  (Halliday and Resnick 1974).

**Light scattering:** The redirection of light waves due to interaction with molecules or aerosols. If the size of the body causing the scattering is small compared to the wavelength of the incident radiation, the scattering is termed "Rayleigh scattering." If the size is large compared to the wavelength, the scattering is termed "Mie scattering." Scattering by molecules is generally Rayleigh scattering, and scattering by aerosols is Mie scattering. As light travels through a medium, two physical processes diminish the intensity in the forward direction – scattering and absorption. The sum of these two effects is called extinction (van de Hulst 1981).

**Long-path monitoring:** This is a monitoring technique that uses an extended, open path. LIDAR systems can make measurements over a path length of a few kilometers. DOAS systems can make measurements of ozone over a path of up to 2 km. The FT-IR systems customarily use paths with length less than 1 km.

**Minimum detection limit:** The minimum concentration of a compound that can be detected by an instrument with a given statistical probability. Usually the detection limit is given as 3 times the standard deviation of the noise in the system. In this case, the minimum concentration can be detected with a probability of 99.7% (Calvert 1990; Long and Winefordner 1983).

**Monitoring path:** The actual path in space over which the pollutant concentration is measured and averaged.

**Monitoring path length:** The length of the monitoring path in the atmosphere over which the average pollutant concentration measurement is determined (U.S. Environmental Protection Agency 1994).

**Monostatic system:** A system with the source and the receiver at the same end of the path. For FT-IR systems and for DOAS systems, the beam is generally returned by a retroreflector. For LIDAR systems, the backscattered portion of the laser beam is measured directly.

**Open-ended system:** A system in which the remote sensor uses light reflected from targets of opportunity (walls, trees, etc.) or skylight as a source.

**Open-path analyzer:** An automated analytical instrument that is used for a method of measuring the average atmospheric pollutant concentration in situ along one or more monitoring paths that are 5 m or more in length (U.S. Environmental Protection Agency 1994).

**Open-path monitoring:** Remote sensing over a path that is completely open to the atmosphere. Thus, the concentration of a particular gas in the beam path can be changed by winds and diffusion. The open path is the most frequently used in remote sensing.

**Optical remote sensing:** A generic term used to describe any of a number of optical measurement techniques that measure some quantity or constituent of the atmosphere.



These techniques include DIAL, DOAS, FT-IR, GASPEC, LIDAR, etc. One thing that is common to all the techniques is that no sample must be collected.

**Parts per million meters:** The unit term for the quantity that is measured by many remote sensors. It is the unit associated with the quantity path-integrated concentration. It is a possible unit of choice for reporting data from remote sensors because it is independent of the path length.

**Passive system:** Any system that does not radiate energy to its surroundings.

**Path-averaged concentration:** The result of dividing the path-integrated concentration by the path length. Path-averaged concentration gives the average value of the concentration along the path (McClenny and Russwurm 1978).

**Path-integrated concentration:** The quantity that is measured by a remote sensor over a long path. It has units of concentration times length.

**Plume:** The gaseous and aerosol effluents emitted from a chimney or other source and the volume of space they occupy. The shape of a plume and the concentration of pollutants within it are very sensitive to meteorological conditions (Calvert 1990).

**Point analyzer:** An automated analytical method that measures pollutant concentration in an ambient air sample extracted from the atmosphere at a specific

inlet probe point (proposed changes [U.S. Environmental Protection Agency 1994]).

**Probe:** The actual inlet where an air sample is extracted from the atmosphere for delivery to a sampler or point analyzer (proposed changes [U.S. Environmental Protection Agency 1994]).

**Radiometry:** The measurement of various quantities such as intensity associated with radiant energy (Calvert 1990). This is in contrast to the term photometry, which assumes the spectral sensitivity of the human eye as the detector (Walsh 1965).

**Real-time system:** Any monitoring system that acquires and records data at a rate that is comparable to the rate at which the concentration is changing.

**Reference spectra:** Spectra of the absorbance versus wave number for a pure sample of a set of gases. The spectra are obtained under controlled conditions of pressure and temperature and with known concentrations. For most instruments, the pure sample is pressure-broadened with nitrogen so that the spectra are representative of atmospherically broadened lines. These spectra are used for obtaining the unknown concentrations of gases in ambient air samples.

**Resolution:** The minimum separation that two spectral features can have and still, in some manner, be distinguished from one another. A commonly used requirement for two spectral features to be considered just

resolved is the Raleigh criterion. This states that two features are just resolved when the maximum intensity of one falls at the first minimum of the other (Jenkins and White 1950; Tolansky 1962). This definition of resolution and the Raleigh criterion are also valid for the FT-IR, although there is another definition in common use for this technique. This definition states that the minimum separation in wave numbers of two spectral features that can be resolved is the reciprocal of the maximum optical path difference (in centimeters) of the two interferometer mirrors employed (Griffiths and deHaseth 1986; Nicolet 1986).

**Retroreflector:** The CIE (Commission Internationale de l'Eclairage) defines retroreflection as "radiation returned in directions close to the direction from which it came, this property being maintained over wide variations of the direction of the incident radiation." Retroreflector devices come in a variety of forms and have many uses. The one commonly described by workers in remote sensing uses total internal reflection from three mutually perpendicular surfaces. This kind of retroreflector is usually called a corner cube or prismatic retroreflector (Rennilson 1980).

**Slit function:** See "Instrument function."

**Source:** The device that supplies the electromagnetic energy for the various instruments used to measure atmospheric gases. These generally are a Nernst glower or globar for the infrared region or a xenon arc lamp for the ultraviolet region. There are

several lasers that also are used as sources for DIAL and LIDAR instruments.

**Spectral intensity:** See "Intensity."

**Spectral interference:** When the absorbance features from two or more gases cover the same wave number regions, the gases are said to exhibit spectral interference. Water vapor produces the strongest spectral interference for infrared spectroscopic instruments that take atmospheric data.

**Synthetic background:** A spectrum that is made from a field spectrum by choosing points along the baseline and connecting them with a high-order polynomial or short, straight lines. The synthetic background is then used to find the absorbance spectrum.

**Truncation:** The act of stopping a process before it is complete. In FT-IR spectrometers, the theoretically infinite scale of the interferogram is truncated by the finite movement of the interferometer mirror.

**Unistatic system:** A system that has the source and the receiver at the same place; now more commonly referred to as a monostatic system.

**Wave number:** The number of waves per centimeter. This term has units of reciprocal centimeters ( $\text{cm}^{-1}$ ).

### 11.3 References

Calvert, J.G. 1990. Glossary of Atmospheric Chemistry Terms

- (recommendations 1990). *Pure Appl. Chem.* 62 (11):2167-2219.
- Champeney, D.C. 1973. *Fourier Transforms and Their Physical Applications*. Academic Press, London.
- Griffiths, P.R., and J.A. deHaseth. 1986. *Fourier Transform Infrared Spectrometry*. John Wiley and Sons, New York.
- Halliday, D., and R. Resnick. 1974. *Fundamentals of Physics*. Wiley and Sons, New York.
- Jenkins, F.A., and H.E. White. 1950. *Fundamentals of Optics*. McGraw-Hill, New York.
- Long, G.L., and J.D. Winefordner. 1983. Limit of Detection: A Closer Look at the IUPAC Definition. *Anal. Chem.* 55(7): 712A-724A.
- Lothian, G.F. 1963. Beer's Law and Its Use in Analysis. *Analyst* 88:678.
- Lengyel, B.A. 1971. *Lasers*, 2nd Ed. Wiley-Interscience, New York.
- Luft, K.F. 1943. Über Eine Neue Methode der Registrierenden Gas Analyze Mit Hilfe der Absorption Ultraroter Stahlen Ohne Spektrale Zerlegung. *J. Tech. Phys.* 24:97.
- McClenny, W.A., and G.M. Russwurm. 1978. Laser-Based Long Path Monitoring of Ambient Gases - Analysis of Two Systems. *Atmos. Environ.* 12:1443.
- Nicolet Analytical Instruments. 1986. *FT-IR Theory*. Nicolet Analytical Instruments, Madison, WI.
- Penner, S.S. 1959. *Quantitative Molecular Spectroscopy and Gas Emissivities*. Addison-Wesley, Reading, MA.
- Pfeiffer, H.G., and H.A. Liebhafsky. 1951. The Origins of Beer's Law. *J. Chem. Educ.* 28:123-125.
- Rennilson, J.J. 1980. Retroreflection Measurements: A Review. *Appl. Opt.* 19:1234.
- Stone, J.M. 1963. *Radiation and Optics*. McGraw-Hill, New York.
- Tolansky, S. 1962. *An Introduction to Interferometry*. John Wiley and Sons, New York.
- U.S. Environmental Protection Agency. 1994. Ambient air quality surveillance siting criteria for open path analyzers (proposed rule). *Fed. Reg.* 59(159):42541-42552.
- van de Hulst, H.C. 1981. *Light Scattering by Small Particles*. Dover Publications, New York.
- Walsh, J.W.T. 1965. *Photometry*. Dover Publications, New York.
- Ward, T.V., and H.H. Zwick. 1975. Gas Cell Correlation Spectrometer: GASPEC. *Appl. Opt.* 14:2896.
- Willard, H.H., L.L. Merritt, and J.A. Dean. 1974. *Instrumental Methods of Analysis*, 5th Ed. D. Van Nostrand, Princeton, NJ.

## Chapter 12

### Bibliography

#### 12.1 Introduction and Overview

This chapter contains a bibliography of journal articles, books, and conference proceedings that address FT-IR long-path monitoring, as well as general references that present discussions of the basic principles of FT-IR spectrometry. This is not a reference section for literature cited in the text of this guidance document, but is a general bibliography. References in this document are listed at the end of the chapter in which they are cited.

This bibliography is by no means exhaustive, but is intended to give a broad overview of the available literature in the FT-IR long-path discipline. During the initial phase of this overview, a computer-assisted on-line literature search was conducted for citations listed in *Chemical Abstracts* through September 29, 1992. A subsequent on-line search was conducted for citations listed in *Chemical Abstracts* from 1992 through July 22, 1994. These literature searches focused on, but were not limited to, current publications regarding FT-IR long-path, open-path monitoring, in keeping with the emphasis of this document. For this latest edition, a literature search of the documents available through NTIS in Springfield, VA, was conducted through 1998. Other citations were gleaned from the reference sections of articles on file. Several early citations are also given to provide an

important, historical perspective into long-path IR monitoring in environmental analysis. Only articles that are on file in our laboratory are listed in the bibliography. This bibliography will continue to be updated as revisions to this document are made.

Several of the more recent citations are from conference proceedings, which may limit their general availability. They are included to give the reader access to current research in the field that has in many cases not yet appeared in the peer-reviewed literature. Also, inclusion of the conference proceedings provides the reader with pertinent information regarding conferences and meetings that typically address FT-IR long-path or remote-sensing issues.

#### 12.2 Publications

Amoto, I. 1988. Remote Sensing: A Distant View of Chemistry. *Anal. Chem.* 60(23):1339A-1344A.

Anderson, R.J., and P.R. Griffiths. 1975. Errors in Absorbance Measurements in Infrared Fourier Transform Spectrometry Because of Limited Instrument Resolution. *Anal. Chem.* 47(14):2339-2347.

Andreas, E.L., J.R. Gosz, and C.N. Dahm. 1992. Can Long-Path FTIR Spectroscopy Yield Gas Flux Measurements Through a Variance Technique? *Atmos. Environ.* 26A(2):225-233.

Bangalore, A.S., G.W. Small, R.J. Combs, R.B. Knapp, R.T. Kroutil, C.A. Traynor, and

- J.D. Ko. 1997. Automated Detection of Trichloroethylene by Fourier Transform Infrared Remote Sensing Measurements. *Anal. Chem.* 26:118-129.
- Barnes, H.W., Jr., W.F. Herget, and R. Rollins. 1974. Remote Sensing of Sulfur Dioxide in Power Plant Plumes Using Ultraviolet Absorption and Infrared Emission Spectroscopy. *Analytical Methods Applied to Air Pollution Measurements* (R.K. Stevens and W.F. Herget, Eds.), Ann Arbor Science, Ann Arbor, MI, pp. 245-266.
- Barnett, R.W., and B.T. Smith. 1994. Modeling Background Temperatures in Passive Infrared Remote Sensing. *SP-89 Optical Sensing for Environmental Monitoring*, Air & Waste Management Association, Pittsburgh, PA, pp. 293-304.
- Batterman, S.A., C. Peng, and P. Milne. 1994. Sequential Extractive Sampling of Indoor Air Contaminants Using FT-IR Spectroscopy. *SP-89 Optical Sensing for Environmental Monitoring*, Air & Waste Management Association, Pittsburgh, PA, pp. 242-254.
- Beer, A. 1852. *Ann. Physik* 86:78.
- Beer, R. 1992. *Remote Sensing by Fourier Transform Spectrometry*, John Wiley and Sons, New York.
- Beil, A., R. Daum, R. Harig, and G. Matz. 1998. Remote Sensing of Atmospheric Pollution by Passive FTIR Spectrometry. *Proc. SPIE* 3493:32-43.
- Bell, R.J. 1972. *Introductory Fourier Transform Spectroscopy*, Academic Press, New York.
- Bennett, C.L. 1994. FTIR Measurements of Thermal Infrared Sky Radiance and Transmission. Department of Energy Report UCRL-117864.
- Bhattacharyya, R., and L.A. Todd. 1995. Two Dimensional Mapping of Air Contaminant Movement Using a Tomographic System. *Proceedings of the SPIE Specialty Conference Optical Sensing for Environmental and Process Monitoring, McClean, VA*, International Society for Optical Engineering, Bellingham, WA.
- Biermann, H.W., E.C. Tuazon, A.M. Winer, T.J. Wallington, and J.N. Pitts, Jr. 1988. Simultaneous Absolute Measurements of Gaseous Nitrogen Species in Urban Ambient Air by Long Pathlength Infrared and Ultraviolet-Visible Spectroscopy. *Atmos. Environ.* 22(8):1545-1554.
- Bishop, G.A., J.R. Starkey, A. Ihlenfeldt, W.J. Williams, and D.H. Stedman. 1989. IR Long-Path Photometry: A Remote Sensing Tool for Automobile Emissions. *Anal. Chem.* 61(10):671A-677A.
- Bishop, G.A., and D.H. Stedman. 1990. On-Road Carbon Monoxide Emission Measurement Comparisons for the 1988-1989 Colorado Oxy-Fuels Program. *Environ. Sci. Technol.* 24(6):843-847.
- Bishop, G.A., D.H. Stedman, and T. Jessop. 1992. Infrared Emission and Remote Sensing. *J. Air Waste Manage. Assoc.* 42(5):695-697.
- Bittner, H., T. Eisenmann, H. Mosebach, M. Erhard, and M. Resch. 1994. Measurements of Diffuse Emissions of Volatile Organic Compounds by High Resolution FTIR Remote Sensing. *SP-89 Optical Sensing for Environmental Monitoring*, Air & Waste Management Association, Pittsburgh, PA, pp. 443-454.
- Blumenstock, T., H. Fischer, A. Friedle, F. Hase, and P. Thomas. 1997. Column Amounts of ClONO<sub>2</sub>, HCl, HNO<sub>3</sub> and HF from Ground Based FTIR Measurements Made

- near Kiruna, Sweden in Late Winter 1994. *J. Atmos. Chem.* 26 (3):311-321.
- Brandon, R.W., S.D. Garbis, and R.H. Kagann. 1992. Quantitative Gas Standards for the Calibration of Open Path Optical Sensors. *SP-81 Optical Remote Sensing. Applications to Environmental and Industrial Safety Problems*, Air & Waste Management Association, Pittsburgh, PA, pp. 434-445.
- Briz, S., A.J. De Castro, J. Melendez, J. Meneses, J.M. Aranda, and F. Lopez. 1997. *Proc. SPIE* 3106:159-170.
- Brown, C.W., P.F. Lynch, R.J. Obremski, and D.S. Lavery. 1982. Matrix Representations and Criteria for Selecting Analytical Wavelengths for Multicomponent Spectroscopic Analysis. *Anal. Chem.* 54(9):1472-1479.
- Byrd, L.A.B. 1994. Ambient Air Monitoring Siting Criteria for Open Path Analyzers Measuring Nitrogen Dioxide, Ozone, and Sulfur Dioxide. *SP-89 Optical Sensing for Environmental Monitoring*, Air & Waste Management Association, Pittsburgh, PA, pp. 349-357.
- Calvert, J.G. 1990. Glossary of Atmospheric Chemistry Terms (recommendations 1990). *Pure Appl. Chem.* 62(11):2167-2219.
- Cantu, A., G. Pophal, S. Hall, and C.T. Laush. 1998. Unique Application of an Extractive FTIR Ambient Air Monitoring System for the Simultaneous Detection of Multiple ppb Level VOC's. *Appl. Phys. B. Lasers Opt.* 67 (4):493-496.
- Carlson, R.C., A.F. Hayden, and W.B. Telfair. 1988. Remote Observation of Effluents from Small Building Smokestacks Using FT-IR Spectroscopy. *Appl. Opt.* 27(23):4952-4959.
- Carter, R.E., Jr., D.D. Lane, G.A. Marotz, M.J. Thomas, and J.L. Hudson. 1992. A Method of Interconversion Between Point and Path-Averaged Ambient Air VOC Concentrations, Using Wind Data. *SP-81 Optical Remote Sensing. Applications to Environmental and Industrial Safety Problems*, Air & Waste Management Association, Pittsburgh, PA, pp. 529-540.
- Carter, R.E., Jr., D.D. Lane, G.A. Marotz, C.T. Chaffin, T.L. Marshall, M. Tucker, M.R. Witkowski, R.M. Hammaker, W.G. Fateley, M.J. Thomas, and J.L. Hudson. 1993. A Method of Predicting Point and Path-Averaged Ambient Air VOC Concentrations, Using Meteorological Data. *J. Air Waste Manage. Assoc.* 43:480-488.
- Carter, R.E., Jr., M.J. Thomas, G.A. Marotz, D.D. Lane, and J.L. Hudson. 1992. Compound Detection and Concentration Estimation by Open-Path Fourier Transform Infrared Spectrometry and Canisters Under Controlled Field Conditions. *Environ. Sci. Technol.* 26(11):2175-2181.
- Carter, R.O., III, N.E. Lindsay, and D. Beduhn. 1990. A Solution to Baseline Uncertainty Due to MCT Detector Nonlinearity in FT-IR. *Appl. Spectrosc.* 44(7):1147-1151.
- Chaffin, T., T.L. Marshall, J.M. Poholarz, M.D. Tucker, M. Hammaker, and W.G. Fateley. 1993. What Height for Remote FTIR Sensing of Volatile Organic Compounds Emitted near Ground Level. *Proceedings of the 86<sup>th</sup> Annual Meeting and Exhibition*, Air & Waste Management Association, Pittsburgh, PA.
- Chaffin, C.T., Jr., W.G. Fateley, M.D. Tucker, and R.M. Hammaker. 1994. An Alternative Sampling Technique for Fourier Transform Infrared (FT-IR) Remote Sensing of Fugitive Emissions from Industrial Sites. *SP-89 Optical Sensing for Environmental*

- Monitoring, Air & Waste Management Association, Pittsburgh, PA, pp. 814-825.
- Chaffin, C.T., T.L. Marshall, R.J. Combs, R.B. Knapp, R.T. Kroutil, W.G. Fatel, and R.M. Hammaker. 1995. Passive Fourier Transform (FTIR) Monitoring of SO<sub>2</sub> in Plumes: A Comparison of Remote Passive Spectra of an Actual Emission Spectra Collected with a Heatable Cell. *Proc. SPIE* 2365:303-313.
- Champeney, D.C. 1973. *Fourier Transforms and Their Physical Applications*. Academic Press, London.
- Chakraborty, D.K. 1995. Examination of the Long Path Open Air FTIR Technique for Air in the State of Kentucky. *Proc. SPIE* 2365: 347-358.
- Chaney, L.W. 1983. The Remote Measurement of Traffic Generated Carbon Monoxide. *J. Air Pollut. Control Assoc.* 33(3):220-222.
- Chang, S.-Y., and T.-L. Tso. 1994. Measurement of the Taiwan Ambient Trace Gas Concentration by Kilometer-Path Length Fourier-Transform Infrared Spectroscopy. *Anal. Sci.* 10(1):193-201.
- Chang, S.-Y., and T.-L. Tso. 1994. Field Applications of Long Infrared Absorption in Taiwan. *SP-89 Optical Sensing for Environmental Monitoring*, Air & Waste Management Association, Pittsburgh, PA, pp. 157-181.
- Childers, J.W. 1993. Resolution Considerations in Long-Path, Open-Path FT-IR Spectrometry. Paper 93-RA-121.05, *Proceedings of the 86th Annual Meeting and Exhibition*, Air & Waste Management Association, Pittsburgh, PA.
- Childers, J.W., and E.L. Thompson, Jr. 1994. Resolution Requirements in Long-Path FT-IR Spectrometry. *SP-89 Optical Sensing for Environmental Monitoring*, Air & Waste Management Association, Pittsburgh, PA, pp. 38-46.
- Childers, J.W., G.M. Russwurm, and E.L. Thompson, Jr. 1996. Instrumental Parameters and Their Effect on Open-Path FT-IR Data. *Proceedings of the 89th Annual Meeting & Exhibition of the Air & Waste Management Association*. Paper 96-MP5.07, Air & Waste Management Association, Pittsburgh, PA.
- Childers, J.W., G.M. Russwurm, and E.L. Thompson. 1997. QA/QC Issues in OP/FTIR Monitoring. *Proceedings of the 1997 Annual Meeting AWMA*, Air & Waste Management Association, Pittsburgh, PA.
- Childers L.O. 1996. USEPA QA Auditor Is Scheduled for a Visit. What Can I Expect? *Proceedings of the 1995 Specialty Conference In San Francisco*, Air & Waste Management Association, Pittsburgh, PA.
- Chu, P.M., G.C. Rhoderick, W.J. Lafferty, F. R. Guenther, and S.J. Wetzel. 1997. Quantitative Infrared Data Base of Hazardous Air Pollutants. *Proceedings of the 89th Annual Meeting of AWMA in Nashville, Tenn.* Air & Waste Management Association, Pittsburgh, PA.
- Chughtai, A.R., and D.M. Smith. 1991. Long Optical Path Cell for Photochemical Kinetics in Heterogeneous Systems of Low Concentration. *Appl. Spectrosc.* 45(7):1204-1207.
- Clark, J.M. 1994. Mercury Cadmium Telluride Cryocooled Detector Performance Parameters for FTIR Spectroscopy. *SP-89 Optical Sensing for Environmental Monitoring*, Air & Waste Management Association, Pittsburgh, PA, pp. 591-606.

- Collins, J.D., and L.A. Todd. 1992. Evaluation of Infrared Optical Remote Sensing Equipment in an Exposure Chamber. *SP-81 Optical Remote Sensing. Applications to Environmental and Industrial Safety Problems*, Air & Waste Management Association, Pittsburgh, PA, pp. 351-355.
- Cronin, J.T. 1992. Stack-Gas Monitoring Using FT-IR Spectroscopy. *Spectroscopy* 7(5):33-39.
- Dando, N.R., T.O. Montgomery, L.A. Schneider, and J.E. Gibb. 1994. Applications of Open-Path FTIR Spectroscopy for Characterizing Fugitive Emissions at Metal Production Plants. *SP-89 Optical Sensing for Environmental Monitoring*, Air & Waste Management Association, Pittsburgh, PA, pp. 123-133.
- Demirgian, J.C., and M.D. Erickson. 1990. The Potential of Continuous Emission Monitoring of Hazardous Waste Incinerators Using Fourier Transform Infrared Spectroscopy. *Waste Manage.* 10:227.
- Demirgian, J.C., C.L. Hammer, and R.T. Kroutil. 1992. The Potential of Passive-Remote Fourier Transform Infrared Spectroscopy to Detect Organic Emissions Under the Clean Air Act. *SP-81 Optical Remote Sensing. Applications to Environmental and Industrial Safety Problems*, Air & Waste Management Association, Pittsburgh, PA, pp. 464-476.
- Demirgian, J.C., C. Hammer, E. Hwang, and Z. Mao. 1994. Advances in Passive-Remote and Extractive Fourier Transform Infrared Systems. *SP-89 Optical Sensing for Environmental Monitoring*, Air & Waste Management Association, Pittsburgh, PA, pp. 780-790.
- Douard, M., J. Zentzius-Reitz, T. Lamp. A. Ropertz, and K. Weber. 1997. Quality Assurance Procedures and Measurements for Open Path FTIR Spectroscopy. *Proc. SPIE* 3107:114-125.
- Dowling, J.A. 1994. A Review of the Naval Research Laboratory Program of Long-Path Air Measurements Using Lasers and FT-IR. *SP-89 Optical Sensing for Environmental Monitoring*, Air & Waste Management Association, Pittsburgh, PA, pp. 145-156.
- Draves, J.A., J.P. LaCosse, D.M. Hull, and R.L. Spellicy. 1992. A Comparison of Open Path Fourier Transform Infrared Spectrometry with Conventional Ambient Air Monitoring Methods. *SP-81 Optical Remote Sensing. Applications to Environmental and Industrial Safety Problems*, Air & Waste Management Association, Pittsburgh, PA, pp. 252-265.
- Dresscher, A.C., M.G. Yost, D.Y. Park, S.P. Levine, A.J. Gadgil, M.L. Fischer, and W.W. Nazaroff. 1995. Measurement of Tracer Gas Distributions Using an Open Path Coupled with Computed Topography. *Proceedings of Specialty SPIE Conference in McLean, Va.* International Society for Optical Engineering, Bellingham, WA.
- Dubois, A.E., J.W. Engle, P.L. McKane, and S.H. Perry. 1996. Open Path FTIR Quality Assurance Data: Demonstration of Technology Reliability. *Proceedings of AWMA Specialty Conference in San Francisco*. Air & Waste Management Association, Pittsburgh, PA.
- Edney, E.O., J.W. Spence, and P.L. Hanst. 1979. Synthesis and Thermal Stability of Peroxy Alkyl Nitrates. *J. Air Pollut. Control Assoc.* 29(7):741-743.
- Egert, S., D. Peri and Y. Danziger. 1996. Efficient Monitoring of Toxic Gases over an Industrial Zone Using Remote Sensors. *Proceedings of SPIE/AWMA Specialty Conference in San Francisco*. Air & Waste Management Association, Pittsburgh, PA.



- Eisenmann, T., H. Mosebach, H. Bittner, M. Resch, R. Haus, and K. Schäfer. 1993. Selected Applications of Remote Sensing Measurements with the Double Pendulum Interferometer in Germany with Special Consideration of Quality Assurance Aspects. Paper 93-FA-165.01, *Proceedings of the 86th Annual Meeting and Exhibition*, Air & Waste Management Association, Pittsburgh, PA.
- Eisenmann, T., H. Mosebach, and H. Bittner. 1994. Remote Sensing FTIR-System for Emission Monitoring and Ambient Air Control of Atmospheric Trace Gases and Air Pollutants. *Erdoel Erdgas Kohle* 110(1):28-34.
- Fischer, H. 1992. Remote Sensing of Atmospheric Trace Constituents Using Fourier Transform Spectrometry. *Ber. Bunsen-Ges. Phys. Chem.* 96(3):306-314.
- Flanagan, J., R. Shores and S. Thorneloe, 1996. Uncertainty Estimate for Open Path Remote Sensing of Fugitive Emissions. EPA/600/A-96/067, U.S. Environmental Protection Agency.
- Franzblau, A., S.P. Levine, L.A. Burgess, A.S. Qu, R.M. Schreck, and J.B. D'Arcy. 1992. The Use of a Transportable Fourier Transform Infrared (FTIR) Spectrometer for the Direct Measurement of Solvents in Breath and Ambient Air - I: Methanol. *Am. Ind. Hyg. Assoc. J.* 53(4):221-7.
- Garbis, S.D., and R.W. Brandon. 1994. An Assessment of Dynamic Equilibrium Methods of Generating FTIR Reference Spectra., *SP-89 Optical Sensing for Environmental Monitoring*, Air & Waste Management Association, Pittsburgh, PA, pp. 281-292.
- Gardner, D.G., W.J. Phillips, D.J. Gonnion, L.T. Lay, and R. Dishakjian. 1994. High Temperature Reference Spectra. *SP-89 Optical Sensing for Environmental Monitoring*, Air & Waste Management Association, Pittsburgh, PA, pp. 266-280.
- Gay, B.W., P.L. Hanst, J.J. Bufalini, and R.C. Noonan. 1976. Atmospheric Oxidation of Chlorinated Ethylenes. *Environ. Sci. Technol.* 10(1):58-67.
- Gay, B.W., R.C. Noonan, J.J. Bufalini, and P.L. Hanst. 1976. Photochemical Synthesis of Peroxyacyl Nitrates in Gas Phase via Chlorine-Aldehyde Reaction. *Environ. Sci. Technol.* 10(1):82-85.
- Gay, B.W., Jr., R.C. Noonan, P.L. Hanst, and J.J. Bufalini. 1975. Photolysis of Alkyl Nitrites and Benzyl Nitrite at Low Concentrations—An Infrared Study. *Removal of Trace Contaminants from the Air*, ACS Symp. Ser. 17:132-151.
- Giese-Bogdan, S., M. Simonds-Malachowski, and S.P. Levine. 1994. Evaluation of the Role of Fixed Beam Open Path Fourier Transform Infrared Spectroscopy in Air Monitoring Strategies. *SP-89 Optical Sensing for Environmental Monitoring*, Air & Waste Management Association, Pittsburgh, PA, pp. 263-265.
- Gosz, J.R., C.L. Dahm, and P.G. Risser. 1988. Long-Path FTIR Measurement of Atmospheric Trace Gas Concentrations. *Ecology* 69(5):1326-1330.
- Gosz, J.R., D.I. Moore, C.N. Dahm, and S. Hofstadler. 1990. Field Testing Long-Path Fourier Transform Infrared (FTIR) Spectroscopy for Measurements of Atmospheric Gas Concentrations. *Remote Sens. Environ.* 32:103-110.
- Grant, W.B., Kagann, R.H., and W.A. McClenny. 1992. Optical Remote Measurement of Toxic Gases. *J. Air Waste Manage. Assoc.* 42(1):18-30.

- Grant, W.B., and R.T. Menzies. 1983. A Survey of Laser and Selected Optical Systems for Remote Measurement of Pollutant Gas Concentrations. *J. Air Pollut. Control Assoc.* 33(3):187-194.
- Grasselli, J.G., P.R. Griffiths, and R.W. Hannah. 1982. Criteria for Presentation of Spectra from Computerized IR Instruments. *Appl. Spectrosc.* 36(2):87-91.
- Gravel, D., A. Rilling, V. Karfik, and M. Schmaeh. 1997. Fourier Transform Infrared Spectrometry—A Mature Analytical Method for Industrial-Level Emission Monitoring. *Proceedings of the AWMA Annual Meeting in Toronto, Canada, Air & Waste Management Association, Pittsburgh, PA.*
- Green, M., Seiber, J.N., and Biermann, H.W. 1991. In Situ Measurement of Methyl Bromide in Indoor Air Using Long-Path FTIR Spectroscopy. *Measurement of Atmospheric Gases, Proc. SPIE* 1433:270-274.
- Green, M., H.W. Biermann, and J.N. Seiber. 1992. Long-Path Fourier Transform Infrared Spectroscopy for Post-Fumigation Indoor Air Measurements. *Analisis* 20(8):455-460.
- Green, M., J.N. Seiber, and H.W. Biermann. 1993. In-Situ Measurements of Volatile Toxic Organics in Indoor Air Using Long-Path Fourier Transform Infrared Spectroscopy. *Proc. SPIE* 1716:157-64.
- Griffiths, P.R., and J.A. de Haseth. 1986. *Fourier Transform Infrared Spectrometry*, John Wiley and Sons, New York.
- Griffiths, P.R., A.R.H. Cole, P.L. Hanst, W.J. Lafferty, R.J. Obremski, J.H. Shaw, and R.N. Jones. 1983. Specifications for Infrared Reference Spectra of Molecules in the Vapor Phase. *Appl. Spectrosc.* 37(5):458-463.
- Griffiths, P.R., R.L. Richardson, D. Qin, and C. Zhu. 1995. Open-Path Atmospheric Monitoring with a Low-Resolution FT-IR Spectrometer. *Proceedings of Optical Sensing for Environmental and Process Monitoring* (O.A. Simpson, Ed.). VIP-37, Air & Waste Management Association, Pittsburgh, PA, pp. 274-284.
- Griggs, M., and C.B. Ludwig. 1978. Legal Aspects of Remote Sensing and Air Enforcement. *J. Air Pollut. Control Assoc.* 28(2):119-122.
- Grim, L.B., Th.C. Gruber, Jr., and J. Ditillo. 1996. Algorithm development for passive FTIR. *Proceedings of the 1995 AWMA/SPIE Specialty Conf in San Francisco*. Air & Waste Management Association, Pittsburgh, PA.
- Grosjean, D., E.C. Tuazon, and E. Fujita. 1990. Ambient Formic Acid in Southern California Air: A Comparison of Two Methods, Fourier Transform Infrared Spectroscopy and Alkaline Trap-Liquid Chromatography with UV Detection. *Environ. Sci. Technol.* 24(1):144-146.
- Haaland, D.M. 1990. Multivariate Calibration Methods Applied to Quantitative FT-IR Analyses. *Practical Fourier Transform Infrared Spectroscopy—Industrial and Laboratory Chemical Analysis*, J.R. Ferrar and K. Krishnan, Eds., Academic Press, San Diego, CA, pp. 396-468.
- Haaland, D.M., and R.G. Easterling. 1980. Improved Sensitivity of Infrared Spectroscopy by the Application of Least Squares Methods. *Appl. Spectrosc.* 34(5):539-548.
- Haaland, D.M., and R.G. Easterling. 1982. Application of New Least-Squares Methods for the Quantitative Infrared Analysis of Multicomponent Samples. *Appl. Spectrosc.* 36(6):665-673.

- Haaland, D.M., R.G. Easterling, and D.A. Vopicka. 1985. Multivariate Least-Squares Methods Applied to the Quantitative Spectral Analysis of Multicomponent Samples. *Appl. Spectrosc.* 39(1):73-84.
- Hall, M.J., D. Lucas, and C.P. Koshland. 1991. Measuring Chlorinated Hydrocarbons in Combustion by Use of Fourier Transform Infrared Spectroscopy. *Environ. Sci. Technol.* 25(2):260-267.
- Halliday, D. and R. Resnick. 1974. *Fundamental of Physics*. John Wiley and Sons, New York.
- Hammaker, R.M., W.G. Fateley, C.T. Chaffin, T.L. Marshall, M.D. Tucker, V.D. Makepeace, and J.M. Poholarz. 1993. FT-IR Remote Sensing of Industrial Atmosphere for Spatial Characterization. *Appl. Spectrosc.* 47:1471-1475.
- Hanst, P.L. 1970. Infrared Spectroscopy and Infrared Lasers in Air Pollution Research and Monitoring. *Appl. Spectrosc.* 24(2):161-174.
- Hanst, P.L. 1971. Mechanism of Peroxyacetyl Nitrate Formation. *J. Air Pollut. Control Assoc.* 21(5):269-271.
- Hanst, P.L. 1971. Spectroscopic Methods for Air Pollution Measurement. *Advances in Environmental Science and Technology*, Vol. 2 (J.N. Pitts, Jr., and R.L. Metcalf, Eds.), Wiley-Interscience, New York, pp. 91-213.
- Hanst, P.L. 1976. Optical Measurement of Atmospheric Pollutants: Accomplishments and Problems. *Opt. Quantum Electron.* 8:87-93.
- Hanst, P.L. 1978. Air Pollution Measurement by Fourier Transform Spectroscopy. *Appl. Opt.* 17(9):1360-1366.
- Hanst, P.L. 1978. Noxious Trace Gases in the Air. Part I. Photochemical Smog. *Chemistry* 51(1):8-15.
- Hanst, P.L. 1978. Noxious Trace Gases in the Air. Part II. Halogenated Pollutants. *Chemistry* 51(2):6-12.
- Hanst, P.L. 1979. Pollution: Trace Gas Analysis. *Fourier Transform Infrared Spectroscopy. Applications to Chemical Systems*, Vol. 2 (J.R. Ferraro and L.J. Basile, Eds.), Academic Press, New York, pp. 79-110.
- Hanst, P.L. 1986. IR-Spectroscopy of the Atmosphere. *Fresenius Z. Anal. Chem.* 324(6):579-588(209-218).
- Hanst, P.L. 1989. Infrared Analysis of Engine Exhausts: Methyl Nitrite Formation from Methanol Fuel. *Spectroscopy* 4(9):33-38.
- Hanst, P.L. 1991. Earliest Spectroscopic Studies of Polluted Air: A Tribute to Dr. Edgar R. Stephens. *Proceedings of the 1991 U.S. EPA/A&WMA International Symposium on the Measurement of Toxic and Related Air Pollutants*, Air & Waste Management Association, Pittsburgh, PA, pp. 37-38.
- Hanst, P.L. 1991. Analyzing Air for PPB Concentrations of Trace Gases, Using Spectral Subtraction. *Proceedings of the 1991 U.S. EPA/A&WMA International Symposium on the Measurement of Toxic and Related Air Pollutants*, Air & Waste Management Association, Pittsburgh, PA, pp. 83-96.
- Hanst, P.L. 1992. Infrared Spectra for Quantitative Analysis of Gases. *SP-81 Optical Remote Sensing. Applications to Environmental and Industrial Safety Problems*, Air & Waste Management Association, Pittsburgh, PA, pp. 490-510.

- Hanst, P.L., and B.W. Gay, Jr. 1977. Photochemical Reactions Among Formaldehyde, Chlorine, and Nitrogen Dioxide in Air. *Environ. Sci. Technol.* 11(12):1105-1109.
- Hanst, P.L., and B.W. Gay, Jr. 1983. Atmospheric Oxidation of Hydrocarbons: Formation of Hydroperoxides and Peroxyacids. *Atmos. Environ.* 17(11):2259-2265.
- Hanst, P.L., and J.A. Morreal. 1968. Detection and Measurement of Air Pollutants by Absorptions of Infrared Radiation. *J. Air Pollut. Control Assoc.* 18(11):754-759.
- Hanst, P.L., A.S. Lefohn, and B.W. Gay, Jr. 1973. Detection of Atmospheric Pollutants at Parts-per-Billion Levels by Infrared Spectroscopy. *Appl. Spectrosc.* 27(3):188-198.
- Hanst, P.L., L.L. Spiller, D.M. Watts, J.W. Spence, and M.F. Miller. 1975. Infrared Measurement of Fluorocarbons, Carbon Tetrachloride, Carbonyl Sulfide, and Other Atmospheric Trace Gases. *J. Air Pollut. Control Assoc.* 25(12):1220-1226.
- Hanst, P.L., J.A. Cooney, E. Hesstvedt, P.L. Kelly, J.J. Kennedy, J.E. Lovelock, C.K.N. Patel, and G. Wang. 1976. Stratospheric Chemistry and Measurement Techniques. *Opt. Quantum Electron.* 8:187-191.
- Hanst, P.L., J.W. Spence, and M. Miller. 1977. Atmospheric Chemistry of *N*-Nitroso Dimethylamine. *Environ. Sci. Technol.* 11(4):403-405.
- Hanst, P.L., N.W. Wong, and J. Bragin. 1982. A Long-Path Infra-Red Study of Los Angeles Smog. *Atmos. Environ.* 16(5):969-981.
- Harris, D.B., and E. L. Thompson. 1998. Evaluation of Ammonia Emissions from Swine Operations in North Carolina. EPA/600/A-98/142. U.S. Environmental Protection Agency.
- Hashmoneh, R.A., Y. Mamane, Y. Benayahu, and A. Cohen. 1996. Estimation of Emission Rates from Non-homogeneous Fugitive Sources Using Open Path FTIR and Inversion Techniques. *Proceedings of the 1995 SPIE/AWMA Specialty Conference in San Francisco.* Air & Waste Management Association, Pittsburgh, PA.
- Haus, R., and K. Schaefer. 1992. Modeling of Smoke Stack Emissions for FTIR Remote Sensing. *Proc. SPIE* 1575:328-330.
- Haus, R., K. Schäfer, D. Wehner, H. Bittner, and H. Mosebach. 1992. Remote Sensing of Air Pollution by Mobile Fourier-Transform Spectroscopy: Modeling and First Results of Measurements. *SP-81 Optical Remote Sensing. Applications to Environmental and Industrial Safety Problems,* Air & Waste Management Association, Pittsburgh, PA, pp. 67-75.
- Haus, R., K. Schäfer, J. Heland, H. Mosebach, and T. Eisenmann. 1993. FTIS in Environmental Research: Mobile Remote Sensing of Air Pollution. *Proc. SPIE* 2089:318-319.
- Haus, R., K. Schäfer, W. Bautzer, H. Mosebach, H. Bittner, and T. Eisenmann. 1994. Mobile FTIS-Monitoring of Air Pollution. *Appl. Opt.* 33(24):5682-5689.
- Haus, R., K. Schaefer, J. Hughes, J. Heland, and W. Bautzer. 1995. FTIR Remote Sensing of Smoke Stack and Test Flare Emissions. *Proc. SPIE* 2506:45-54.
- Heland, J., K. Schaefer and R. Haus. 1995. FTIR Emission Spectroscopy and Modeling of

- Radiative Transfer Layered Plume: Analysis of Aircraft Engine Exhausts. *Proc. SPIE* 236.
- Heland, J., and K. Schaefer. 1997. Analysis of Aircraft Exhausts with Fourier Transform Infrared Emission Spectroscopy. *J. Eng. Appl. Sci.* 36(21):4922-4931.
- Herget, W.F. 1979. Air Pollution: Ground-Based Sensing of Source Emissions. *Fourier Transform Infrared Spectroscopy. Applications to Chemical Systems, Vol. 2* (J.R. Ferraro and L.J. Basile, Eds.), Academic Press, New York, pp. 111-127.
- Herget, W.F. 1981. Measurement of Gaseous Pollutants Using a Mobile Fourier Transform Infrared (FTIR) System. *Proc. SPIE* 289:449-456.
- Herget, W.F. 1982. Analysis of Gaseous Air Pollutants Using a Mobile FTIR System. *Am. Lab.* 14(12):72-78.
- Herget, W.F. 1982. Remote and Cross-Stack Measurement of Stack Gas Concentrations Using a Mobile FT-IR System. *Appl. Opt.* 21(4):635-641.
- Herget, W.F., and J.D. Brasher. 1979. Remote Measurement of Gaseous Pollutant Concentrations Using a Mobile Fourier Transform Interferometer System. *Appl. Opt.* 18(20):3404-3420.
- Herget, W.F., and J.D. Brasher. 1980. Remote Fourier Transform Infrared Air Pollution Studies. *Opt. Eng.* 19(4):508-514.
- Herget, W.F., and W.D. Conner. 1977. Instrumental Sensing of Stationary Source Emissions. *Environ. Sci. Technol.* 11(10):962-967.
- Herget, W.F., and S.P. Levine. 1986. Fourier Transform Infrared (FTIR) Spectroscopy for Monitoring Semiconductor Process Gas Emissions. *Appl. Ind. Hyg.* 1(2):110-112.
- Herget, W.F., and J.W. Muirhead. 1970. Infrared Spectral Absorption Coefficients for Water Vapor. *J. Opt. Soc. Am.* 60(2):180-183.
- Herget, W.F., J.A. Jahnke, D.E. Burch, and D.A. Gryvnak. 1976. Infrared Gas-Filter Correlation Instrument for In Situ Measurement of Gaseous Pollutant Concentrations. *Appl. Opt.* 15(5):1222-1228.
- Herres, W., and J. Gronholz. 1984. Understanding FT-IR Data Processing Part 1: Data Acquisition and Fourier Transformation. *Computer Applications in the Laboratory* 4:216-220.
- Hilton, M., A.H. Lettington, and I.M. Mills. 1994. Passive Remote Detection of Atmospheric Pollutants Using Fourier Transform Infrared Spectroscopy. *SP-89 Optical Sensing for Environmental Monitoring, Air & Waste Management Association, Pittsburgh, PA*, pp. 134-144.
- Hirshfeld, T. 1979. Quantitative FT-IR: A Detailed Look at the Problems Involved. *Fourier Transform Infrared Spectroscopy. Applications to Chemical Systems, Vol. 2* (J.R. Ferraro and L.J. Basile, Eds.), Academic Press, New York, pp. 193-242.
- Hodgeson, J.A., W.A. McClenny, and P.L. Hanst. 1973. Air Pollution Monitoring by Advanced Spectroscopic Techniques. *Science* 182:248-258.
- Hommrich, D.N., R.L. Kump, and R.H. Kagann. 1992. An Evaluation of Remote Sensing FTIR vs. Point Source Sample Collection and Analysis. *SP-81 Optical Remote Sensing. Applications to Environmental and Industrial Safety Problems, Air & Waste Management Association, Pittsburgh, PA*, pp. 207-211.

- Hook, S.J., and A.B. Kahle. 1996. Micro Fourier Transform Interferometer (muFTIR)—A New Field Spectrometer for Acquisition of Infrared Data of Natural Surfaces. *Remote Sens. Environ.* 56(3):172-181.
- Horlick, G. 1968. Introduction to Fourier Transform Spectroscopy. *Appl. Spectrosc.* 22:617-626.
- Hudson, J.L., J. Arello, M.J. Thomas, H.E. Kimball, T.T. Holloway, B.J. Fairless, M.L. Spartz, M.R. Witkowski, T.L. Marshall, C.P. Chaffin, R.M. Hammaker, W.G. Fateley, and D.F. Gurka. 1991. Remote Sensing of Toxic Air Pollutants at a High Risk Point Source Using Open-Path Fourier Transform Infrared Spectroscopy: A Case Study. Paper 91-57.1, *Proceedings of the 84th Annual Meeting and Exhibition*, Air & Waste Management Association, Pittsburgh, PA.
- Hudson, J.L., M.J. Thomas, J. Arello, J.R. Helvig, B.J. Fairless, R.E. Carter, Jr., D.D. Lane, and G.A. Marotz. 1992. An Overview Assessment of the Intercomparability and Performance of Multiple Open-Path FTIR Systems as Applied to the Measurement of Air Toxics. *SP-81 Optical Remote Sensing. Applications to Environmental and Industrial Safety Problems*, Air & Waste Management Association, Pittsburgh, PA, pp. 112-122.
- Hudson, J.L., M.J. Thomas, J. Arello, J.R. Helvig, T.T. Holloway, B.J. Fairless, R.E. Carter, Jr., D.D. Lane, and G.A. Marotz. 1992. The Kansas Open-Path Fourier Transform Infrared Spectrometer Intercomparison Study: A Project Overview. Paper 92-73.08, *Proceedings of the 85th Annual Meeting and Exhibition*, Air & Waste Management Association, Pittsburgh, PA.
- Hull, D., R. Brewer, W. Dieringer, J. Lange, J. Pophal, and R. Spellacy. 1996. Full Perimeter FTIR Fence Line Monitor. *Proc. AWMA/SPIE Specialty Conference in San Francisco*. Air & Waste Management Association, Pittsburgh, PA.
- Hunt, R.N. 1992. Continuous Monitoring of Atmospheric Pollutants by Remote Sensing FTIR. *SP-81 Optical Remote Sensing. Applications to Environmental and Industrial Safety Problems*, Air & Waste Management Association, Pittsburgh, PA, pp. 446-455.
- Hunt, R.N. 1994. Installation of Industrial Bistatic Long-Path FTIR Systems. Paper 807-813, *SP-89 Optical Sensing for Environmental Monitoring*, Air & Waste Management Association, Pittsburgh, PA.
- Hunt, R.N., and P.A. Fuchs. 1995. Applications in Continuous Monitoring of Atmospheric Sensing. *Proc. SPIE* 2365.
- Jenkins, F.A., and H.E. White. 1950. *Fundamentals of Optics*. McGraw-Hill, New York.
- Kagann, R.H., and O.A. Simpson. 1990. Open Path FTIR Measurements of Gaseous Emissions from a Chemical Plant Waste Water Treatment Basin. Paper 90-86-7, *Proceedings of the 83rd Annual Meeting and Exhibition*, Air & Waste Management Association, Pittsburgh, PA.
- Kagann, R.H., and O.A. Simpson. 1992. FTIR Remote Sensor Data from the EPA Region VII FTIR Intercomparison Study. *SP-81 Optical Remote Sensing. Applications to Environmental and Industrial Safety Problems*, Air & Waste Management Association, Pittsburgh, PA, pp. 145-156.
- Kagann, R.H., R. DeSimone, O.A. Simpson, and W.F. Herget. 1990. Remote FTIR Measurement of Chemical Emissions. *Proceedings of the 1990 U.S. EPA/A&WMA International Symposium on the Measurement of Toxic and Related Air Pollutants*, Air & Waste Management Association, Pittsburgh, PA, pp. 244-247.

- Kagann, R.H., O.A. Simpson, G.M. Russwurm, and W.A. McClenny. 1991. New Developments in the FTIR Remote Sensor. Paper 91-57.7, *Proceedings of the 84th Annual Meeting and Exhibition, Air & Waste Management Association, Pittsburgh, PA.*
- Kagann, R.H., and O.A. Simpson. 1992. Comparison of Open Path FTIR Data with Point Samplers in the EPA Region VII FTIR Intercomparison Study. Paper 92-73.09, *Proceedings of the 85th Annual Meeting and Exhibition, Air & Waste Management Association, Pittsburgh, PA.*
- Kagann, R.H., J.G. Jolley, D.S. Shoop, M.R. Hankins, and J.M. Jackson. 1994. Validation of Open-Path FTIR Data at Treatment, Storage, and Disposal Facilities. *SP-89 Optical Sensing for Environmental Monitoring, Air & Waste Management Association, Pittsburgh, PA, pp. 437-442.*
- Kagann, R.H., W.T. Walter, C.D. Wang, D.K. Kotter, and G.J. McManus. 1995. Field Test on Signal Processing Methods for Passive FTIR Remote Sensing Measurements. *Proc. SPIE 2366.*
- Kagan, R.H. 1997. Instrumentation for Optical Remote Sensing. *Proceedings of the 1997 Annual AWMA Meeting in Toronto, Air & Waste Management Association, Pittsburgh, PA.*
- Kert, J. 1992. Remote Sensing of On-Road Vehicle Emissions by an FTIR. *SP-81. Optical Remote Sensing. Applications to Environmental and Industrial Safety Problems, Air & Waste Management Association, Pittsburgh, PA, pp. 325-330.*
- Kirchgessner, D.A., S.D. Piccot, and A. Chadha. 1993. Estimation of Methane Emissions from a Surface Coal Mine Using Open-Path FTIR Spectroscopy and Modeling Techniques. *Chemosphere 26:23-44.*
- Koehler, F.W., and G.W. Small. 1998. Calibration Transfer Results for Automated Detection of Acetone and SF<sub>6</sub> by FTIR Remote Sensing Measurements. *AIP Conf. Proc. 430:231-234.*
- Kricks, R.J., T.R. Minnich, D.E. Pescatore, P.J. Solinski, D. Mickunas, L. Kaelin, O. Simpson, M.J. Czerniawski, and T.H. Pritchett. 1991. Perimeter Monitoring at Lipari Landfill Using Open-Path FTIR Spectroscopy: An Overview of Lessons Learned. Paper 91-57.11, *Proceedings of the 84th Annual Meeting and Exhibition, Air & Waste Management Association, Pittsburgh, PA.*
- Kricks, R.J., R.L. Scotto, T.H. Pritchett, G.M. Russwurm, R.H. Kagann, and D.B. Mickunas. 1992. Quality Assurance Issues Concerning the Operation of Open-Path FTIR Spectrometers. *SP-81 Optical Remote Sensing. Applications to Environmental and Industrial Safety Problems, Air & Waste Management Association, Pittsburgh, PA, pp. 224-231.*
- Kricks, R.J., S.H. Perry, and D.E. Pescatore. 1994. Continued Investigation of an Automated I<sub>0</sub> Generation Technique for Open-Path FTIR Application. *SP-89 Optical Sensing for Environmental Monitoring, Air & Waste Management Association, Pittsburgh, PA, pp. 47-55.*
- Kricks, R.J., and R.L. Scotto, 1997. Update of QA/QC Issues for Field Data. *Proceedings of the 1997 AWMA Meeting in Toronto, Air & Waste Management Association, Pittsburgh, PA.*
- Kroutil, R.T., J.T. Ditillo, and G.W. Small. 1990. Signal Processing Techniques for Remote Infrared Chemical Sensing. *Comput.-Enhanced Anal. Spectrosc., Vol. 2 (H.L.C. Meuzelaar, Ed.), pp. 71-111.*

- Kump, R.L., and D.N. Hommrich. 1992. Fenceline and Ambient Air Monitoring with Open Path FTIR Optical Remote Sensing. *SP-81 Optical Remote Sensing. Applications to Environmental and Industrial Safety Problems*, Air & Waste Management Association, Pittsburgh, PA, pp. 269-272.
- Lacey, R.F. 1989. Elimination of Interferences in Spectral Data. *Appl. Spectrosc.* 43(7):1135-1139.
- LaCrosse, J.P., W.F. Herget, and R.L. Spellicy. 1994. Measurements of Ambient CS<sub>2</sub> Concentrations Using FTIR Spectroscopy. *SP-89 Optical Sensing for Environmental Monitoring*, Air & Waste Management Association, Pittsburgh, PA, pp. 466-491.
- Lamp, T., M. Radmacher, K. Weber, A. Gaertner, R. Nitz, and G. Broeker. 1997. Calibration of an Open Path FTIR Spectrometer for Methane Ethylene and Carbon Monoxide. *Proceedings of the 1997 AWMA Meeting in Toronto*. Air & Waste Management Association, Pittsburgh, PA.
- Lane, D.D., R.E. Carter, Jr., G.A. Marotz, M.J. Thomas, and J.L. Hudson. 1992. The Design of and Results from a Study to Intercompare Open-Path FTIRs and Canisters under Controlled Field Conditions. Paper 92-73.06, *Proceedings of the 85th Annual Meeting and Exhibition*, Air & Waste Management Association, Pittsburgh, PA.
- Lawson, D.R., P.J. Groblicki, D.H. Stedman, G.A. Bishop, and P.L. Guenther. 1990. Emissions from In-Use Motor Vehicles in Los Angeles: A Pilot Study of Remote Sensing and the Inspection and Maintenance Program. *J. Air Waste Manage. Assoc.* 40(8):1096-1105.
- Lengyel, B.A. 1971. *Lasers*, 2nd Ed., Wiley-Interscience, New York.
- Leo, M.R., T.R. Minnich, R.L. Scotto, R. Lute, D.B. Mickunas, and T.H. Pritchett. 1994. Estimation of Hydrocarbon Emission Rates Using Open-Path FTIR Spectroscopy During a Controlled Evaporation Study. *SP-89 Optical Sensing for Environmental Monitoring*, Air & Waste Management Association, Pittsburgh, PA, pp. 639-658.
- Levine, S.P. 1992. Metrological Recommendations for Air-Monitoring Instruments - A Guidance Document. *Am. Ind. Hyg. Assoc. J.* 53(10):673-676.
- Levine, S.P., H-K. Xiao, T. Pritchett, and R.D. Turpin. 1990. Fourier Transform Infrared (FTIR) Spectroscopy for Monitoring Polar and Labile Airborne Gases and Vapors. *Proceedings of the 1991 U.S. EPA/A&WMA International Symposium on the Measurement of Toxic and Related Air Pollutants*, Air & Waste Management Association, Pittsburgh, PA, pp. 176-182.
- Levine, S., H. Xiao, W. Herget, R. Spear, and T. Pritchett. 1991. Remote Sensing (ROSE) FTIR. *Proceedings of the 1991 U.S. EPA/A&WMA International Symposium on the Measurement of Toxic and Related Air Pollutants*, Air & Waste Management Association, Pittsburgh, PA, pp. 707-711.
- Levine, S.P., and G.M. Russwurm. 1994. Fourier Transform Infrared Optical Remote Sensing for Monitoring Airborne Gas and Vapor Contaminants in the Field. *Trends Anal. Chem.* 13(7):258-262.
- Liebhafsky, H.A., and H.G. Pfeiffer. 1953. Beer's Law in Analytical Chemistry. *J. Chem. Educ.* 30(9):450-452.
- Long, G.L. and J.D. Winefordner. 1983. Limit of Detection: A Closer Look at the IUPAC Definition. *Anal. Chem.* 55(7):712A-724A.
- Lord, H.C. 1974. Absorption Spectroscopy Applied to Stationary Source Emissions



- Monitoring. *Analytical Methods Applied to Air Pollution Measurements* (R.K. Stevens and W.F. Herget, Eds.), Ann Arbor Science, Ann Arbor, MI, pp. 233-243.
- Lothian, G.F. 1963. Beer's Law and Its Use in Analysis. *Analyst* 88:678.
- Low, M.J.D., and F.K. Clancy. 1967. Remote Sensing and Characterization of Stack Gases by Infrared Spectroscopy. *Environ. Sci. Technol.* 1(1):73-74.
- Lubin, D., and S.A. Simpson. 1994. The Longwave Emission Signature of Urban Pollution: Radiometric FTIR Measurement. *Geophys. Res. Lett.* 21(1):37-40.
- Luft, K.F. 1943. Über Eine Neue Methode der Registrierenden Gas Analyse Mit Hilfe der Absorption Ultraroter Strahlen Ohne Spektrale Zerlegung. *J. Tech. Phys.* 24:97.
- Lupo, M.J., C.E. Magnuson, R.L. Shriver, F.K. Hamilton, R.L. Scotto, T.R. Minnich, D.E. Pescatore, R.H. Kagann, O.A. Simpson, S.E. McLaren, and D.H. Stedman. 1991. Air Pathway Monitoring for a Land Ban No-Migration Petition. Paper 91-57.4, *Proceedings of the 84th Annual Meeting and Exhibition*, Air & Waste Management Association, Pittsburgh, PA.
- Lupo, M.J., C.E. Magnuson, Z. Wang, G.B. Evans, Jr., R.L. Shiver, T.R. Minnich, R.L. Scotto, D.E. Pescatore, and R.J. Kricks. 1991. The Suitability of Open Path Air Monitoring for RCRA Application: A Case Study. Part I. Project Overview. *Proceedings of the 1991 U.S. EPA/A&WMA International Symposium on the Measurement of Toxic and Related Air Pollutants*, Air & Waste Management Association, Pittsburgh, PA, pp. 685-690.
- Lute, R., R.J. Kricks, D.E. Pescatore, and P.J. Solinski. 1992. Effects of Atmospheric Water Vapor on Open-Path FTIR Spectroscopy Data. *SP-81 Optical Remote Sensing. Applications to Environmental and Industrial Safety Problems*, Air & Waste Management Association, Pittsburgh, PA, pp. 425-433.
- Mellqvist, J., D.W. Arlander, B. Galle, and B. Berqvist. 1995. *Measurements of Industrial Fugitive Emissions by the FTIR Tracer Method*. IVL Report B 1214, Swedish Environmental Research Institute, Goteborg, Sweden.
- Marotz, G.A., R.E. Carter, Jr., and D.D. Lane. 1992. Sampling Design and Protocols Used in a Recent Study of Long-Path FTIR and Canister Compound Detection and Estimation Under Controlled Field Conditions. *SP-81 Optical Remote Sensing. Applications to Environmental and Industrial Safety Problems*, Air & Waste Management Association, Pittsburgh, PA, pp. 123-132.
- Marshall, A.G. and F.R. Verdun. 1990. *Fourier Transforms in NMR, Optical, and Mass Spectrometry*, Elsevier, Amsterdam.
- Marshall, T.L., C.T. Chaffin, R.M. Hammaker, and W.G. Fateley. 1994. An Introduction to Open-Path FT-IR Atmospheric Monitoring. *Environ. Sci. Technol.* 28:224A-232A.
- Marshall, T.L., C.T. Chaffin, V.D. Makepeace, R.M. Hoffman, R.M. Hammaker, W.G. Fateley, P. Saarinen, and J. Kauppinen. 1994. Investigation of the Effects of Resolution on the Performance of Classical Least-Squares (CLS) Spectral Interpretation Programs When Applied to Volatile Organic Compounds (VOCs) of Interest in Remote Sensing Using Open-Air Long-Path Fourier Transform Infrared (FT-IR) Spectrometry. *J. Mol. Struct.* 324:19-28.
- Martino, P.A. 1992. A Comparison of Remote Sensing and Point Sampling Measurements of Aromatic Hydrocarbon Emissions. *SP-81 Optical Remote Sensing. Applications to Environmental and Industrial*

- Safety Problems*, Air & Waste Management Association, Pittsburgh, PA, pp. 212-223.
- McCauley, C.L., M.J. Czerniawski, R.H. Kagann, and O.A. Simpson. 1992. Development of a User-Friendly Intelligent Spectroscopic Computer System: A Case Study. *SP-81 Optical Remote Sensing. Applications to Environmental and Industrial Safety Problems*, Air & Waste Management Association, Pittsburgh, PA, pp. 456-463.
- McClenny, W.A., and G.M. Russwurm. 1978. Laser-Based, Long Path Monitoring of Ambient Gases—Analysis of Two Systems. *Atmos. Environ.* 12:1443-1453.
- McClenny, W.A., W.F. Herget, and R.K. Stevens. 1974. Comparative Review of Open-Path Spectroscopic Absorption Methods for Ambient Air Pollutants. *Analytical Methods Applied to Air Pollution Measurements* (R.K. Stevens and W.F. Herget, Eds.), Ann Arbor Science, Ann Arbor, MI, pp. 107-120.
- McClenny, W.A., Baumgardner, R.E., Jr., Baity, F.W., Jr., and R.A. Gray. 1974. Methodology for Comparison of Open-Path Monitors with Point Monitors. *J. Air Pollut. Control Assoc.* 24(11):1044-1046.
- McClenny, W.A., G.M. Russwurm, M.W. Holdren, A.J. Pollack, J.D. Pleil, J.L. Varns, J.D. Mulik, K.D. Oliver, R.E. Berkley, D.D. Williams, K.J. Krost, and W.T. McLeod. 1991. *Superfund Innovative Technology Evaluation. The Delaware SITE Study, 1989*. EPA 600/3-91/071. U.S. Environmental Protection Agency, Research Triangle Park, NC.
- McLaren, S.E., J.W. Hannigan, D.L. New, and D.H. Stedman. 1991. Direct Measurement of Freeway Emissions Using Long-Path Spectroscopy. *Proceedings of the 1991 U.S. EPA/A&WMA International Symposium on the Measurement of Toxic and Related Air Pollutants*, Air & Waste Management Association, Pittsburgh, PA, pp. 741-746.
- McLaren, S.E., D.H. Stedman, P.D. Greenlaw, R.J. Bath, and R.D. Spear. 1992. Comparison of an Open Path UV and FTIR Spectrophotometer. Paper 92-73.10, *Proceedings of the 85th Annual Meeting and Exhibition*, Air & Waste Management Association, Pittsburgh, PA.
- McNesby, K.L., C.F. Chabalowski, and R.A. Fifer. 1991. Approximation to True Peak Absorbance from Observed Peak Absorbance for Gas Phase Fourier Transform Spectroscopy. *Appl. Opt.* 30(4):378-379.
- Michelson, A.A. 1881. The Relative Motion of the Earth and the Luminiferous Ether. *Am. J. Sci.* 22(3):120-129.
- Michelson, A.A. 1882. Interference Phenomena in a New Form of Refractometer. *Phil. Mag.* 13:236-242.
- Michelson, A.A. 1891. Visibility of Interference-Fringes in the Focus of a Telescope. *Phil. Mag.* 31:256-259.
- Minnich, T.R., R.L. Scotto, and T.H. Pritchett. 1990. Remote Optical Sensing of VOCs: Application to Superfund Activities. *Proceedings of the 1990 U.S. EPA/A&WMA International Symposium on the Measurement of Toxic and Related Air Pollutants*, Air & Waste Management Association, Pittsburgh, PA, pp. 928-936.
- Minnich, T.R., M.R. Leo, R.L. Scotto, M.J. Czerniawski, R.H. Kagann, and O.A. Simpson. 1991. A Software Package for Assessing Downwind Air Quality Impact in Real Time Based on Open-Path FTIR Measurement Data. *Proceedings of the 1991 U.S. EPA/A&WMA International Symposium on the Measurement of Toxic and Related Air*

- Pollutants*, Air & Waste Management Association, Pittsburgh, PA, pp. 704-706.
- Minnich, T.R., R.L. Scotto, M.R. Leo, B.C. Sanders, S.H. Perry, and T.H. Pritchett. 1992. A Practical Methodology Using Open-Path FTIR Spectroscopy to Generate Gaseous Fugitive-Source Emission Factors at Industrial Facilities. *SP-81 Optical Remote Sensing. Applications to Environmental and Industrial Safety Problems*, Air & Waste Management Association, Pittsburgh, PA, pp. 513-518.
- Minnich, T.R., R.L. Scotto, R.H. Kagann, and O.A. Simpson. 1990. Optical Remote Sensors Ready to Tackle Superfund, RCRA Emissions Monitoring Tasks. *Hazmat World* 3:42.
- Minnich, T.R., and R.L. Scotto. 1994. The Role of Open-Path FTIR Spectroscopy in the Development of a Successful Accidental Release Detection Program. *SP-89 Optical Sensing for Environmental Monitoring*, Air & Waste Management Association, Pittsburgh, PA, pp. 340-348.
- Mosebach, H., T. Eisenmann, Y. Schulz-Spahr, I. Neureither, H. Bittner, H. Rippel, K. Schäfer, D. Wehner, and R. Haus. 1992. Remote Sensing of Smoke Stack Emissions Using a Mobile Environmental Laboratory. *Proc. SPIE* 1717:149-158.
- Muthusubramanian, P., and S.P.M. Deborrah. 1989. Design Considerations of a 32 m Optical Path Multiple Reflection Cell for Air Pollution Studies. *Indian J. Environ. Prot.* 9(2):144-146.
- Nelson, C.M., K.S. Knight, A.S. Bonanno, M.A. Serio, P.R. Solomon, and M.A. Halter. 1994. On-Line FT-IR Analysis of Fossil Fuel-Fired Power Plants. *SP-89 Optical Sensing for Environmental Monitoring*, Air & Waste Management Association, Pittsburgh, PA, pp. 826-840.
- Nicolet Analytical Instruments. 1986. *FT-IR Theory*. Nicolet Analytical Instruments, Madison, WI.
- Niki, H., and P.D. Maker. 1990. Atmospheric Reactions Involving Hydrocarbons: Long Path-FTIR Studies. *Adv. Photochem.* 15: 69-137.
- Nyden, M.R., W. Grosshandler, D. Lowe, R. Harris, and E. Braun. 1994. Application of FTIR Remote Sensing Spectroscopy in Environmental Impact Assessments of Oil Fires. *SP-89 Optical Sensing for Environmental Monitoring*, Air & Waste Management Association, Pittsburgh, PA, pp. 767-779.
- Oppenheimer, C., P. Francis, M. Burton, A.J.H. Maciejewski, and L. Boardman. 1998. Remote Measurement of Volcanic Gases by Fourier Transform Infrared Spectroscopy. *Appl. Phys. B.* 76(4):505-515.
- Paine, R.J., J.O. Zwicker, and H. Feldman. 1997. Project OPTEx: Field Study at a Petrochemical Facility to Assess Optical Remote Sensing and Dispersion Modeling Techniques. *Proceedings of the AWMA Annual Meeting in Toronto*, Air & Waste Management Association, Pittsburgh, PA.
- Park, D.Y., S. Levine, and G.M. Russwurm. 1998. Fourier Transform Infrared Optical Remote Sensing. *Encyclopedia of Environmental Analysis and Remediation*. Vol.7, Chapter 7, pp. 4137-4149.
- Pawloski, J.N. and D.G. Iverson. 1998. The Use of Optical Remote Sensing to Monitor Facility Releases. *Hydrocarbon Process.* 77(9) September.
- Penner, S.S. 1959. *Quantitative Molecular Spectroscopy and Gas Emissivities*. Addison-Wesley, Reading, MA.

- Perry, S.H., P.L. McKane, D.E. Pescatore, A.E. Dubois, and R.J. Kricks. 1996. Maximizing the Use of Open-Path FTIR for 24 Hour Monitoring Around the Process Area of an Industrial Chemical Facility. *Proceedings of the AWMA Specialty Conference in San Francisco*, Air & Waste Management Association, Pittsburgh, PA.
- Pescatore, D.E., S.H. Perry, R.J. Kricks, and G.R. Pollack. 1994. Use of Open-Path FTIR Spectroscopy to Investigate Unknown Airborne Contaminants at a Sludge Dewatering Facility. *SP-89 Optical Sensing for Environmental Monitoring*, Air & Waste Management Association, Pittsburgh, PA, pp. 93-104.
- Pfeiffer, H.G., and H.A. Liebhafsky. 1951. The Origins of Beer's Law. *J. Chem. Educ.* 28:123-125.
- Phillips, B. and Roy Brandon. 1993. FTIR Remote Sensing Data Reduction Technique for Elevated Temperature Gas Emissions from an Aluminum Smelting Plant. *Proceedings AWMA Annual Meeting*. Air & Waste Management Association, Pittsburgh, PA.
- Phillips, B., D. Brown, G.M. Russwurm, J. Childers, E. Thompson, and L.T. Lay, 1996. Innovative Open-Path FTIR Data Reduction Algorithm. *Proceedings of the AWMA Specialty Conference in San Francisco*, Air & Waste Management Association, Pittsburgh, PA.
- Phillips, B., R. Moyers, and L.T. Lay. 1995. Improved FTIR Open-Path Remote Sensing Data Reduction. *Proceedings of the AWMA Specialty Conference in San Francisco*, Air & Waste Management Association, Pittsburgh, PA.
- Piccot, S.D., A. Chadha, D.A. Kirchgessner, R. Kagann, M.J. Czerniawski, and T. Minnich. 1991. Measurement of Methane Emissions in the Plume of a Large Surface Coal Mine Using Open-Path FTIR Spectroscopy. Paper 91-57.6, *Proceedings of the 84th Annual Meeting and Exhibition*, Air & Waste Management Association, Pittsburgh, PA.
- Piccot, S.D., D.A. Kirchgessner, S.S. Masemore, W.F. Herget, and E. Ringler. 1994. Validation of a Method for Estimating Pollution Emission Rates Using Open-Path FTIR Spectroscopy and Modeling Techniques. *SP-89 Optical Sensing for Environmental Monitoring*, Air & Waste Management Association, Pittsburgh, PA, pp. 322-339.
- Piccot, S.D., S.S. Masemore, E.S. Ringler, S. Srinivasan, D.A. Kirchgessner, and W.F. Herget. 1994. Validation of a Method for Estimating Pollution Emission Rates from Area Sources Using Open-Path FTIR Spectroscopy and Dispersion Modeling Techniques. *J. Air Waste Manage. Assoc.* 44:271-279.
- Pitts, J.N., B.J. Finlayson-Pitts, and A.M. Winer. 1977. Optical Systems Unravel Smog Chemistry. *Environ. Sci. Technol.* 11(6):568-573.
- Plummer, G.M. 1994. Current and Future Spectroscopic Emission Test Method Development Topics. *SP-89 Optical Sensing for Environmental Monitoring*, Air & Waste Management Association, Pittsburgh, PA, pp. 492-502.
- Polak, M.L., J.L. Hall, G.J. Sherer, and K.C. Herr. 1996. *Proceedings of the AWMA Specialty Conference in San Francisco*, Air & Waste Management Association, Pittsburgh, PA.
- Powell, J.R., F.M. Wasacz, and R.J. Jakobsen. 1986. An Algorithm for the Reproducible Spectral Subtraction of Water from the FT-IR Spectra of Proteins in Dilute

- Solutions and Adsorbed Monolayers. *Appl. Spectrosc.* 40(3):339-344.
- Prengle, H.W., Jr., C.A. Morgan, C-S. Fang, L-K. Huang, P. Campani, and W.W. Wu. 1973. Infrared Remote Sensing and Determination of Pollutants in Gas Plumes. *Environ. Sci. Technol.* 7(5):417-423.
- Pruitt, G.R. 1992. Status of Cryogenic Coolers for Remote Sensing Applications. *SP-81 Optical Remote Sensing. Applications to Environmental and Industrial Safety Problems*, Air & Waste Management Association, Pittsburgh, PA, pp. 313-324.
- Reid, S.A., J.I.L. Hughes, P.T. Roberts, I. Archibald, and K. Gregory. 1994. Development of Open Path Systems for Emission Rate Measurements. *SP-89 Optical Sensing for Environmental Monitoring*, Air & Waste Management Association, Pittsburgh, PA, pp. 305-321.
- Rennilson, J.J. 1980. Retroreflection Measurements: A Review. *Appl. Opt.* 19:1234.
- Ropertz, A., T. Lamp, K. Weber, M. Douard, A. Gaertner, and R. Nitz. 1997. Calibration of High Resolution OP-FTIR Spectrometer Combined with an Adjustable 100 m Multipass Cell. *Proc SPIE* 3107:137-147.
- Rossi, B. 1957. *Optics*. Addison-Wesley Publishing Company, Inc., Reading, MA.
- Russwurm, G.M. 1992. Quality Assurance, Water Vapor, and the Analysis of FTIR Data. Paper 92-73.03, *Proceedings of the 85th Annual Meeting and Exhibition*, Air & Waste Management Association, Pittsburgh, PA.
- Russwurm, G.M. 1992. Quality Assurance and the Effects of Spectral Shifts and Interfering Species in FTIR Analysis. *SP-81 Optical Remote Sensing. Applications to Environmental and Industrial Safety Problems*, Air & Waste Management Association, Pittsburgh, PA, pp. 105-111.
- Russwurm, G.M. 1994. A Technique for the Quantitative Comparison of FT-IR Spectra. *SP-89 Optical Sensing for Environmental Monitoring*, Air & Waste Management Association, Pittsburgh, PA, pp. 15-25.
- Russwurm, G.M. 1997. Long-Path Open-Path Fourier Transform Infrared Monitoring of Atmospheric Gases. Compendium Method TO-16. *Proc. SPIE* 3107.
- Russwurm, G.M. 1997. Methodological Questions in the Application of Spectroscopic Techniques. *Proc. SPIE* 3107.
- Russwurm G.M. 1997. Quality Assurance/Quality Control Issues in Open-Path FTIR Monitoring. *Proc. SPIE* 3107.
- Russwurm, G.M., and J.W. Childers. 1994. An Overview of the Fourier Transform Infrared Remote Sensing Technique. *Environ. Lab.* June/July:15-18.
- Russwurm, G.M., and J.W. Childers. 1995. FT-IR Spectrometers Perform Environmental Monitoring. *Laser Focus World*, April.
- Russwurm, G.M. and J.W. Childers. 1996. Compendium Method TO-16: Long Path Open Path Fourier Transform Infrared Method for Monitoring Ambient Air. *Proceedings of the 89th Annual Meeting & Exhibition of the Air & Waste Management Association*. Paper 96-MP5.04, Air & Waste Management Association, Pittsburgh, PA.
- Russwurm, G.M., and J.W. Childers. 1997. Quality Assurance/Quality Control Issues in Open-Path FT-IR Monitoring. *Proc. SPIE* 3107.
- Russwurm, G.M., and W.A. McClenny. 1990. A Comparison of FTIR Open Path Ambient Data with Method TO-14 Canister

- Data. *Proceedings of the 1990 U.S. EPA/A&WMA International Symposium on the Measurement of Toxic and Related Air Pollutants*, Air & Waste Management Association, Pittsburgh, PA, pp. 248-253.
- Russwurm, G.M., and B. Phillips. 1998. Uncertainties in FTIR Data Due to a Nonlinear Response. Presented at the SPIE Specialty Conference on Environmental Monitoring and Remediation Techniques, Boston, November.
- Russwurm, G.M., R.H. Kagann, O.A. Simpson, W.A. McClenny, and W.F. Herget. 1991. Long-Path FTIR Measurements of Volatile Organic Compounds in an Industrial Setting. *J. Air Waste Manage. Assoc.* 41(8):1062-1066.
- Russwurm, G.M., R.H. Kagann, O.A. Simpson, and W.A. McClenny. 1991. Use of a Fourier Transform Spectrometer as a Remote Sensor at Superfund Sites. *Proc. SPIE* 1433:302-314.
- Sandridge, R.L. 1994. Calibration of Bistatic Long-Path FTIR Monitoring Systems. *SP-89 Optical Sensing for Environmental Monitoring*, Air & Waste Management Association, Pittsburgh, PA, pp. 255-262.
- Schäfer, K., R. Haus, D. Wehner, and H. Mosebach. 1992. Modelling of Radiative Transfer for FTIR Remote Sensing of Smoke Stack Emissions. Paper IU-9B.05, *Waste Management, Proceedings of the 9th World Clean Air Congress*, Air & Waste Management Association, Pittsburgh, PA.
- Schäfer, K., R. Haus, D. Wehner, H. Mosebach, H. Bittner, and N. Neureither. 1992. Fourier-Transform-Infrared-Spectroscopy of Air Pollution by a Mobile System. *Proceedings of the International Symposium on Environmental Contamination in Central and Eastern Europe*, pp. 843-845.
- Schäfer, K., R. Haus, and J. Heland. 1994. Measurements of Gaseous Compounds from Emissions Sources and in Ambient Air by Fourier Transform Infrared Spectroscopy: Method and Results of FTIS-MAPS. *SP-89 Optical Sensing for Environmental Monitoring*, Air & Waste Management Association, Pittsburgh, PA, pp. 455-465.
- Schäfer K., J. Heland, R. Haus, C. Werner, and F. Koeppe. 1995. Contribution of Remote Sensing for Diagnostics of Aircraft Engine Combustion. *Proc. SPIE* 2506:55-61.
- Schäfer, K., R.Haus, J. Heland, and C. Werner. 1995. Determination of Emission Sources by Remote Sensing. *Proceedings of the 1995 3<sup>rd</sup> International Conference on Air Pollution*, Vol. 2, Comp. Mechanics Inc., Billerica, MA.
- Schäfer, K., R. Haus, and S. Heinz. 1996. Determination of Emission Rates from Diffuse Sources by Ambient FTIR-absorption-spectroscopy and Adapted Dispersion Modeling. *Proceedings of the AWMA Specialty Conferences in San Francisco*, Air & Waste Management Association, Pittsburgh, PA.
- Schlosser, R.L., and R.W. Brandon. 1992. FTIR Remote Sensor Measurements of Hydrogen Fluoride and Other Fugitive Emissions at Aluminum Smelting Facilities. *SP-81 Optical Remote Sensing. Applications to Environmental and Industrial Safety Problems*, Air & Waste Management Association, Pittsburgh, PA, pp. 286-295.
- Scotto, R.L., T.R. Minnich, and M.R. Leo. 1991. A Method for Estimating VOC Emission Rates from Area Sources Using Remote Optical Sensing. *Proceedings of the 1991 U.S. EPA/A&WMA International Symposium on the Measurement of Toxic and Related Air Pollutants*, Air & Waste Management Association, Pittsburgh, PA, pp. 698-703.

- Scotto, R.L., B.C. Sanders, R.H. Kagann, and O.A. Simpson. 1992. Validation of a Gaussian Plume Dispersion Model Based on Data from the Kansas Open-Path FTIR Intercomparison Study. Paper 92-73.04, *Proceedings of the 85th Annual Meeting and Exhibition, Air & Waste Management Association, Pittsburgh, PA.*
- Shepherd, O., A.G. Hurd, R.B. Wattson, H.J.P. Smith, and G.A. Vanasse. 1981. Spectral Measurements of Stack Effluents Using a Double Beam Interferometer with Background Suppression. *Appl. Opt.* 20(22):3972-3980.
- Simonds-Malachowski, M., S.P. Levine, G. Herrin, R.C. Spear, M. Yost, and Z. Yi. 1994. Workplace and Environmental Air Contaminant Concentrations Measured by Open Path Fourier Transform Infrared Spectroscopy: A Statistical Process Control Technique to Detect Changes from Normal Operating Conditions. *J. Air Waste Manage. Assoc.* 44:673-682.
- Simpson, O.A., and R.H. Kagann. 1990. Measurements of Emissions at a Chemical Waste Water Treatment Site with an Open Path Remote Fourier Transform Interferometer. *Proceedings of the 1990 U.S. EPA/A&WMA International Symposium on the Measurement of Toxic and Related Air Pollutants, Air & Waste Management Association, Pittsburgh, PA, pp. 937-940.*
- Small, G.W., R.T. Kroutil, J.T. Ditillo, and W.R. Loerop. 1988. Detection of Atmospheric Pollutants by Direct Analysis of Passive Fourier Transform Infrared Interferograms. *Anal. Chem.* 60(3):264-269.
- Small, G.W., A.C. Harms, R.T. Kroutil, J.T. Ditillo, and W.R. Loerop. 1990. Design of Optimized Finite Impulse Response Digital Filters for Use with Passive Fourier Transform Infrared Interferograms. *Anal. Chem.* 62(17):1768-1777.
- Small, G.W., T.F. Kaltenbach, and R.T. Kroutil. 1991. Rapid Signal Processing Techniques for Fourier Transform Infrared Remote Sensing. *Trends Anal. Chem.* 10(5):149-155.
- Solomon, P.R., P.W. Morrison, Jr., M.A. Serio, R.M. Carangelo, J.R. Markham, S.C. Bates, and J.E. Cosgrove. 1992. Fourier Transform Infrared Spectroscopy for Open-Path Monitoring. *SP 81 Optical Remote Sensing. Applications to Environmental and Industrial Safety Problems, Air & Waste Management Association, Pittsburgh, PA, pp. 479-489.*
- Spartz, M.L., M.R. Witkowski, J.H. Fateley, J.M. Jarvis, J.S. White, J.V. Paukstelis, R.M. Hammaker, W.G. Fateley, R.E. Carter, M. Thomas, D.D. Lane, G.A. Marotz, B.J. Fairless, T. Holloway, J.L. Hudson, and D.F. Gurka. 1989. Evaluation of a Mobile FT-IR System for Rapid VOC Determination. Part 1: Preliminary Qualitative and Quantitative Calibration Results. *Am. Environ. Lab.* 1(2):15-30.
- Spartz, M.L., M.R. Witkowski, J.H. Fateley, R.M. Hammaker, W.G. Fateley, R.E. Carter, M. Thomas, D.D. Lane, B.J. Fairless, T. Holloway, J.L. Hudson, J. Arello, and D.F. Gurka. 1990. Comparison of Long Path FT-IR Data to Whole Air Canister Data from a Controlled Upwind Point Source. *Proceedings of the 1990 EPA/A&WMA International Symposium on the Measurement of Toxic and Related Air Pollutants, Air & Waste Management Association, Pittsburgh, PA, pp. 685-692.*
- Spear, R.D., G.M. Rojek, P.D. Greenlaw, and R.J. Bath. 1991. A Case Study Using Remote Sensing in the Region II Site Assessment FASP Program. *Proceedings of the 1991 U.S. EPA/A&WMA International Symposium on the Measurement of Toxic and Related Air Pollutants, Air & Waste*

- Management Association, Pittsburgh, PA, pp. 729-740.
- Spear, R.D., P. Boone, P.D. Greenlaw, and R.J. Bath. 1991. Standard Field Operating Guidelines for the Determination of Air Toxics in the Region II Site Assessment FASP Program. *Proceedings of the 1991 U.S. EPA/A&WMA International Symposium on the Measurement of Toxic and Related Air Pollutants*, Air & Waste Management Association, Pittsburgh, PA, pp. 712-718.
- Spear, R.D., P. Greenlaw, and R. Bath. 1991. System Selection and Design for the Determination of Air Toxics in the Region II Site Assessment FASP Program. *Proceedings of the 1991 U.S. EPA/A&WMA International Symposium on the Measurement of Toxic and Related Air Pollutants*, Air & Waste Management Association, Pittsburgh, PA, pp. 719-728.
- Spellicy, R.L., W.L. Crow, J.A. Draves, W.F. Buchholtz, and W.F. Herget. 1991. Spectroscopic Remote Sensing: Addressing Requirements of the Clean Air Act. *Spectroscopy* 6(9):24-34.
- Spellicy, R.L., J.A. Draves, W.L. Crow, W.F. Herget, and W.F. Buchholtz. 1992. A Demonstration of Optical Remote Sensing in a Petrochemical Environment. *SP-81 Optical Remote Sensing. Applications to Environmental and Industrial Safety Problems*, Air & Waste Management Association, Pittsburgh, PA, pp. 273-285.
- Spellicy, R.L., J.A. Draves, W. Crow, W.F. Herget, and W. Buchholtz. 1992. A Demonstration of Open-Path Fenceline and Extractive Workplace Monitoring with FTIR and UV-DOAS Systems. Paper 92-73.05, *Proceedings of the 85th Annual Meeting and Exhibition*, Air & Waste Management Association, Pittsburgh, PA.
- Spellicy, R.L., W.F. Herget, and J.A. Draves. 1994. Integrated Stack and Open-Path Measurements of Industrial Facilities Using FTIR. *SP-89 Optical Sensing for Environmental Monitoring*, Air & Waste Management Association, Pittsburgh, PA, pp. 105-122.
- Spellicy, R., and S.E. Hall. 1997. Early Test Results on a FTIR Industrial Process Monitoring System. *Proceedings of the AWMA Annual Meeting in Toronto*. Air & Waste Management Association, Pittsburgh, PA.
- Spellicy, R. 1997. Analytical Methods for Optical Remote Sensing. *Proceedings of the AWMA Annual Meeting in Toronto*. Air & Waste Management Association, Pittsburgh, PA.
- Spence, J.W., and P.L. Hanst. 1978. Oxidation of Chlorinated Ethanes. *J. Air Pollut. Control Assoc.* 28(3):250-253.
- Spence, J.W., P.L. Hanst, and B.W. Gay, Jr. 1976. Atmospheric Oxidation of Methyl Chloride, Methylene Chloride, and Chloroform. *J. Air Pollut. Control Assoc.* 26(10):994-996.
- Spence, J.W., E.O. Edney, and P.L. Hanst. 1978. Peroxychloroformyl Nitrate: Synthesis and Thermal Stability. *Chem. Phys. Lett.* 56(3):478-483.
- Spence, J.W., E.O. Edney, and P.L. Hanst. 1980. Infrared and Ultraviolet Spectral Study of HOCl. *J. Air Pollut. Control Assoc.* 30(1):50-52.
- Stedman, D.H., and S.E. McLaren. 1990. Flux Measurements Using Simultaneous Long Path Ultraviolet and Infrared Spectroscopy. Paper 90-86.6, *Proceedings of the 83rd Annual Meeting and Exhibition*, Air & Waste Management Association, Pittsburgh, PA.



- Stephens, E.R. 1958. Long-Path Infrared Spectroscopy for Air Pollution Research. *Appl. Spectrosc.* 12:80.
- Stephens, E.R., P.L. Hanst, and R.C. Doerr. 1957. Infrared Spectra of Aliphatic Peroxyacids. *Anal. Chem.* 29:776-777.
- Stephens, R.D., and S.H. Cadle. 1991. Remote Sensing Measurements of Carbon Monoxide Emissions from On-Road Vehicles. *J. Air Waste Manage. Assoc.* 41:39.
- Stone, J.M. 1963. *Radiation and Optics.* McGraw-Hill, New York.
- Strang, C.R., and S.P. Levine. 1989. The Limits of Detection for the Monitoring of Semiconductor Manufacturing Gas and Vapor Emissions by Fourier Transform Infrared (FTIR) Spectroscopy. *Am. Ind. Hyg. Assoc. J.* 50(2):78-84.
- Strang, C.R., S.P. Levine, and W.F. Herget. 1989. A Preliminary Evaluation of the Fourier Transform Infrared (FTIR) Spectrometer as a Quantitative Air Monitor for Semiconductor Manufacturing Process Emissions. *Am. Ind. Hyg. Assoc. J.* 50(2):70-77.
- Stuffer, T., V. Klein, and M. Resch. 1995. CO<sub>2</sub> LIDAR System for the Detection of Atmospheric Pollutants and Comparisons of the Measurement Results with Those of a Passive Remote Sensing System: An FTIR Spectrometer. *SPIE Specialty Conference in Munich*, Vol. 2505, International Society for Optical Engineering, Bellingham, WA.
- Tannenbaum, H., R.L. Byer, S.F. Clifford, K.S. Fu, E.D. Hinkley, T. Jaeger, A.G. Kjellass, K.W. Nill, M. Slatkine, and A. Wood. 1976. Long-Path Monitoring of Atmospheric Pollutant Gases. *Opt. Quantum Electron.* 8:194-196.
- Tate, J.D., J.P. Chauvel, and K. Taylor. 1994. Application of Industrial Open-Path FTIR for Continuous Monitoring. *SP-89 Optical Sensing for Environmental Monitoring, Air & Waste Management Association*, Pittsburgh, PA, pp. 791-806.
- Theriault, J.M., C. Bradette, and J. Gilbert. 1996. Atmospheric Remote Sensing with a Ground Based Spectrometer System. *Proc. SPIE* 2744.
- Theriault, J.M., L. Bissonnette, and G. Roy. 1997. Monitoring Cloud Parameters Using a Ground Based FTIR System. *Proc. SPIE* 3106:7-16
- Thomas, M.J., J.L. Hudson, G.A. Marotz, D.D. Lane, and R.E. Carter, Jr. 1992. Data Variability and Use Factors Compared Based on Open-Path FTIR and Canister Sampling Techniques. *SP-81 Optical Remote Sensing. Applications to Environmental and Industrial Safety Problems*, Air & Waste Management Association, Pittsburgh, PA, pp. 133-144.
- Thomas, M.J., J.L. Hudson, D.D. Lane, R.E. Carter, Jr., and G.A. Marotz. 1992. A Statistical and Data Use Comparison of a Canister-Based Sampling Technique with That of Open-Path Remote Sensing. Paper 92-73.07, *Proceedings of the 85th Annual Meeting and Exhibition*, Air & Waste Management Association, Pittsburgh, PA.
- Todd, L.A. 1992. Optical Remote Sensing/Computed Tomography Systems for Workplace Exposure Assessments. *SP-81 Optical Remote Sensing. Applications to Environmental and Industrial Safety Problems*, Air & Waste Management Association, Pittsburgh, PA, pp. 356-360.
- Todd, L., and D. Leith. 1990. Remote Sensing and Computed Tomography in Industrial Hygiene. *Am. Ind. Hyg. Assoc. J.* 51(4):224-233.
- Tolansky, S. 1962. *An Introduction to Interferometry.* John Wiley and Sons, New York.

- Toth, R.A., R.L. Abrams, G. Birnbaum, S.T. Eng, R.A. McClatchey, P.E. Nordal, and S.O. Olsen. 1976. Infrared Spectral Properties of Atmospheric Molecules. *Opt. Quantum Electron.* 8:191-194.
- Tso, T.L., W.C. Liao, and S.I. Chang. 1992. Portable Long Open Path FTIR Applied in In-Situ Measurement of Trace Gases of Ambient Air Pollution. *Proc. SPIE* 1637:95-106.
- Tuazon, E.C., R.A. Graham, A.M. Winer, R.R. Easton, J.N. Pitts, Jr., and P.L. Hanst. 1978. A Kilometer Pathlength Fourier-Transform Infrared System for the Study of Trace Pollutants in Ambient and Synthetic Atmospheres. *Atmos. Environ.* 12:865-875.
- Tuazon, E.C., A.M. Winer, R.A. Graham, and J.N. Pitts, Jr. 1980. Atmospheric Measurements of Trace Pollutants by Kilometer-Pathlength FT-IR Spectroscopy. *Advances in Environmental Science and Technology*, Vol. 10 (J.N. Pitts, Jr., and R.L. Metcalf, Eds.), John Wiley and Sons, New York, pp. 259-299.
- University of South Florida. 1993. USF HITRAN-PC. University of South Florida, Tampa, FL.
- Vandaele, A.C., M. Carleer, R. Colin, and P.C. Simon. 1993. Detection of Urban Ozone, Nitrogen Dioxide, Formaldehyde, and Sulfur Dioxide Using Fourier Transform Spectroscopy. *Proc. SPIE* 1715:288-92.
- van de Hulst, H.C. 1981. *Light Scattering by Small Particles*. Dover Publications, New York.
- Vaughan, W.M. 1991. Remote Sensing Terminology. *J. Air Waste Manage. Assoc.* 41(11):1489-1493.
- Vaughan, W.M., J.O. Zwicker, R.H. Dunaway, and P. Martino. 1994. The Feasibility of Using Optical Remote Sensing Systems to Determine Fugitive Emissions from Petroleum Refineries: A Review of the Present State of the Technology. *SP-89 Optical Sensing for Environmental Monitoring, Air & Waste Management Association*, Pittsburgh, PA, pp. 517-528.
- Vazquez, G.J. 1995. FTIR Remote Sensing of Atmospheric Species: Application to Air Pollution. *Proc. SPIE* 2365:438-463.
- Walsh, J.W.T. 1965. *Photometry*. Dover Publications, New York.
- Walter, B. 1889. *Ann. Physik* 36:502-518
- Wang, C. D., W.T. Walter, and R.H. Kagann. 1995. Neural Network and Classical Least Squares Methods for Quantitative Analysis in Remote Sensing FTIR Systems. *Proc. SPIE* 2366:251-262.
- Ward, T.V., and H.H. Zwick 1975. Gas Cell Correlation Spectrometer: GASPEC. *Appl. Opt.* 14:2896.
- Wassell, P.T., R.P. Wayne, J. Ballard, and W.B. Johnston. 1989. Laboratory Spectroscopic Studies of Atmospherically Important Radicals Using Fourier Transform Spectroscopy, *J. Atmos. Chem.* 8(1):63-85.
- Webb, J.D., K.R. Loos, C.L. Yao, D.C. Kreuger, S.A. Reid, S. Williamson, M.J. DeLong, and P.I. Chipman. 1995. Initial Applications of Open Path FTIR to Three Shell Oil Facilities—a Chemical Plant, a Refinery, and a Gas Processing Plant. *Proceedings of the AWMA Specialty Conference in San Francisco*. Air & Waste Management Association, Pittsburgh, PA.
- Weber, K., H.J. van de Wiel, A.C.F. Junker, and C. de LaRiva. 1992. Definition and Determination of Performance Characteristics of Air Quality Measuring Methods as Given by the International Organization for

- Standardization (ISO): Applicability to Optical Remote Sensing. *SP-81. Optical Remote Sensing. Applications to Environmental and Industrial Safety Problems*, Air & Waste Management Association, Pittsburgh, PA, pp. 30-42.
- Weber, K., V. Klein, and C. Werner. 1992. The Measurement of Gaseous Air Pollutants in the Troposphere by Optical Remote Sensing: Developments and Applications in Germany. *SP-81 Optical Remote Sensing. Applications to Environmental and Industrial Safety Problems*, Air & Waste Management Association, Pittsburgh, PA, pp. 44-54.
- Werner, C., R. Haus, F. Koepp, and K. Schäfer. 1995. Remote Sensing of Mass Fluxes of Trace Gases in the Boundary Layer. *Appl. Phys. B* 61:249-251.
- White, J.U. 1942. Long Paths of Large Apertures. *J. Opt. Soc. Am.* 32:285.
- Whitecraft, W.K., and K.N. Wood. 1990. Use of Remote Sensing to Measure Wastewater Treatment Plant Emissions. Paper 90-86.4, *Proceedings of the 83rd Annual Meeting and Exhibition*, Air & Waste Management Association, Pittsburgh, PA.
- Willard, H.H., L.L. Merritt, and J.A. Dean. 1974. *Instrumental Methods of Analysis*, 5th Ed., D. Van Nostrand, Princeton, NJ.
- Winkler, C., H. DeWitt, T. Eisenmann, and H. Mosebach. 1997. Surveillance System for Air Pollutants by Combination of the Decision Support System COMPAS and the FTIR Optical Remote Sensing System K300. *Proceedings of the 1997 1st International Conference on Measurements and Modeling in Environmental Pollution. Madrid, Spain*. Computational Mechanics Publ., Southampton, England.
- Witkowski, M.R., T.L. Marshall, C.T. Chaffin, R.M. Hammaker, and W.G. Fateley. 1992. Field Monitoring of Volatile Organic Compounds (VOCs) with a Mobile Fourier Transform Infrared (FT-IR) Spectrometer System. 1992. *SP-81 Optical Remote Sensing. Applications to Environmental and Industrial Safety Problems*, Air & Waste Management Association, Pittsburgh, PA, pp. 157-168.
- Woods, P.T., R.H. Partridge, M.J. Milton, B.W. Jolliffe, and N.R. Swann. 1992. Remote Sensing Techniques for Gas Detection, Air Pollution and Fugitive Loss Monitoring. *SP-81 Optical Remote Sensing. Applications to Environmental and Industrial Safety Problems*, Air & Waste Management Association; Pittsburgh, PA, pp. 3-29.
- Wu, R.T., S.Y. Chang, Y.W. Chung, H.C. Tzou, and T.L. Tso. 1995. FTIR Remote Sensor Measurements of Air Pollutants in the Petrochemical Industrial Park. *Proceedings of the SPIE Conference on Infrared Technology XXI in San Diego*. International Society for Optical Engineering, Bellingham, WA.
- Xiao, H-K., S.P. Levine, and J.B. D'Arcy. 1989. Iterative Least-Squares Fit Procedures for the Identification of Organic Vapor Mixtures by Fourier Transform Infrared Spectro-photometry. *Anal. Chem.* 61(24): 2708-2714.
- Xiao, H-K., S.P. Levine, J.B. D'Arcy, G. Kinnes, and D. Almaguer. 1990. Comparison of the Fourier Transform Infrared (FTIR) Spectrophotometer and the Miniature Infrared Analyzer (MIRAN) for the Determination of Trichloroethylene (TCE) in the Presence of Freon-113 in Workplace Air. *Am. Ind. Hyg. Assoc. J.* 51(7):395-401.
- Xiao, H-K., S.P. Levine, W.F. Herget, J.B. D'Arcy, R. Spear, and T. Pritchett. 1991. A Transportable, Remote Sensing, Infrared Air Monitoring System. *Am. Ind. Hyg. Assoc. J.* 52(11):449-457.

- Ying, L-S., and S.P. Levine. 1989. Evaluation of the Applicability of Fourier Transform Infrared (FTIR) Spectroscopy for Quantitation of the Compounds of Airborne Solvent Vapors in Air. *Am. Ind. Hyg. Assoc. J.* 50(7):360-365.
- Ying, L-S., and S.P. Levine. 1989. Fourier Transform Infrared Least-Squares Methods for the Quantitative Analysis of Multicomponent Mixtures of Airborne Vapors of Industrial Hygiene Concern. *Anal. Chem.* 61(7):677-683.
- Ying, L-S., S.P. Levine, C.R. Strang, and W.F. Herget. 1989. Fourier Transform Infrared (FTIR) Spectroscopy for Monitoring Airborne Gases and Vapors of Industrial Hygiene Concern. *Am. Ind. Hyg. Assoc. J.* 50(7):354-359.
- Yokelson, R.J., D.W.T. Griffith, J.B. Burkholder, and D.E. Ward. 1996. Accuracy and Advantages of Synthetic Calibration of Smoke Spectra. *Proceedings of the AWMA Specialty Conference in San Francisco*. Air & Waste Management Association, Pittsburgh, PA.
- Yost, M.G., H.K. Xiao, R.C. Spear, and S.P. Levine. 1992. Comparative Testing of an FTIR Remote Optical Sensor with Area Samplers in a Controlled Ventilation Chamber. *Am. Ind. Hyg. Assoc. J.* 53(10):611-616.
- Zhang, Y., D.H. Stedman, G.A. Bishop, P.L. Guenther, S.P. Beaton, and J.E. Peterson. 1993. On-Road Hydrocarbon Remote Sensing in the Denver Area. *Environ. Sci. Technol.* 27(9):1885-1891.
- Zwicker, J.O., W.M. Vaughan, R.H. Dunaway, and R.H. Kagann. 1994. Open-Path FTIR Measurements of Carpet/Water Sealant Emissions to Determine Indoor Air Quality. *SP-89 Optical Sensing for Environmental Monitoring*, Air & Waste Management Association, Pittsburgh, PA, pp. 225-241.
- Zwicker, J.O. 1995. Intercomparison of Data from Open-Path Fourier Transform Infrared Spectrometers Collected During the EPA/API Cooperative Remote Sensing Dispersion Field Study at Duke Forest, North Carolina, January 9 to 27, 1995. *Proceedings of the AWMA Specialty Conference in San Francisco*. Air & Waste Management Association, Pittsburgh, PA.